ISBN 978-82-326-4814-6 (printed version)
ISBN 978-82-326-4815-3 (electronic version)
ISSN 1503-8181




Doctoral theses at NTNU, 2020:233

Haavard Holta

# Kick & Loss Detection and Estimation using Distributed Models

**NTNU**
Norwegian University of
Science and Technology
Faculty of Information Technology
and Electrical Engineering
Department of Engineering Cybernetics

NTNU
Norwegian University of
Science and Technology

Doctoral theses at NTNU, 2020:233

NTNU

NTNU
Norwegian University of
Science and Technology

Haavard Holta

# Kick & Loss Detection and Estimation using Distributed Models

Thesis for the degree of Philosophiae Doctor

Trondheim, August 2020

Norwegian University of Science and Technology
Faculty of Information Technology
and Electrical Engineering
Department of Engineering Cybernetics

NTNU
Norwegian University of
Science and Technology

**NTNU**
Norwegian University of Science and Technology

Thesis for the degree of Philosophiae Doctor

Faculty of Information Technology
and Electrical Engineering
Department of Engineering Cybernetics



ISBN 978-82-326-4814-6 (printed version)
ISBN 978-82-326-4815-3 (electronic version)
ISSN 1503-8181
ITK-report: 2020-7-W

Doctoral theses at NTNU, 2020:233

Printed by Skipnes Kommunikasjon as

# Summary

A *kick* in oil and gas drilling is an unwanted, unexpected leak of oil and gas from the reservoir into the well-bore. This can happen when the surrounding formation pore pressure exceeds the well-bore pressure. A *loss* of circulation is the leak of drilling mud from the well-bore into the surrounding formation which occurs if the well-bore pressure is sufficiently higher than the formation pressure. Both types of leaks can have severe consequences related to the safety of the drilling crew, the rig itself and the surrounding environment. Even if the risk of severe safety related incidents is minimal, leaks are associated with high purely economical costs, both related to down-time (non-productive time), or fracturing of the well which might affect the future revenue-generating capabilities of the well. Besides preventive actions to reduce the likelihood that a leak occurs, it is evident that the ability to attenuate a leak when they do happen is an important part of any drilling operation. Early *kick & loss detection* is an important factor in fast leak attenuation. Almost equally important is early *kick & loss estimation* where information about the leak, such as pore pressure, well pressure, formation permeability and inflow size, is estimated in real-time and used to guide the controller for faster leak attenuation.

The well-bore can be several kilometers long and transient fluid flow effects are significant. The fluid flow is therefore often modeled by hyperbolic partial differential equations (PDEs). Previous results on kick and loss detection and estimation has mainly focused on using *lumped* ODE models (with some notable exceptions), where the infinite dimensional PDE model is approximated by a finite dimensional ordinary differential equation model. This thesis investigates the possibility of using distributed PDE models directly in kick and loss estimation schemes.

# Preface

This thesis is submitted in partial fulfillment of the requirements for the degree of philosophiae doctor (PhD) at the Norwegian University of Science and Technology (NTNU). The research has been carried out at the Department of Engineering Cybernetics from August 2017 to May 2020 under the guidance of Professor Ole Morten Aamo. The project has been funded by The Research Council of Norway and Equinor ASA through project no. 255348/E30 "Sensors and models for improved kick/loss detection in drilling (Semi-kidd)".

**Acknowledgments**

I would like thank my supervisor, Professor Ole Morten Aamo for offering me the PhD position and for guidance throughout the PhD. Thanks to Professor Bernt Lie, Dr. Asanthi Jinasena, Dr. Prasanna Welahettige, Dr. Morten Hansen Jondahl and the rest of the Semi-Kidd group for collaboration and motivating discussions during the Semi-Kidd meetings. I would also like to thank Dr. John-Morten Godhavn for inviting me to Equinor, Rotvoll. A special thanks to PostDoc Henrik Anfinsen for collaboration and constructive, motivating discussions during the last year. Finally, I would like to thank my family, Mom, Dad, Astri, Inger, and Ann Christin for all support during the last three years.

*Haavard Holta*
*Trondheim, May 2020*

# Contents

# Abbreviations

| | |
|---|---|
| DFM | Drift-Flux Model |
| LOL | Low-order Lumped (model) |
| LWD | Logging While Drilling |
| MPD | Managed Pressure Drilling |
| ODE | Ordinary Differential Equation |
| PDE | Partial Differential Equation |
| PE | Persistently Exciting |
| PI | Productivity Index |

# CHAPTER 1

# Introduction

## 1.1 The kick & loss problem in oil & gas drilling

Figure 1.1 shows an illustration of an offshore drilling system. A rotating drill string with a drill bit at the end is lowered down to the seabed and used to dig a hole down to a prospective reservoir where oil and gas can be extracted through porous formations. The drill string is hollow allowing a drilling fluid, referred to as mud, to be circulated down into the well using a pump top-side at the rig. The mud exits through nozzles on the drill bit down-hole and is circulated up in the annulus between the drill string outer walls and the well. Between the seabed and the rig, a riser is installed to separate the drilling system from the surrounding sea water.

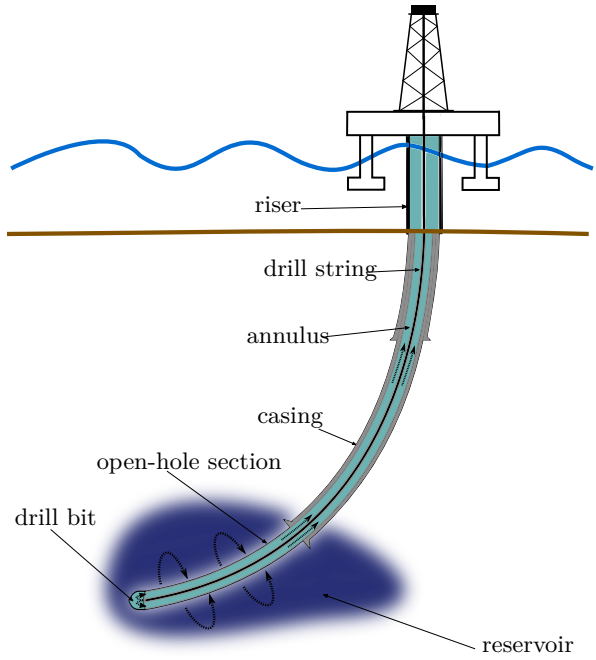


**Figure 1.1:** Illustration of an offshore drilling system.

The drilling mud is used to transport rock cuttings out of the well to the rig, where the cuttings are separated from the mud and the mud recirculated down the drill string. Equally important is that the mud provides well pressure control [26]. In steady state, the well pressure is the sum of the hydrostatic pressure, frictional pressure loss and top-side pressure. Figure 1.2 shows a typical well pressure profile and associated lower and upper pressure bounds. The process of isolating the well

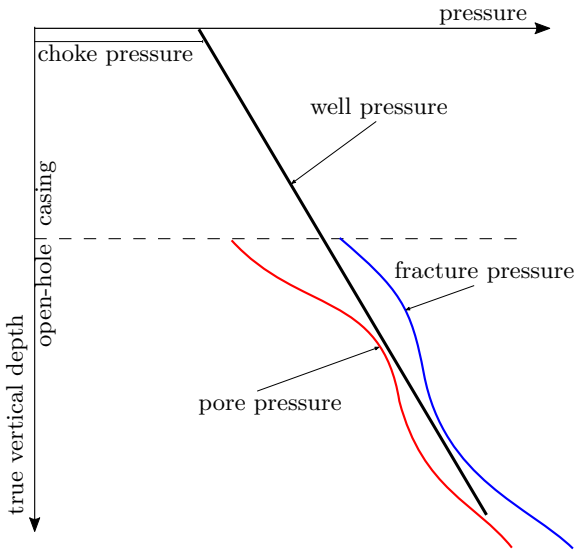


**Figure 1.2:** Pressure margins in drilling.

from the surrounding formation is called completion and involves the insertion of a casing pipe in the annulus which is typically cemented in place. The section below the casing pipe is open to the surrounding formation and the well pressure in this region must be carefully controlled. The lower pressure bound is determined by the pore pressure. If the pore pressure exceeds the annular pressure, fluids from the surrounding formations, which can be water, oil or gas, will start flowing into the well. This phenomenon is called a *kick*. If not handled, a kick will lead to a blowout on the surface endangering both the safety of personnel and the drilling rig. The opposite situation with a high annular pressure might lead to fracturing of the well and flow of drilling mud into the surrounding formation, potentially damaging the formation. This phenomenon is called a *loss* (*loss* of circulation or *loss* of drilling fluid). Even more severe, a loss of drilling fluids leads to a lower hydrostatic pressure which in turn might cause a kick further up the annulus.

In *conventional drilling* the annular pressure gradient is controlled by varying the density of the drilling mud. However, with a circulation speed in the magnitude of $\sim 1\,\mathrm{m\,s^{-1}}$, this process is too slow to handle an unexpected rise in reservoir pressure and the resulting kick. Instead, various time-consuming shut-in and circulation procedures must be initiated. This entails stopping the rotation of the drill string, lifting the drill-bit up from the well-bottom, closing the top-side annular seal known as a *blow out preventer* and circulating out any reservoir fluid in the

annulus.

In *Managed Pressure Drilling* (MPD), the annular pressure is controlled more actively. Various technologies exist, the most common being *annular back-pressure* and *dual-gradient* systems. A back-pressure can be applied by sealing the annulus top-side at the rig using a *rotating control device* and restricting the return flow through a choke valve. This allows for continuous pressure control while drilling by adjusting the valve opening. In addition, a *back pressure pump* can be used to maintain the hydrostatic pressure in the case of lost circulation by pumping additional mud into the annulus. In addition to being an enabling technology by making wells with tight pressure margins drillable, MPD can be used for fast kick attenuation by actively adjusting top-side pressure in response to changes in the down-hole situation [82]. Using MPD, the kick can be attenuated without stopping drilling, avoiding the costly shut-in procedures. However, the top-side separator equipment can only handle a limited amount of production fluids. Early kick detection and estimation are therefore essential to prevent the kick from developing in magnitude to a level where shut-in procedures must be initiated [47, 50, 85, 92, 102].

## 1.2 Mathematical preliminaries: Hyperbolic PDEs

The models used to describe the drilling systems in this thesis are hyperbolic partial differential equations (PDEs), so before presenting the physical drilling models, some background material on hyperbolic PDEs are provided.

### 1.2.1 Notation

For a signal $z : [0, 1] \times [0, \infty) \to \mathbb{R}^n$, partial derivatives with respect to e.g. space are denoted $z_x$ or $\partial_x z_i$ for each element $i = 1, ..., n$. The $L_2$-norm is denoted

$$||z|| := \sqrt{\int_0^1 z^T(x,t)z(x,t)dx}. \tag{1.1}$$

For $f : [0, \infty) \to \mathbb{R}$, we use the vector spaces

$$f \in \mathcal{L}_p \leftrightarrow \left( \int_0^\infty |f(t)|^p dt \right)^{\frac{1}{p}} < \infty \tag{1.2}$$

for $p \geq 1$ with the particular case

$$f \in \mathcal{L}_\infty \leftrightarrow \sup_{t \geq 0} |f(t)| < \infty. \tag{1.3}$$

Derivatives with respect to time are denoted $\dot{f}$.

To simplify the notation, for functions of time and space the temporal and spatial arguments $(x, t)$ are sometimes omitted.

### 1.2.2 Classes of hyperbolic PDEs

The most general system considered in this thesis has the form

$$z_t + F(z, x)z_x = S(z, x) \tag{1.4}$$

with solution $z : [0,1] \times [0,\infty) \to \mathcal{Z} : (x,t) \mapsto u(x,t)$ for some open subset $\mathcal{Z}$ of $\mathbb{R}^n$ for any $n \geq 1$, where $x \in [0,1]$ is the independent (normalized) space variable and $t \in [0,\infty)$ the independent time variable. The *flux density* $F : \mathcal{Z} \times [0,1] \to \mathbb{R}^{n \times n}$ and *source term* $S : \mathcal{Z} \times [0,1] \to \mathbb{R}^n$ are continuously differentiable functions with respect to both $z$ and $x$. As the system (1.4) is linear in the first order derivatives $z_t$ and $z_x$, but generally non-linear in $z$, it is referred to as a *quasi-linear* system. If the flux density $F(x)$ is independent of $z$, the system is called *semi-linear* and if also the source term $S(z,x) = S_0(x)z$ is linear in $z$, the system is referred to as a *linear* system. Systems in the form (1.4) arise naturally from various physical *balance laws* describing how a certain quantity in the domain is balanced through consumption/production and in- or out-fluxes through the boundaries. If $S(z,x) \equiv 0$, the quantity is preserved in the domain, and the system is used to represent *conservation laws*.

Only *hyperbolic* systems are considered which are systems where the flux density matrix $F(z)$ has $n$, real, eigenvalues. If, in addition, all eigenvalues are distinct, the system is called *strictly hyperbolic*. If there exists a similarity transformation $P : \mathcal{Z} \to \mathcal{U} \subset \mathbb{R}^n : (z,x) \mapsto P(z,x) =: w$ such that the diagonal matrix $\Lambda(w,x)$ is similar to $F(z,x)$, i.e. satisfying

$$\Lambda(w,x)P(z,x) = P(z,x)F(u) \tag{1.5}$$

for all $(w,x) \in \mathcal{W} \times [0,1]$, the system is said to be *diagonalizable*. The resulting system is said to be on *characteristic form* and the coordinates $w := P(z,x)$ are called *Riemann coordinates* for general balance laws, or *Riemann invariants* for conservation laws. In the following, only diagonalizable systems will be considered. The diagonal elements of $\Lambda(w,x)$, often called *characteristic velocities* for general balance laws or *transport velocities* for conservation laws, are typically denoted $\mu_i(w,x)$ for $i = 1,...,m$ and $\lambda_i(w,x)$ for $i = 1,...,n$ and ordered such that

$$-\mu_1(w,x) \leq \cdots \leq -\mu_m(w,x) < 0 < \lambda_1(w,x) \leq \cdots \leq \lambda_n(w,x). \tag{1.6}$$

Remark that $\lambda_i(w,x), \mu_i(w,x) > 0$, i.e. non-vanishing in $\mathcal{W} \times [0,1]$. For strictly hyperbolic linear or semi-linear systems, the system is always diagonalizable.

For linear systems on characteristic form, the system state $w(x,t)$ is often divided into a positive convecting part $u(x,t) \in \mathbb{R}^n$ associated with the positive characteristic velocities $\Lambda^+(x) := \text{diag}(\lambda_1(x),...,\lambda_n(x))$ and a negative convecting part $v(x,t) \in \mathbb{R}^m$ associated with the negative characteristic velocities $-\Lambda^-(x) := \text{diag}(-\mu_1(x),...,-\mu_m(x))$:

$$u_t + \Lambda^+(x) = \Sigma^{++}(x)u + \Sigma^{+-}(x)v \tag{1.7a}$$

$$v_t - \Lambda^-(x) = \Sigma^{-+}(x)u + \Sigma^{--}(x)v \tag{1.7b}$$

where

$$\begin{bmatrix} \Sigma^{++}(x)u & \Sigma^{+-}(x) \\ \Sigma^{-+}(x)u & \Sigma^{--}(x) \end{bmatrix} := P(x)S_0(x)P^{-1}(x). \tag{1.8}$$

The special case $m = 1$, referred to as $n+1$ systems, is often used to model multiphase flow systems, where $n \geq 1$ denotes the number of phases (see Section 1.3.2). Such systems are usually written in the form

$$u_t + \Lambda(x) = \Sigma^{++}(x)u + \sigma^{+-}(x)v \tag{1.9a}$$

$$v_t - \mu(x) = \sigma^{-+}(x)u \tag{1.9b}$$

where $\Lambda(x)$ is the diagonal matrix with elements $\{\lambda_i(x)\}_{i=1,..,n}$, and source terms $\sigma^{+-}(x) \in \mathbb{R}^{n\times 1}$ and $\sigma^{+-}(x) \in \mathbb{R}^{1\times n}$. The missing source term $\sigma^{--} \in \mathbb{R}$ can always be removed through a linear coordinate transformation and is therefore omitted. The next special case, where also $n = 1$, is commonly used to model single-phase flow systems. They are referred to as $2 \times 2$ systems and are usually written in the form

$$u_t + \lambda(x)u_x = \sigma^{+}(x)v \tag{1.10a}$$
$$v_t - \mu(x)v_x = \sigma^{-}(x)u \tag{1.10b}$$

with source terms $\sigma^{+}(x), \sigma^{-}(x) \in \mathbb{R}$, where again the diagonal source terms can be removed by defining a linear coordinate transformation. Finally, the trivial system with $n = 0$ and $m = 1$,

$$v_t - \mu(x)v_x = 0, \tag{1.11}$$

is used to model various quantity conservative transport phenomena.

### 1.2.3 Well-posedness

A system is said to be *well-posed* if the system has a unique solution which depends continuously on the input data. In order to guarantee well-posedness, both the boundary and initial conditions must therefore be specified. For many open-loop systems or systems with static feedback written in characteristic form, this usually amounts to specifying the *incoming information* as a function of the *outgoing information* [96], where incoming and outgoing information are defined to be the originating and terminating boundary, respectively, of each convecting Riemann state, i.e.

$$u(0,t) = \mathcal{B}_0(u(1,t), v(0,t)) \tag{1.12a}$$
$$v(1,t) = \mathcal{B}_1(u(1,t), v(0,t)) \tag{1.12b}$$

for some boundary functions $\mathcal{B}_0 : \mathbb{R}^n \times \mathbb{R}^m \to \mathbb{R}^n$ and $\mathcal{B}_1 : \mathbb{R}^n \times \mathbb{R}^m \to \mathbb{R}^m$. In this thesis, dynamic boundary control laws are often used, i.e.

$$u(0,t) = \mathcal{B}_0(u(1,\cdot), v(0,\cdot), t) \tag{1.13a}$$
$$v(1,t) = \mathcal{B}_1(u(1,\cdot), v(0,\cdot), t) \tag{1.13b}$$

where now the boundary functions, called control laws if specifiable, takes the arguments $u(1,\cdot)$ and $v(0,\cdot)$ which are functions $[0,\infty) \to \mathbb{R}^n$ and $[0,\infty) \to \mathbb{R}^m$ respectively. In this case, proving well-posedness is non-trivial without some restriction on the type of control law [10, Theorem 1.1]. Linear boundary conditions are usually written in the form

$$u(0,t) = Q_0 v(0,t) + d(t) \tag{1.14a}$$
$$v(1,t) = R_1 u(1,t) + U(t) \tag{1.14b}$$

for some constant matrices $Q_0 \in \mathbb{R}^{n\times m}$ and $R_1 \in \mathbb{R}^{m\times n}$ and control law functions $d : [0,1] \to \mathbb{R}^n$ and $U : [0,1] \to \mathbb{R}^m$. The signal $d(t)$ can also be used to model

exogenous disturbances such as oil & gas reservoir interactions in a drilling system (see Section 1.3.4). Here, opposite boundary dependencies (i.e. $u(0,t)$ dependent on $u(\cdot,t)$ and $v(1,t)$ dependent on $v(\cdot,t)$ ), if they exist, are embedded into the control laws.

### 1.2.4 Stability of PDEs

Based on the definitions in Section 1.2.1, various notions of stability are studied throughout this thesis. For infinite dimensional vector spaces the $L_p$ norms are not equivalent. However, since the spatial domain has finite measure, the inclusion $L_p([0,1]) \subset L_q([0,1])$ holds for any $1 < p < q$. Although many of the systems studied can be shown to have continuous or even continuously differentiable solutions, most stability results are proved in terms of the $L_2([0,1])$-norm, meaning that the solution is only required to be square integrable.

A function $u : [0,\infty) \to L_2([0,1]) : t \mapsto ||u(\cdot,t)||$ is said to be

- *bounded in the $L_2$-sense*, or simply *bounded*, if $||u|| \in \mathcal{L}_\infty$,
- *square integrable in the $L_2$-sense*, or simply *square integrable*, if $||u|| \in \mathcal{L}_2$,
- *converge to zero in the $L_2$-sense*, or simply *converge to zero* if $||u|| \to 0$ as $t \to \infty$.

Many hyperbolic PDE systems, particularly non-adaptive systems, also have the property that convergence to zero is achieved in a *finite time* specified by the characteristic velocities. In particular, this is true for many systems without boundary reflection (e.g. $Q_0 = 0, R_1 = 0$ in (1.14)).

## 1.3 Models for estimation and control in drilling

Transient effects in fluid flow systems have been studied for centuries [49, 93, 108]. Initial interest in transient analysis of fluid flows in pipe systems was motivated by the observed *water hammer problem* in hydroelectric penstocks [49] which can be described as the sudden change in pressure caused by a sudden change in fluid velocity, often caused by opening or closing a valve. The Joukowsky equation [108], also called the *fundamental equation of water hammer*, captures this relationship:

$$\Delta p = z \Delta q \tag{1.15}$$

where $\Delta q$ is the change in volumetric flow rate, $z$ is the *hydraulic impedance*, and $\Delta p$ is the resulting change in pressure. The hydraulic impedance is given by $z = \frac{\rho\lambda}{A}$ where $\rho$ is the fluid density, $A$ is the cross-sectional area of the pipe and $\lambda$ the speed of sound in the fluid.

Due to the initial interest in the water hammer problem, the model describing unidirectional, axisymmetric flow of a compressible fluid in a pipe where the Mach number is very small [49], has therefore been called the *water hammer equations*. This model is presented in Section 1.3.1. Structurally similar models include the *Saint-Venant shallow water equations*, the *telegrapher equations*, or the *Euler equations*. An overview can be found in [18].

Some phenomena in fluid flow systems are only captured by a distributed model such as the hyperbolic PDE systems described in Section 1.2. The significance of these phenomena, such as the water hammer effect, when modeling for estimation and control in oil & gas drilling systems however, is still an open question [5, 38, 79, 84, 105]. There is also a trade-of between increased model accuracy and model complexity. For many applications, simple *low order lumped*-models (LOL-models) may be adequate. In the following, a linear single-phase model (the water hammer equations) and a more complex two-phase model (the drift-flux model) will be presented. Qualitative aspects of these two models are then compared to a commonly used LOL-model.

For the specific problem of kick & loss estimation and attenuation considered in this thesis, modeling the well–reservoir interaction is important. Reservoir models, sensing, actuation and control objectives specific to the kick & loss application are therefore also briefly presented.

### 1.3.1 Single-phase distributed PDE models

For single-phase flows, the mass and momentum balance in the drill string and annulus can be described by

$$\partial_t p_i(x,t) + \frac{\beta_i}{A_i(x)}\partial_x q_i(x,t) = \varphi_i(p_i(x,t), q_i(x,t), x) \tag{1.16a}$$

$$\partial_t q_i(x,t) + \frac{A_i(x)}{\rho_i}\partial_x p_i(x,t) = \phi_i(p_i(x,t), q_i(x,t), x) \tag{1.16b}$$

where $i = d$ for the drill string and $i = a$ for the annulus, the pressure $p_i(x,t)$ and volumetric flow $q_i(x,t)$ are functions of the along-string distance $x \in [0, L]$ (measured depth where $L$ is the well length), and time $t \in [0, \infty)$. $A_i(x)$ is the cross-sectional area, $\beta_i$ the bulk modulus of the drilling mud and $\rho_i$ the drilling mud density. For the annulus with inflow $q_{in}(x,t)$, flow-induced friction $F_a(q_a(x,t), x)$ and force equivalent momentum influx from the surrounding formation $F_r(q_{in}(x,t), x)$, the source terms have the general structure

$$\varphi_a(p_a(x,t), q_a(x,t), x) = \frac{\beta_a}{A_a(x)}\partial_x q_{in}(x,t) \tag{1.17a}$$

$$\begin{aligned}\phi_a(p_a(x,t), q_a(x,t), x) = &- A_a(x) g \cos(\psi(x)) \\ &- \rho_a^{-1}\partial_x F_a(q_a(x,t), x) + \rho_a^{-1}\partial_x F_r(q_{in}(x,t), x),\end{aligned} \tag{1.17b}$$

where $\psi(x)$ is the inclination of the well and $g$ the gravitational acceleration. For the drill string with flow-induced friction $F_d(q_a(x,t), x)$ (and no reservoir inflow), the source terms have the general structure

$$\varphi_d(p_d(x,t), q_d(x,t), x) = 0 \tag{1.18a}$$

$$\phi_d(p_d(x,t), q_d(x,t), x) = A_d(x) g \cos(\psi(x)) - \rho_d^{-1}\partial_x F_d(q_d(x,t), x). \tag{1.18b}$$

However, for most problems considered in this thesis, only the flow in the annulus is considered, reservoir inflow is assumed to only happen at the boundary, and the friction terms are assumed to be linear in $q_a$. In that case,

$$\varphi_a(p_a(x,t), q_a(x,t), x) = 0 \tag{1.19a}$$

$$\phi_a(p_a(x,t), q_a(x,t), x) = -A_a(x)g\cos(\psi(x)) - f_a(x)q_a(x,t), \tag{1.19b}$$

for some friction coefficient $f_a(x) \geq 0$.

The boundary conditions can be modeled as

$$p_d(0,t) = \begin{cases} p_a(0,t) + k_{bit}q_d^2(0,t), & q_d(0,t) > 0 \\ 0, & q_d(0,t) \leq 0 \end{cases} \tag{1.20a}$$

$$q_d(L,t) = q_p(t) \tag{1.20b}$$

$$p_a(L,t) = p_c(t) \tag{1.20c}$$

$$q_a(0,t) = q_a(0,t) + q_{in}(t) \tag{1.20d}$$

where $q_p(t)$ is the stand pipe pump rate, $k_{bit}$ is a constant relating the bit flow and differential pressure over the bit, $q_{in}(t)$ is the reservoir inflow (see Section 1.3.4 below), and $p_c(t)$ is the choke pressure which for conventional drilling can be set to $p_c(t) = 1\,\text{bar}$ (atmospheric pressure). In Managed Pressure Drilling, the return flow is usually modeled by the choke equation

$$q_c(t) = k_{choke}(t)\text{sign}(p_a(L,t) - p_0)\sqrt{|p_a(L,t) - p_0|} \tag{1.21}$$

where $p_0$ is the pressure at the separator side, and $k_{choke}(t)$ the adjustable choke coefficient modeling both the specific choke characteristics and the variable choke opening.

Let $z_i(x,t) = [p_i(x,t), q_i(x,t)]$. The system (1.16) has the general form (1.4) with flux density matrix

$$F(x) = \begin{bmatrix} 0 & \frac{\beta_i}{A_i(x)} \\ \frac{A_i(x)}{\rho_i} & 0 \end{bmatrix} \tag{1.22}$$

which has constant eigenvalues $\lambda = \sqrt{\frac{\beta_i}{\rho_i}}$ and $-\mu = -\sqrt{\frac{\beta_i}{\rho_i}}$, and there exists a linear transformation $z(x,t) \to (u(x,t), v(x,t))$ transforming (1.16) into characteristic form. For the linear case (1.19) with spatially constant cross-sectional area $A_i$ and friction factor $f_i$, the system (1.16) is equivalent to the $2 \times 2$ system (1.10) with

$$\sigma^+(x) = \sigma^-(-x) = -\frac{f_i}{2\rho_i}\exp(\frac{Lf_i}{\sqrt{\beta_i\rho_i}}x). \tag{1.23}$$

The details can be found in Appendix A which are based on [1, 17].

For a typical drilling fluid with density $1500\,\text{kg}\,\text{m}^{-3}$ and bulk modulus 1.5 GPa, the characteristic velocity is $\lambda = \mu = 1000\,\text{m}\,\text{s}^{-1}$, but it can also be as low as $\lambda = \mu = 10\,\text{m}\,\text{s}^{-1}$ in certain gas-oil-water-mud mixtures. This mode represents the propagation of pressure waves, or sound waves, and $\lambda = |-\mu| = \sqrt{\frac{\beta_i}{\rho_i}}$ is often called the *speed of sound* of the medium. The Joukowsky equation (1.15) is obtained by integrating the mass-balance (1.16a) (with $\varphi_i = 0$) along the characteristic lines over the spatial interval $[L - \lambda t - \epsilon, L - \lambda t + \epsilon]$ and then taking the limit $\epsilon \to 0$.

In the linear case, the source terms are dissipative in the sense that $\sigma^+(x), \sigma^-(x) \leq 0$ for all $x \in [0,1]$. In that case, the only source of instability is through the boundaries. Even in the non-linear case, for many applications the momentum source $\phi_i$ is dissipative in the sense that

$$\frac{\phi_i(p_i, q_1, x) - \phi_i(p_i, q_2, x)}{q_1 - q_2} \leq 0 \tag{1.24}$$

for any $q_1, q_2$ and all $x \in [0,1]$. This fact is exploited in Chapter 3 for observer design.

### 1.3.2 Multi-phase distributed model: The drift-flux model

If the well consists only of liquids such as water, oil, mud and even cuttings, the single-phase model in Section 1.3.1 is commonly used by lumping all phases into a single state assuming uniform density. If, however, gas is present in the well, the multi-phase flow dynamics are not accurately captured by the semi-linear model (1.16). Gas–liquid multi-phase flows are commonly modeled by the classical *Drift-Flux Model* (DFM) (see e.g. the review article [4])

$$\partial_t(\alpha_L\rho_L) = -\partial_z(\alpha_L\rho_L v_L) \tag{1.25a}$$
$$\partial_t(\alpha_G\rho_G) = -\partial_z(\alpha_G\rho_G v_G) \tag{1.25b}$$
$$\begin{aligned}\partial_t(\alpha_L\rho_L v_L + \alpha_G\rho_G v_G) = &-\partial_z(p + \alpha_L\rho_L v_L^2 + \alpha_G\rho_G v_G^2) \\ &- \rho_M g\cos\psi - \rho_M F(v_M)\end{aligned} \tag{1.25c}$$

where mud, oil and water are lumped into a single liquid state with density $\rho_L$, volume fraction $\alpha_L$ and velocity $v_L$, and the gas phase with density $\rho_G$, volume fraction $\alpha_G$ and velocity $v_G$ is kept separate. $F(v_M)$ models frictional forces and $\psi$ is the inclination angle of the well. The mean density $\rho_M$ and mean velocity $v_M$ are defined as

$$\rho_M := \alpha_G\rho_G + \alpha_L\rho_L \quad v_M := \alpha_G v_G + \alpha_L v_L. \tag{1.26}$$

In addition, since the liquid and gas phase are lumped into a single momentum balance (1.25c), a set of closure relations must be specified. The pressure $p$ is related to the densities by

$$\rho_G = \frac{p}{c_G^2}, \quad \rho_L = \rho_{L,0} + \frac{p - p_{L,0}}{c_L^2} \tag{1.27}$$

where $c_G$ and $c_L$ are the speeds of sound, in the gas and liquid phase, respectively, and $p_{L,0}$ and $\rho_{L,0}$ are constants. The gas and liquid velocities are related by the slip law

$$v_G = \frac{v_M}{1-\alpha_L^*} + v_\infty \tag{1.28}$$

where $\alpha_L^*$ and $v_\infty$ are empirically estimated constant parameters. Moreover, the former acts as a lower bound on $\alpha_L$ as it was shown in [20] that the DFM is hyperbolic for $\alpha_L > \alpha_L^*$. Similar to the single-phase model (1.16), the DFM can be extended to model in-domain in- or out-flow [43]. The dissolution of gas into the liquid phase is not modeled by (1.25). In cases where the gas solubility is significant, such as when using oil-based mud, an additional mass balance must be included. In [9] it was shown that the reduction in pit gain due to gas solubility when using oil-based mud (as compared to water-based mud) is significant.

With in- or out-flow at the bottom-hole location $x = 0$, the boundary condition takes the form

$$\alpha_L\rho_L v_L + \alpha_G\rho_G v_G = \frac{1}{A}(W_{L,res} + W_{G,res} + W_{L,bit}) \tag{1.29}$$

where $A$ is the cross-sectional area of the annulus, $W_{L,res}$ and $W_{G,res}$ are the mass influx rate of formation liquid and formation gas respectively, and $W_{L,bit}$ is the mud flow velocity through the drill-bit. For the top-side boundary condition, the top-side pressure is either set constant as in conventional drilling or, as in MPD, specified by the choke equation

$$\left[\frac{\alpha_L\rho_L v_L}{\sqrt{\rho_L}} + \frac{\alpha_G\rho_G v_G}{Y\sqrt{\rho_G}}\right]_{x=L} = k_{1,choke}(t)\text{sign}(p_a(L,t)-p_0)\sqrt{|p_a(L,t)-p_0|} \quad (1.30)$$

where $p_0$ is the pressure at the separator side, $k_{1,choke}(t)$ the adjustable choke coefficient modeling both the specific choke characteristics and the variable choke opening, and $Y \in [0,1]$ is a gas expansion factor.

Mathematical properties of the drift-flux model have been studied extensively. However, without any simplifying assumptions such as liquid incompressibility, low gas density ($\alpha_G\rho G \ll \alpha_L\rho_L$), or the no-slip case ($v_G = v_M$), the quasi-linear form (1.4) with analytical expressions for the flux density matrix is hard to obtain [20]. In this thesis, with a focus on gas-kicks, the analysis of the DFM will be simplified by using model reductions that isolate the dynamics relevant in a gas-kick scenario. More specifically, following the approach in [48] and [3], by defining the *pseudo density*

$$\rho = \rho_M - \alpha_L^*\rho_L, \quad (1.31)$$

the *pseudo mass concentration*

$$\chi = \frac{(\alpha_L - \alpha_L^*)\rho_L}{\rho_M - \alpha_L^*\rho_L}, \quad (1.32)$$

and neglecting higher order terms, it can be shown that system (1.25) can be written in the quasi linear form (1.4) in terms of the coordinates $w = (\chi, \rho, v_G)$ as

$$\chi_t + v_G\chi_x = 0 \quad (1.33a)$$

$$\partial_t\begin{bmatrix}\rho\\ v_G\end{bmatrix} + \frac{\bar{\alpha}_0(w)c_M^2(w)}{\rho}\chi_x + \begin{bmatrix} v_G & \rho \\ \frac{c_M^2(w)}{\rho} & v_G\end{bmatrix}\partial_x\begin{bmatrix}\rho\\ v_G\end{bmatrix} = \begin{bmatrix}0\\ S(w)\end{bmatrix} \quad (1.33b)$$

where

$$\bar{\alpha}_0 := \frac{\rho(\rho_G-\rho_L)}{\rho_L(1-\alpha_L^*)\rho_G}, \quad c_M^2(w) := \frac{(1-\alpha_L^*)p}{\alpha_G\rho} \quad (1.34)$$

and

$$\begin{aligned} S(w) &:= -\frac{\rho_M}{\rho}g\cos\psi - \frac{\rho_M}{\rho}F(v_M) \\ &= -\left(1+\frac{\alpha_L^*\rho_L}{\rho}\right)\left(g\cos\psi - F((1-\alpha_L^*)(v_G - v_\infty))\right). \end{aligned} \quad (1.35)$$

Observe that the pseudo mass concentration $\chi$ is a *Riemann invariant* propagating with speed $v_G$. The two other eigenvalues, denoted $\lambda$ and $-\mu$, are given by

$$\lambda(w) = v_G + c_M(w), \quad -\mu(w) = v_G - c_M(w). \quad (1.36)$$

In [37], the flux density matrix and eigenvalues of the original system as posed in [20] (without neglecting higher order terms) are characterized. Since $c_M \gg v_G$, for

high frequencies, the pseudo mass concentration $\chi$ can be considered constant. The pressure wave dynamics (1.33b) with eigenvalues $\lambda$ and $\mu$ can then be considered decoupled from the void fraction wave (1.33a) with eigenvalue $v_G$. Indeed, the flux density matrix associated with the subsystem (1.33b) resembles the isentropic Euler equation which has been studied extensively. The linear coordinate transformation $w \mapsto P(w)[\rho, v_G]^T$ where

$$P(w) := \frac{1}{2}\begin{bmatrix} \frac{c_M(w)}{\rho} & 1 \\ -\frac{c_M(w)}{\rho} & 1 \end{bmatrix} \tag{1.37}$$

with Riemann coordinates $[u, v]^T := P(w)[\rho, v_G]^T$, maps the sub-system (1.33b) into the characteristic form

$$\partial_t \begin{bmatrix} u \\ v \end{bmatrix} + \Lambda(\chi, u, v)\partial_x \begin{bmatrix} u \\ v \end{bmatrix} = \begin{bmatrix} \tilde{S}(\chi, u, v) \\ \tilde{S}(\chi, u, v) \end{bmatrix} \tag{1.38}$$

where $\Lambda(\chi, u, v) := \mathrm{diag}(\lambda(\chi, u, v), -\mu(\chi, u, v))$ and

$$\begin{aligned} \tilde{S}(\chi; u, v) :=& \frac{1}{2} S(V^{-1}(u, v)^T) \\ &- \frac{\bar{\alpha}_0(V^{-1}(u, v)^T)c_M^2(V^{-1}(u, v)^T)}{2\rho}\chi_x. \end{aligned} \tag{1.39}$$

The quasi-linear system (1.38) is often simplified to a semi-linear system. First, note that since $c_M \gg v_G$, $\lambda, \mu \approx c_M^2$ is a reasonable approximation. Second, the sound velocity model (1.34) is derived assuming the liquid is incompressible. This assumption can not be used to model transitions between single to two-phase flows as the pressure is undefined for $\alpha_G = 0$. To model such transitions, [44] proposes to use the switching model

$$\lambda = \mu = \begin{cases} c_L, & \text{if } \alpha_G < \epsilon \\ c_M, & \text{if } \epsilon \leq \alpha_G < 1 - \alpha_L^* \end{cases} \tag{1.40}$$

where $\epsilon > 0$ is a small parameter. The case $\lambda = \mu = c_L$ for $\alpha_G < \epsilon$ follows easily when computing the eigenvalues of (1.25) in the limiting case $\alpha_G \rho_G \ll \alpha_L \rho_L$, which as expected corresponds to the eigenvalues in the corresponding single-phase flow model. Lastly, observing that $c_M^2$ in (1.34) can be written in the form

$$c_M^2 = \frac{1 - \alpha_L^*}{\alpha_G^2} c_G^2 (1 - \chi) \tag{1.41}$$

and that $\alpha_G(s) \approx \alpha_G(\chi, \bar{\rho}, \bar{v}_G)$ where $(\bar{\rho}, \bar{v}_G)$ are the steady state values of $(\rho, v_G)$ for constant $\chi$, we have $\alpha \approx \alpha(\chi)$, so that $c_M \approx c_M(\chi)$ and $\Lambda \approx \Lambda(\chi)$. That is, the quasi-linear system (1.38) can be approximated by the *semi-linear* system

$$\partial_t \begin{bmatrix} u \\ v \end{bmatrix} + \Lambda(\chi)\partial_x \begin{bmatrix} u \\ v \end{bmatrix} = \begin{bmatrix} \tilde{S}(\chi; u, v) \\ \tilde{S}(\chi; u, v) \end{bmatrix} \tag{1.42}$$

where $\chi$ is regarded as an external parameter governed by the separate system (1.33a). The simplification $\chi = const$, which makes the characteristic velocity matrix $\Lambda$ time-invariant, is exploited in Chapter 5 for observer design.

Summarizing, DFM can be analyzed as having two distinct modes: The slowly gas-convection wave governed by (1.33a) with a transport speed $v_G$ in the range of magnitude $1\,\mathrm{m\,s^{-1}}$, and the fast propagating pressure wave governed by the semi-linear, time-varying, system (1.42), which is similar to the $2 \times 2$ system in Section 1.3.1.

### 1.3.3 Finite dimensional models

Lumping the distributed density into a single state by integrating (1.16) with boundary conditions (1.20) over the spatial domain gives the low order lumped mass balance from [75],

$$\dot{p}_p = \frac{\beta_d}{V_d}(q_p - q_{bit}) \tag{1.43}$$

for the drill string, where $V_d = \int_0^L A_d(x)dx$ is the total volume of the drill string, and

$$\dot{p}_c = \frac{\beta_a}{V_a}(q_{bit} - q_c + q_{in}) \tag{1.44}$$

for the annulus, where $V_a = \int_0^L A_a(x)dx$ is the total volume of the annulus. Similarly, the model in [75] also includes a lumping of the momentum balance, obtained by averaging over the spatial domain between two points. In particular, the momentum balance

$$\dot{q}_{bit} = \frac{1}{M}(p_p - p_c - F_d(q_p) - F_a(q_c) - (\rho_a - \rho_d)gh) \tag{1.45}$$

is obtained by averaging flow over the combined drill string – annulus system, with

$$M = \int_0^L \frac{\rho_d(x)}{A_d(x)}dx + \int_0^L \frac{\rho_a(x)}{A_a(x)}dx. \tag{1.46}$$

With constant pump-flow $p_p$ and choke flow $p_c$ given by the choke equation (1.21), the time-constant of the system (1.43)–(1.45) is usually in the range of magnitude 1 min. However, for two-phase systems, as a varying gas fraction $\alpha_G$ propagates through the system, the values of $\beta_a$ will vary and affect the time-constant significantly. In any case, the mode, often called the *compression mode*, usually has a time-constant somewhere between the fast propagating pressure waves and the slower gas-convection wave.

The compression mode is also present in the distributed models presented in Sections 1.3.1 and 1.3.2, where the same time-constant can be identified by studying the dissipative properties of the boundary conditions. As mentioned in Section 1.3.1, for many distributed systems, the only source of instability is through the boundaries and investigating the boundary conditions are important in order to understand the asymptotic behavior of a system. In fact, studying the stability of the ODE model (1.43)–(1.45) obtained through spatial averaging, is structurally similar to studying stability of a distributed system using the notions of stability presented in Section 1.2.4.

### 1.3.4 Reservoir and fault modeling

Darcy's law states a relationship between flow through a porous medium and the pressure differential over the same medium. Originally formulated for water flows, it has later been generalized to fluids with different viscosity and varying density. Assuming constant density, Darcy's law can be stated as

$$q_{in} = \frac{kA}{\mu}\frac{dp}{dr} \tag{1.47}$$

where $\mu$ is the viscosity, $k$ is a constant characterizing the porous medium called the *permeability*, $A$ is the radial area (any area parallel to the formation–well interface area), and $\frac{dp}{dr}$ is the radial pressure differential. Following [36, Section 4.7], assume that the inflow rate $q_{in}$ is constant over a well section with length $h$, then the flow rate over any radial area $A = 2\pi rh$ at the radial distance $r$ from the well–formation interface is also $q_{in}$. Then for any $r$,

$$q_{in} = \frac{2\pi kh}{\mu}\frac{dp}{dr}. \tag{1.48}$$

Separating the variables, integrating between the well radius $r_w$ and any radius $r > r_w$, and defining $p_w = p(r_w)$ gives the solution

$$p(r) - p_w = \frac{q_{in}\mu}{2\pi kh}\ln\frac{r}{r_w}. \tag{1.49}$$

In particular, it is common to consider a *far away* radius $r_e$ where the pressure gradient is zero, and define the formation pressure as $p_{res} = p(r_e)$ [36, Section 4.7]. Then, in steady state, the following linear relationship between the pressure differential $(p_{res} - p_w)$ and the inflow $q_{in}$ holds

$$q_{in} = \frac{2\pi kh}{\mu(\ln\frac{r_e}{r_w} + S)}(p_{res} - p_w), \tag{1.50}$$

where in addition, a so-called *skin factor* $S$ is included. The skin factor models the additional pressure drop due to a partial plugging of the formation caused by loss of drilling mud in overbalanced drilling. The constant coefficient

$$J := \frac{q_{in}}{p_{res} - p_w} = \frac{2\pi kh}{\mu(\ln\frac{r_e}{r_w} + S)} \tag{1.51}$$

is often called the *productivity index* (PI). The constant flow assumption is obviously violated in a kick scenario. As an alternative to the steady state model (1.50), the transient flow can be modeled by the following parabolic PDE [36, Section 5.2]

$$p_t = \frac{k}{r\phi c\mu}\partial_r(r\partial_r p) \tag{1.52}$$

where $c$ is a compressibility constant and $\phi$ a porosity constant. The sol-called *constant terminal rate solution* [36] is obtained by assuming constant flow and a zero pressure gradient infinitely far away (at $r_e = \infty$)

$$q_{in} = \frac{4\pi kh}{\mu}\frac{p_{res} - p_w}{\ln(\frac{4kt}{\gamma\phi\mu cr_w^2}) + 2S} \tag{1.53}$$

where $\gamma$ is the exponent of Euler's constant ($= 1.782...$).

Both the linear, steady state, PI model (1.50) [8, 99, 120] and the transient constant terminal rate solution model (1.53) [90, 114] have been used for reservoir characterization and estimation during drilling. There even exists some results designing observers for the parabolic model (1.52) directly [115].

In this thesis however, due to its simplicity, the linear inflow model $q_{in} = J(p_w - p_{res})$ is used exclusively. Moreover, in an adaptive setting where $J$ is assumed unknown, parameter adaptation on $J$ adds some flexibility and robustness with respect to varying flow regimes. For multi-phase systems with both liquid and gas inflow, a separate PI model is used for each phase. That is,

$$W_{L,res} = J_L \rho_L (p_{res} - p(0,t)) \tag{1.54a}$$
$$W_{G,res} = J_G \rho_G (p_{res} - p(0,t)). \tag{1.54b}$$

The linear inflow model (1.50) can be used to model both spatially distributed inflow, or a single point bottom-hole inflow. In the latter case, the inflow model specifies the bottom-hole boundary conditions. Using Riemann coordinates, the model (1.50) can be written in the form

$$u(0,t) + v(0,t) = k(\theta - v(0)) \tag{1.55}$$

where $k$ is a function of the PI, and $\theta$ is proportional to $p_{res}$. Note that (1.55) can be written in the affine form (1.14a) with $Q_0 = -(1+k)$ and $d = k\theta$. Alternatively, if the bottom-hole pressure $p(0,t)$ is measured, the boundary condition can be written in the form

$$u(0,t) + v(0,t) = k_0(\theta_0 - y_0(t)) \tag{1.56}$$

for some $k_0$ dependent on the PI, $\theta_0$ proportional to $p_{res}$, and $y_0(t)$ proportional to $p(0,t)$. The details can be found in Appendix A.

## 1.4 Sensing, actuation and control objectives

### 1.4.1 Flow and pressure sensing

A pervasive problem in drilling systems is the absence of reliable measurements. The flow into the drill string, provided by the mud pump, is a clean, single-phase fluid with known rheological properties and conventional meters such a mud pump stroke counter, a rotary speed transducer, a magnetic flowmeter, or a Doppler ultrasonic flowmeter can be used [98]. The return flow, on the other hand, is contaminated by rock cuttings and formation fluids. The most common return flow indicator used in conventional drilling is still a simple flow paddle. This, however, is not a direct flow measurement, and can only be considered indicative [28, 29]. Coriolis, electromagnetic and ultrasonic flow meters are also used [80, 91, 94]. Of these, the Coriolis meter is the most accurate and is increasingly being used in both MPD and conventional drilling. The Semi-kidd project (see Section 1.7.1) aims at developing low-cost return flow estimates using an open flow Venturi channel. For kick detection, [91] claims that an accuracy of minimum $3\,\mathrm{L\,s^{-1}}$ in the return flow measurements is necessary.

At the rig-side, both the mud pump pressure (stand pipe pressure) and return-flow pressure (discharge pressure) measurements are fairly accurate, and depending

on the range, can typically provide an accuracy of 1 bar. Bottom-hole, various logging tools collectively referred to as *logging while drilling* (LWD), are embedded into the bottom-hole assembly [41]. While these measurements are fairly accurate, the transmission bandwidth is often insufficient. Traditionally, mud pulse telemetry has been used to transmit LWD data to the rig in real-time. The bandwidth of mud pulse telemetry is typically in the range of $10 - 40$ bit/second, but can drop to as low as 0.5 bit/s in long wells [116]. Either way, it is too low for kick & loss detection. As an alternative, wired pipe technology offers bandwidths up to 1 Mbit/s [7]. However, possibly due to high cost and complexity of deployment, this technology has so far seen limited use. Another interesting application of wired drill-pipe is along-string pressure sensing where pressure sensors are installed at a fixed interval inside the annulus [45]. This application is the topic of Chapter 3.

### 1.4.2 Sensing and actuation in Riemann coordinates

In the flow – pressure models discussed in Section 1.3, there is a clear distinction between measured quantities and controlled quantities: The stand pipe pressure and discharge pressure are measured while the pump flow and choke opening are controlled. If the system is formulated in characteristic form using Riemann coordinates, this distinction becomes less clear. The Riemann coordinates are uniquely related to the physical quantities through a diffeomorphism, but does not represent any physical quantity directly. Instead, the Riemann coordinates are abstractly said to represent unidirectional convecting *information* (see Appendix A). By convention, if all physical quantities at a boundary are either measured or controlled, the signals defining the Riemann coordinates originating at the boundary are called control laws and the Riemann coordinates terminating at the boundary are said to be measured at the boundary. Furthermore, a distinction is made between systems only using sensing at the same boundary as the control law, which is called *collocated* control and sensing, and systems with sensing on the opposite boundary, which is called *non-collocated* sensing and control. Some authors reserve the designation *non-collocated* to systems with sensing and control on opposite boundaries *only*. In this thesis, however, *non-collocated* is used to describe all systems with sensing and control on opposite boundaries, which includes systems with sensing at both boundaries. Control and estimation schemes using only top-side measurements are therefore said to employ collocated sensing and control, while schemes also relying on down-hole pressure measurements are said to employ non-collocated sensing and control.

### 1.4.3 Kick & loss attenuation and actuation

A striking feature of closed loop output-feedback adaptive control schemes is that parameter convergence is often not necessary to achieve output regulation. As such, isolating the estimation problem and studying the parameter and state estimation properties in open-loop rather than in combination with feedback control, does not fully illustrate the utility of the estimation scheme.

Traditionally, kicks are handled by changing the mud density and thereby changing the hydrostatic pressure in the well. Various procedures of circulating out and replacing the mud are in use with generalizing names such as the *driller's method* or *engineer's method* (also called *wait and weight*) (see e.g. [51]). Common to both

methods is that they require a full shut-in of the well and at least one full circulation of drilling fluid. The MPD technology offers an alternative to the traditional time-consuming shut-in methods, often called *dynamic shut-in* [27]. In MPD, the choke opening and back pressure pump can be used to actively manage the top-side return flow, and the bottom-hole pressure can be controlled with an accuracy of up to $\sim 2\,\text{bar}$ [82]. More importantly, MPD is an enabling technology, enabling the use of automated well control systems [50, 85, 92]. Adaptive estimation schemes based on flow and pressure measurements are therefore well suited to be used in a closed loop system with active MPD choke control.

### 1.4.4 Estimation and control objectives

Most of the results included in this thesis are formulated using Riemann coordinates, but the particular form of presentation is selected with the kick & loss application in mind. For example, for single phase system, the objective is often to stabilize the bottom-hole pressure at the reservoir pressure. That is,

$$p(0) \to p_{res}. \tag{1.57}$$

In Riemann coordinates, for the $2 \times 2$ hyperbolic system (1.10) with boundary condition (1.55), this objective can be shown to be equivalent to

$$u(0) + v(0) \to 0 \tag{1.58}$$

or

$$v(0) \to \theta. \tag{1.59}$$

In adaptive output-feedback problems where $(k, \theta)$ and $(u, v)$ are unknown, the estimation problem is typically to design state parameter estimates $(\hat{u}, \hat{v})$ and $(\hat{k}, \hat{\theta})$ such that

$$||u - \hat{u}||, ||v - \hat{v}|| \to 0 \tag{1.60}$$

and

$$\hat{\theta} \to \theta. \tag{1.61}$$

Generally in adaptive control, parameter convergence is only guaranteed if the input data $\psi$ is sufficiently rich. More formally, the parameter estimates converge to their true value if the *persistence of excitation* (PE) condition

$$k_1 I \geq \frac{1}{T} \int_t^{t+T} \psi(\tau)\psi^T(\tau)d\tau \geq k_2 I \tag{1.62}$$

for some positive constants $T, k_1, k_2$, is satisfied for $t > T$. For the specific parametrization (1.55), this condition can be shown to be trivially satisfied if $v(0) \to \theta$. In other words, if the bottom-hole pressure $p(0)$ stabilizes at the reservoir pressure $p_{res}$, then the estimate of the reservoir pressure will converge to the true value. From the structure (1.55), it can also be observed that whenever $v(0) \to \theta$, identifiability of $k$, which models the unknown permeability, is lost. In other words, identification of permeability and simultaneous stabilization of the well are incompatible goals.

## 1.5 Control of distributed systems

Most model-based observer and controller schemes developed for drilling systems are based on finite dimensional lumped models. Moreover, schemes based on PDE models are often derived by first doing a spatial discretization of the PDE, approximating the PDE as a set of ODEs and then applying the rich observer and control toolbox developed for finite dimensional ODE systems. Even schemes derived in a fully distributed sense, must at some point be discretized if they are to be implemented in a computer. It is therefore timely to question the added value of using more complicated schemes based on distributed models. The difference between lumped model and fully distributed models might seem fundamental. At the same time, many of the design and analysis methods developed for finite dimensional systems have intuitive extensions into the domain of infinite dimensional systems, so that the practical utility of schemes based on finite dimensional methods and that of infinite dimensional might be more similar than expected. This section presents an overview of some control design and stability analysis methods for hyperbolic PDEs, and an overview of previous results related to the specific problem of kick and loss estimation in drilling using both distributed and lumped models.

### 1.5.1 Early vs. late lumping

There exist several methods for numerical integration of hyperbolic PDEs. E.g. finite element methods [24, 101, 107], various collocation methods [42, 109], or finite difference schemes: As an example, consider the $2 \times 2$ system (1.10). Let $x_1, ..., x_N$ be uniformly distributed points on $[0, 1]$ such that $x_i - x_{i-1} = \frac{1}{N+1} =: \Delta x$ and let $u_i(t) := u(x_i, t)$, $v_i(t) := v(x_i, t)$ for $i = 1, ..., N$ such that

$$\partial_t u_i + \lambda(x_i)\partial_x u_i = \sigma^+(x_i)v_i \tag{1.63a}$$
$$\partial_t v_i - \mu(x_i)\partial_x v_i = \sigma^-(x_i)u_i. \tag{1.63b}$$

The spatial derivatives can be approximated using various types of finite difference schemes, e.g. the second order *upwind* scheme

$$\partial_x u_i \approx \frac{3u_i - 4u_{i-1} + u_{i-2}}{2\Delta x} \tag{1.64a}$$
$$\partial_x v_i \approx \frac{-3v_i + 4v_{i+1} - v_{i+2}}{2\Delta x}. \tag{1.64b}$$

With linear boundary conditions in the form (1.14), the endpoints are found by extrapolation as

$$u_0(t) = Q_0 v_0(t) + d(t) \tag{1.65}$$
$$\approx Q_0(2v_1(t) - v_2(t)) + d(t) \tag{1.66}$$

and

$$v_{N+1}(t) = R_1 u_{N+1}(t) + U(t) \tag{1.67}$$
$$\approx R_1(2u_N(t) - v_{N-1}(t)) + U(t). \tag{1.68}$$

As a special case, the spatial derivatives closest to the boundary can be approximated using the first order upwind scheme

$$\partial_x u_1 \approx \frac{u_1 - u_0}{\Delta x} \tag{1.69a}$$

$$\partial_x v_N \approx \frac{v_{N+1} - v_N}{\Delta x}. \tag{1.69b}$$

Defining $w = [u_1, ..., u_N, v_1, ..., v_N]$ gives the following set of ODEs on state space form:

$$\dot{w} = Aw + B_1 d(t) + B_2 U(t) \tag{1.70}$$

where

$$A = M \begin{bmatrix} A_1 & Q_0 D_1 + C_1 \\ R_1 D_2 + C_2 & A_2 \end{bmatrix}, \tag{1.71}$$

$$M = \text{diag}(-\lambda(x_1), ..., -\lambda(x_N), \mu(x_1), ..., \mu(x_N)), \tag{1.72}$$

$$A_1 = \frac{1}{2\Delta x} \begin{bmatrix} 2 & 0 & 0 & \cdots & 0 & 0 & 0 \\ -4 & 3 & 0 & \cdots & 0 & 0 & 0 \\ 1 & -4 & 3 & \cdots & 0 & 0 & 0 \\ \vdots & \vdots & \vdots & \ddots & \vdots & \vdots & \vdots \\ 0 & 0 & 0 & \cdots & 1 & -4 & 3 \end{bmatrix}, \tag{1.73}$$

$$A_2 = \frac{1}{2\Delta x} \begin{bmatrix} -3 & 4 & -1 & \cdots & 0 & 0 & 0 \\ \vdots & \vdots & \vdots & \ddots & \vdots & \vdots & \vdots \\ 0 & 0 & 0 & \cdots & -3 & 4 & -1 \\ 0 & 0 & 0 & \cdots & 0 & -3 & 4 \\ 0 & 0 & 0 & \cdots & 0 & 0 & -2 \end{bmatrix}, \tag{1.74}$$

$$D_1 = \frac{1}{2\Delta x} \begin{bmatrix} -4 & 2 & 0 & \cdots & 0 \\ 2 & -1 & 0 & \cdots & 0 \\ \vdots & \vdots & \vdots & \ddots & \vdots \\ 0 & 0 & 0 & \cdots & 0 \end{bmatrix}, \tag{1.75}$$

$$D_2 = \frac{1}{2\Delta x} \begin{bmatrix} 0 & \cdots & 0 & 0 & 0 \\ \vdots & \ddots & \vdots & \vdots & \vdots \\ 0 & \cdots & 0 & 1 & -2 \\ 0 & \cdots & 0 & -2 & 4 \end{bmatrix}, \tag{1.76}$$

$$B_1 = \frac{1}{2\Delta x} M \begin{bmatrix} -2 & 1 & 0 & \cdots & 0 \end{bmatrix}^T, \tag{1.77}$$

$$B_2 = \frac{1}{2\Delta x} M \begin{bmatrix} 0 & \cdots & -1 & 2 \end{bmatrix}^T, \tag{1.78}$$

and

$$C_i = \begin{bmatrix} \sigma^+(x_1) & \cdots & \sigma^+(x_N) \end{bmatrix}^T, i = 1, 2. \tag{1.79}$$

Similar discretization procedures as shown above where a PDE system in the form (1.10) is approximated by the ODE system (1.70)–(1.79) are used in all computer implemented controller or observer schemes. In *early lumping* schemes, the PDE

model is discretized before estimation methods for finite dimensional systems are applied. In the alternative *late-lumping* schemes, the design is carried out for the original distributed model and the system is only discretized before simulation or computer implementation.

An important feature of the PDE model, is the *finite-time* propagation property which is another way of saying that information can not travel infinitely fast. For the ODE model, this feature only holds in the limiting case where $\Delta x \to 0$ (in which case (1.64) holds exactly). An implication of the finite-time propagation property is that without any boundary reflection ($Q_0 = R_1 = 0$) or internal damping ($\sigma^+(x) = \sigma^-(x) = 0$) the PDE model will actually converge in finite time. This property is used extensively in control of PDEs, in particular the infinite-dimensional backstepping method discussed in Section 1.5.3 where internal damping (the source terms) are actively compensated for using boundary control and the PDE system can be controlled in finite-time. Also in adaptive control, where even though the adaptive laws only converge asymptotically, the finite-time propagation property is used extensively to find parametric relationships that hold exactly after some finite initial time. In the ODE approximation (1.70)–(1.79) on the other hand, even without any boundary reflection or internal damping ($C_1 = C_2 = Q_1 = R_1 = 0$) so that the off-diagonal elements in (1.71) are all zero, the system will still include state feedback terms, however small, whenever $\Delta x$ is non-zero.

Note that the lumped model discussed in Section 1.3.3 is the special case $N = 1$ in which no attempt to capture the distributed effects are made. As such, this model only models the boundary effects and the cumulative in-domain sources/sinks.

### 1.5.2 Stability conditions and control Lyapunov functions

To further highlight some stability properties of hyperbolic PDEs, consider as an example the $n + m$ system (1.7) with all source terms identically equal to zero ($\Sigma^{ij} = 0, i, j = \{+, -\}$ for all $x \in [0, 1]$), and linear boundary conditions (1.14). Consider the Lyapunov function

$$V = \int_0^1 \left( \sum_{i=1}^{n} a_i e^{-\delta_1 x} u_i^2(x) dx + \sum_{i=1}^{m} b_i e^{\delta_2 x} v_i^2(x) \right) dx \tag{1.80}$$

for some positive constants $a_i, b_i, \delta_1, \delta_2$. Since,

$$c_1 (\sum_{i=1}^{n} ||u_i||^2 + \sum_{i=1}^{m} ||v||^2) \leq V \leq c_2 (\sum_{i=1}^{n} ||u_i||^2 + \sum_{i=1}^{m} ||v||^2) \tag{1.81}$$

can be shown to hold for some $c_1, c_2 > 0$, the Lyapunov function (1.80) can be used to study stability in the $L_2([0, 1])$ norm. The weights $e^{-\delta_1 x}$ and $e^{\delta_2 x}$ are essential to get a Lyapunov function with a strictly negative derivative, and was first used in [32] for stabilization of the Euler equation.

By lumping the state into a single scalar variable, local stability properties are ignored and similar stability conditions should be expected to hold for the lumped model described in the previous section, including the lowest order model with $N = 1$. Indeed it was shown in [33] that if

$$\inf \left\{ ||\Delta \text{diag}(Q_0, R_1)\Delta^{-1}||_2, \, \Delta \in \mathcal{D}_{n+m}^{+} \right\} < 1 \tag{1.82}$$

where $\mathcal{D}_n^+$ denotes the set of diagonal strictly positive matrices in $\mathbb{R}^{n\times n}$, then $\dot{V} \leq -cV$ for some $c > 0$. In other words, as pointed out in [18, Section 3.1.1.], the stability condition is independent of the system dynamics (1.7). To further highlight this point, [18] suggest to view (1.7) and (1.14) as two interconnected systems where the former has unit gain (if the source terms are identically equal to zero), and the latter has gain given by (the left hand side of) (1.82).

### 1.5.3 Infinite dimensional backstepping

The idea behind (infinite-dimensional) backstepping is to *shift* the gain of the input-output system (1.7) to the input-output system (1.14) where it easier can be handled [78]. This technique is particularly useful for systems with either boundary sensing or boundary control. For observers, the necessary in-domain damping needed to ensure stability is first identified. Using a backstepping transformation, this necessary *in-domain* damping can be represented as the equivalent necessary *boundary* damping. Since the boundary is measured, the boundary condition can be specified so that this necessary boundary damping is achieved. Equivalently, for boundary control, for any unwanted *in-domain* source terms, the necessary *boundary* damping needed to cancel these terms can be identified using a backstepping transformation. The boundary control signal can then be used to provide this level of boundary damping.

As an example, in [35, 111] it was shown that the backstepping transformation

$$\alpha(x,t) = u(x,t) - \int_0^x K^{uu}(x,\xi)u(\xi,t)d\xi - \int_0^x K^{uv}(x,\xi)v(\xi,t)d\xi \tag{1.83a}$$

$$\beta(x,t) = v(x,t) - \int_0^x K^{vu}(x,\xi)u(\xi,t)d\xi - \int_0^x K^{vv}(x,\xi)v(\xi,t)d\xi \tag{1.83b}$$

where the kernels $K^{uu}, K^{uv}, K^{vu}, K^{vv} : \{(x,\xi) : 0 \leq \xi \leq x \leq 1\} \to \mathbb{R}$ are the solution to a well-posed $4\times 4$ hyperbolic system (see [35] or Paper [68] included in Section 4.3), maps the $2\times 2$ system (1.10) with boundary conditions (1.14) (for the special case $d = 0$ and $R_1 = 1$) into the system

$$\alpha_t + \lambda(x)\alpha_x = 0 \tag{1.84a}$$

$$\beta_t - \mu(x)\beta_x = 0 \tag{1.84b}$$

with boundary conditions

$$\alpha(0,t) = Q_0\beta(0,t) \tag{1.85a}$$

$$\beta(1,t) = R_1u(1,t) + U(t) - \int_0^1 K^{vu}(1,\xi)u(\xi,t)d\xi - \int_0^1 K^{vv}(1,\xi)v(\xi,t)d\xi. \tag{1.85b}$$

As discussed in the previous section, (1.84) has unit gain, and the potentially problematic source terms are now included in the input-output system (1.85). The system can now be formulated as a difference equation for $\beta(1,t)$ and stability

conditions in terms of $\lambda, \mu, c_1, c_2, Q_0, R_1$ can be formulated by studying the characteristic equation associated with the resulting difference equation [14, 97]. More importantly, using boundary control, the boundary terms can be canceled by selecting

$$U(t) = \int_0^1 K^{vu}(1,\xi)u(\xi,t)d\xi - \int_0^1 K^{vv}(1,\xi)v(\xi,t)d\xi - R_1 u(1,t). \tag{1.86}$$

As a side note, in [13] it was shown that preserving some boundary reflection might be preferable in certain situations in order to provide some robustness to actuation and sensing delays, i.e. selecting $U(t)$ such that

$$\beta(1,t) = \bar{R}_1 \beta(1,t). \tag{1.87}$$

for some $\bar{R}_1$ such that $|Q_0 \bar{R}_1| \leq 1$.

The idea of using Volterra integral transformation to study observability and stabilization properties of PDEs dates back to at least the 1970's [31, 95]. In [31] the method was referred to as *the method of integral operators*. The name *infinite-dimensional backstepping* came into use in the 1990's when the recursive backstepping method for finite dimensional ODE systems was extended to PDEs [16, 25, 81, 103, 104]. The method of infinite-dimensional backstepping was first used to stabilize a first-order hyperbolic PDE in [77] and has later been extended to linear $2 \times 2$ systems [111], $n+1$ system [40] and general $n+m$ systems [70]. The method has also been used to (locally) stabilize quasi-linear systems [35, 71]. Infinite-dimensional backstepping is especially well suited for adaptive control. The topic of adaptive control of hyperbolic PDE using infinite-dimensional backstepping has been studied extensively in [10].

## 1.6 Previous results on model-based kick & loss estimation

Early examples of model-based in-/out-flux estimation include problems studied in the framework of pipeline leak detection and estimation which are modeled using the water-hammer equations (1.16). Most examples are based on some form of early lumping. In [22, 23, 76, 100], various finite difference schemes are used, while [109, 110] use collocation methods. Using the lumped models, leak size and location can be estimated using Kalman filters [22, 76, 109, 110], special correlation methods [19] or Lyapunov-based non-linear observers [100]. As an alternative to the early lumping approaches, a late-lumping approach is presented in [2] where boundary output injection is used to design observers estimating the distributed pipe-flow, and adaptive laws are used to estimate the leak size and location.

In contrast to pipe-flow leak problems, where the leak is either assumed constant or governed by some choke equation with known external pressure (atmospheric), in- and out-flows in drilling systems depend on both the well dynamics and the reservoir dynamics. As discussed in Section 1.3.4, the well-reservoir relationships are complicated and even estimation schemes based on the simple linear PI model (1.50) with only two unknown parameters (or $n+1$ parameters for systems with $n$-phases), will require some level of excitation to achieve parameter convergence. If,

however, the in- or out-flow can be assumed constant, the well-reservoir dynamics can be ignored. In [53], the low order lumped model described in Section 1.3.3 (from [75]) is used to estimate and locate unknown constant inflow rates using an adaptive observer. The same model is used in [118, 119] to detect, isolate and locate various drilling faults, such as in- or out-fluxes, using a set of adaptive observers and distributed pressure measurements. Yet another low order lumped model for percolating gas is used in [55] for gas kick estimation and localization using an unscented Kalman filter. The first results on using late-lumping infinite-dimensional backstepping for inflow estimation was presented in [1, 54] where the inflow is modeled as a constant additive term appearing in the boundary condition of the single phase model (1.16).

An adaptive observer for flow estimation assuming constant inflow was also presented in [121]. However, the main contribution of this paper is a closed loop kick estimation and mitigation scheme. It was shown that in a closed loop setting where $p_{bit} \to p_{res}$, pore pressure estimation is also possible using the linear PI model (1.50). The necessary excitation is here achieved by attenuating the kick. In [112, 113, 114], the inflow is modeled by the transient reservoir model (1.53). The drift-flux model is then approximated by a lumped model and both pore pressure and permeability are estimated using non-linear least squares estimation in [112, 114] and ensemble Kalman filters in [113, 114]. Forced excitation of the well is however needed for parameter convergence. Various other schemes based on early lumping approximations of the drift-flux models using Kalman filters for reservoir characterization are also presented in [6, 52, 86] . Even low order lumped models have been used for reservoir characterization. In [89], reservoir permeability estimation schemes using extended, unscented and ensemble Kalman filters are compared. Permeability estimation using a moving horizon estimation scheme is presented in [87], and using a non-linear adaptive observer is presented in [88], both using low order lumped models. In [8], the pore pressure and permeability are estimated using a recursive least squares estimation scheme for the reduced drift-flux model and early lumping scheme presented in [3]. In a result similar to the adaptive backstepping observer in [1], an adaptive observer based on the method of infinite-dimensional backstepping is used in [39] to estimate the pore pressure, which is formulated as an unknown additive term in the boundary condition of a linearized version of the drift-flux model.

## 1.7 Contributions

### 1.7.1 The Semi-Kidd project

This PhD study is part of the *Semi-Kidd* project (Sensors and models for improved Kick/loss detection in drilling), which is funded by the Research Council of Norway and Equinor ASA (project no. 255348/E30). The primary objective of the project is to

> "enable cost-effective and automatic kick/loss detection by developing new knowledge on model-based estimation and utilization of new sensor technology for drilling operations".

The central idea of the project is to use an open Venturi channel to measure the

return flow rates in real-time [72, 117]. This, as an *easy-to-implement* alternative to the still commonly used flow paddle and possibly also as an alternative to existing flow meters such as Coriolis, electromagnetic or ultrasonic flow meters [21, 30]. Information about the return flow rate obtained from the Venturi channel can be used both for early kick & loss detection and as input to a kick & loss estimation algorithm.

The project is divided into 4 research tasks. In the first research task [117], a model of the flow rate and fluid level in the Venturi channel with cuttings transport effects is developed and simulated. In the second research task [72], a real-time, model-based estimator for the flow rate of the return flow is developed. This thesis is the product of the third research task, which aims at developing new model-based kick & loss estimation schemes. Data fusion of new and existing sensors for flow estimation is the topic of the fourth research task [74].

From the perspective of research task 3, research task 1, 2 and 4 will provide reliable return flow estimates as input to research task 3. This relationship is depicted in Figure 1.3.

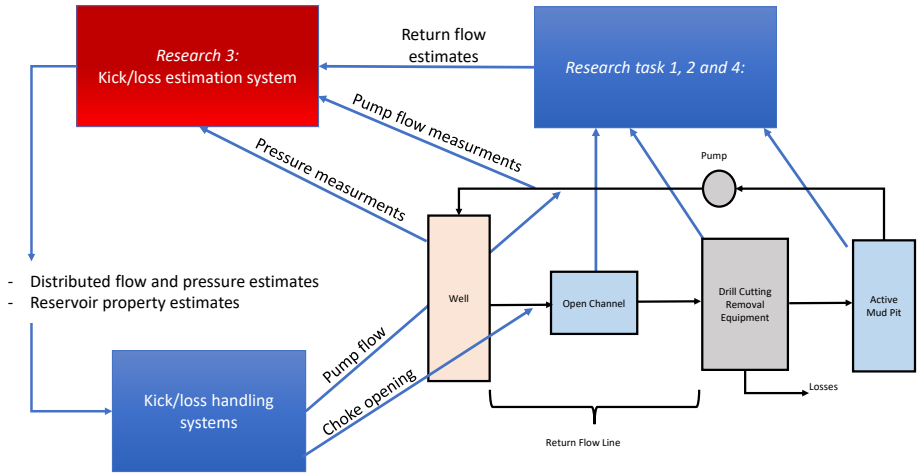


**Figure 1.3:** Schematic overview of the Semi-Kidd research tasks from the perspective of research task 3. Modified from [72].

### 1.7.2 Scope and Outline

In naturally fractured reservoirs, the reservoir can act as a buffer-tank for drilling mud: For increasing well pressures, drilling mud flows into the reservoir, filling up the reservoir buffer-tank. If the pressure is reduced, drilling fluid will flow back into the well. This effect, called *breathing* or *ballooning* [56, 83], is often misinterpreted as a kick. Another effect often misinterpreted as a kick is the change in pressure and temperature in high pressure, high temperature wells, caused by starting or stopping the circulation [15]. Characterizing all such effects will require a large set

of different models. Alternatively, an attempt to incorporate all possible effects in any single model will yield a high order model too complicated to be useful in any real-time estimation or control scheme. Furthermore, measurements corrupted by noise and un-modeled dynamics makes the model output uncertain. The problem of kick detection is consequently a statistical problem, where competing explanatory models should be weighted against each other based on uncertain observed and estimated data.

Early kick detection and key performance indicators for kick detection and handling are discussed in [46]. The following two key performance indicators (KPIs) are proposed.

1. Kick Detection Volume: How much of an influx occurs before it is positively identified as a kick?

2. Kick Response Time: Once a kick has been positively identified, how much time elapses before well control procedures have stopped the influx from progressing?

The first KPI is related to the kick detection problem and the second KPI is related to the kick handling problem. Somewhere in between is the kick *estimation* problem. Kick & loss *estimation* is a different problem downstream the kick & loss detection problem. That is, kick & loss estimation schemes answer question about size, location and type, *given* that a kick is detected. Although not directly affecting the first KPI proposed in [46], the second KPI is improved by providing faster and more accurate decision support data to the kick & handling systems (see Figure 1.3).

A final word of caution: The output of a kick (or loss) detection system is binary; a kick is detected or not detected. Although the model-based estimation schemes presented in this thesis might be useful in a larger kick detection system to confirm the presence of a kick, using any of the schemes on a stand-alone basis to answer the binary kick detection question is a logical fallacy. The kick & loss *estimates* provided by the schemes in this thesis will only be reliable *after* all other possible causes are eliminated.

This thesis has the following structure.

- **Chapter 2** presents state and parameter estimation schemes for kick & loss estimation. The observers are derived using infinite-dimensional backstepping and boundary sensing only.

- The schemes in **Chapter 3** utilize distributed pressure measurements for in-domain *fault* estimation and localization. A wide range of drilling faults, including in- and out-flows, can be modeled by the proposed design.

- Closed loop kick & loss attenuation schemes are presented in **Chapter 4**. As discussed in Section 1.4.3, some properties of adaptive observer systems are not well illustrated in open-loop estimation schemes. The closed loop attenuation schemes presented here are direct extensions of the estimation schemes in Chapter 2.

- **Chapter 5** investigates gas kick estimation in over-balanced drilling, using the modeling assumption that the well dynamics prior to a gas kick, and some time after, can be approximated by a single-phase model.

Some of the papers are purely theoretical with no mentioning of the kick & loss problem. Yet, the motivation for studying each theoretical problem is clear. An introduction to each paper and the relevance to the kick & loss problem is provided in the introduction to each chapter. Each chapter is concluded by a section discussing various limitations and flaws in the proposed designs the authors have been made aware of after submission or publication.

### 1.7.3 List of publications

**Journal papers**

- Holta, H., Anfinsen, H., and Aamo, O. M. (2020a). Adaptive set-point regulation of linear $2 \times 2$ hyperbolic systems with application to the kick and loss problem in drilling. *Automatica*, 119:109078 (Section 4.3)
- Holta, H. and Aamo, O. M. (2019c). Observer design for a class of semi-linear hyperbolic PDEs with distributed sensing and parametric uncertainties. *Under review, IEEE Transactions on Automatic Control, submitted September 2019* (Section 3.3)
- Holta, H. and Aamo, O. M. (2020c). Exploiting wired-pipe technology in an adaptive observer for drilling incident detection and estimation. *Under review, SPE Journal, submitted January 2020* (Section 3.5)
- Holta, H. and Aamo, O. M. (2020b). Adaptive set-point regulation of linear n+1 hyperbolic systems with uncertain affine boundary condition using collocated sensing and control. *Under review, Systems & Control Letters, submitted January 2020* (Section 4.4)
- Holta, H., Anfinsen, H., and Aamo, O. M. (2020b). Observer design for a two-time-scale quasi-linear system. *Unpublished* (Section 5.3)

**Conference papers**

- Holta, H., Anfinsen, H., and Aamo, O. M. (2018). Improved kick and loss detection and attenuation in managed pressure drilling by utilizing wired drill pipe. *In Proceedings of the 3rd IFAC Workshop on Automatic Control in Offshore Oil and Gas Production (OOGP)*, 51(8):44–49 (Section 2.2)
- Holta, H. and Aamo, O. M. (2018). Boundary set-point regulation of a linear $2 \times 2$ hyperbolic PDE with uncertain bilinear boundary condition. In *Proceedings of the 2018 IEEE Conference on Decision and Control (CDC)*, pages 2156–2163. IEEE (Section 4.2)
- Holta, H. and Aamo, O. M. (2019a). An adaptive observer design for $2 \times 2$ semi-linear hyberbolic systems using distributed sensing. In *Proceedings of the 2019 American Control Conference (ACC)*, pages 2540–2545 (Section 3.2)
- Holta, H. and Aamo, O. M. (2019b). A least-squares scheme utilizing fast propagating shock waves for early kick estimation in drilling. In *Proceedings of the 2019 IEEE Conference on Control Technology and Applications (CCTA)*, pages 1081–1086 (Section 5.2)

- Holta, H. and Aamo, O. M. (2020a). Adaptive observer design for an n+1 hyperbolic PDE with uncertainty and sensing on opposite ends. In *Proceedings of the 2020 European Control Conference (ECC)*, pages 1159–1164 (Section 2.3)

- Holta, H. and Aamo, O. M. (2020d). A heuristic observer design for an uncertain hyperbolic PDE using distributed sensing. In *Proceedings of the IFAC world congress 2020* (Section 3.4)

**Publications not included in this thesis** The following list of publications includes work conducted during the time-span of this project, but that are outside the scope of this thesis.

- Holta, H., Anfinsen, H., and Aamo, O. M. (2017a). Adaptive set-point regulation of linear $2 \times 2$ hyperbolic systems with uncertain affine boundary condition using collocated sensing and control. In *Proceedings of the 2017 Asian Control Conference (ASCC)*, pages 2766–2771

- Holta, H., Anfinsen, H., and Aamo, O. M. (2017b). Estimation of an uncertain bilinear boundary condition in linear $2\times2$ hyperbolic systems with application to drilling. In *Proceedings of the 17th International Conference on Control, Automation, and Systems (ICCAS)*, pages 188–193

- Anfinsen, H., Holta, H., and Aamo, O. M. (2020b). Adaptive control of a scalar 1-D linear hyperbolic PDE with an uncertain transport speed using boundary sensing. In *Proceedings of the 2020 American Control Conference (ACC)*

- Anfinsen, H., Holta, H., and Aamo, O. M. (2020a). Adaptive control of a linear hyperbolic PDE with an uncertain transport speed and a spatially varying coefficient. In *Proceedings of the 28th Mediterranean Conference on Control and Automation (MED)*

- Jinasena, A., Holta, H., Jondahl, M. H., Welahettige, P., Sharma, R., Aamo, O. M., and Lie, B. (2020). Model based early kick/loss detection and attenuation in managed pressure drilling with topside sensing using a Venturi flowmeter. *Submitted to the 61st International Conference of Scandinavian Simulation Society, SIMS*

# CHAPTER 2

# Kick & loss estimation using boundary sensing

## 2.1 Introduction

In the first paper [67], an adaptive observer derived using infinite-dimensional backstepping and a set of swapping filters is used to estimate the distributed pressure and flow in the annulus and bottom-hole unknown parameters. The bottom-hole pressure is assumed measured using wired drill-pipe. The bottom-hole reservoir inflow is modeled using the linear PI model (1.50) where both parameters are assumed unknown.

In the second paper [61], the results from [67] are extended in two directions. First, measurements are assumed to be only taken at one boundary (top-side), anti-collocated with the uncertain parameters. Second, the design is extended to any linear $n + 1$ system. The analysis is carried out using Riemann coordinates. Possible applications include under-balanced drilling where the drift-flux model is linearized around a constant draw-down pressure.

## 2.2 Paper [67]: *Improved kick and loss detection and attenuation in managed pressure drilling by utilizing wired drill pipe*

Holta, H., Anfinsen, H., and Aamo, O. M. (2018). Improved kick and loss detection and attenuation in managed pressure drilling by utilizing wired drill pipe. *In Proceedings of the 3rd IFAC Workshop on Automatic Control in Offshore Oil and Gas Production (OOGP)*, 51(8):44–49

Available online at www.sciencedirect.com

ScienceDirect

IFAC PapersOnLine 51-8 (2018) 44–49

IFAC Papers Online CONFERENCE PAPER ARCHIVE

# Improved Kick and Loss Detection and Attenuation in Managed Pressure Drilling by Utilizing Wired Drill Pipe

**Haavard Holta** * **Henrik Anfinsen** * **Ole Morten Aamo** *

* *Department of Engineering Cybernetics. Norwegian University of Science and Technology, Trondheim N-7034, Norway (e-mail: haavard.holta@ntnu.no; henrik.anfinsen@ntnu.no; aamo@ntnu.no).*

**Abstract:** A model based method for kick and loss detection and attenuation in Managed Pressure Drilling is presented. The drilling system is modeled as a distributed parameter system combined with a reservoir flow equation containing reservoir pressure and the so-called productivity index as uncertain parameters. A swapping-based design for state and parameter estimation utilizing bottom-hole pressure measurements available via wired drill pipe is combined with a closed loop controller for kick and loss attenuation. The performance of the proposed method is compared to earlier results on kick attenuation in a simulation, showing significant improvement.



*Keywords:* Distributed-parameter systems, adaptive control, parameter estimation, managed pressure drilling, kick detection

## 1. INTRODUCTION

### 1.1 Problem Statement

In order to carry cuttings to the surface and maintain an appropriate pressure barrier down-hole during drilling, a drilling mud is circulated down the drill string, through the drill bit and up in a casing surrounding the drill string (see Figure 1). In cases where pressure margins are tight, a control choke and a back pressure pump are installed at the top side end of the annulus so that pressure can be controlled quickly and precisely. The method utilizing this equipment is referred to as managed pressure drilling (MPD) with applied back pressure (ABP). To model the flow dynamics in the annulus, the following model from Landet et al. (2013) is used

$$p_t(z,t) = -\frac{\beta}{A_1} q_z(z,t) \tag{1a}$$

$$q_t(z,t) = -\frac{A_1}{\rho} p_z(z,t) - \frac{F_1}{\rho} q(z,t) - A_1 g \tag{1b}$$

where $z \in [0, l]$ and $t \geq 0$ are the independent variables of space and time respectively, $l$ is the well depth, $p(z,t)$ is pressure, $q(z,t)$ is volumetric flow, $\rho$ is the density of the mud, $\beta$ is the bulk modulus of the mud, $F_1$ is the friction factor, $A_1$ is the cross sectional area of the annulus and $g$ is the acceleration of gravity.

When drilling into an oil reservoir, the bottom-hole end of the drill-string is exposed to the reservoir pressure. If the reservoir pressure is higher than the bottom-hole pressure in the annulus, the result is a net inflow of formation fluids into the annulus. This situation is called a *kick*. Similarly, a *loss* is a net outflow of drilling-mud into the reservoir caused by a higher bottom-hole mud pressure in the annulus than formation pressure. To model this relationship, a simple *productivity-based-inflow* model is used. Together with the top-side actuation signal $p_l(t)$, this gives the boundary conditions

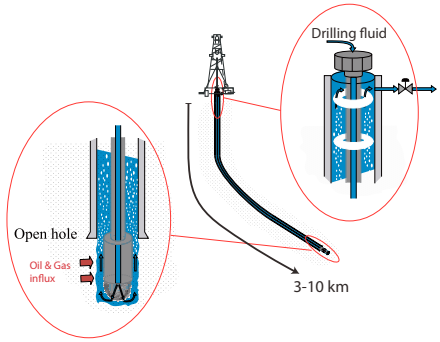


Fig. 1. Schematic of the drilling system. Courtesy of Ulf Jakob Aarsnes (Aarsnes et al. (2016b)).

$$q(0,t) = J\left(p_r - p(0,t)\right) + q_{bit} \tag{2a}$$

$$p(l,t) = p_l(t) \tag{2b}$$

where $J > 0$ is called the productivity index and is assumed unknown, $p_r$ is the unknown reservoir pressure, and $q_{bit}$ the known flow through the drill bit. It is assumed that $p_r$ satisfies $0 < p_r \leq \bar{p}_r$ where $\bar{p}_r$ is some known upper bound for the reservoir pressure. Moreover, it is assumed that the choke controller has significantly faster dynamics than the rest of the system so that the actuation dynamics can be ignored and the top-side pressure $p_l$ regarded as a control input. The design utilizes both bottom-hole pressure measurements $p(0,t)$, which are assumed available in real time when using a wired drill pipe, and the top-side flow $q(l,t)$.

The design goal is to keep the bottom-hole pressure equal to the unknown reservoir pressure, that is $p(0,t) = p_r$ such that flow


10.1016/j.ifacol.2018.06.353

from the reservoir into the drill string is zero. This implies that the flow through the annulus is equal to the drill bit flow.

### 1.2 Previous Work

Control of coupled distributed systems like (1) and (3) can be achieved by using the method of *infinite-dimensional backstepping* for PDEs. This method was first introduced for parabolic PDEs in Liu (2003); Smyshlyaev and Krstic (2004, 2005), where the gain kernel was expressed as a solution to a well-posed PDE. The first result for hyperbolic PDEs was in Krstic and Smyshlyaev (2008) for first order systems, for second order hyperbolic systems in Smyshlyaev et al. (2010), and to two coupled first order hyperbolic systems in Vazquez et al. (2011). The results in the latter were used in Aamo (2013) for disturbance attenuation in managed pressure drilling which has similarities to the problem considered in this paper.

Results on adaptive control for parabolic PDEs can be found in Smyshlyaev and Krstic (2010). Adaptive observers for $n+1$ hyperbolic systems using sensing collocated with the uncertain boundary parameters can be found in Anfinsen et al. (2016) using swapping filters, and in Bin and Di Meglio (2017) using a Lyapunov approach. The extension to general $m+n$ systems is given in Anfinsen et al. (2017). The extension to stabilization, without additive boundary parameter and sensing at the left boundary restricted to the form $y_0(t) = v(0,t)$, is given in Anfinsen and Aamo (2017c) ($n+1$ case) and Anfinsen and Aamo (2017b) ($m+n$ case). An adaptive observer for $n+1$ systems with a multiplicative boundary condition is developed in Di Meglio et al. (2014) and for $2\times 2$ systems with an affine boundary condition in Anfinsen and Aamo (2016). Adaptive stabilization of the same type of systems, but without the additive parameter is considered in Anfinsen and Aamo (2017a) and with only the additive parameter unknown in Aamo (2013).

Kick attenuation in MPD has mainly been studied in the context of lumped drilling models. A lumped ODE model is applied to a gas kick detection and mitigation problem in Zhou et al. (2011) by using a method for switched control of the bottom-hole pressure. Another lumped model for estimation and control of in-/outflux is presented in Hauge et al. (2012). Kick handling methods for a first-order approximation to the PDE system is presented in Aarsnes et al. (2016a) using LMI (Linear Matrix Inequality) based controller design. An infinite-dimensional observer for kick & loss detection is presented in Hauge et al. (2013). Another observer for state and reservoir pressure estimation in under-balanced drilling is given in Di Meglio et al. (2014). In Holta et al. (2018, 2017), a distributed PDE model is combined with a model of the reservoir inflow relation (given in Equation 2a). Kick & loss detection with sensing non-collocated with control is studied in Holta et al. (2017), while a method for kick & loss attenuation for the same system is presented in Holta et al. (2018).

### 1.3 Contributions and Paper Structure

This paper considers both kick/loss detection and attenuation. The main contribution of this paper is an improved version of the parameter estimation scheme presented in Holta et al. (2018), better utilizing the bottom-hole pressure measurement. The estimation scheme presented in this paper is combined with the closed loop controller derived in Holta et al. (2018) and applied to the kick & loss application. In Section 2, the main results from Holta et al. (2018) are included for completeness. Section 3 presents the improved estimation scheme. In Section 4 the estimator from Section 3 is combined with the control law from Holta et al. (2018) and applied to the kick & loss problem in MPD where the performance of the new estimation scheme is compared to results from Holta et al. (2018) in a simulation.

### 1.4 Mapping to Riemann Invariants

To ease the design process, as well as generalize the control problem, it can be shown that system (1) with boundary conditions (2) can be transformed, through a suitable coordinate transformation (see Holta et al. (2018)), to an equivalent system written in terms of Riemann invariants as

$$u_t(x,t) + \lambda u_x(x,t) = c_1(x)v(x,t) \tag{3a}$$
$$v_t(x,t) - \mu v_x(x,t) = c_2(x)u(x,t) \tag{3b}$$
$$u(0,t) = rv(0,t) + k(\theta - y_0(t)) \tag{3c}$$
$$v(1,t) = U(t) \tag{3d}$$

defined for $x\in[0,1]$, $t\geq 0$, where $u, v$ are the system states, $U(t)$ is the control input, $\lambda,\mu>0$ and $c_1(x), c_2(x)\in C([0,1])$ are known, while $k\in\mathbb{R}$ and $\theta\in\mathbb{R}$ are unknown boundary parameters, but where $\text{sign}(k)$ is known. The measurement collocated with actuation is given by

$$y_1(t) = u(1,t) \tag{4}$$

while the measurement anti-collocated with actuation is generated as a linear combination of the system states. That is,

$$y_0(t) = a_0u(0,t) + b_0v(0,t) \tag{5}$$

with $a_0\neq 0$. The objective is generalized to stabilization in the $L_2$-sense and boundedness uniformly and point-wise in $x$. In addition, based on the design goal $p(0,t) = p_r(t)$, we select the weaker control objective

$$\lim_{t\to\infty}\int_t^{t+T} |rv(0,\tau) - u(0,\tau)|\, d\tau = 0 \tag{6}$$

for

$$r \neq -\frac{b_0}{a_0} \tag{7}$$

and for some arbitrary $T>0$. Furthermore, it is assumed that the initial conditions $u(x,0) = u_0(x)$, $v(x,0) = v_0(x)$ satisfy $u_0,\ v_0\in L_2([0,1])$.

## 2. ESTIMATION AND CONTROL WITH ADAPTATION BASED ON TOP-SIDE SENSING (OLD METHOD)

The main results on state and parameter estimation from Holta et al. (2017) are given in Section 2.1 and Theorem 1 in particular. Section 2.2 presents the main results from Holta et al. (2018) with the control law given formally in Theorem 2.

### 2.1 State and Parameter Estimation

In Holta et al. (2017), a swapping based design is used to generate on-line state and parameter estimates. The same swapping filters will be used in this paper. The filters are given by

$$a_t(x,t) + \lambda a_x(x,t) = c_1(x)b(x,t) + P_1(x)(y_1(t) - a(1,t)) \tag{8a}$$
$$b_t(x,t) - \mu b_x(x,t) = c_2(x)a(x,t) + P_2(x)(y_1(t) - a(1,t)) \tag{8b}$$
$$a(0,t) = rb(0,t) \tag{8c}$$
$$b(1,t) = U(t) \tag{8d}$$

and parameter filters

$$m_t(x,t)+\lambda m_x(x,t) = c_1(x)n(x,t) - P_1(x)m(1,t) \quad (9a)$$
$$n_t(x,t)-\mu n_x(x,t) = c_2(x)m(x,t) - P_2(x)m(1,t) \quad (9b)$$
$$m(0) = rn(0,t)+1 \quad (9c)$$
$$n(1) = 0 \quad (9d)$$

and

$$w_t(x,t)+\lambda w_x(x,t) = c_1(x)z(x,t) - P_1(x)w(1,t) \quad (10a)$$
$$z_t(x,t)-\mu z_x(x,t) = c_2(x)w(x,t) - P_2(x)w(1,t) \quad (10b)$$
$$w(0,t) = rz(0,t) - y_0(t) \quad (10c)$$
$$z(1,t) = 0 \quad (10d)$$

where $P_1, P_2$ are gains to be designed. The input filters model how the control signal $U(t)$ affect the system states $u, v$, while the parameter filters model the effect of the boundary parameters $k$ and $\theta$ on the system states.

Using the swapping filters, the following static relationship between the system states $(u, v)$ and unknown parameters $k$ and $\theta$ can be found

$$u(x,t) = a(x,t) + k\left(\theta m(x,t) + w(x,t)\right) + e(x,t) \quad (11a)$$
$$v(x,t) = b(x,t) + k\left(\theta n(x,t) + z(x,t)\right) + \epsilon(x,t) \quad (11b)$$

where $e, \epsilon$ represent the *non-adaptive* estimation error. It is shown in Holta et al. (2017) that if the gains $P_1, P_2$ are selected as

$$P_1(x) = \lambda P^{uu}(x,1) \quad (12a)$$
$$P_2(x) = \lambda P^{vu}(x,1), \quad (12b)$$

where $(P^{uu}, P^{vu})$ is the solution to

$$\lambda P^{uu}_x(x,\xi) + \lambda P^{uu}_\xi(x,\xi) = c_1(x)P^{vu}(x,\xi) \quad (13a)$$
$$\mu P^{vu}_x(x,\xi) - \lambda P^{vu}_\xi(x,\xi) = -c_2(x)P^{uu}(x,\xi) \quad (13b)$$
$$P^{vu}(x,x)\lambda + P^{vu}(x,x)\mu = c_2(x) \quad (13c)$$
$$P^{uu}(0,\xi) = rP^{vu}(0,\xi) \quad (13d)$$

defined over $\mathcal{T}_1 = \{(x,\xi)\,|\,0 \le x \le \xi \le 1\}$, then the error terms $e, \epsilon$ will tend to zero in a finite time given by

$$t_F = \frac{1}{\lambda} + \frac{1}{\mu}. \quad (14)$$

It is shown in Coron et al. (2013) that the system (13) has a continuous, bounded and unique solution $(P^{uu}, P^{vu})$.

Motivated by the bilinear form of the static relationship (11), the following *adaptive* state estimates are generated:

$$\hat{u}(x,t) = a(x,t) + \hat{k}(t)\left(\hat{\theta}(t)m(x,t) + w(x,t)\right) = u(x,t) - \hat{e}(x,t) \quad (15a)$$
$$\hat{v}(x,t) = b(x,t) + \hat{k}(t)\left(\hat{\theta}(t)n(x,t) + z(x,t)\right) = v(x,t) - \hat{\epsilon}(x,t) \quad (15b)$$

where $\hat{e}, \hat{\epsilon}$ represent the *adaptive* estimation error, and $\hat{\theta}$ and $\hat{k}$ are estimates of $\theta$ and $k$, respectively.

Evaluating (15a) at $x = 1$, inserting (4) and rearranging then give

$$\hat{e}(1,t) = y_1(t) - a(1,t) - \hat{k}(t)\left(\hat{\theta}(t)m(1,t) + w(1,t)\right). \quad (16)$$

Assuming the sign of $k$ is known, the *gradient method for bilinear parametric models* in Ioannou and Sun (2012, Theorem 4.52) can be used to minimize a cost function based on the square error $\hat{e}^2(1,t)$ and thereby forming an adaptive law for the parameter estimates $\hat{\theta}, \hat{k}$. The following theorem presents the main results from Ioannou and Sun (2012, Theorem 4.52) together with some additional properties needed to prove stability of the closed loop system.

*Theorem 1.* Consider the adaptive laws

$$\dot{\hat{\theta}}(t) = \gamma_1 \text{sign}(k)\frac{\hat{e}(1,t)}{1+w^2(1,t)}m(1,t) \quad (17a)$$
$$\dot{\hat{k}}(t) = \gamma_2\left[\hat{\theta}(t)m(1,t) + w(1,t)\right]\frac{\hat{e}(1,t)}{1+w^2(1,t)} \quad (17b)$$

for $t \ge t_F$ and $\dot{\hat{\theta}}(t) = \dot{\hat{k}}(t) = 0$ for $t < t_F$, where $\gamma_1, \gamma_2 > 0$ are the adaptation gains, $m(1,t)$ and $w(1,t)$ are the filters given in (9) and (10), $\hat{e}(1,t)$ is the adaptive estimation error in (16) and $t_F$ is defined in (14). Suppose system (3) has a unique solution $u, v$ for all $t \ge 0$. Then, the adaptive laws (17) have the following properties:

(1) $\hat{\theta}, \hat{k}, \in \mathcal{L}_\infty$.
(2) $\dot{\hat{\theta}}, \dot{\hat{k}}, \in \mathcal{L}_\infty \cap \mathcal{L}_2$.
(3) $\hat{\theta}(t) \to \hat{\theta}(t - d_\beta)$ and $\hat{k}(t) \to \hat{k}(t - d_\beta)$.
(4) $\frac{\tilde{k}(\theta - y_0) + \hat{k}\tilde{\theta}}{\sqrt{1+w^2(1,\cdot)}} \in \mathcal{L}_2$ where $\tilde{\theta} = \theta - \hat{\theta}$ and $\tilde{k} = k - \hat{k}$.
(5) If $w(1,\cdot) \in \mathcal{L}_\infty$ and $\hat{\theta}m(1,\cdot) + w(1,\cdot) \in \mathcal{L}_2$, then $\hat{\theta}$ converges to $\theta$ and $\hat{k}$ converges to some constant.

**Proof.** See Holta et al. (2017).

### 2.2 Closed Loop Adaptive Control

The control law from Holta et al. (2018) is given in terms of the state estimates $(\hat{u}, \hat{v})$ and parameter estimates $\hat{\theta}, \hat{k}$. The parameter estimates are generated from the adaptive laws in Theorem 1. Once these estimates are found, the adaptive relationship (15) can be used to generate state estimates.

*Theorem 2.* Consider system (3), the state estimates (15) and the adaptive law (17), and suppose (7) holds. Then, the control law

$$U(t) = \mathcal{K}[\hat{u}, \hat{v}](1) + \frac{1}{a_0 r + b_0}\hat{\theta}(t) \quad (18)$$

where $\mathcal{K} : L_2([0,1]) \times L_2([0,1]) \to L_2([0,1])$ is the operator given by

$$\mathcal{K}[\hat{u}, \hat{v}](x) = \hat{v}(x) - \int_0^x K^{vu}(x,\xi)\hat{u}(\xi)d\xi - \int_0^x K^{vv}(x,\xi)\hat{v}(\xi)d\xi \quad (19)$$

defined for $x \in [0,1]$ where $(K^{vu}, K^{vv})$ is the unique solution to (see Coron et al. (2013))

$$K^{vu}_x(x,\xi)\mu - K^{vu}_\xi(x,\xi)\lambda = K^{vv}(x,\xi)c_2(x) \quad (20a)$$
$$K^{vv}_x(x,\xi)\mu + K^{vv}_\xi(x,\xi)\mu = K^{vu}(x,\xi)c_1(x) \quad (20b)$$
$$K^{vu}(x,x)\lambda + K^{vu}(x,x)\mu = -c_2(x) \quad (20c)$$
$$K^{vu}(x,0)\lambda r = K^{vv}(x,0)\mu \quad (20d)$$

defined over $\mathcal{T}_2 = \{(x,\xi)\,|\,0 \le \xi \le x \le 1\}$, guarantees (6). Moreover, all signals in the closed loop system are bounded and the parameter estimate $\hat{\theta}$ converges to its true value $\theta$ in the sense

$$\int_t^{t+T} |\hat{\theta}(\tau) - \theta| d\tau \to 0 \quad (21)$$

for some $T > 0$.

### 3. ESTIMATION WITH ADAPTATION BASED ON BOTTOM-HOLE SENSING (NEW METHOD)

The adaptive law in Theorem 1 is designed to minimize the top-side estimation error and the bottom-hole pressure measurement is only used indirectly in the filters (8)-(10). Even though new measurements $y_0(t)$ are instantly available to the control unit by wired drill-pipe technology, the old design forces new measurements to propagate through the filter systems before the state estimates are updated, and consequently, the top-side error $\hat{e}(1,t)$ is only affected by $y_0(t-\lambda^{-1})$. In contrast, the proposed method of this section, which is the main result of the paper, utilizes the bottom-hole pressure measurement immediately and directly in the adaptive law, which is designed to minimizes the bottom-hole estimation error rather than the top-side error. The artificial time delay introduced by the filters in the old method is therefore avoided and the parameter and state estimates approach their true values significantly faster, as demonstrated in simulations in Section 4.

The new design goes as follows. Using that $e(0,t)=\epsilon(0,t)=0$ for all $t \geq t_F$ and inserting (5) into the static relationship (11), and evaluating at $x=0$ give

$$\begin{aligned} y_0(t) =& a_0 u(0,t) + b_0 v(0,t) \\ =& a_0 \left(a(0,t) + k\left(\theta m(0,t) + w(0,t)\right)\right) \\ &+ b_0 \left(b(0,t) + k\left(\theta n(0,t) + z(0,t)\right)\right). \end{aligned} \tag{22}$$

Defining

$$\breve{a}(t) = a_0 a(0,t) + b_0 b(0,t) \tag{23a}$$
$$\breve{m}(t) = a_0 m(0,t) + b_0 n(0,t) \tag{23b}$$
$$\breve{w}(t) = a_0 w(0,t) + b_0 z(0,t) \tag{23c}$$

and rearranging the terms, give the bilinear parametric model

$$y_0(t) - \breve{a}(t) = k\left(\theta \breve{m}(t) + \breve{w}(t)\right). \tag{24}$$

The same adaptive state estimates (15) will be reused here. Evaluating (15) at $x=0$, inserting (5) and defining

$$\breve{e}(t) = a_0 \hat{e}(0,t) + b_0 \hat{\epsilon}(0,t) \tag{25}$$

then give

$$\breve{e}(t) = y_0(t) - \breve{a}(t) - \hat{k}(t)\left(\hat{\theta}(t)\breve{m}(t) + \breve{w}(t)\right). \tag{26}$$

Assuming the sign of $k$ is known, the gradient method for bilinear parametric models in Ioannou and Sun (2012, Theorem 4.52) can be used to minimize a cost function based on the square error $\breve{e}^2(t)$ and thereby forming an adaptive law for the parameter estimates $\hat{\theta}, \hat{k}$.

*Theorem 3.* Consider the adaptive laws

$$\dot{\hat{\theta}}(t) = \begin{cases} \gamma_1 \text{sign}(k) \dfrac{\breve{e}(t)}{1+\breve{w}^2(t)} \breve{m}(t) & t \geq t_F \\ 0 & \text{otherwise} \end{cases} \tag{27a}$$

$$\dot{\hat{k}}(t) = \begin{cases} \gamma_2 \left[\hat{\theta}(t)\breve{m}(t) + \breve{w}(t)\right] \dfrac{\breve{e}(t)}{1+\breve{w}^2(t)} & t \geq t_F \\ 0 & \text{otherwise} \end{cases} \tag{27b}$$

for some adaptation gains $\gamma_1, \gamma_2 > 0$ where $\breve{m}(t)$ and $\breve{w}(t)$ are given in (23), $\breve{e}(t)$ is the adaptive estimation error (25) and $t_F$ is defined in (14). Suppose system (3) has a unique solution $u, v$ for all $t \geq 0$. Then, the adaptive laws (27) have the following properties:

(1) $\hat{\theta}, \hat{k} \in \mathcal{L}_\infty$.
(2) $\dot{\hat{\theta}}, \dot{\hat{k}} \in \mathcal{L}_2 \cap \mathcal{L}_\infty$.
(3) $\dfrac{\breve{e}}{\sqrt{1+\breve{w}^2(1,\cdot)}} \in \mathcal{L}_\infty \cap \mathcal{L}_2$
(4) If $\breve{w} \in \mathcal{L}_\infty$ and $\hat{\theta}\breve{m} + \breve{w} \in \mathcal{L}_2$, then $\hat{\theta}$ converges to $\theta$ and $\hat{k}$ converges to some constant.

**Proof.** Consider the Lyapunov function candidate

$$V_0 = |k| \frac{1}{2\gamma_1} \tilde{\theta}^2 + \frac{1}{2\gamma_2} \tilde{k}^2 \tag{28}$$

where $\tilde{\theta} = \theta - \hat{\theta}$ and $\tilde{k} = k - \hat{k}$. Differentiating, inserting the adaptive laws (27) for $t \geq t_F$ and using relation (26) give

$$\begin{aligned} \dot{V}_0 =& -|k| \frac{1}{\gamma_1} \tilde{\theta}\dot{\hat{\theta}} - \frac{1}{\gamma_2} \tilde{k}\dot{\hat{k}} \\ =& -\frac{\breve{e}(t)}{1+\breve{w}^2(t)} \left(|k|\tilde{\theta}\text{sign}(k)\breve{m}(t) - \tilde{k}\left[\hat{\theta}(t)\breve{m}(t) + \breve{w}(t)\right]\right) \\ =& -\frac{\breve{e}(t)}{1+\breve{w}^2(t)} \left(a_0 u(0,t) + b_0 v(0,t) - a_0 \hat{u}(0,t) - b_0 \hat{v}(0,t)\right) \\ =& -\frac{\breve{e}^2(t)}{1+\breve{w}^2(t)} \leq 0 \end{aligned} \tag{29}$$

which shows that $V_0, \tilde{\theta}, \tilde{k} \in \mathcal{L}_\infty$. The adaptive estimation error $\breve{e}$ can be written on the form

$$\breve{e}(t) = \Theta(t)^T \Psi(t) \tag{30}$$

where

$$\Theta(t) = \left[\tilde{k}(t),\ \sqrt{|k|}\tilde{\theta}(t)\right]^T \tag{31a}$$
$$\Psi(t) = \left[\hat{\theta}\breve{m}(t) + \breve{w}(t),\ \text{sign}(k)\sqrt{|k|}\breve{m}(t)\right]^T \tag{31b}$$

It is shown in Holta et al. (2017) that the filter system $(m,n)$ in (9) is bounded point-wise in $x$. We then have

$$\frac{1}{\sqrt{1+\breve{w}^2(1,\cdot)}} \Psi(t) \in \mathcal{L}_\infty \tag{32}$$

which together with Property 1 and (30) give

$$\frac{\breve{e}}{\sqrt{1+\breve{w}^2(1,\cdot)}} \in \mathcal{L}_\infty. \tag{33}$$

Integrating (29) from $t=0$ to $t=\infty$ and using that $V_0 \geq 0$ is a non-increasing function of time give

$$\begin{aligned} \int_0^\infty \left(\frac{\breve{e}^2(1,\tau)}{1+\breve{w}^2(\tau)}\right) d\tau =& -\int_0^\infty \dot{V}_0(\tau) d\tau \\ =& V_0(0) - V_0(\infty) < \infty \end{aligned} \tag{34}$$

and therefore

$$\frac{\breve{e}(1,\cdot)}{\sqrt{1+\breve{w}^2(\cdot)}} \in \mathcal{L}_2. \tag{35}$$

From (27a), one has

$$\left|\dot{\hat{\theta}}(t)\right| \leq \gamma_1 \left|\frac{\breve{e}(t)}{\sqrt{1+\breve{w}^2(t)}}\right| \left|\frac{\breve{m}(t)}{\sqrt{1+\breve{w}^2(t)}}\right| \tag{36}$$

which together with (33), (35) and boundedness of $\breve{m}$ give $\dot{\hat{\theta}} \in \mathcal{L}_\infty \cap \mathcal{L}_2$ and the first part of Property 2. For the second part, one has similarly

$$\left|\dot{\hat{k}}(t)\right| \leq \gamma_2 \left|\frac{\breve{e}(t)}{\sqrt{1+\breve{w}^2(t)}}\right| \left|\frac{\hat{\theta}\breve{m}(t) + \breve{w}(t)}{\sqrt{1+\breve{w}^2(t)}}\right| \tag{37}$$

which together with (33), (35) and boundedness of $\breve{m}$ give $\dot{\hat{k}} \in \mathcal{L}_\infty \cap \mathcal{L}_2$ and the second part of Property 2. Inserting (26) into (27a) yields

$$\dot{\hat{\theta}}(t) = -\frac{\gamma_1 \text{sign}(k)}{1+\breve{w}^2(t)} \left( k\tilde{\theta}\breve{m}(t) + \tilde{k}(t) \left( \hat{\theta}\breve{m}(t) + \breve{w}(t) \right) \right) \breve{m}(t) \tag{38}$$

where the last term can be treated as an external input. Using that $\breve{m} \in \mathcal{L}_\infty$ and if the last term $\tilde{k}(t) \left( \hat{\theta}\breve{m}(t) + \breve{w}(t) \right)$ is square integrable, then (38) forms an *exponentially stable* system and it follows that $\tilde{\theta} \to 0$ as $t \to \infty$ or equivalently the first part of Property 4. The second part of Property 4 can be seen by applying Cauchy-Schwarz' inequality to (27b).

*Remark 4.* Property 4 in Theorem 3 gives sufficient conditions for parameter convergence. For $t > t_F$, we have $\breve{m}(t) = m(0,t) = 1$ and $\breve{w}(t) = w(0,t) = -y_0(t)$. The conditions are then simplified to $y_0 \in \mathcal{L}_\infty$ and $(\hat{\theta} - y_0) \in \mathcal{L}_2$. If the adaptive laws are used in conjunction with a closed loop controller guaranteeing these properties, parameter convergence will follow.

## 4. SIMULATION

The swapping based estimation scheme presented in Section 3, consisting of the swapping filters (8)-(10), state estimates (15) and the adaptive law of Theorem 3, is combined with the control law from Holta et al. (2018) given in Theorem 2 and implemented in MATLAB (the new method). This design is compared to the design from Holta et al. (2017) (the old method), consisting of the swapping filters (8)-(10), state estimates (15), the adaptive law of Theorem 1 and the control law of Theorem 2, which is also implemented in MATLAB. In addition, a simple controller (the simple method) where the top-side flow is kept equal to the drill bit flow $q(l,t) = q_{bit}$ is also implemented. For all control schemes, the system parameters are chosen as

$$\beta = 7317\,\text{Pa}, \qquad \rho = 1250\,\text{kg}\,\text{m}^{-3} \tag{39a}$$

$$l = 2500\,\text{m}, \qquad A_1 = 0.024\,\text{m}^2 \tag{39b}$$

$$F_1 = 200, \qquad g = 9.81\,\text{m}\,\text{s}^{-2} \tag{39c}$$

$$q_{bit} = 1/60\text{m}^3\,\text{s}^{-1}, \quad J = 1.1 \times 10^{-8}\,\text{m}^3\,\text{s}^{-1}\,\text{Pa}^{-1}. \tag{39d}$$

The reservoir pressure is initially set to $p_r(0) = 400\,\text{bar}$ and kept constant until a step to $p_r(t \geq t_0) = 450\,\text{bar}$ occurs at $t_0 = 10\,\text{s}$. The system is at steady state at $t = 0$ with the initial bottom-hole pressure set equal to the reservoir pressure and the bottom-hole flow equal to the drill bit flow. The adaptation gains are selected as $\gamma_1 = \gamma_2 = 5$.

Figures 2 and 3 show the bottom-hole pressure and flow when using the three methods. The figures show that all three methods are able to attenuate the kick. The bottom-hole pressure is stabilized at the reservoir pressure and the net gain into the well converges to zero. It is seen that both the new method and the old method converge in an approximately finite time after $\sim 10\,\text{s}$, whereas the simple method has a much slower asymptotic convergence time. In addition, as can be seen from Figure 6, the new method offers a $\sim 35\,\%$ reduction in total accumulated inflow compared to the old method. This is due to the better utilization of the bottom-hole measurement as can be seen from the state estimation error in Figures 4, 5 and 7. Figure 7 also shows that the reservoir pressure estimates converge to the true value for both methods.

## 5. CONCLUSIONS AND FURTHER WORK

A new method for kick detection and attenuation in managed pressure drilling is presented. A swapping based estimator utilizing bottom-hole pressure estimates for fast parameter adaption is presented. The estimation scheme is combined with a recently developed closed loop controller for kick & loss attenuation. The new design was compared to earlier works on kick & loss attenuation in a simulation, suggesting that significant performance improvement is possible by exploiting downhole pressure measurements made available in real-time by wired drill-pipe technology. Further work include a rigorous proof of closed loop stability in the $L_2$-sense and convergence of the bottom-hole pressure to the desired set-point.

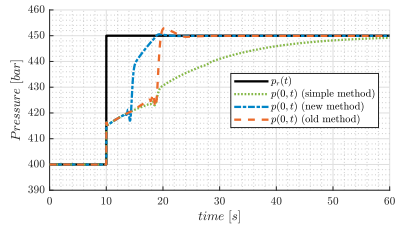


Fig. 2. Bottom-hole pressure.

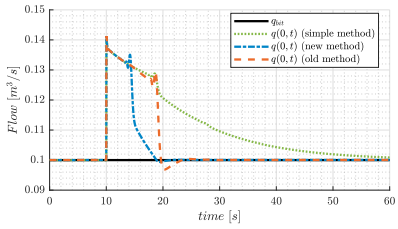


Fig. 3. Bottom-hole flow.

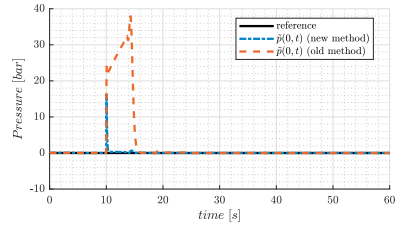


Fig. 4. Bottom-hole pressure estimation error.

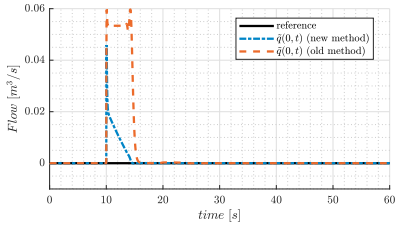


Fig. 5. Bottom-hole flow estimation error.

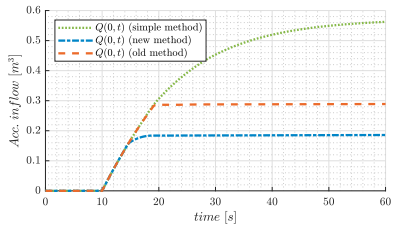


Fig. 6. Accumulated net inflow.

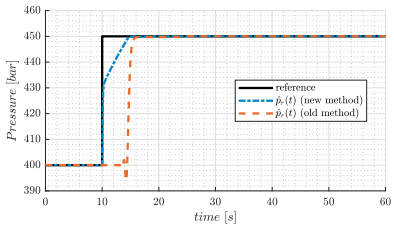


Fig. 7. Reservoir pressure estimate.

## REFERENCES


Aamo, O.M. (2013). Disturbance rejection in $2 \times 2$ linear hyperbolic systems. *IEEE Transactions on Automatic Control*, 58(5), 1095–1106.

Aarsnes, U.J.F., Açıkmeşe, B., Ambrus, A., and Aamo, O.M. (2016a). Robust controller design for automated kick handling in managed pressure drilling. *Journal of Process Control*, 47, 46–57.

Aarsnes, U.J.F., Flåtten, T., and Aamo, O.M. (2016b). Review of two-phase flow models for control and estimation. *Annual Reviews in Control*, 42, 50 – 62.

Anfinsen, H. and Aamo, O.M. (2016). Boundary parameter and state estimation in $2 \times 2$ linear hyperbolic PDEs using adaptive backstepping. In *Proceedings of the 55th Conference on Decision and Control*, 2054–2060.

Anfinsen, H. and Aamo, O.M. (2017a). Adaptive stabilization of $2 \times 2$ linear hyperbolic systems with an unknown boundary parameter from collocated sensing and control. *IEEE Transactions on Automatic Control*, 62(12), 6237–6249.

Anfinsen, H., Diagne, M., Aamo, O.M., and Krstic, M. (2016). An adaptive observer design for $n+1$ coupled linear hyperbolic PDEs based on swapping. *IEEE Transactions on Automatic Control*, 61(12), 3979–3990.

Anfinsen, H. and Aamo, O.M. (2017b). Adaptive output feedback stabilization of $n+m$ coupled linear hyperbolic PDEs with uncertain boundary conditions. *SIAM Journal on Control and Optimization*, 55(6), 3928–3946.

Anfinsen, H. and Aamo, O.M. (2017c). Adaptive stabilization of $n+1$ coupled linear hyperbolic systems with uncertain boundary parameters using boundary sensing. *Systems & Control Letters*, 99, 72 – 84.

Anfinsen, H., Diagne, M., Aamo, O.M., and Krstic, M. (2017). Estimation of boundary parameters in general heterodirectional linear hyperbolic systems. *Automatica*, 79, 185 – 197.

Bin, M. and Di Meglio, F. (2017). Boundary estimation of parameters for linear hyperbolic PDEs. *IEEE Transactions on Automatic Control*, 62(8), 3890–3904.

Coron, J.M., Vazquez, R., Krstic, M., and Bastin, G. (2013). Local exponential $H^2$ stabilization of a $2 \times 2$ quasilinear hyperbolic system using backstepping. *SIAM Journal on Control and Optimization*, 51(3), 2005–2035.

Di Meglio, F., Bresch-Pietri, D., and Aarsnes, U.J.F. (2014). An adaptive observer for hyperbolic systems with application to underbalanced drilling. *IFAC Proceedings Volumes*, 47(3), 11391 – 11397.

Hauge, E., Aamo, O.M., and Godhavn, J.M. (2012). Model-based estimation and control of in/out-flux during drilling. In *Proceeding of the 2012 American Control Conference*, 4909–4914. IEEE.

Hauge, E., Aamo, O.M., and Godhavn, J.M. (2013). Application of an infinite-dimensional observer for drilling systems incorporating kick and loss detection. In *Proceedings of the 12th European Control Conference*, 1065–1070. IEEE.

Holta, H., Anfinsen, H., and Aamo, O.M. (2017). Estimation of an uncertain bilinear boundary condition in linear 2x2 hyperbolic systems with application to drilling. In *Proceedings of the 17th International Conference on Control, Automation, and Systems*, 188–193.

Holta, H., Anfinsen, H., and Aamo, O.M. (2018). Adaptive set-point regulation of linear $2 \times 2$ hyperbolic systems with application to the kick problem in managed pressure drilling. *Submitted*.

Ioannou, P.A. and Sun, J. (2012). *Robust Adaptive Control*. Courier Corporation.

Krstic, M. and Smyshlyaev, A. (2008). Backstepping boundary control for first-order hyperbolic PDEs and application to systems with actuator and sensor delays. *Systems & Control Letters*, 57(9), 750–758.

Landet, I.S., Pavlov, A., and Aamo, O.M. (2013). Modeling and control of heave-induced pressure fluctuations in managed pressure drilling. *IEEE Transactions on Control Systems Technology*, 21(4), 1340–1351.

Liu, W. (2003). Boundary feedback stabilization of an unstable heat equation. *SIAM Journal on Control and Optimization*, 42(3), 1033–1043.

Smyshlyaev, A., Cerpa, E., and Krstic, M. (2010). Boundary stabilization of a 1-D wave equation with in-domain anti-damping. *SIAM Journal on Control and Optimization*, 48(6), 4014–4031.

Smyshlyaev, A. and Krstic, M. (2004). Closed-form boundary state feedbacks for a class of 1-D partial integro-differential equations. *IEEE Transactions on Automatic Control*, 49(12), 2185–2202.

Smyshlyaev, A. and Krstic, M. (2005). On control design for PDEs with space-dependent diffusivity or time-dependent reactivity. *Automatica*, 41(9), 1601–1608.

Smyshlyaev, A. and Krstic, M. (2010). *Adaptive Control of Parabolic PDEs*. Princeton University Press.

Vazquez, R., Krstic, M., and Coron, J.M. (2011). Backstepping boundary stabilization and state estimation of a $2 \times 2$ linear hyperbolic system. In *Proceedings of the 50th IEEE Conference on Decision and Control and European Control Conference*, 4937–4942.

Zhou, J., Stamnes, Ø.N., Aamo, O.M., and Kaasa, G.O. (2011). Switched control for pressure regulation and kick attenuation in a managed pressure drilling system. *IEEE Transactions on Control Systems Technology*, 19(2), 337–350.

## 2.3 Paper [61]: *Adaptive observer design for an $n+1$ hyperbolic PDE with uncertainty and sensing on opposite ends*

Holta, H. and Aamo, O. M. (2020a). Adaptive observer design for an n+1 hyperbolic PDE with uncertainty and sensing on opposite ends. In *Proceedings of the 2020 European Control Conference (ECC)*, pages 1159–1164

# Adaptive Observer Design for an $n+1$ Hyperbolic PDE with Uncertainty and Sensing on Opposite Ends

Haavard Holta and Ole Morten Aamo

***Abstract*— An adaptive observer design for a system of $n+1$ coupled 1-D linear hyperbolic partial differential equations with an uncertain boundary condition is presented, extending previous results by removing the need for sensing collocated with the uncertainty. This modification is important and motivated by applications in oil & gas drilling where information about the down-hole situation is crucial in order to prevent or deal with unwanted incidents. Uncertainties are usually present down-hole while measurements are available top-side at the rig, only. Boundedness of the state and parameter estimates is proved in the general case, while convergence to true values requires bounded system states and, for parameter convergence, persistent excitation. The central tool for analysis is the infinite-dimensional backstepping method applied in two steps, the first of which is time-invariant, while the second is time-varying induced by the time-varying parameter estimates.**

## I. Introduction

### A. Problem formulation

We consider the system of linear first-order hyperbolic Partial Differential Equations (PDEs) with $n$ positive convecting invariants and 1 negative convecting invariant given by

$$u_t + \Lambda u_x = \Sigma(x)u + \omega(x)v \tag{1a}$$
$$v_t - \mu v_x = \varpi(x)u \tag{1b}$$

where $u \in \mathbb{R}^n$ is the *upward* propagating Riemann invariants, $v \in \mathbb{R}$ is the single *downward* propagating Riemann invariant, $\Sigma : [0,1] \to \mathbb{R}^{n\times n}$ with diagonal terms being zero, $\omega : [0,1] \to \mathbb{R}^{n\times 1}$, $\varpi : [0,1] \to \mathbb{R}^{1\times n}$, and $\Lambda = \text{diag}(\lambda_1, ..., \lambda_n)$ and $\mu$ satisfying $-\mu < 0 < \lambda_1 < \cdots < \lambda_n$. We consider boundary conditions on the form

$$u(0,t) = qv(0,t) + d \tag{2a}$$
$$v(1,t) = \rho u(1,t) + U(t) \tag{2b}$$

where $q = \{q_i\}_{1\le i\le n} \in \mathbb{R}^n$ and $d = \{d_i\}_{1\le i\le n} \in \mathbb{R}^n$ are unknown, $\rho \in \mathbb{R}^{1\times n}$ is known, and $U : [0,\infty) \to \mathbb{R}$ can be any known time-varying function. In addition, we assume that

$$y(t) := u(1,t) \tag{3}$$

is measured. The initial conditions

$$u(x,0) =: u_{ic}(x) \tag{4a}$$
$$v(x,0) =: v_{ic}(x) \tag{4b}$$

The authors are with the Department of Engineering Cybernetics. Norwegian University of Science and Technology, Trondheim N-7491, Norway (e-mail: haavard.holta@ntnu.no; aamo@ntnu.no).

Economic support from The Research Council of Norway and Equinor ASA through project no. 255348/E30 Sensors and models for improved kick/loss detection in drilling (Semi-kidd) is gratefully acknowledged.

satisfy certain compatibility conditions, making the Cauchy problem (1)–(4) well-posed (see e.g. [1, Theorem 3.1]).

### B. A motivating application

The system (1) can be used to model, among others, various phenomena in multiphase fluid flows. An overview of other possible applications ranging from open-channel networks to transmission lines can be found in [2]. In this paper, we are concerned with the problem of state estimation in fluid flow systems where one of the boundaries is specified in terms of uncertain parameters and sensing is limited to the opposite boundary. The motivation is an application in oil & gas drilling where only top-side flow measurements are available and the bottom-hole flow is influenced by an oil/gas reservoir with unknown properties.

In the drilling application, mud is circulated down the drill-string, through the drill-bit at the bottom, and up in the open annulus surrounding the drill-string back up to the rig where flow is measured. See Figure 1. If the pressure down-hole is lower than the reservoir pressure, oil, water or even gas might start flowing into the well and up the annulus. This is called a kick and can, if not handled, lead to catastrophic consequences when the reservoir fluids reach the surface. If properties such as the reservoir pressure is unknown, handling and even detecting such influxes of reservoir fluids is a very challenging problem. Previous methods of detecting and estimating influxes have mainly focused on lumped-order models [3]–[11], were the distributed dynamics are neglected. Some results using the so called *early-lumping* approach where the PDE model is spatially discretized and approximated by a set of ODEs have also been explored [12]–[14]. In this paper, we propose to use the contrasting *late-lumping* approach where the observer is derived for the distributed model, and discretization is only necessary for computer implementation.

In the drift-flux model, which is the most commonly used model for drilling applications involving gas, all liquids (mud, oil, water) are lumped into a single phase, and gas is considered separately. Following [15], the drift flux model proposed in [16] can be written on conservative form in terms of pressure, gas fraction and gas velocity by the quasi-linear $3\times 3$ system

$$w_t + A(w)w_x = S(w) \tag{5}$$

over the domain $(x,t) \in [0,1] \times [0,\infty)$, where $A$ and $S$ are complicated and given in [15]. System (5) can be linearized around a given operating profile, diagonalized and written in terms of Riemann invariants to obtain the form (1) with $n = 2$ [17].

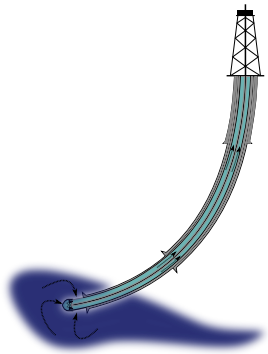

Fig. 1. Schematic of the drilling system.

Interaction with the reservoir is modeled by the boundary conditions which are assumed to equal the bottom-hole net liquid and gas inflow $q_L(0,t)$ and $q_G(0,t)$, respectively. It is common to model them as proportional to the pressure difference between the bottom-hole pressure $p(0,t)$ and reservoir pressure $p_{res}(t)$, that is,

$$q_L(0,t) = J_L(p_{res}(t) - p(0,t)) \tag{6a}$$
$$q_G(0,t) = J_G(p_{res}(t) - p(0,t)) \tag{6b}$$

where $J_L$ and $J_G$ are constants called *production indices* (PI). Both PI's $J_G$ and $J_L$ and the reservoir pressure $p_{res}$ are assumed to be unknown and (6) can be rephrased in the form (2a). For the top-side boundary condition at $x = 1$, we assume that the pressure $p(1,t)$ and flow $q(1,t)$ are known (one is measured, the other is a control input).

### C. Relevant previous results

We use the much celebrated backstepping method for infinite dimensional systems, first derived for hyperbolic systems in [18] and later extended to $2\times 2$ systems [19] and $m+n$ systems [20]. In the adaptive setting with uncertain boundary parameters, an observer for a $2\times 2$ system only relying on measurements on the boundary opposite of the boundary with the uncertain parameters is derived in [21], [22]. For $n+1$ systems, the adaptive observer problem has been solved in [23]–[25] utilizing sensing at the same boundary as the uncertain parameters. Particularly relevant to this paper is [25] which considers an application in under-balanced drilling. Worth mentioning is also [17] where the backstepping approach is used to control multiphase flows in drilling using state-feedback.

In this paper, we extend the observer in [21] and derive an observer for $n+1$ systems with parametric uncertainties on one boundary and measurements taken at the opposite boundary. A disadvantage of the method in [21] is that the observer injection gains have to be updated on-line with every new time-varying parameter estimate. We propose a design avoiding the on-line recalculation of injection gains by instead solving a set of computationally simpler transport equations on-line. The estimation scheme with state observer and adaptive laws including stability proofs are presented in Section II. Some concluding remarks are offered in Section III.

### D. Notation

For a signal $z : [0,1]\times[0,\infty) \to \mathbb{R}^n$ , partial derivatives with respect to i.e. space are denoted $z_x$ or $\partial_x z_i$ for each element $i = 1,...,n$. The $L_2$-norm is denoted

$$||z|| := \sqrt{\int_0^1 z^T(x,t)z(x,t)dx}. \tag{7}$$

For $f : [0,\infty) \to \mathbb{R}$, we use the vector spaces

$$f \in \mathscr{L}_p \leftrightarrow \left(\int_0^\infty |f(t)|^p dt\right)^{\frac{1}{p}} < \infty \tag{8}$$

for $p \geq 1$ with the particular case

$$f \in \mathscr{L}_\infty \leftrightarrow \sup_{t\geq 0} |f(t)| < \infty. \tag{9}$$

Derivatives with respect to time are denoted $\dot{f}$. If not otherwise stated, a statement for a variable with subscript $i$ refers to all variables with subscript $i = 1,...,n$.

## II. State and parameter estimation

Let $(\hat{u},\hat{v}) \in \mathbb{R}^{n+1}$ denote the state estimates. We consider the observer system

$$\begin{aligned}\hat{u}_t + \Lambda\hat{u}_x =& \Sigma(x)\hat{u} + \omega(x)\hat{v} \\ &+ P_1(x,t)(y(t) - \hat{u}(1,t))\end{aligned} \tag{10a}$$
$$\hat{v}_t - \mu\hat{v}_x = \varpi(x)\hat{u} + P_2(x,t)(y(t) - \hat{u}(1,t)) \tag{10b}$$
$$\hat{u}(0,t) = \hat{q}(t)\hat{v}(0,t) + \hat{d}(t) \tag{10c}$$
$$\hat{v}(1,t) = \rho u(1,t) + U(t) \tag{10d}$$

with compatible initial conditions $(\hat{u}(x,0),\hat{v}(x,0)) = (\hat{u}_{ic}(x),\hat{v}_{ic}(x))$ and where $\hat{q}_i(t)$ and $\hat{d}_i(t)$ are the parameter estimates of $q$ and $d$. The injection gains $P_1$ and $P_2$ have the structure

$$\begin{aligned}P_1(x,t) =& M(x,1)\Lambda + G(x,1,t)\Lambda \\ &+ \int_x^1 M(x,\xi)G(\xi,1,t)\Lambda d\xi\end{aligned} \tag{11a}$$
$$P_2(x,t) = N(x,1)\Lambda + \int_x^1 N(x,\xi)G(\xi,1,t)\Lambda d\xi \tag{11b}$$

where $(M,N,G)$ are Volterra integral kernels and will be specified further in the next sections. The state estimation error $\tilde{u} = u - \hat{u}$, $\tilde{v} = v - \hat{v}$ then satisfies

$$\tilde{u}_t + \Lambda\tilde{u}_x = \Sigma(x)\tilde{u} + \omega(x)\tilde{v} - P_1(x,t)\tilde{u}(1,t) \tag{12a}$$
$$\tilde{v}_t - \mu\tilde{v}_x = \varpi(x)\tilde{u} - P_2(x,t)\tilde{u}(1,t) \tag{12b}$$
$$\tilde{u}(0,t) = \hat{q}(t)\tilde{v}(0,t) + \tilde{q}(t)v(0,t) + \tilde{d}(t) \tag{12c}$$
$$\tilde{v}(1,t) = 0 \tag{12d}$$

where $\tilde{q}(t) = q - \hat{q}(t)$ and $\tilde{d} = d - \hat{d}(t)$. The design strategy is as follows: In Section II-A, we specify the $(M,N)$-kernels

and show that the estimation error system (12) is equivalent to a simpler target system. This target system is used to derive a parametric model relating the unknown parameters to some known signals in Section II-B. Equivalence to yet another target system are shown in Section II-C by specifying the remaining $G$-kernel. Properties of this final target system together with appropriate adaptive laws based on the parametric model are used in Theorem 1 in Section II-D to state the main contribution of this paper on state end parameter estimation.

### A. Backstepping transformation

*Lemma 1:* Let $\bar{q} = \{\bar{q}_i\}_{1\le i\le n} \in \mathbb{R}^n$. On the triangular domain $\mathscr{T}_1 = \{(x,\xi)|0 \le x \le \xi \le 1\}$, the backstepping transformation

$$\tilde{u}(x,t) = \alpha(x,t) + \int_x^1 M(x,\xi)\alpha(\xi,t)d\xi \tag{13a}$$

$$\tilde{v}(x,t) = \beta(x,t) + \int_x^1 N(x,\xi)\alpha(\xi,t)d\xi, \tag{13b}$$

with kernels $M = \{M_{ij}(x,t)\}_{1\le i,j\le n} : \mathscr{T}_1 \to \mathbb{R}^{n\times n}$, $N = \{N_i(x,t)\}_{1\le i\le n} : \mathscr{T}_1 \to \mathbb{R}^{1\times n}$ satisfying

$$M_\xi\Lambda + \Lambda M_x = \Sigma(x)M + \omega(x)N \tag{14a}$$

$$N_\xi\Lambda - \mu N_x = \varpi(x)M, \tag{14b}$$

$$\Sigma(x) = M(x,x)\Lambda - \Lambda M(x,x) \tag{15a}$$

$$\varpi(x) = N(x,x)\Lambda + \mu N(x,x), \tag{15b}$$

$$M_{ij}(0,\xi) = \bar{q}_i N_j(0,\xi),\ 1 \le i \le j \le n \tag{16}$$

and

$$M_{ij}(x,1) = \frac{\Sigma_{ij}(x)}{\lambda_j - \lambda_i}, \quad 1 \le j < i \le n \tag{17}$$

is invertible and maps the target system

$$\alpha_t(x,t) + \Lambda\alpha_x(x,t) = \omega(x)\beta(x,t) - G(x,1,t)\Lambda\alpha(1,t) - \int_x^1 A(x,\xi)\beta(\xi,t)d\xi \tag{18a}$$

$$\beta_t(x,t) - \mu\beta_x(x,t) = -\int_x^1 B(x,\xi)\beta(\xi,t)d\xi \tag{18b}$$

$$\alpha(0,t) = \hat{q}(t)\beta(0,t) + \int_0^1 H(\xi,t)\alpha(\xi,t)d\xi + \tilde{q}(t)v(0,t) + \tilde{d}(t) \tag{18c}$$

$$\beta(1,t) = 0 \tag{18d}$$

where $G = \{g_{ij}(x,t)\}_{1\le i,j\le n}$ is an upper triangular matrix to be decided, $A$ and $B$ satisfy

$$A(x,\xi) = M(x,\xi)\omega - \int_x^\xi M(x,s)A(s,\xi)ds \tag{19a}$$

$$B(x,\xi) = N(x,\xi)\omega - \int_x^\xi N(x,s)A(s,\xi)ds, \tag{19b}$$

and $H(\xi,t) = \{h_{ij}(\xi,t)\}_{1\le i,j\le n}$ is defined by

$$h_{ij}(\xi,t) := \hat{q}_i(t)N_j(0,\xi) - M_{ij}(0,\xi), \tag{20}$$

into the error system (12) with injection gains (11). Moreover, the kernel equation (14)–(17) has a unique solution. The target system (18), but without the $G(x,1,t)\alpha(1,t)$ term, and injection gains $P_1(x) = M(x,1)\Lambda$ and $P_2(x) = N(x,1)\Lambda$, was first used in [24] for non-collocated observer design for $n+1$ systems, which itself was a straightforward application of the kernel equations derived in [20]. The effect of including the $G(x,1,t)\alpha(1,t)$ term in the target system can be seen by substituting $G(x,1,t)\alpha(1,t)$ for $\alpha(\xi,t)$ in (13) showing the origin of the injection gains (11). The proof of Lemma 1 is therefore omitted.

*Remark 1:* The constant $\bar{q}$ can be chosen arbitrarily, but better performance is expected if it is chosen as close to $q$ as possible, i.e. $\bar{q} = \hat{q}(0)$, presuming $\hat{q}(0)$ is our best guess of $q$ at $t = 0$. Due to (16), we have

$$h_{ij}(\xi,t) = (\hat{q}_i - \bar{q}_i)N_j \tag{21}$$

for all $j \ge i$, meaning that $H(\xi,t)$ will in general only be strictly lower triangular for all $\xi \in [0,1]$ if $\bar{q} = \hat{q}(t)$. The remaining injection gain $G(x,1,t)\Lambda$ left unspecified in (18a) (specified later in Section II-C) will be used to handle the time-varying discrepancy $(\tilde{q} - \hat{q}(t))$.

### B. Parametric model

The advantage of transforming the error system to the form (18) is that, for $t \ge \mu^{-1}$, $\beta \equiv 0$ and the $\alpha$-dynamics can be solved independently for each element $\alpha_i$. This solution is exploited in the next lemma to obtain a bilinear parametric model relating the unknown parameters to known signals.

*Lemma 2:* Let $\lambda = \min_i \lambda_i = \lambda_1$. For $t \ge t_F := \mu^{-1} + 2\lambda^{-1}$,

$$\psi_i(t) = q_i\phi(t) + d_i, \quad 1 \le i \le n \tag{22}$$

where

$$\begin{aligned}\psi_i(t) =& \tilde{y}_i(t + \lambda_i^{-1} - \lambda^{-1}) \\ &+ \hat{q}_i(t - \lambda^{-1})\phi(t) + \hat{d}_i(t - \lambda^{-1}) \\ &- \sum_{j=i}^n \int_{t-\lambda^{-1}}^{t+\lambda_i^{-1}-\lambda^{-1}} g_{ij}((\tau - t + \lambda^{-1})\lambda_i, \tau)\lambda_j\tilde{y}_j(\tau)d\tau \\ &- \sum_{j=1}^n \int_0^1 h_{ij}(\xi, t - \lambda^{-1}) \Bigg(\tilde{y}_j(t + \lambda^{-1}(1-\xi) - \lambda^{-1}) \\ &- \sum_{l=j}^n \int_{t-\lambda^{-1}}^{t+\lambda_j^{-1}(1-\xi)-\lambda^{-1}} k_{jl}(\xi + \lambda_j(\tau + \lambda^{-1} - t), \tau) \\ &\times \tilde{y}_l(\tau)d\tau\Bigg)d\xi,\end{aligned} \tag{23}$$

$$\begin{aligned}\phi(t) \equiv& -\hat{v}(0, t - \lambda^{-1}) + \sum_{i=1}^n \int_0^1 N_i(0,\xi, t - \lambda^{-1}) \\ &\times \Bigg(\sum_{j=1}^n \int_{t-\lambda^{-1}}^{t+\lambda_i^{-1}(1-\xi)-\lambda^{-1}} g_{ij}(\xi + \lambda_i(\tau + \lambda^{-1} - t), \tau) \\ &\times\lambda_j\tilde{y}_j(\tau)d\tau - \tilde{y}_i(t + \lambda_i^{-1}(1-\xi) - \lambda^{-1})\Bigg)d\xi,\end{aligned} \tag{24}$$

and

$$\tilde{y}_i(t) := \alpha_i(1,t) = y_i(t) - \hat{u}_i(1,t). \tag{25}$$

*Proof:* Consider the target system (18) in Lemma 1. Since $\beta \equiv 0$ for $t \geq \mu^{-1}$, we have on component form

$$\partial_t \alpha_i + \lambda_i \partial_x \alpha_i = \sum_{j=i}^{n} g_{ij}(x,t)\lambda_j \tilde{y}_j(t) \tag{26a}$$

$$\alpha_i(0,t) = \sum_{j=1}^{n} \int_0^1 h_{ij}(\xi,t)\alpha_j(\xi,t)d\xi + \tilde{q}_i(t)v(0,t) + \tilde{d}_i(t) \tag{26b}$$

with the solution

$$\alpha_i(x,t) = \sum_{j=i}^{n} \int_{t+\lambda_i^{-1}(x_0-x)}^{t} g_{ij}(x+\lambda_i(\tau-t),\tau)\lambda_j \tilde{y}_j(\tau)d\tau + \alpha_i(x_0, t+\lambda_i^{-1}(x_0-x)) \tag{27}$$

valid for all $t \geq \mu^{-1} + \lambda_i^{-1}$ and some $x_0 \in [0,1]$. Selecting $x_0 = 0$ and inserting (18c) yield

$$\begin{aligned}\alpha_i(x,t) =& \sum_{j=i}^{n} \int_{t-\lambda_i^{-1}x}^{t} g_{ij}(x+\lambda_i(\tau-t),\tau)\lambda_j \tilde{y}_j(\tau)d\tau \\ &+ \sum_{j=1}^{n} \int_0^1 h_{ij}(\xi, t-\lambda_i^{-1}x)\alpha_j(\xi, t-\lambda_i^{-1}x)d\xi \\ &+ \tilde{q}_i(t-\lambda_i^{-1}x)v(0,t-\lambda_i^{-1}x) + \tilde{d}_i(t-\lambda_i^{-1}x).\end{aligned} \tag{28}$$

Selecting $x_0 = 1$ and inserting (25) yield

$$\begin{aligned}\alpha_i(x,t) =& -\sum_{j=i}^{n} \int_{t}^{t+\lambda_i^{-1}(1-x)} g_{ij}(x+\lambda_i(\tau-t),\tau)\lambda_j \tilde{y}_j(\tau)d\tau \\ &+ \tilde{y}_i(t+\lambda_i^{-1}(1-x)).\end{aligned} \tag{29}$$

We have from (13b) for $t \geq \mu^{-1}$, and (29) that

$$\begin{aligned}v(0,t) =& \hat{v}(0,t) + \int_0^1 N(0,\xi)\alpha(\xi,t)d\xi \\ =& \hat{v}(0,t) + \sum_{i=1}^{n} \int_0^1 N_i(0,\xi) \quad \tilde{y}_i(t+\lambda_i^{-1}(1-\xi)) \\ &- \sum_{j=i}^{n} \int_{t}^{t+\lambda_i^{-1}(1-\xi)} g_{ij}(\xi+\lambda_i(\tau-t),\tau)\lambda_j \tilde{y}_j(\tau)d\tau \Bigg) d\xi.\end{aligned} \tag{30}$$

Thus,

$$v(0,t-\lambda^{-1}) = -\phi(t). \tag{31}$$

Next, inserting the right hand side of (29) into the left hand side of (28) evaluated at $x = 1$ and $t = t + \lambda_i^{-1} - \lambda^{-1} \leq t$ yields

$$\begin{aligned}&\tilde{y}_i(t+\lambda_i^{-1}-\lambda^{-1}) = \tilde{q}_i(t-\lambda^{-1})v(0,t-\lambda^{-1}) + \tilde{d}_i(t-\lambda^{-1}) \\ &+ \sum_{j=i}^{n} \int_{t-\lambda^{-1}}^{t+\lambda_i^{-1}-\lambda^{-1}} g_{ij}((\tau-t+\lambda^{-1})\lambda_i,\tau)\lambda_j \tilde{y}_j(\tau)d\tau \\ &+ \sum_{j=1}^{n} \int_0^1 h_{ij}(\xi, t-\lambda^{-1})\alpha_j(\xi, t-\lambda^{-1})d\xi \\ =& \sum_{j=i}^{n} \int_{t-\lambda^{-1}}^{t+\lambda_i^{-1}-\lambda^{-1}} g_{ij}((\tau-t+\lambda^{-1})\lambda_i,\tau)\lambda_j \tilde{y}_j(\tau)d\tau \\ &+ q_i v(0,t-\lambda^{-1}) + d_i \\ &- \hat{q}_i(t-\lambda^{-1})v(0,t-\lambda^{-1}) - \hat{d}_i(t-\lambda^{-1}) \\ &+ \sum_{j=1}^{n} \int_0^1 h_{ij}(\xi,t-\lambda^{-1}) \Bigg( \tilde{y}_j(t+\lambda^{-1}(1-\xi)-\lambda^{-1}) \\ &- \sum_{l=j}^{n} \int_{t-\lambda^{-1}}^{t+\lambda_j^{-1}(1-\xi)-\lambda^{-1}} k_{jl}(\xi+\lambda_j(\tau+\lambda^{-1}-t),\tau) \\ &\times \tilde{y}_l(\tau)d\tau \Bigg) d\xi\end{aligned} \tag{32}$$

which is equivalent to (22) in view of (23)–(25) and (31). ■

### C. Properties of estimation error target system

We now show equivalence to yet another target system by specifying the $G$-kernel.

*Lemma 3:* For $t \geq \mu^{-1}$, the backstepping transformation

$$\alpha(x,t) = \eta(x,t) + \int_x^1 G(x,\xi,t)\eta(\xi,t)d\xi \tag{33}$$

with kernel $G = \{g_{ij}\}_{1\leq i,j\leq n} : \mathscr{T}_1 \times [0,\infty) \to \mathbb{R}^{n\times n}$ satisfying

$$\partial_t g_{ij} = -\lambda_j \partial_\xi g_{ij} - \lambda_i \partial_x g_{ij} \tag{34a}$$

$$g_{ij}(x,x,t) = 0 \tag{34b}$$

$$g_{ij}(0,\xi,t) = h_{ij}(\xi,t) + \sum_{k=1}^{j} \int_0^\xi h_{ik}(s,t)g_{kj}(s,\xi,t)ds \tag{34c}$$

for $1 \leq i \leq j \leq n$ and $g_{ij} \equiv 0$ for $1 \leq j < i \leq n$, which has a unique, bounded solution for every bounded $h_{ij}$, maps the sub-system (18a) and (18c) (recall that $\beta \equiv 0$ for $t \geq \mu^{-1}$) into the target system

$$\eta_t(x,t) + \Lambda\eta_x(x,t) = 0 \tag{35a}$$

$$\eta(0,t) = \int_0^1 \bar{H}(\xi,t)\eta(\xi,t)d\xi + \tilde{q}(t)v(0,t) + \tilde{d}(t) \tag{35b}$$

where $\bar{H}$ is the strictly lower triangular matrix

$$\bar{H}(\xi,t) := H(\xi,t) - G(0,\xi,t) + \int_0^\xi H(s,t)G(s,\xi,t)ds. \tag{36}$$

*Proof:* Differentiating (33) with respect to time and space, inserting the dynamics (35), and integrating by parts yield

$$\begin{aligned}&\alpha_t(x,t) + \Lambda\alpha_x(x,t) + G(\xi,1,t)\Lambda\alpha(1,t) \\ =& \eta_t(x,t) + \Lambda\eta_x(x,t) + G(\xi,1,t)\Lambda\alpha(1,t) \\ &+ \int_x^1 G_t(x,\xi,t)\eta(\xi,t)dsd\xi \\ &+ G(x,x,t)\Lambda\eta(1,t) - G(x,1,t)\Lambda\eta(1,t) \\ &+ \int_x^1 G_\xi(x,\xi,t)\Lambda\eta(\xi,t)d\xi \\ &- \Lambda G(x,x,t)\eta(x,t) + \int_x^1 \Lambda G_x(x,\xi,t)\eta(\xi,t)d\xi \\ =& \int_x^1 \left(G_t(x,\xi,t) + G_\xi(x,\xi,t)\Lambda + \Lambda G_x(x,\xi,t)\right)\eta(\xi,t)d\xi \\ &+ (G(x,x,t)\Lambda - \Lambda G(x,x,t))\eta(x,t) \\ &+ G(x,1,t)\Lambda(\alpha(1,t) - \eta(1,t))\end{aligned} \tag{37}$$

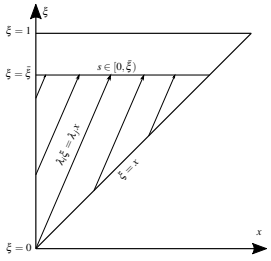


Fig. 2. Characteristic lines of $g_{ij}$ for $j > i$.

which in view of (34) and $\alpha(1,t) = \eta(1,t)$ verifies (18) (with $\beta \equiv 0$). For the boundary condition, we have

$$\begin{aligned}\eta(0,t) =&\tilde{q}(t)v(0,t) + \tilde{d}(t) - \int_0^1 G(0,\xi,t)\eta(\xi,t)d\xi \\ &+ \int_0^1 H(\xi,t)\left(\eta(\xi,t) + \int_\xi^1 G(\xi,s,t)\eta(s,t)ds\right)d\xi \\ =&\int_0^1 \left(H(\xi,t) - G(0,\xi,t) + \int_0^\xi H(s,t)G(s,\xi,t)ds\right) \\ &\times \eta(\xi,t)d\xi + \tilde{q}(t)v(0,t) + \tilde{d}(t). \end{aligned} \tag{38}$$

Defining $\bar{H}$ as in (36), which due to (34c) is strictly lower triangular, yields (35b).

The system (34) is a set of Riemann invariants parameterized by $(\xi,t)$ with characteristic lines $(\lambda_i\lambda_j^{-1}s, \xi + s, t + \lambda_j^{-1}s)$ originating from the $(0,\xi,t)$-boundary for $\lambda_i\xi - \lambda_j x \geq 0$ . See Figure 2. Since (34c) is causal for all $\xi \in [0,1]$ in the sense that $g_{ij}(0,\xi,t)$ is uniquely specified by $h_{ij}(\xi,t)$, $h_{ik} = (s,t)$ and $g_{kj}(0,s,t-\lambda_j^{-1})$ for $s \in [0,\xi), k = 1,...,j$, it follows that there exist a unique solution $g_{ij}(0,\xi,t)$ to (34c), which in turn implies the existence of a unique solution $g_{ij}(x,\xi,t)$ to (34) for all bounded $h_{ij}$. Since $g_{ij}(0,\xi,t)$ can be upper bounded in terms of $h_{ij}$, $g_{ij}(x,\xi,t)$ is bounded. ■

### *D. Adaptive law and stability of estimation error*

*Theorem 1:* Consider the system (1) and observer (10). Let $\tilde{q}_i(t) = q_i - \hat{q}_i(t)$, $\tilde{d}_i(t) = d - \hat{d}_i(t)$ and $\tilde{\psi}_i(t) := \psi_i(t) - \hat{q}_i(t)\phi(t) + \hat{d}_i(t)$. If

$$\dot{\hat{q}}_i = \gamma_{q_i}\frac{\tilde{\psi}_i(t)\phi(t)}{2+\phi^2(t)}, \quad \dot{\hat{d}}_i = \gamma_{d_i}\frac{\tilde{\psi}_i(t)}{2+\phi^2(t)} \tag{39}$$

for $t \geq t_F$ and $\dot{\hat{q}}_i = \dot{\hat{d}} = 0$ otherwise, where $\gamma_{q_i}, \gamma_{d_i} > 0$ are the adaptation gains, then

$$\hat{q}_i, \hat{d}_i \in \mathscr{L}_\infty, \quad \dot{\hat{q}}_i, \dot{\hat{d}}_i \in \mathscr{L}_\infty \cap \mathscr{L}_2 \tag{40}$$

and

$$(\tilde{u}(x,\cdot), \tilde{v}(x,\cdot)) \in \mathscr{L}_\infty. \tag{41}$$

If in addition $v(0,t)$ is bounded for all $t \geq 0$, then

$$||\tilde{u}||, ||\tilde{v}|| \to 0. \tag{42}$$

Lastly, if the *persistence of excitation* condition

$$c_1 I_{2\times 2} \geq \frac{1}{T}\int_t^{t+T} [\phi(\tau),1]^T[\phi(\tau),1]d\tau \geq c_2 I_{2\times 2} \tag{43}$$

is satisfied for some constants $c_1, c_2, T > 0$, the parameter estimates $\hat{q}_i$ and $\hat{d}_i$ converge exponentially to their true values $q_i$ and $d_i$.

*Proof:* Consider the parametric model (22) in Lemma 2. The properties (40) of $\hat{q}$ and $\hat{d}$ follow from [26, Theorem 4.3.2], along with the fact that $\tilde{\psi}_i(2+\phi^2)^{-1} \in \mathscr{L}_2 \cap \mathscr{L}_\infty$. Let

$$\tilde{\Theta}_i(t) =: \left[\tilde{q}_i(t), \tilde{d}_i(t)\right]^T \tag{44}$$

$$\Phi_i(t) =: \frac{1}{\sqrt{1+\phi^2(t)}}[\phi(t),1]^T. \tag{45}$$

so that $\tilde{\psi}_i(t)(2+\phi^2(t))^{-1} = \Phi_i^T(t)\tilde{\Theta}_i(t)$. We have

$$\Phi_i^T(t)\tilde{\Theta}_i(t) = \Phi_i^T(t)\left(\int_{t-\lambda^{-1}}^t \dot{\tilde{\Theta}}_i(\tau)d\tau + \tilde{\Theta}_i(t-\lambda^{-1})\right) \tag{46}$$

which after rearranging and squaring both sides give the inequality

$$\begin{aligned}&(\Phi_i^T(t)\tilde{\Theta}_i(t-\lambda^{-1}))^2 \\ &\leq 2(\Phi_i^T(t)\tilde{\Theta}_i(t))^2 + 2\left(\Phi_i^T(t)\int_{t-\lambda^{-1}}^t \dot{\tilde{\Theta}}_i(\tau)d\tau\right)^2 \\ &\leq 2(\Phi_i^T(t)\tilde{\Theta}_i(t))^2 + c\int_{t-\lambda^{-1}}^t \dot{\tilde{q}}_i^2(\tau) + \dot{\tilde{d}}_i^2(\tau)d\tau \end{aligned} \tag{47}$$

for some constant $c > 0$. As already stated, the first term is integrable. For the second term, we have by changing the order of integration

$$\begin{aligned}&\lim_{T\to\infty}\int_{\lambda^{-1}}^T\int_{t-\lambda^{-1}}^t \dot{\tilde{q}}_i^2(\tau)d\tau dt \\ &= \lim_{T\to\infty}\int_0^{\lambda^{-1}}\int_{\lambda^{-1}}^{\tau+\lambda^{-1}} dt\lambda\dot{\tilde{q}}_i^2(\tau)d\tau \\ &\quad + \int_{\lambda^{-1}}^{T-\lambda^{-1}}\int_\tau^{\tau+\lambda^{-1}} dt\lambda\dot{\tilde{q}}_i^2(\tau)d\tau \\ &\quad + \int_{T-\lambda^{-1}}^T\int_\tau^T dt\lambda\dot{\tilde{q}}_i^2(\tau)d\tau \end{aligned} \tag{48}$$

Since all the inner integrals evaluate to $\lambda^{-1}$ or less,

$$\lim_{T\to\infty}\int_{\lambda^{-1}}^T\int_{t-\lambda^{-1}}^t \dot{\tilde{q}}_i^2(\tau)d\tau dt \leq \lim_{T\to\infty}\lambda^{-1}\int_{\lambda^{-1}}^T \dot{\tilde{q}}_i^2(\tau)d\tau \tag{49}$$

which by (40) is bounded. The term involving $\dot{\tilde{d}}_i$ can similarly be shown to be bounded and integrable, showing that the left hand side of (47) is bounded and integrable. That is

$$\pi_i := \frac{\tilde{q}_i v(0,\cdot) + \tilde{d}_i}{\sqrt{2+v^2(0,\cdot)}} \in \mathscr{L}_2 \cap \mathscr{L}_\infty. \tag{50}$$

We construct the Lyapunov function candidate

$$V(t) = \int_0^1 e^{-x}\eta^T(x,t)\Pi\eta(x,t)dx \tag{51}$$

where $\Pi$ is a positive definite diagonal matrix. Differentiating (51) with respect to time inserting the system dynamics (35)

and integrating by parts give the upper bound

$$\dot{V}(t) \leq -\int_0^1 \eta^T(x,t)\left[\Pi\lambda_1 - \bar{H}^T(x,t)\Pi\bar{H}(x,t)\lambda_n\right]\eta(x,t)dx - c_1\eta^T(1,t)\eta(1,t) + c_2\pi^T(t)\pi(t). \quad (52)$$

where $\pi = \{\pi_i\}_{1\leq i\leq n}$. Since $\bar{H}(x,t)$ is strictly lower triangular and by (40) bounded for all $t \geq 0$, it is possible to (recursively, see e.g. [27, Appendix B.2.]) select $\Pi$ such that $\Pi\lambda_1 - \bar{H}^T(x,t)\Pi\bar{H}(x,t)\lambda_n \succ 0$ yielding

$$\dot{V}(t) \leq -c_3V_1(t) - c_1\eta^T(1,t)\eta(1,t) + c_2\pi^T(t)\pi(t) \quad (53)$$

for some constants $c_1, c_2, c_3 > 0$. The bound (53) is of the form considered [28, Lemma 3] yielding $V \to 0$ which in turn implies $||\eta|| \to 0$. Invertibility of the transformations (13) and (33) and boundedness of all kernels finally give (42). ■

## III. Concluding remarks

We have designed an adaptive observer estimating boundary parameters and distributed states in an $n+1$ linear hyperbolic system using measurements on the boundary opposite the uncertainty. Boundedness of state estimates are proved. The state and parameter estimates are shown to converge to their true value assuming bounded system states and persistence of excitation, respectively. The observer can be applied to a multiphase fluid flow system in drilling to estimate distributed flow and pressure profiles and reservoir properties. The drift-flux model mentioned in Section I-B is quasi-linear and linearization is only a valid simplification for limited variations around an equilibrium profile. This is violated for kick and loss scenarios, but may be fine for underbalanced drilling operations. An interesting option to pursue in applications, is to allow the non-linear terms in the observer even though output injections are designed for the linearization.

## References


[1] D. L. Russell, "Controllability and stabilizability theory for linear partial differential equations: Recent progress and open questions," *SIAM Review*, vol. 20, no. 4, pp. 639–739, 1978.

[2] G. Bastin and J.-M. Coron, *Stability and boundary stabilization of 1-D hyperbolic systems*. Springer, 2016, vol. 88.

[3] A. Nikoofard, T. A. Johansen, and G.-O. Kaasa, "Nonlinear moving horizon observer for estimation of states and parameters in underbalanced drilling operations," in *ASME 2014 Dynamic Systems and Control Conference*. ASME, oct 2014.

[4] ——, "Reservoir characterization in under-balanced drilling using low-order lumped model," *Journal of Process Control*, vol. 62, pp. 24–36, feb 2018.

[5] G. Nygaard, G. Naedal, and S. Mylvaganam, "Evaluating nonlinear kalman filters for parameter estimation in reservoirs during petroleum well drilling," in *2006 IEEE Conference on Computer Aided Control System Design*. IEEE, oct 2006.

[6] M. Paasche, T. A. Johansen, and L. Imsland, "Regularized and adaptive nonlinear moving horizon estimation of bottomhole pressure during oil well drilling," *IFAC Proceedings Volumes*, vol. 44, no. 1, pp. 10 511–10 516, jan 2011.

[7] D. Sui, R. Nybø, G. Gola, D. Roverso, and M. Hoffmann, "Ensemble methods for process monitoring in oil and gas industry operations," *Journal of Natural Gas Science and Engineering*, vol. 3, no. 6, pp. 748–753, dec 2011.

[8] E. Hauge, O. M. Aamo, and J.-M. Godhavn, "Model-based estimation and control of in/out-flux during drilling," in *Proceeding of the 2012 American Control Conference*. IEEE, 2012, pp. 4909–4914.

[9] E. Hauge, O. Aamo, J.-M. Godhavn, and G. Nygaard, "A novel model-based scheme for kick and loss mitigation during drilling," *Journal of Process Control*, vol. 23, no. 4, pp. 463–472, 2013.

[10] J. Zhou, Ø. N. Stamnes, O. M. Aamo, and G.-O. Kaasa, "Switched control for pressure regulation and kick attenuation in a managed pressure drilling system," *IEEE Transactions on Control Systems Technology*, vol. 19, no. 2, pp. 337–350, 2011.

[11] ——, "Pressure regulation with kick attenuation in a managed pressure drilling system," in *Proceedings of the 48th IEEE Conference on Decision and Control and 28th Chinese Control Conference*. IEEE, 2009, pp. 5586–5591.

[12] R. J. Lorentzen, K. K. Fjelde, J. Frøyen, A. C. Lage, G. Nævdal, and E. H. Vefring, "Underbalanced and low-head drilling operations: Real time interpretation of measured data and operational support," in *SPE Annual Technical Conference and Exhibition*. Society of Petroleum Engineers, 2001.

[13] R. Lorentzen, G. Nævdal, and A. Lage, "Tuning of parameters in a two-phase flow model using an ensemble kalman filter," *International Journal of Multiphase Flow*, vol. 29, no. 8, pp. 1283–1309, aug 2003.

[14] A. Nikoofard, U. J. F. Aarsnes, T. A. Johansen, and G.-O. Kaasa, "Estimation of states and parameters of a drift-flux model with unscented kalman filter," *IFAC-PapersOnLine*, vol. 48, no. 6, pp. 165–170, 2015.

[15] F. Di Meglio, G.-O. Kaasa, N. Petit, and V. Alstad, "Slugging in multiphase flow as a mixed initial-boundary value problem for a quasilinear hyperbolic system," in *Proceedings of the 2011 American Control Conference*. IEEE, jun 2011.

[16] F. Di Meglio, "Dynamics and control of slugging in oil production," Theses, École Nationale Supérieure des Mines de Paris, July 2011.

[17] F. Di Meglio, R. Vazquez, M. Krstic, and N. Petit, "Backstepping stabilization of an underactuated $3\times3$ linear hyperbolic system of fluid flow equations," in *Proceedings of American Control Conference (ACC)*. IEEE, jun 2012.

[18] M. Krstic and A. Smyshlyaev, "Backstepping boundary control for first-order hyperbolic pdes and application to systems with actuator and sensor delays," *Systems & Control Letters*, vol. 57, no. 9, pp. 750 – 758, 2008.

[19] R. Vazquez, M. Krstic, and J.-M. Coron, "Backstepping boundary stabilization and state estimation of a $2\times2$ linear hyperbolic system," in *Proceedings of the 50th IEEE Conference on Decision and Control and European Control Conference*, Dec. 2011, pp. 4937–4942.

[20] L. Hu, F. Di Meglio, R. Vazquez, and M. Krstic, "Control of homodirectional and general heterodirectional linear coupled hyperbolic PDEs," *IEEE Transactions on Automatic Control*, vol. 61, no. 11, pp. 3301–3314, Nov. 2016.

[21] H. Anfinsen and O. M. Aamo, "Boundary parameter and state estimation in $2\times2$ linear hyperbolic PDEs using adaptive backstepping," in *Proceedings of the 55th Conference on Decision and Control*, 2016, pp. 2054–2060.

[22] O. M. Aamo, "Disturbance rejection in $2\times2$ linear hyperbolic systems," *IEEE Transactions on Automatic Control*, vol. 58, no. 5, pp. 1095–1106, 2013.

[23] H. Anfinsen, M. Diagne, O. M. Aamo, and M. Krstic, "An adaptive observer design for $n+1$ coupled linear hyperbolic PDEs based on swapping," *IEEE Transactions on Automatic Control*, vol. 61, no. 12, pp. 3979–3990, Dec. 2016.

[24] M. Bin and F. Di Meglio, "Boundary estimation of parameters for linear hyperbolic PDEs," *IEEE Transactions on Automatic Control*, vol. 62, no. 8, pp. 3890–3904, Aug 2017.

[25] F. Di Meglio, D. Bresch-Pietri, and U. J. F. Aarsnes, "An adaptive observer for hyperbolic systems with application to underbalanced drilling," *IFAC Proceedings Volumes*, vol. 47, no. 3, pp. 11 391 – 11 397, 2014, 19th IFAC World Congress.

[26] P. A. Ioannou and J. Sun, *Robust Adaptive Control*. Courier Corporation, 2012.

[27] H. Anfinsen and O. M. Aamo, "Adaptive output feedback stabilization of $n+m$ coupled linear hyperbolic PDEs with uncertain boundary conditions," *SIAM Journal on Control and Optimization*, vol. 55, no. 6, pp. 3928–3946, 2017.

[28] ——, "A note on establishing convergence in adaptive systems," *Automatica*, vol. 93, pp. 545–549, jul 2018.

## 2.4 Comments, flaws, limitations and further work

The swapping filters introduced in [67] are unnecessary. The states can be estimated in finite time using a clever restatement of the system and observer boundary condition. This is done in [68] in Chapter 4. The original bilinear boundary condition is still used when designing the adaptive laws, however.

In [61], it is suggested that the drift-flux model is linearized around a given operating profile and thereby in the form of the linear, $n + 1$, homo-directional, hyperbolic PDE considered in the paper. The validity of this linearized drift-flux model is questionable. As discussed in the last section of the paper, the linearized drift-flux model is certainly not sufficiently accurate to be used in a gas-kick scenario where the flow regime is fast changing. Even in under-balanced drilling where the flow regimes are more stable, any linearization must be carried out with care, and the boundaries of the operating envelope of the model must be investigated. If too narrow, the model might be useless in some scenarios.

# CHAPTER 3

# Fault estimation & localization using distributed sensing

## 3.1 Introduction

In the first paper [58], the annulus flow dynamics are modeled by the general single-phase model (1.16) with source terms (1.17). The pressure in the annulus is assumed measured using along-string pressure measurements and wired drill pipe. The dissipative structure of source terms and boundary conditions are utilized in an observer estimating the distributed flow in the annulus. In addition, the momentum balance source terms are modeled by a set of unknown parameters which can be used to model various drilling faults. The unknown parameters are estimated by a set of adaptive laws.

In the second paper [60], the method from [58], developed for single-phase $2 \times 2$ systems, is extended to general hetero-directional hyperbolic systems with general boundary structures.

In the third paper [64], the method from [58] is extended to allow parametric uncertainties also in the mass balance.

In the final fourth paper [63], the theoretical observer designs from [58, 60, 64] are applied to a drilling system and used to estimate a set of drilling faults.

## 3.2 Paper [58]: *An adaptive observer design for 2×2 semi-linear hyperbolic systems using distributed sensing*

Holta, H. and Aamo, O. M. (2019a). An adaptive observer design for 2 × 2 semi-linear hyberbolic systems using distributed sensing. In *Proceedings of the 2019 American Control Conference (ACC)*, pages 2540–2545

## 3.3 Paper [60]: *Observer design for a class of semi-linear hyperbolic PDEs with distributed sensing and parametric uncertainties*

Holta, H. and Aamo, O. M. (2019c). Observer design for a class of semi-linear hyperbolic PDEs with distributed sensing and parametric uncertainties. *Under review, IEEE Transactions on Automatic Control, submitted September 2019*

# Observer Design for a Class of Semi-linear Hyperbolic PDEs with Distributed Sensing and Parametric Uncertainties

Haavard Holta and Ole Morten Aamo

***Abstract*—We study a class of heterodirectional semi-linear hyperbolic PDEs where the distributed state vector is partially measured. An observer estimating the unmeasured part of the state vector is designed. The design is, for instance, applicable to multi-phase one-dimensional fluid models where the pressure is measured, but the distributed flow and phase-concentrations are not. Furthermore, the observer is extended to systems with parametric uncertainties appearing in the dynamics of the unmeasured part of the state. While required to be linear in the uncertain parameter, the uncertain term may be nonlinear in the state, even in the unmeasured part of the state. Terms of this type appear often in applications, and cover for instance viscous drag in fluid flow systems. A noteworthy property of the design is that convergence of the state estimate is achieved without requiring persistent excitation. Two example applications are presented and the design is illustrated in a simulation.**

## I. Introduction

### A. Motivation

Hyperbolic PDE systems are used to model various physical systems ranging from fluid flows in pipes, heat exchangers and electrical transmission lines to road traffic models (see [7] for an overview). In this paper, we consider a class of hyperbolic PDEs termed *systems of semi-linear balance laws*. They allow the source terms, which model in-domain production or consumption of the balanced quantities, to be nonlinear. Our main motivation for studying such systems comes from an application in oil and gas drilling, where the balanced quantities are mass and momentum of drilling mud, oil, gas, water, etc. inside the well bore-hole. Before casings are inserted into the bore-hole, the bottom section is open to the surrounding formations. Depending on the pressure in the well relative to the formation pressure, drilling fluids and formation fluids like oil, gas or water might flow either way, representing either a production or consumption of mass and momentum in the system modeling flow inside the bore-hole. A sufficiently accurate model capturing this relationship between well and formation pressure and resulting mass and momentum production or consumption can be very complex and nonlinear. Furthermore, even if the structure of the relationship is known, the exact parameters for a specific well might be unknown and even varying with operating conditions. For this reason we also study systems with linearly parametrized (non-linear) source terms where the parameters are assumed unknown.

The problem we study is state and parameter estimation. This is a challenging problem even for linear systems without parametric uncertainties. Observer design for hyperbolic systems are often based on the backstepping approach using boundary sensing. To tackle the semi-linear problem, we go one step further and assume that some in-domain measurements are available. That is, a part of the state is measured in the entire domain, while the rest of the state remains unmeasured. In the drilling application, so-called wired pipe technology allows a finite number of pressure sensors to be placed along the drill-string, providing in an approximate manner measurement of the pressure distribution in the well. The other part of the state vector, which is related to flow and concentration of each phase (oil,gas,water,mud etc.), is unmeasured, but observable. The theoretical results obtained in this paper have been applied in a simulation study in [15], demonstrating detection capability of various important fault scenarios in oil well drilling by means of state and parameter estimation exploiting wired pipe technology. In what follows, the class of systems considered contains the drilling application, but is more general with an arbitrary number of states convecting in each direction through the domain.

The authors are with the Department of Engineering Cybernetics. Norwegian University of Science and Technology, Trondheim N-7491, Norway (e-mail: haavard.holta@ntnu.no; aamo@ntnu.no).

Economic support from The Research Council of Norway and Equinor ASA through project no. 255348/E30 Sensors and models for improved kick/loss detection in drilling (Semi-kidd) is gratefully acknowledged.

### B. Notation

A function $u:[0,1]\to\mathbb{R}^n$ is said to be in $L_2([0,1],\mathbb{R}^n)$ if

$$\sqrt{\int_0^1 u^T(x)u(x)dx}<\infty. \tag{1}$$

For $u_1,u_2\in L_2([0,1],\mathbb{R}^n)$ the inner product is

$$\langle u_1,u_2\rangle := \int_0^1 u_1^T(x)u_2(x)dx \tag{2}$$

with the associated norm $||u||=\sqrt{\langle u,u\rangle}$. Furthermore, for a function $u:[0,1]\times\mathbb{R}^+\to\mathbb{R}^n$, we denote by $u(\cdot,t)$ the function $[0,1]\to\mathbb{R}^n$ obtained from $u$ at $t$, and by $u(x,\cdot)$ the function $\mathbb{R}^+\to\mathbb{R}^n$ obtained from $u$ at $x$. For convenience, we will sometimes omit the arguments. In particular, we will sometimes write $||u||$ for the scalar-valued function of time $||u(\cdot,t)||$, and $\phi(y,z)$ instead of $\phi(y(x,t),z(x,t),x)$.

For $f:[0,\infty)\to\mathbb{R}$, we use the spaces

$$f\in\mathscr{L}_p \leftrightarrow \left(\int_0^\infty |f(t)|^p dt\right)^{\frac{1}{p}}<\infty \tag{3}$$

for $p\geq 1$ with the particular case $f\in\mathscr{L}_\infty\leftrightarrow \sup_{t\geq 0}|f(t)|<\infty$.

The notation $f\to 0$ means that $f$ converges to zero as time goes to infinity, i.e. $\lim_{t\to\infty} f(t)=0$.

The partial derivative of a function is denoted with a subscript, for example $u_t(x,t)=\frac{\partial}{\partial t}u(x,t)$. For a function of one variable, the derivative is denoted using a prime, that is $f'(x)=\frac{d}{dx}f(x)$. The dot notation is reserved for the derivative of functions of time only; $\dot{f}(t)=\frac{d}{dt}f(t)$.

# 3. FAULT ESTIMATION & LOCALIZATION USING DISTRIBUTED SENSING

An operator $\Xi : L_2([0,1],\mathbb{R}^n) \to \mathbb{R}$ is called *Fréchet differentiable* at $u \in L_2([0,1],\mathbb{R}^n)$ if there exists a bounded linear operator $\mathscr{D}_u\Xi : L_2([0,1],\mathbb{R}^n) \to \mathbb{R}$ such that

$$\lim_{h\to 0} \frac{|\Xi[u+h] - \Xi[u] - \mathscr{D}_u\Xi[h]|}{||h||} = 0 \tag{4}$$

for $h \in L_2([0,1],\mathbb{R}^n)$. If there exist bounded linear operators $\mathscr{D}^a_{(a,b)}\Xi : L_2([0,1],\mathbb{R}^m) \to \mathbb{R}$ and $\mathscr{D}^b_{(a,b)}\Xi : L_2([0,1],\mathbb{R}^{n-m}) \to \mathbb{R}$ such that

$$\lim_{h_1\to 0} \frac{|\Xi[(a+h_1,b)] - \Xi[(a,b)] - \mathscr{D}^a_{(a,b)}\Xi[h_1]|}{||h_1||} = 0 \tag{5a}$$

$$\lim_{h_2\to 0} \frac{|\Xi[(a,b+h_2)] - \Xi[(a,b)] - \mathscr{D}^b_{(a,b)}\Xi[h_2]|}{||h_2||} = 0 \tag{5b}$$

for $a, h_1 \in L_2([0,1],\mathbb{R}^m)$ and $b, h_2 \in L_2([0,1],\mathbb{R}^{n-m})$ we call $\mathscr{D}^a_{(a,b)}\Xi$ and $\mathscr{D}^b_{(a,b)}\Xi$ the *Fréchet partial derivatives* of $\Xi$ at $(a,b)$ with respect to $a$ and $b$ respectively. If the operators exist, they are unique.

### C. Problem statement

We study a class of $n \times n$ semi-linear heterodirectional hyperbolic systems where an $m$-dimensional part of the state vector is measured. Consider

$$y_t(x,t) + Ay_x(x,t) + Bz_x(x,t) = f(y(x,t),x) \tag{6a}$$

$$z_t(x,t) + Cy_x(x,t) + Dz_x(x,t) = g(y(x,t),x) + \phi(y(x,t),z(x,t),x)\theta \tag{6b}$$

where $y : [0,1]\times\mathbb{R}^+ \to \mathbb{R}^m$ is the measured part of the state and $z : [0,1]\times\mathbb{R}^+ \to \mathbb{R}^{n-m}$ is the unmeasured part of the state. The known functions $f : \mathbb{R}^m \times [0,1] \to \mathbb{R}^m$, $g : \mathbb{R}^m \times [0,1] \to \mathbb{R}^{n-m}$ and $\phi : \mathbb{R}^m \times \mathbb{R}^{n-m} \times [0,1] \to \mathbb{R}^{(m-n)\times q}$ together with the potentially uncertain parameter $\theta \in \mathbb{R}^q$ define the source terms, and may be nonlinear. The system coefficient matrix

$$\begin{bmatrix} A & B \\ C & D \end{bmatrix} \tag{7}$$

is nonsingular with $n$ real, distinct, eigenvalues so that (6) is strictly hyperbolic with non-zero characteristic speeds. Although the method can be extended to spatially varying coefficient matrices, for simplicity the method is derived assuming constant matrices.

To estimate the unmeasured state $z$ based on measurements $y$ we rely on the following observability condition.

**Assumption 1.** *The pair $(D,B)$ is observable.*

A complicating factor is that the uncertainty $\phi((y(x,t),z(x,t)),x)\theta$ appears in the *unmeasured dynamics* (6b) and depends on the unmeasured state $z$. Dealing with uncertainties appearing in this way is difficult even for the ODE case [22], [23]. The regressor $\phi$ and source terms $f$ and $g$ are known functions and satisfy the following assumption.

**Assumption 2.** *For all $(y,z) \in L_2([0,1],\mathbb{R}^n)$, we have*

$$(f(y,\cdot),g(y,\cdot)) \in L_2([0,1],\mathbb{R}^n), \tag{8}$$

$$\phi((y,z),\cdot) \in L_2([0,1],\mathbb{R}^{(n-m)\times q}) \tag{9}$$

*and*

$$||(y,z)|| \in \mathscr{L}_\infty \Rightarrow ||f(y,\cdot)||, ||g(y,\cdot))||, ||\phi((y,z),\cdot)|| \in \mathscr{L}_\infty. \tag{10}$$

*Furthermore, in the analysis that follows we will require that the uncertain term $\phi(y,z,x)\theta$ satisfy a* monotone damping property *specified by the sector condition*

$$(z_1 - z_2)^T Q(x)(\phi(y,z_1,x) - \phi(y,z_2,x))\theta \le 0 \tag{11}$$

*for all $y \in \mathbb{R}^m$, $z_1, z_2 \in \mathbb{R}^{n-m}$ and $x \in [0,1]$, where $Q(x)$ is a symmetric positive definite matrix ($Q(x) > 0$ for all $x \in [0,1]$) that will be further characterized in the next section.*

**Remark 1.** *For the special case when $Q(x)$ is diagonal, and the $i^{th}$ row of $\phi(y,z,x)$, denoted $\phi_i$, depends only on the $i^{th}$ element of $z$, denoted $z_i$, then the sector conditions are separated and can be written element-wise as*

$$\phi_i(y,z_{1,i},x)\theta - \phi_i(y,z_{2,i},x)\theta \le z_{1,i} - z_{2,i} \tag{12}$$

*for any $y \in \mathbb{R}^m$, $z_{1,i}, z_{2,i} \in \mathbb{R}$, $x \in [0,1]$, and $i = 1,\ldots,n-m$. Condition* (12) *implies that $\phi_i(y,z_i,x)\theta$ is monotonic in $z_i$, and is satisfied for a large class of passive elements, for example resistive loads in transmission lines in terms of electric current or friction loss in fluid flows in terms of volumetric flow.*

The observer design in this paper is valid for a broad range of boundary conditions and boundary measurements which will be specified later (Assumption 3). For now we assume that the associated Cauchy problem for (6) with a given set of boundary conditions and initial conditions

$$y(x,0) =: y_{ic}(x) \tag{13a}$$

$$z(x,0) =: z_{ic}(x) \tag{13b}$$

with $(y_{ic}, z_{ic}) \in L_2([0,1],\mathbb{R}^n)$, has a unique solution $(y,z)(\cdot,t) \in L_2([0,1],\mathbb{R}^n)$ for all $t \ge 0$.

### D. Background and previous work

In recent years, the infinite dimensional *backstepping* approach has become a popular method for observer design using boundary sensing. The method was originally developed for parabolic PDEs and has been extended to $2\times 2$ and general $m+n$ linear hyperbolic systems in [27] and [16], respectively. Local results for quasilinear systems using the same approach was presented in [26], [17]. A global result was presented in [24] for semi-linear systems and for quasi-linear systems in [25], both using a method where the solution are predicted along each characteristic. Adaptive estimation and control of linear hyperbolic systems with uncertain boundary parameters are extensively studied in [3], with the most relevant result for state and boundary parameter estimation first presented in [4] for $n+1$ systems and [5] for $m+n$ linear systems. Estimation of uncertain source terms are also studied in [3], but these results either require full state measurements [1], or rely on transformations involving the unknown parameters into so-called *canonical* form such that true state estimates can only be reconstructed if the system is *persistently excited* [2], [8]. Adaptive output feedback estimation of semi-linear systems without relying on PE, seems to be a challenging

topic. Transformations into canonical forms have also been used to design observers for non-linear ODEs. All systems that can be observed using such canonical transformations are characterized in [20], [21]. Provided the systems satisfies a *uniform observability* condition [12], the high-gain approach can be used to design adaptive observer [9], [13]. The extension to hyperbolic systems was presented in [18] for systems with distributed state measurements. Various results using semigroup-based methods for observer design of hypertbolics systems with distributed measurements has also been investigated [10]. For systems with non-linear terms satisfying a sector condition, stability can be proved using a passivity argument without relying on any dominating input gain [6]. This approach was used in [22], [23] to design adaptive observers for finite dimensional systems, and recently for a $2\times 2$ hyperbolic system in [14].

### *E. Contribution and paper structure*

We extend the result from [14] in several directions. Firstly, the method is extended to general hetero-directional systems and the special coefficient matrix in [14] is replaced by a general observability condition. Secondly, we study more general source terms all depending on the measured state $y$. Thirdly, since measurements might be corrupted by noise, to which reduced order designs are sensitive, we replace the reduced order observer in [14] by a full state observer including filtering of the $y$-dynamics. Lastly, the boundary conditions and boundary measurements are generalized.

In Section II, we first consider the non-adaptive state estimation problem with $\theta$ known. Then, in Section III we study the full adaptive state and parameter estimation problem assuming uncertain $\theta$. A simulation example is presented in Section IV.

## II. Non-adaptive state estimation

To estimate the unknown state component $z$, we utilize the $y$-measurements and define a coordinate transformation $(y,z)\mapsto P(y,z)$ of the form

$$P := \begin{bmatrix} P_1 & 0 \\ P_2 L & P_2 \end{bmatrix}. \tag{14}$$

**Lemma 1.** *For any diagonal $\Lambda_1\in\mathbb{R}^{m\times m}$ and $\Lambda_2\in\mathbb{R}^{(n-m)\times(n-m)}$ with distinct entries, and any $\bar C\in\mathbb{R}^{(n-m)\times m}$, there exist matrices $K_1\in\mathbb{R}^{m\times m}$, $K_2\in\mathbb{R}^{(n-m)\times m}$, $L\in\mathbb{R}^{(n-m)\times m}$ and $\operatorname{diag}(P_1,P_2)\in\mathbb{R}^{n\times n}$ such that $[\alpha,\beta]^T := P[y,z]^T$ maps system (6) into*

$$\alpha_t+\Lambda_1\alpha_x+\bar B\beta_x = \bar f(\alpha,x)-\bar K_1\alpha_x \tag{15a}$$
$$\beta_t+\bar C\alpha_x+\Lambda_2\beta_x = \bar g(\alpha,x)+\bar\phi((\alpha,\beta),x)\theta-\bar K_2\alpha_x \tag{15b}$$
$$(\alpha(x,0),\beta(x,0)) = P(y_{ic}(x),z_{ic}(x)) \tag{15c}$$

*where*

$$\bar K_1 = P_1K_1P_1^{-1},\quad \bar B = P_1BP_2^{-1} \tag{16a}$$
$$\bar K_2 = P_2K_2P_1^{-1},\quad \bar C = P_2(C-(D+LB)L+LA-K_2)P_1 \tag{16b}$$

*and*

$$\begin{bmatrix}\bar f(\alpha,x)\\ \bar g(\alpha,x)\end{bmatrix} = P\begin{bmatrix} f(P_1^{-1}\alpha,x)\\ g(P_1^{-1}\alpha,x)\end{bmatrix} \tag{17}$$
$$\bar\phi((\alpha,\beta),x) = P_2\phi(P^{-1}(\alpha,\beta),x). \tag{18}$$

*Proof.* Pre-multiplying equation (6) by $P$, inserting $[y,z]^T = P^{-1}[\alpha,\beta]^T$ and then subtracting $[\bar K_1,\bar K_2]^T\alpha_x$ from both sides yield (15)–(18) where

$$\begin{bmatrix}\Lambda_1 & \bar B\\ \bar C & \Lambda_2\end{bmatrix} := P\begin{bmatrix}A & B\\ C & D\end{bmatrix}P^{-1} - \begin{bmatrix}\bar K_1 & 0\\ \bar K_2 & 0\end{bmatrix} = \begin{bmatrix} P_1(A-BL-K_1)P_1^{-1} & P_1BP_2^{-1}\\ P_2(C-(D+LB)L+LA-K_2)P_1^{-1} & P_2(D+LB)P_2^{-1}\end{bmatrix}. \tag{19}$$

Since $(D,B)$ is observable (Assumption 1), there exists $L$ such that the eigenvalues of $D+LB$ correspond to the entries in $\Lambda_2$. Since the entries in $\Lambda_2$ are distinct, $D+LB$ is diagonalizable and $P_2$ exists such that $\Lambda_2 = P_2(D+LB)P_2^{-1}$. We then select $K_1$ such that $A-BL-K_1$ has eigenvalues corresponding to the entries in $\Lambda_1$. Since the entries in $\Lambda_1$ are distinct, $A-BL-K_1$ is diagonalizable and $P_1$ exists such that $\Lambda_1 = P_1(A-BL-K_1)P_1^{-1}$. □

The significance of (15) is that the eigenvalues of $\Lambda_2$ for the $\beta$-subsystem (15b) can be specified as desired. To shape the system's dependence on $\alpha$, we rely on the measurements and design an observer with output injection terms in $\alpha_x = P_2y_x$ and scaled by the *output injection gains* $(K_1,K_2)$. We suggest the following observer for the $(\alpha,\beta)$-system:

$$\hat\alpha_t+\Lambda_1\hat\alpha_x+\bar B\hat\beta_x = \bar f(\alpha,x)-\bar K_1\alpha_x \tag{20a}$$
$$\hat\beta_t+\bar C\hat\alpha_x+\Lambda_2\hat\beta_x = \bar g(\alpha,x)+\bar\phi((\alpha,\hat\beta),x)\hat\theta-\bar K_2\alpha_x \tag{20b}$$
$$\hat\alpha(x,0) = \hat\alpha_{ic}(x) \tag{20c}$$
$$\hat\beta(x,0) = \hat\beta_{ic}(x), \tag{20d}$$
$$(\hat y(x,t),\hat z(x,t)) = P^{-1}(\hat\alpha(x,t),\hat\beta(x,t)) \tag{20e}$$

where $(\hat\alpha_{ic},\hat\beta_{ic})\in L_2([0,1],\mathbb{R}^n)$ and $\hat\theta(t)\in\mathbb{R}^q$ is the parameter estimate. Remark that $\hat\theta=\theta$ for the non-adaptive case studied in this section. But since the observer equations (20) is being reused in the next section where $\theta$ is assumed unknown, the notation $\hat\theta$ is used.

The estimation error $\tilde\alpha := \alpha-\hat\alpha$ and $\tilde\beta := \beta-\hat\beta$ satisfy

$$\tilde\alpha_t+\Lambda_1\tilde\alpha_x+\bar B\tilde\beta_x = 0 \tag{21a}$$
$$\tilde\beta_t+\bar C\tilde\alpha_x+\Lambda_2\tilde\beta_x = \tilde\phi(\alpha,\beta,\tilde\beta,x)\theta+\bar\phi((\alpha,\hat\beta),x)\tilde\theta \tag{21b}$$
$$\tilde\alpha(x,0) = \tilde\alpha_{ic}(x) := \alpha_{ic}(x)-\hat\alpha_{ic}(x) \tag{21c}$$
$$\tilde\beta(x,0) = \tilde\beta_{ic}(x) := \beta_{ic}(x)-\hat\beta_{ic}(x) \tag{21d}$$
$$(\tilde y(x,t),\tilde z(x,t)) = P^{-1}(\tilde\alpha(x,t),\tilde\beta(x,t)). \tag{21e}$$

where $\tilde\theta=\theta-\hat\theta$ and

$$\tilde\phi(\alpha,\beta,\tilde\beta,x) := \bar\phi((\alpha,\beta),x)-\bar\phi((\alpha,\beta-\tilde\beta),x). \tag{22}$$

where

$$\tilde\beta^T\bar Q(x)\tilde\phi(\alpha,\beta,\tilde\beta,x)\theta \le 0 \tag{23}$$

as can be seen from Assumption 2 with $y=P_1^{-1}\alpha$, $z_1 = -LP_1^{-1}\alpha+P_2^{-1}\beta$, $z_2 = -LP_1^{-1}\alpha+P_2^{-1}\hat\beta$ and $\bar Q(x) = P_2^{-T}Q(x)P_2^{-1}$.

**Remark 2.** *Even though $\alpha(\cdot,t)$ is measured, we include an observer for the $\alpha$-dynamics and achieve some robustness with respect to measurement noise and modeling errors. The injection gains add some degrees of freedom in that $K_1$ specifies the convergence rate of $\tilde{\alpha}$ and $K_2$ can be used to achieve anywhere between zero and full cancellation of the $\bar{C}\tilde{\alpha}_x$ coupling term. Note also that for each $t \geq 0$, the signal $\alpha(x,t)$, which is a linear combination of $y(x,t)$, is causal for all $x \in [0,1]$ and delay-free filtering techniques can be applied to suppress noise and estimate $\alpha_x(x,t)$ for all $x \in [0,1]$.*

To characterize the boundaries, let

$$\Pi_1 := \begin{bmatrix} E_1^+ \\ E_1^- \end{bmatrix} \in \mathbb{R}^{m\times m}, \quad \Pi_2 := \begin{bmatrix} E_2^+ \\ E_2^- \end{bmatrix} \in \mathbb{R}^{(n-m)\times(n-m)} \tag{24}$$

be permutation matrices such that

$$E_1^+\Lambda_1(E_1^+)^T \succ 0, \quad E_1^-\Lambda_1(E_1^-)^T \prec 0 \tag{25}$$

and

$$E_2^+\Lambda_2(E_2^+)^T \succ 0, \quad E_2^-\Lambda_2(E_2^-)^T \prec 0. \tag{26}$$

As mentioned in the introduction, the observer design in this paper is valid for a broad range of boundary conditions and boundary measurements. We will thus not state explicit boundary conditions for either the system (15) nor the observer system (20) directly. Instead, to proceed with the stability analysis of (21), for the $\tilde{\beta}$ dynamics, we assume the following.

**Assumption 3.** *The boundary condition is* dissipative *in the sense that*

$$\tilde{\beta}^T(x,t)\bar{Q}(x)\Lambda_2\tilde{\beta}(x,t)\Big|_{x=0}^{x=1} \leq 0 \tag{27}$$

*for all $t \geq 0$. Furhteremore, the state estimation error system* (21) *with the selected boundary conditions, is well-posed.*

For the $\tilde{\alpha}$-subsystem, since $y(x,t)$ is measured for all $x \in [0,1]$ we have the additional freedom of specifying zero boundary conditions by choosing $E_1^+P_1^{-1}\hat{y}(0,t) = E_1^+P_1^{-1}y(0,t)$ and $E_1^-P_1^{-1}\hat{y}(1,t) = E_1^-P_1^{-1}y(1,t)$. We can thus select $E_1^+\hat{\alpha}(0,t)$ and $E_1^-\hat{\alpha}(1,t)$ such that

$$E_1^+\tilde{\alpha}(0,t) = E_1^-\tilde{\alpha}(1,t) = 0. \tag{28}$$

Before proceeding with the stability analysis, we provide two examples of boundary conditions satisfying Assumption 3.

**Example 1.** *For each element $\beta_i$ in $\beta$, measurements are available at least on one of the boundaries. That is, for $i = 1,\ldots,n$, $\beta_i(0,t)$ and/or $\beta_i(1,t)$ are measured. For each diagonal element $\lambda_{2,i}$ in $\Lambda_2$, we select $\lambda_{2,i} > 0$ if $\beta_i(0,t)$ is measured and $\lambda_{2,i} < 0$ if $\beta_i(1,t)$ is measured. A well posed estimation error system is then constructed by selecting boundary conditions for the observer as $E_2^+\hat{\beta}(0,t) = E_2^+\beta(0,t)$ and $E_2^-\hat{\beta}(1,t) = E_2^-\beta(1,t)$, so that Assumption 3 holds trivially with*

$$E_2^+\tilde{\beta}(0,t) = E_2^-\tilde{\beta}(1,t) = 0 \tag{29}$$

.

**Example 2.** *Suppose the boundary functions are linear and have the form*

$$\begin{bmatrix} E_2^+\tilde{\beta}(0,t) \\ E_2^-\tilde{\beta}(1,t) \end{bmatrix} = H \begin{bmatrix} E_2^-\tilde{\beta}(0,t) \\ E_2^+\tilde{\beta}(1,t) \end{bmatrix} \tag{30}$$

*with $H \in \mathbb{R}^{(n-m)\times(n-m)}$ satisfying*

$$\inf\left\{||\Delta H\Delta^{-1}||_2, \Delta \in \mathscr{D}_{n-m}^+\right\} < 1 \tag{31}$$

*where $\mathscr{D}_n^+$ denotes the set of diagonal strictly positive matrices in $\mathbb{R}^{n\times n}$. Then by [11, Theorem 2.3], Assumption 3 is satisfied.*

To study the stability of the state estimation error system (21), consider the Lyapunov function candidate

$$V_0 = \frac{1}{2}\int_0^1 \alpha^T W_1(x)\alpha dx + \int_0^1 \tilde{\beta}^T W_2(x)\tilde{\beta}dx \tag{32}$$

where $W_i(x)$ are positive definite diagonal matrices for all $x \in [0,1]$ and such that (23) holds with $\bar{Q}(x) = W_2(x)$. In addition, we impose the restriction

$$W_i'(x) = -c_1 W_i(x)\Lambda_i^{-1}, \quad i,j = 1,2 \tag{33}$$

for all $x \in [0,1]$ for some $c_1 > 0$. Differentiating (32) with respect to time gives

$$\begin{aligned}\dot{V}_0 = &-\int_0^1 \tilde{\alpha}^T W_1(x)(\Lambda_1\tilde{\alpha}_x + \bar{B}\tilde{\beta}_x)dx \\ &-\int_0^1 (\Lambda_1\tilde{\alpha}_x + \bar{B}\tilde{\beta}_x)^T W_1(x)\tilde{\alpha}dx \\ &-\int_0^1 \tilde{\beta}^T W_2(x)(\Lambda_2\tilde{\beta}_x + \bar{C}\tilde{\alpha}_x)dx \\ &-\int_0^1 (\Lambda_2\tilde{\beta}_x + \bar{C}\tilde{\alpha}_x)^T W_2(x)\tilde{\beta}dx \\ &+\int_0^1 \tilde{\beta}^T W_2(x)\tilde{\phi}(\alpha,\beta,\tilde{\beta},x)\theta dx \\ &+\int_0^1 \tilde{\beta}^T W_2(x)\bar{\phi}((\alpha,\hat{\beta}),x)\tilde{\theta}dx.\end{aligned} \tag{34}$$

Integrating by parts and using (33) yield

$$\begin{aligned}\dot{V}_0 = &-\left[\tilde{\alpha}^T W_1(x)(\Lambda_1\tilde{\alpha} + \bar{B}\tilde{\beta}) + \tilde{\beta}^T W_2(x)(\Lambda_2\tilde{\beta} + \bar{C}\tilde{\alpha})\right]_{x=0}^{x=1} \\ &-c_1\int_0^1 \tilde{\alpha}^T W_1(x)(\tilde{\alpha} + \Lambda_1^{-1}\bar{B}\tilde{\beta}) + \tilde{\beta}^T W_2(x)(\tilde{\beta} + \Lambda_2^{-1}\bar{C}\tilde{\alpha})dx \\ &-c_1\int_0^1 (\tilde{\alpha} + \Lambda_1^{-1}\bar{B}\tilde{\beta})^T W_1(x)\tilde{\alpha} + (\tilde{\beta} + \Lambda_2^{-1}\bar{C}\tilde{\alpha})^T W_2(x)\tilde{\beta}dx \\ &+\int_0^1 \tilde{\beta}^T W_2(x)\tilde{\phi}(\alpha,\beta,\tilde{\beta},x)\theta dx \\ &+\int_0^1 \tilde{\beta}^T W_2(x)\bar{\phi}((\alpha,\hat{\beta}),x)\tilde{\theta}dx.\end{aligned} \tag{35}$$

The second and third term are quadratic in $(\tilde{\alpha},\tilde{\beta})$ and since the products $\Lambda_1^{-1}\bar{B}$ and $\Lambda_2^{-1}\bar{C}$ can be made arbitrary small by selecting sufficiently large $\Lambda_1$ and $\Lambda_2$, we have

$$\begin{aligned}&c_1\begin{bmatrix} 2W_1(x) & W_1\Lambda_1^{-1}\bar{B} + \bar{C}^T\Lambda_2^{-1}W_2(x) \\ W_2(x)\Lambda_2^{-1}\bar{C} + \bar{B}^T\Lambda_1^{-1}W_1(x) & 2W_2(x)\end{bmatrix} \\ &-c_2\mathrm{diag}(W_1,W_2) \succeq 0.\end{aligned} \tag{36}$$

for sufficiently large $\Lambda_1$ and $\Lambda_2$ and some $c_2 > 0$. The boundary terms, quadratic in $(\tilde{\alpha}(1,t),\tilde{\beta}(1,t)$ and $(\tilde{\alpha}(0,t),\tilde{\beta}(0,t)$, are rewritten using the definitions (24) and boundary conditions (28) as a term quadratic in $(E_1^+\tilde{\alpha}(1,t),E_1^-\tilde{\alpha}(0,t)),\tilde{\beta}(1,t),\tilde{\beta}(0,t))$ with coefficient matrix

$$G = \begin{bmatrix} G_{11} & G_{12} \\ G_{21} & G_{22}\end{bmatrix} \tag{37}$$

$$G_{11} = \text{diag}(2E_1^+ W_1(1)\Lambda_1(E_1^+)^T, -2E_1^- W_1(0)\Lambda_1(E_1^-)^T) \quad (38)$$
$$G_{12} = G_{12}^T = \text{diag}(E_1^+(W_1(1)\bar{B} + \bar{C}^T W_2(1)), - E_1^-(W_1(0)\bar{B} + \bar{C}^T W_2(0))) \quad (39)$$
$$G_{22} = \text{diag}(2W_2(1)\Lambda_2, -2W_2(0)\Lambda_2). \quad (40)$$

By (25) and commutativity of $W_1$ and $\Lambda_1$, $G_{11} \succ 0$. By Assumption 3 , commutativity of $W_2$ and $\Lambda_2$ and since $W_2(x)$ is selected such that (27) holds with $W_2(x) = \bar{Q}$ for all $x \in [0,1]$, $G_{22} \succeq 0$. And again, there exist some $\Lambda_1$ and $\Lambda_2$ such that $G \succeq 0$. Non-positivity of the two quadratic terms along with property (23) then yield

$$\dot{V}_0 \leq -c_2 V_0 + \int_0^1 \tilde{\beta}^T W_2(x)\tilde{\phi}((\alpha,\hat{\beta}),x)\tilde{\theta}dx. \quad (41)$$

Summarizing for the non-adaptive case $\tilde{\theta} = 0$ where $\dot{V}_0 \leq -c_2 V_0$, we obtain the following intermediate result.

**Proposition 1.** *Consider the error dynamics* (21) *with boundary conditions satisfying Assumption 3 and* (28)*, let* $\tilde{\theta} = 0$*, and suppose that there exist* $\Lambda_1, W_1(x) \in \mathbb{R}^{m\times m}$ *and* $\Lambda_2, W_2(x) \in \mathbb{R}^{(n-m)\times(m-n)}$ *such that:*

1) *The error dynamics* (21) *with boundary conditions is well posed.*
2) $\Lambda_1$ *and* $\Lambda_2$ *are diagonal with distinct entries and sufficiently large to satisfy* (36)*.*
3) $W_1(x)$ *and* $W_2(x)$ *are diagonal positive definite and satisfy* (33) *for all* $x \in [0,1]$*.*
4) *Inequality* (23) *and Assumption 3 hold for all* $x \in [0,1]$ *with* $\bar{Q}(x) = W_2(x)$*.*

*Then, the origin of* (21) *is exponentially stable in the* $L_2$*-norm, implying that*

$$||\bar{y}||, ||\bar{z}|| \to 0 \quad (42)$$

*exponentially fast.*

**Remark 3.** *If the source terms* $f$ *and* $g$ *are functions of the unknown state* $z$ *and satisfy the sector condition*

$$\begin{bmatrix} y_1 - y_2 \\ z_1 - z_2 \end{bmatrix}^T Q \begin{bmatrix} f((y_i,z_i),x)|_{i=1}^{i=2} \\ g((y_i,z_i),x)|_{i=1}^{i=2} + \phi((y_i,z_i),x)\theta|_{i=1}^{i=2} \end{bmatrix} \leq 0 \quad (43)$$

*we claim that a result, similar to Proposition 1 can be shown for the non-adaptive case. However, the stability proof would be tedious, i.e. involving a non-diagonal Lyapunov function, so to simplify the presentation we omit this extension. In addition, the extension is non-trivial in the adaptive case studied in the next section.*

## III. Adaptive state and parameter estimation

For the following analysis, we restrict boundary conditions to be in the form considered in Example 1, that is

**Assumption 4.**

$$E_2^+ \tilde{\beta}(0,t) = E_2^- \tilde{\beta}(1,t) = 0. \quad (44)$$

### A. Adaptive law

To make the state estimator robust to parametric uncertainties, we need a scheme to update the parameter estimate $\hat{\theta}$. We augment the Lyapunov function candidate with terms quadratic in the parameter estimation error and select the adaptive law using a passivity argument: Let

$$V = V_0 + \frac{1}{2}\tilde{\theta}^T \Gamma^{-1}\tilde{\theta} \quad (45)$$

where $\Gamma$ is the adaptation gain.

**Lemma 2.** *Consider the error dynamics* (21) *with boundary conditions satisfying Assumption 3 and* (28)*, and the adaptive law*

$$\dot{\hat{\theta}} = \Gamma \int_0^1 \tilde{\phi}^T((\alpha,\hat{\beta}),x)W_2(x)\tilde{\beta}dx \quad (46)$$

*for any initial estimate* $\hat{\theta}(0) = \hat{\theta}_0$ *and diagonal* $\Gamma > 0$*, and suppose the conditions of Proposition 1 hold. Then,*

$$\hat{\theta} \in \mathscr{L}_\infty \quad (47a)$$
$$||\bar{y}||, ||\bar{z}|| \in \mathscr{L}_2 \cap \mathscr{L}_\infty. \quad (47b)$$

*Moreover, if* $||(y,z)||$ *is bounded, then*

$$\dot{\hat{\theta}} \in \mathscr{L}_2 \cap \mathscr{L}_\infty \quad (48a)$$
$$||\bar{y}||, ||\bar{z}|| \to 0. \quad (48b)$$

*Proof.* Differentiating (45) with respect to time yields

$$\dot{V} = \dot{V}_0 - \dot{\hat{\theta}}^T \Gamma^{-1}\tilde{\theta}. \quad (49)$$

Selecting the adaptive law according to (46) cancels the last term in (41) and renders the Lyapunov function negative semidefinite with upper bound

$$\dot{V} \leq -cV_0 \quad (50)$$

so that $||\tilde{\alpha}||, ||\tilde{\beta}||, \tilde{\theta} \in \mathscr{L}_\infty$ follows. Furthermore, from $V > 0, \dot{V} \leq 0$ we have that $\lim_{t\to\infty} V(t) = V(\infty)$ exists and therefore

$$c\int_0^\infty V_0(t)dt \leq V(0) - V(\infty) \quad (51)$$

which implies $||\tilde{\alpha}||, ||\tilde{\beta}|| \in \mathscr{L}_2$. From (46), we have that $|\dot{\hat{\theta}}| \leq ||\Gamma||||W_2||||\tilde{\beta}||||\bar{\phi}(\alpha,\hat{\beta},\cdot)|| \leq ||\Gamma||||W_2||||\tilde{\beta}||||R_2 P||||\phi((y,\hat{z}),\cdot)||$. So, if in addition $||(y,z)|| \in \mathscr{L}_\infty$, $||\tilde{z}|| \leq ||z|| + ||\bar{z}||$ is bounded which in turn implies boundedness of $||\bar{\phi}||$ by Assumption 2 and (48a) follows. Lastly, from (49) and (50) we get

$$\dot{V}_0 \leq -cV_0 + \dot{\hat{\theta}}^T \Gamma^{-1}\tilde{\theta} \quad (52)$$

which shows that $\dot{V}_0(t)$ is upper bounded by some constant. By Lemma 6 (see appendix) $V_0 \to 0$ and in turn $||\tilde{\alpha}||, ||\tilde{\beta}|| \to 0$ or equivalently (48b). □

It is clear that the adaptive law cannot be implemented in the form (46), since $\tilde{\beta}$ is not available. To solve that problem, we borrow an idea from [22], [23] and design an alternative way of computing (46) that relies only on measured quantities. For each column vector $\bar{\phi}_i$ in $\bar{\phi}$, parameter $\hat{\theta}_i$ in $\hat{\theta}$ and diagonal

element $\gamma_i$ in $\Gamma$, $i = 1, ..., q$, the adaptive law (46) can be written in the form

$$\dot{\hat{\theta}}_i = -\dot{\tilde{\theta}}_i = -\gamma_i \langle W_2 \bar{\phi}_i((\alpha,\hat{\beta}),\cdot), \tilde{\beta}\rangle \tag{53}$$

where the first term in the inner product can be separated, by applying (24), as

$$\begin{aligned} W_2(x)\bar{\phi}_i((\alpha,\hat{\beta}),x) &= \Pi_2^T \Pi_2 W_2(x)\bar{\phi}_i((\alpha,\hat{\beta}),x) \\ &= \Pi_2^T \begin{bmatrix} E_2^+ W_2(x)\bar{\phi}_i((\alpha,\hat{\beta}),x) \\ E_2^- W_2(x)\bar{\phi}_i((\alpha,\hat{\beta}),x) \end{bmatrix}. \end{aligned} \tag{54}$$

To ease the notation, for $u \in L_2([0,1],\mathbb{R}^n)$ let

$$\Phi_i[u](x) := \Pi_2^T \begin{bmatrix} -\int_x^1 E_2^+ W_2(\xi)\bar{\phi}_i(u,\xi)d\xi \\ \int_0^x E_2^- W_2(\xi)\bar{\phi}_i(u,\xi)d\xi \end{bmatrix} \tag{55}$$

so that by differentiating (55) evaluated at $u = (\alpha,\hat{\beta})$, (53) can be written as

$$\dot{\tilde{\theta}}_i = -\gamma_i \langle (\Phi_i[(\alpha,\hat{\beta})])', \tilde{\beta}\rangle. \tag{56}$$

Observing that

$$\begin{aligned} &\tilde{\beta}^T(0)\Phi_i[(\alpha,\hat{\beta})](0) \\ &= \begin{bmatrix} 0 \\ E_2^- \tilde{\beta}(0,t) \end{bmatrix}^T \begin{bmatrix} -\int_0^1 E_2^+ W_2(\xi)\bar{\phi}_i((\alpha,\hat{\beta}),\xi)d\xi \\ 0 \end{bmatrix} \\ &= 0 \end{aligned} \tag{57}$$

and similarly $\tilde{\beta}^T(1)\Phi_i[(\alpha,\hat{\beta})](1) = 0$, (56) can be integrated by parts to yield

$$\dot{\tilde{\theta}}_i = \gamma_i \langle \Phi_i[(\alpha,\hat{\beta})], \tilde{\beta}_x\rangle. \tag{58}$$

The above steps show that the original representation of the adaptive law (46), dependent on $\tilde{\beta}$, is equivalent to the representation (58), dependent on $\tilde{\beta}_x$. The strategy is now to utilize the structure of the estimation error system (21a), where $\alpha$ is measured, and design a set of filters to find yet an equivalent representation of the adaptive law only dependent on known and measured signals.

Let the signal $\sigma_i : \mathbb{R}^+ \to \mathbb{R}$ be defined by

$$\sigma_i := \theta_i + \Xi_i[(\alpha,\hat{\beta})] \tag{59}$$

where $\Xi_i$ is an operator to be specified. Based on (59), we set

$$\hat{\theta}_i = \hat{\sigma}_i - \Xi_i[(\alpha,\hat{\beta})] \tag{60}$$

and where $\hat{\sigma}_i : \mathbb{R}^+ \to \mathbb{R}$ is a dynamic filter to be specified. We seek the operator $\Xi$ and update law for $\hat{\sigma}_i$, such that the dynamics of $\hat{\theta}_i$ defined by (60) is identical to (46), so that properties (47)–(48) follow.

### *B. Filter and operator design*

**Lemma 3.** *Suppose there exist some functionals $\eta_i^\alpha : L_2([0,1],\mathbb{R}^n) \to \mathbb{R}^m$ and $\eta_i^{\hat{\beta}} : L_2([0,1],\mathbb{R}^n) \to \mathbb{R}^{n-m}$ satisfying*

$$(P_1 B P_2^{-1})^T \eta_i^\alpha[(\alpha,\hat{\beta})] = -\gamma_i \Phi_i[(\alpha,\hat{\beta})] \tag{61a}$$

$$(P_2 L B P_2^{-1})^T \eta_i^{\hat{\beta}}[(\alpha,\hat{\beta})] = \gamma_i \Phi_i[(\alpha,\hat{\beta})] \tag{61b}$$

*for all $x \in [0,1]$, exists and let the operator $\Xi_i : L_2([0,1],\mathbb{R}^n) \to \mathbb{R}$ be defined by*

$$\mathscr{D}^a_{(a,b)}\Xi_i[h_1] = \langle \eta_i^a[(a,b)], h_1\rangle \tag{62a}$$

$$\mathscr{D}^b_{(a,b)}\Xi_i[h_2] = \langle \eta_i^b[(a,b)], h_2\rangle \tag{62b}$$

*where $a, h_1 \in L_2([0,1],\mathbb{R}^m)$ and $b, h_2 \in L_2([0,1],\mathbb{R}^{n-m})$. Then, $\hat{\theta}_i$ calculated using (60) where $\hat{\sigma}_i$ is defined by*

$$\begin{aligned} \dot{\hat{\sigma}}_i =& \mathscr{D}^\alpha_{(\alpha,\hat{\beta})}\Xi_i[-(\Lambda_1+\bar{K}_1)\alpha_x + \bar{f}(\alpha,\cdot)] \\ &+ \mathscr{D}^{\hat{\beta}}_{(\alpha,\hat{\beta})}\Xi_i[-P_2 D P_2^{-1}\hat{\beta}_x + \Sigma] \end{aligned} \tag{63a}$$

$$\Sigma(x) = \bar{g}(\alpha,x) + \bar{\phi}((\alpha,\hat{\beta}),x)\hat{\theta} - \bar{C}\hat{\alpha}_x - \bar{K}_2\alpha_x \tag{63b}$$

$$\hat{\sigma}_i(0) = \hat{\theta}_{i,0} + \Xi[(\alpha_{ic},\hat{\beta}_{ic}] \tag{63c}$$

*and $\hat{\beta}$ is generated from (20), satisfies (46).*

*Proof.* Differentiating (59) with respect to time by introducing the *Fréchet derivatives* of $\Xi_i$ gives

$$\dot{\sigma}_i = \frac{d}{dt}\Xi_i[(\alpha,\hat{\beta})] = \mathscr{D}^\alpha_{(\alpha,\hat{\beta})}\Xi_i[\alpha_t] + \mathscr{D}^{\hat{\beta}}_{(\alpha,\hat{\beta})}\Xi_i[\hat{\beta}_t]. \tag{64}$$

Inserting the dynamics (15a) and (20b) and using (63b), we get

$$\begin{aligned} \dot{\sigma}_i =& \frac{d}{dt}\Xi_i[(\alpha,\hat{\beta})] = \mathscr{D}^\alpha_{(\alpha,\hat{\beta})}\Xi_i[-(\Lambda_1+\bar{K}_1)\alpha_x - \bar{B}\beta_x + \bar{f}(\alpha,\cdot)] \\ &+ \mathscr{D}^{\hat{\beta}}_{(\alpha,\hat{\beta})}\Xi_i[-\Lambda_2\hat{\beta}_x + \Sigma]. \end{aligned} \tag{65}$$

From (59) and (60), we see that the error $\tilde{\sigma}_i = \sigma_i - \hat{\sigma}_i$ satisfies $\tilde{\theta}_i = \tilde{\sigma}_i$, so that differentiating with respect to time and inserting the dynamics (63a) and (65), and using linearity of Fréchet derivatives, we get

$$\begin{aligned} \dot{\tilde{\theta}}_i =& \mathscr{D}^\alpha_{(\alpha,\hat{\beta})}\Xi_i[-(\Lambda_1+\bar{K}_1)\alpha_x - \bar{B}\beta_x + \bar{f}(\alpha,\cdot)] \\ &- \mathscr{D}^\alpha_{(\alpha,\hat{\beta})}\Xi_i[-(\Lambda_1+\bar{K}_1)\alpha_x + \bar{f}(\alpha,\cdot)] \\ &+ \mathscr{D}^{\hat{\beta}}_{(\alpha,\hat{\beta})}\Xi_i[-\Lambda_2\hat{\beta}_x + \Sigma] - \mathscr{D}^{\hat{\beta}}_{(\alpha,\hat{\beta})}\Xi_i[-P_2 D P_2^{-1}\hat{\beta}_x + \Sigma] \\ =& \mathscr{D}^\alpha_{(\alpha,\hat{\beta})}\Xi_i[-P_1 B P_2^{-1}\beta_x] \\ &+ \mathscr{D}^{\hat{\beta}}_{(\alpha,\hat{\beta})}\Xi_i[-P_2 L B P_2^{-1}\hat{\beta}_x] \end{aligned} \tag{66}$$

where we have used that $\bar{B} = P_1 B P_2^{-1}$ and $\Lambda_2 = P_2(D+LB)P_2^{-1}$. Using (62), we have

$$\begin{aligned} \dot{\tilde{\theta}}_i =& \langle \eta_i^\alpha[(\alpha,\hat{\beta})], -P_1 B P_2^{-1}\beta_x\rangle \\ &+ \langle \eta_i^{\hat{\beta}}[(\alpha,\hat{\beta})], -P_2 L B P_2^{-1}\hat{\beta}_x\rangle \end{aligned} \tag{67}$$

$$\begin{aligned} =& -\langle (P_1 B P_2^{-1})^T \eta_i^\alpha[(\alpha,\hat{\beta})], \beta_x\rangle \\ &- \langle (P_2 L B P_2^{-1})^T \eta_i^{\hat{\beta}}[(\alpha,\hat{\beta})], \hat{\beta}_x\rangle \end{aligned} \tag{68}$$

Therefore, by (61) we get

$$\begin{aligned} \dot{\tilde{\theta}}_i =& \gamma_i \langle \Phi_i[(\alpha,\hat{\beta})], \beta_x\rangle - \gamma_i \langle \Phi_i[(\alpha,\hat{\beta})], \hat{\beta}_x\rangle \\ =& \gamma_i \langle \Phi_i[(\alpha,\hat{\beta})], \tilde{\beta}_x\rangle \end{aligned} \tag{69}$$

which is (58). □

**Remark 4.** *Let*

$$\eta_i^\alpha[(\alpha,\hat{\beta})] = -(P_2 L P_1^{-1})^T \eta_i^{\hat{\beta}}[(\alpha,\hat{\beta})]. \tag{70}$$

*The condition* (61) *is satisfied if*

$$(P_2LBP_2^{-1})^T\eta_i^{\hat{\beta}}[(\alpha,\hat{\beta})] = \gamma_i\Phi_i[(\alpha,\hat{\beta})] \tag{71}$$

*which, by the Rouché-Capelli theorem, has a solution* $\eta_i^{\hat{\beta}}[(\alpha,\hat{\beta})]$ *if and only if the rank of* $(LB)$ *is equal to rank of the augmented matrix* $\begin{bmatrix}(P_2LBP_2^{-1})^T & \Phi_i[(\alpha,\hat{\beta})]\end{bmatrix}$. *So if* $\Phi_i[(\alpha,\hat{\beta})]$ *is full rank,* $2m \geq n$ *is a necessary condition.*

### C. Evaluating the operator $\Xi$

Let $(a_0,b_0)$ and $(a_1,b_1)$ be arbitrary functions in $L_2([0,1];\mathbb{R}^n)$. We seek a method to calculate the incremental value $\Xi_i[(a_1,b_1)] - \Xi_i[(a_0,b_0)]$. To that end, let $S_a : [0,1] \to L_2([0,1];\mathbb{R}^m)$ and $S_b : [0,1] \to L_2([0,1];\mathbb{R}^{n-m})$ be given by

$$S_a(\gamma) = a_0 + \gamma(a_1 - a_0) \tag{72a}$$
$$S_b(\gamma) = b_0 + \gamma(b_1 - b_0). \tag{72b}$$

Differentiating $\Xi_i$ at $S(\gamma) := (S_a(\gamma), S_b(\gamma))$ with respect to $\gamma$ and using (62) yield

$$\begin{aligned}
&\frac{d}{d\gamma}\Xi_i[S(\gamma)] \\
&= \mathscr{D}^{S_a(\gamma)}_{(S_a(\gamma),S_b(\gamma))}\Xi_i[S_a'(\gamma)] + \mathscr{D}^{S_b(\gamma)}_{(S_a(\gamma),S_b(\gamma))}\Xi_i[S_b'(\gamma)] \\
&= \langle \eta_i^a[S(\gamma)], S_a'(\gamma)\rangle + \langle \eta_i^b[S(\gamma)], S_b'(\gamma)\rangle \\
&= \langle \eta_i^a[S(\gamma)], a_1 - a_0\rangle + \langle \eta_i^b[S(\gamma)], b_1 - b_0\rangle.
\end{aligned} \tag{73}$$

Integrating from $\gamma = 0$ to $\gamma = 1$ gives

$$\begin{aligned}
\Xi_i[S(1)] &= \Xi_i[S(0)] \\
&+ \int_0^1 \Big(\langle \eta_i^a[S(\gamma)], a_1 - a_0\rangle + \langle \eta_i^b[S(\gamma)], b_1 - b_0\rangle\Big)\, d\gamma.
\end{aligned} \tag{74}$$

Finally, since $S(1) = (a_1,b_1)$ and $S(0) = (a_0,b_0)$, we obtain

$$\begin{aligned}
\Xi_i[(a_1,b_1)] &= \Xi_i[(a_0,b_0)] \\
&+ \int_0^1 \left\langle \eta_i^a\left[\begin{pmatrix} a_0 + \gamma(a_1 - a_0) \\ b_0 + \gamma(b_1 - b_0)\end{pmatrix}\right], a_1 - a_0 \right\rangle d\gamma \\
&+ \int_0^1 \left\langle \eta_i^b\left[\begin{pmatrix} a_0 + \gamma(a_1 - a_0) \\ b_0 + \gamma(b_1 - b_0)\end{pmatrix}\right], b_1 - b_0 \right\rangle d\gamma.
\end{aligned} \tag{75}$$

The condition (62) in Lemma 3 specifies the operator $\Xi$ uniquely only up to a constant. Therefore, we may select $\Xi$ such that $\Xi[(\alpha(\cdot,0),\hat{\beta}(\cdot,0))] = 0$. Choosing $(a_1(x),b_1(x))) = (\alpha(x,t),\hat{\beta}(x,t))$ and $(a_0(x),b_0(x)) = (\alpha(x,0),\hat{\beta}(x,0))$ yield an expression for the operator evaluated at the current state.

**Lemma 4.** *Suppose the conditions of Lemma 3 hold. Then, the operator* $\Xi_i$ *can be evaluated at* $(\alpha(\cdot,t),\hat{\beta}(\cdot,t))$ *by*

$$\begin{aligned}
&\Xi_i[(\alpha(\cdot,t),\hat{\beta}(\cdot,t))] \\
&= \int_0^1 \left\langle \eta_i^\alpha\left[\begin{pmatrix} \alpha(\cdot,0) + \gamma(\alpha(\cdot,t) - \alpha(\cdot,0)) \\ \hat{\beta}(\cdot,0) + \gamma(\hat{\beta}(\cdot,t) - \hat{\beta}(\cdot,0))\end{pmatrix}\right], \right. \\
&\qquad\qquad \alpha(\cdot,t) - \alpha(\cdot,0)\Big\rangle\, d\gamma \\
&\quad + \int_0^1 \left\langle \eta_i^{\hat{\beta}}\left[\begin{pmatrix} \alpha(\cdot,0) + \gamma(\alpha(\cdot,t) - \alpha(\cdot,0)) \\ \hat{\beta}(\cdot,0) + \gamma(\hat{\beta}(\cdot,t) - \hat{\beta}(\cdot,0))\end{pmatrix}\right], \right. \\
&\qquad\qquad \hat{\beta}(\cdot,t) - \hat{\beta}(\cdot,0)\Big\rangle\, d\gamma.
\end{aligned} \tag{76}$$

The design procedure is summarized in Table I and Figure 1.

TABLE I: Overview of adaptive observer design.

| | |
|---|---|
| System | $y_t + Ay_x + Bz_x = f(y,x)$<br>$z_t + Cy_x + Dz_x = g(y,x) + \phi(y,z)\theta$ |
| Observer | $\hat{\alpha}_t + \Lambda_1\hat{\alpha}_x + \bar{B}\hat{\beta}_x = \bar{f}(\alpha,x) - \bar{K}_1\alpha_x$<br>$\hat{\beta}_t + \bar{C}\hat{\alpha}_x + \Lambda_2\hat{\beta}_x = \bar{g}(\alpha,x) + \bar{\phi}((\alpha,\hat{\beta}),x)\hat{\theta} - \bar{K}_2\alpha_x$<br>$(\hat{y},\hat{z}) = P^{-1}(\hat{\alpha},\hat{\beta})$ |
| Adaptive law | $(\alpha,\hat{\beta}) = P(y,\hat{z})$<br>$\hat{\theta}_i = \hat{\sigma}_i - \Xi_i[(\alpha,\hat{\beta})]$<br>$\dot{\hat{\sigma}}_i = \left\langle \eta_i^\alpha[(\alpha,\hat{\beta})], -(\Lambda_1 + \bar{K}_1)\alpha_x + \bar{f}(\alpha,\cdot)\right\rangle$<br>$\quad + \left\langle \eta_i^{\hat{\beta}}[(\alpha,\hat{\beta})], -P_2DP_2^{-1}\hat{\beta}_x + \Sigma\right\rangle$<br>$\Sigma(x) = \bar{g}(\alpha,x) + \bar{\phi}((\alpha,\hat{\beta}),x)\hat{\theta} - \bar{C}\hat{\alpha}_x - \bar{K}_2\alpha_x$<br>$\hat{\sigma}_i(0) = \hat{\theta}_0 + \Xi[(\alpha_{ic},\hat{\beta}_{ic}]$ |
| Operator evaluation | $\Xi_i[(\alpha(\cdot,t),\hat{\beta}(\cdot,t))]$<br>$= \int_0^1 \left\langle \eta_i^\alpha\left[\begin{pmatrix} \alpha(\cdot,0) + \gamma(\alpha(\cdot,t) - \alpha(\cdot,0)) \\ \hat{\beta}(\cdot,0) + \gamma(\hat{\beta}(\cdot,t) - \hat{\beta}(\cdot,0))\end{pmatrix}\right], \alpha(\cdot,t) - \alpha(\cdot,0)\right\rangle d\gamma$<br>$+ \int_0^1 \left\langle \eta_i^{\hat{\beta}}\left[\begin{pmatrix} \alpha(\cdot,0) + \gamma(\alpha(\cdot,t) - \alpha(\cdot,0)) \\ \hat{\beta}(\cdot,0) + \gamma(\hat{\beta}(\cdot,t) - \hat{\beta}(\cdot,0))\end{pmatrix}\right], \hat{\beta}(\cdot,t) - \hat{\beta}(\cdot,0)\right\rangle d\gamma.$<br>where $(\eta_i^\alpha, \eta_i^{\hat{\beta}})$ solves<br>$(P_1BP_2^{-1})^T\eta_i^\alpha[(\alpha,\hat{\beta})] = -\gamma_i\Phi_i[(\alpha,\hat{\beta})]$<br>$(P_2LBP_2^{-1})^T\eta_i^{\hat{\beta}}[(\alpha,\hat{\beta})] = \gamma_i\Phi_i[(\alpha,\hat{\beta})]$ |

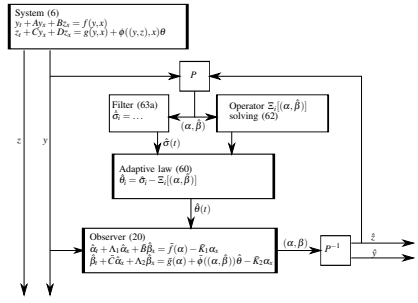


Fig. 1: Structure of the observer design.

Computing (76) at every time step in a computer implementation may be computationally expensive. However, for some special classes of source terms $\phi_i$, the computation simplifies.

**Lemma 5.** *If* $n - m = 1$ *and* $\phi_i$ *is in the form*

$$\phi_i((\gamma a,\gamma b),x) = \rho_i(\gamma)\phi_i((a,b),x) \tag{77}$$

*for some function* $\rho_i : [0,1] \to \mathbb{R}$, *then the operator* $\Xi_i$ *can be evaluated at* $(\alpha(\cdot,t),\beta(\cdot,t))$ *by*

$$\begin{aligned}
\Xi_i[(\alpha(\cdot,t),\beta(\cdot,t))] &= c_i + k_i\langle \eta_i^a[(\alpha(\cdot,t),\beta(\cdot,t))], \alpha(\cdot,t))\rangle \\
&+ k_i\langle \eta_i^b[(\alpha(\cdot,t),\beta(\cdot,t))], \beta(\cdot,t))\rangle
\end{aligned} \tag{78}$$

*where*

$$k_i = \int_0^1 \rho_i(\gamma)d\gamma \tag{79a}$$

$$c_i = -k_i\left\langle \eta_i^a\left[(\alpha(\cdot,0),\hat{\beta}(\cdot,0))\right],\alpha(\cdot,0)\right\rangle - k_i\left\langle \eta_i^b\left[(\alpha(\cdot,0),\hat{\beta}(\cdot,0))\right],\hat{\beta}(\cdot,0)\right\rangle. \tag{79b}$$

*Proof.* From (75), letting $(a_1(x),b_1(x)) = (\alpha(x,t),\hat{\beta}(x,t))$ and $(a_0(x),b_0(x)) = (0,0)$, we have

$$\begin{aligned}\Xi_i[(\alpha(\cdot,t),\hat{\beta}(\cdot,t)] = {}& \Xi_i[(0,0)] \\ &+ \int_0^1 \left\langle \eta_i^a\left[\begin{pmatrix}\gamma\alpha(\cdot,t)\\ \gamma\hat{\beta}(\cdot,t)\end{pmatrix}\right],\alpha(\cdot,t)\right\rangle d\gamma \\ &+ \int_0^1 \left\langle \eta_i^b\left[\begin{pmatrix}\gamma\alpha(\cdot,t)\\ \gamma\hat{\beta}(\cdot,t)\end{pmatrix}\right],\hat{\beta}(\cdot,t)\right\rangle d\gamma\end{aligned} \tag{80}$$

and from letting $(a_1(x),b_1(x)) = (\alpha(0,t),\hat{\beta}(0,t))$ and $(a_0(x),b_0(x)) = (0,0)$, we have

$$\begin{aligned}\Xi_i[(\alpha(\cdot,0),\hat{\beta}(\cdot,0)] = {}& \Xi_i[(0,0)] \\ &+ \int_0^1 \left\langle \eta_i^a\left[\begin{pmatrix}\gamma\alpha(\cdot,0)\\ \gamma\hat{\beta}(\cdot,0)\end{pmatrix}\right],\alpha(\cdot,0)\right\rangle d\gamma \\ &+ \int_0^1 \left\langle \eta_i^b\left[\begin{pmatrix}\gamma\alpha(\cdot,0)\\ \gamma\hat{\beta}(\cdot,0)\end{pmatrix}\right],\hat{\beta}(\cdot,0)\right\rangle d\gamma = 0.\end{aligned} \tag{81}$$

Thus, combining (80) and (81), and recalling that we may select $\Xi$ such that $\Xi[\alpha(\cdot,0,\hat{\beta}(\cdot,0)] = 0$, we get

$$\begin{aligned}\Xi_i[(\alpha(\cdot,t),\hat{\beta}(\cdot,t)] = {}& \\ &+ \int_0^1 \left\langle \eta_i^a\left[\begin{pmatrix}\gamma\alpha(\cdot,t)\\ \gamma\hat{\beta}(\cdot,t)\end{pmatrix}\right],\alpha(\cdot,t)\right\rangle d\gamma \\ &+ \int_0^1 \left\langle \eta_i^b\left[\begin{pmatrix}\gamma\alpha(\cdot,t)\\ \gamma\hat{\beta}(\cdot,t)\end{pmatrix}\right],\hat{\beta}(\cdot,t)\right\rangle d\gamma \\ &- \int_0^1 \left\langle \eta_i^a\left[\begin{pmatrix}\gamma\alpha(\cdot,0)\\ \gamma\hat{\beta}(\cdot,0)\end{pmatrix}\right],\alpha(\cdot,0)\right\rangle d\gamma \\ &- \int_0^1 \left\langle \eta_i^b\left[\begin{pmatrix}\gamma\alpha(\cdot,0)\\ \gamma\hat{\beta}(\cdot,0)\end{pmatrix}\right],\hat{\beta}(\cdot,0)\right\rangle d\gamma.\end{aligned} \tag{82}$$

From (77) and definition (55) it follows that $\Phi_i[(\gamma a,\gamma b)] = \rho(\gamma)\Phi_i[(a,b)]$, and the solution to (61), if it exists, is of the form $\eta_i^a[(\gamma a,\gamma b)] = \rho(\gamma)\eta_i^a[(a,b)]$ and $\eta_i^b[(\gamma a,\gamma b)] = \rho(\gamma)\eta_i^b[(a,b)]$, so that

$$\begin{aligned}\Xi_i[(\alpha(\cdot,t),\hat{\beta}(\cdot,t)] = {}& \int_0^1 \rho_i(\gamma)d\gamma \\ &\times \Big(\left\langle \eta_i^a\left[(\alpha(\cdot,t),\hat{\beta}(\cdot,t))\right],\alpha(\cdot,t)\right\rangle \\ &+ \left\langle \eta_i^b\left[(\alpha(\cdot,t),\hat{\beta}(\cdot,t))\right],\hat{\beta}(\cdot,t)\right\rangle \\ &- \left\langle \eta_i^a\left[(\alpha(\cdot,0),\hat{\beta}(\cdot,0))\right],\alpha(\cdot,0)\right\rangle \\ &- \left\langle \eta_i^b\left[(\alpha(\cdot,0),\hat{\beta}(\cdot,0))\right],\hat{\beta}(\cdot,0)\right\rangle\Big).\end{aligned} \tag{83}$$

□

Lemma 2–5 now provide the following adaptive state and parameter estimation result.

**Proposition 2.** *Consider the error dynamics* (21) *with boundary conditions satisfying Assumption 3 and* (28) *and the parameter update law* (60) *with* $\hat{\sigma}$ *satisfying* (63)*. If the conditions of Lemma 2 and 3 are satisfied, and the operator* $\Xi$ *is computed either by the scheme in Lemma 4 or Lemma 5, then the state estimation error* $(\tilde{y},\tilde{z})$ *and parameter estimate* $\hat{\theta}$ *satisfy properties* (47) *and* (48)*.*

## IV. Simulation example

Consider system (6) with

$$A = -D = \begin{bmatrix}0 & 2\\ 2 & -1\end{bmatrix} \tag{84a}$$

$$C = B = \begin{bmatrix}0 & -4\\ -4 & 0\end{bmatrix} \tag{84b}$$

$$f(y,x) = y_1\begin{bmatrix}-x & 1\end{bmatrix}^T \tag{84c}$$

$$g(y,x) = \begin{bmatrix}\tan^{-1}(y_2) & 0\end{bmatrix}^T \tag{84d}$$

$$\phi(y,z,x) = \begin{bmatrix}-z_1x^2 & -\tan^{-1}(z_1)\\ -z_2|z_2|x & -x^2\end{bmatrix} \tag{84e}$$

$$\theta = \begin{bmatrix}5 & 2\end{bmatrix}^T, \tag{84f}$$

which can be shown to satisfy Assumption 1 and 2, the boundary conditions

$$\begin{bmatrix}1.3 & 2.0 & -0.7 & -0.6\\ 2.1 & 4.0 & 0.8 & 1.4\end{bmatrix}\begin{bmatrix}y(0,t)\\ z(0,t)\end{bmatrix} = \begin{bmatrix}1+sin(t)\\ 0\end{bmatrix} \tag{85a}$$

$$\begin{bmatrix}2.0 & -2.0 & -1.0 & 0.6\\ 0 & 4.0 & 0 & 1.4\end{bmatrix}\begin{bmatrix}y(1,t)\\ z(1,t)\end{bmatrix} = \begin{bmatrix}1.0\\ -0.3\end{bmatrix}, \tag{85b}$$

and suitable initial conditions found by numerically solving the system of ODEs

$$Ay_x(\cdot,0) + Bz_x(\cdot,0) = f(y(\cdot,0),x) \tag{86a}$$

$$Cy_x(\cdot,0) + Dz_x(\cdot,0) = g(y(\cdot,0),x) + \phi((y(\cdot,0),z(\cdot,0)),x)\theta \tag{86b}$$

with (85) for $x\in[0,1]$ (which ensures that all compatibility conditions are satisfied). This Cauchy problem can be shown to be well-posed. Specifically, using the coordinate transformation (14) with

$$L = \frac{1}{4}\begin{bmatrix}-2 & -1\\ 2 & -2\end{bmatrix} \tag{87}$$

transforms the system into (15) with

$$\Lambda_1 = \mathrm{diag}(2,-2) \tag{88a}$$

$$\Lambda_2 = \mathrm{diag}(1,-1) \tag{88b}$$

$$\bar{B} = \begin{bmatrix}0 & -4\\ -4 & 0\end{bmatrix} \tag{88c}$$

$$\bar{C} = \frac{1}{2}\begin{bmatrix}0 & -9\\ -9 & 2\end{bmatrix} \tag{88d}$$

$$\bar{f}(\alpha,x) = \alpha_1\begin{bmatrix}-x\\ 1\end{bmatrix} \tag{88e}$$

$$\bar{g}(\alpha,x) = \begin{bmatrix}\tan^{-1}(\alpha_2) - \alpha_1(\frac{1}{4}-\frac{1}{2}x)\\ \alpha_1(\frac{1}{4}+\frac{1}{2}x)\end{bmatrix} \tag{88f}$$

$$\bar{\phi}_1(\alpha,\beta,x) = \begin{bmatrix}-(\frac{1}{2}\alpha_1+\frac{1}{4}\alpha_2+\beta_1)x^2\\ \frac{1}{4}(\alpha_1-\alpha_2-2\beta_2)|-\alpha_1+\alpha_2+2\beta_2|x\end{bmatrix} \tag{88g}$$

$$\bar{\phi}_2(\alpha,\beta,x) = \begin{bmatrix}-\tan^{-1}(\frac{1}{2}\alpha_1+\frac{1}{4}\alpha_2+\beta_1)\\ -x^2\end{bmatrix} \tag{88h}$$

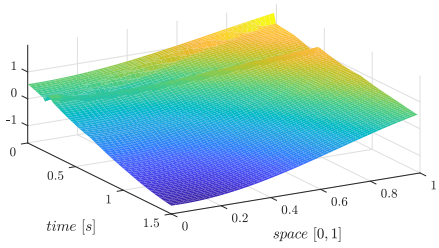


(a) $y_1(x,t)$.

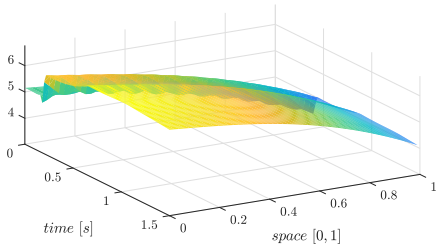


(b) $y_2(x,t)$.

Fig. 2: Measured system state $y$.

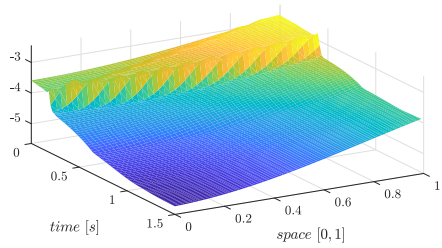


(a) $z_1(x,t)$.

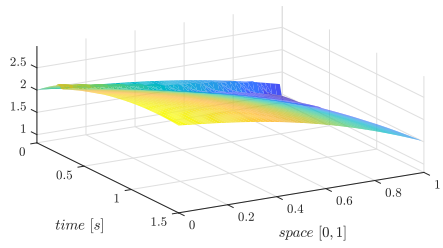


(b) $z_2(x,t)$.

Fig. 3: Unmeasured system states $z$.

and boundary conditions

$$\begin{bmatrix} 1.3 & 2.0 & -0.7 & -0.6 \\ 1.3 & 5.3 & 1.3 & 2.7 \end{bmatrix} \begin{bmatrix} \alpha(0,t) \\ \beta(0,t) \end{bmatrix} = \begin{bmatrix} 1+sin(t) \\ 0 \end{bmatrix} \quad (88ia)$$

$$\begin{bmatrix} 1.3 & -4.0 & -0.7 & 0.5 \\ 0 & 4.0 & 0 & 1.4 \end{bmatrix} \begin{bmatrix} \alpha(1,t) \\ \beta(1,t) \end{bmatrix} = \begin{bmatrix} 1.0 \\ -0.3 \end{bmatrix}. \quad (88ib)$$

which can be solved explicitly for $(\alpha_1(0,t),\alpha_2(1,t))$ and $(\beta_1(0,t),\beta_2(1,t))$. The observer is designed with boundary conditions $(\hat{\alpha}_1(0,t),\hat{\alpha}_2(1,t)) = (\alpha_1(0,t),\alpha_2(1,t))$ and $(\hat{\beta}_1(0,t),\hat{\beta}_2(1,t)) = (\beta_1(0,t),\beta_2(1,t))$ so that Assumption 4 is satisfied and we use the injection gains $K_1 = -\frac{1}{2}\Lambda_1$ and $K_2 = 0$. Since $\phi$ is in the form discussed in Remark 1 and $P_2$ is the identity matrix, any diagonal $W(x)$ will satisfy (33). The choice $W(x) = \text{diag}(2-x, 2-x)$ also satisfies (36). The system and observer scheme with $\Gamma = \text{diag}(5,5)$ and $\hat{\theta}(0) = 0$ are are implemented in MATLAB and simulated for 1.5 seconds using the *method of line* with a *Runge-Kutta* solver using 200 spatial discretization points. The system states are shown in Figures 2 and 3. Figures 4–6 shows that the state estimation error converges to zero in accordance with Proposition 2. In addition, the parameter estimate $\hat{\theta}$ converge to the true value $\theta$ as can be seen in Figures 7 and 8.

## V. Concluding Remarks

A state and parameter estimation scheme for heterodirectional semi-linear hyperbolic systems has been presented. The observer and adaptive law guarantee convergence of the state estimation error to zero. The non-adaptive version of the design is general and requires only a simple observability condition

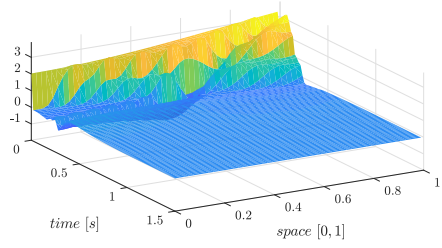


(a) $\tilde{y}_1(x,t)$.

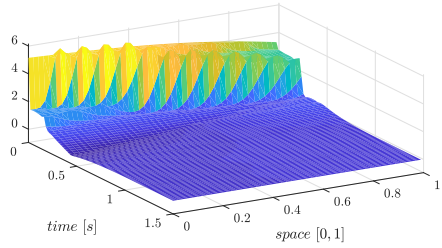


(b) $\tilde{y}_2(x,t)$.

Fig. 4: State estimation error $\tilde{y}$.

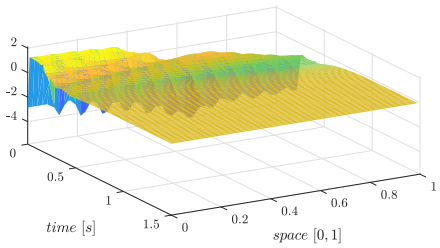


(a) $\tilde{v}_1(x,t)$.

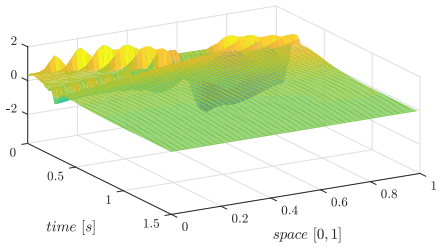


(b) $\tilde{v}_2(x,t)$.

Fig. 5: State estimation error $\tilde{z}$.

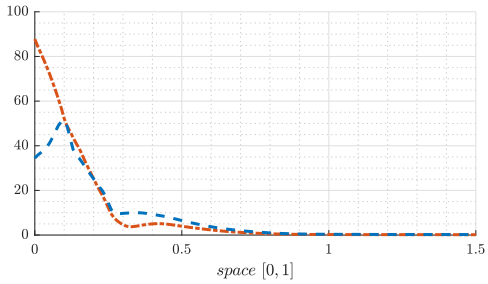


Fig. 6: State estimation error $||(\tilde{y}(\cdot,t)||$ (red) and $||\tilde{z}(\cdot,t))||$ (blue).

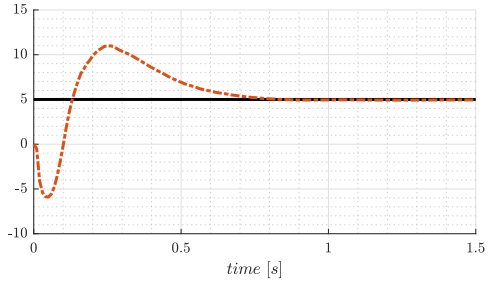


Fig. 7: Parameter estimate $\theta_1(t)$

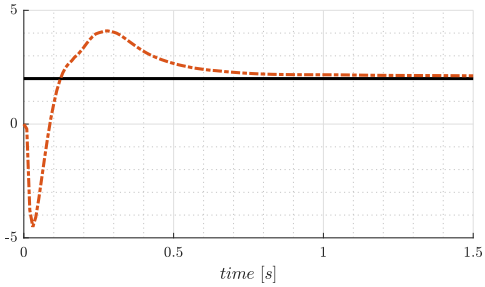


Fig. 8: Parameter estimate $\theta_2(t)$

on the coefficient matrices, in addition to the monotonicity condition on the non-linearity in the unmeasured part of the state. In the presence of uncertainties, the design requires a special rank condition on the coefficient matrices. In view of the property that state estimates converge to their true values regardless of parameter convergence, removal of this constraint is probably hard.

## APPENDIX

**Lemma 6** (Lemma 3.1 from [19])**.** *Let $g$ be a real valued function defined for $t \geq 0$. Suppose:*

1) $g(t) \geq 0$ *for all* $t \in [0,\infty)$,
2) $g(t)$ *is differentiable on* $[0,\infty)$ *and there exists a constant* $M$ *such that* $\dot{g}(t) \leq M$, *for all* $t \geq 0$,
3) $g \in \mathscr{L}_1$.

*Then*

$$\lim_{t\to\infty} g(t) = 0. \tag{1}$$

## REFERENCES

[1] Henrik Anfinsen and Ole Morten Aamo. Adaptive control of linear $2\times2$ hyperbolic systems. *Automatica*, 2017.
[2] Henrik Anfinsen and Ole Morten Aamo. Adaptive output-feedback stabilization of linear $2\times2$ hyperbolic systems using anti-collocated sensing and control. *Systems & Control Letters*, 104:86–94, 2017.
[3] Henrik Anfinsen and Ole Morten Aamo. *Adaptive Control of Hyperbolic PDEs (Communications and Control Engineering)*. Springer, 2019.
[4] Henrik Anfinsen, Mamadou Diagne, Ole Moren Aamo, and Miroslav Krstic. An adaptive observer design for $n+1$ coupled linear hyperbolic PDEs based on swapping. *IEEE Transactions on Automatic Control*, 61(12):3979–3990, December 2016.
[5] Henrik Anfinsen, Mamadou Diagne, Ole Morten Aamo, and Miroslav Krstic. Estimation of boundary parameters in general heterodirectional linear hyperbolic systems. *Automatica*, 79:185–197, 2017.
[6] Murat Arcak and Petar Kokotović. Nonlinear observers: a circle criterion design and robustness analysis. *Automatica*, 37(12):1923–1930, dec 2001.
[7] Georges Bastin and Jean-Michel Coron. *Stability and boundary stabilization of 1-D hyperbolic systems*, volume 88. Springer, 2016.
[8] Pauline Bernard and Miroslav Krstic. Adaptive output-feedback stabilization of non-local hyperbolic PDEs. *Automatica*, 50(10):2692–2699, October 2014.
[9] Gildas Besançon. *Nonlinear Observers and Applications*. Springer Berlin Heidelberg, 2007.
[10] Panagiotis D. Christofides and Prodromos Daoutidis. Feedback control of hyperbolic PDE systems. *AIChE Journal*, 42(11):3063–3086, nov 1996.

[11] Jean-Michel Coron, Georges Bastin, and Brigitte d'Andréa Novel. Dissipative boundary conditions for one-dimensional nonlinear hyperbolic systems. *SIAM Journal on Control and Optimization*, 47(3):1460–1498, jan 2008.

[12] J. Gauthier and G. Bornard. Observability for any $u(t)$ of a class of nonlinear systems. *IEEE Transactions on Automatic Control*, 26(4):922–926, aug 1981.

[13] J.P. Gauthier, H. Hammouri, and S. Othman. A simple observer for nonlinear systems applications to bioreactors. *IEEE Transactions on Automatic Control*, 37(6):875–880, jun 1992.

[14] Haavard Holta and Ole Morten Aamo. An adaptive observer design for $2\times2$ semi-linear hyberbolic systems using distributed sensing. In *Proceedings of the 2019 American Control Conference*, pages 2540–2545, July 2019.

[15] Haavard Holta and Ole Morten Aamo. Exploiting wired-pipe technology in an adaptive observer for detecting faults during oil well drilling. *Under reivew, SPE Journal, submitted January 2020*, 2020.

[16] Long Hu, Florent Di Meglio, Rafael Vazquez, and Miroslav Krstic. Control of homodirectional and general heterodirectional linear coupled hyperbolic PDEs. *IEEE Transactions on Automatic Control*, 61(11):3301–3314, November 2016.

[17] Long Hu, Rafael Vazquez, Florent Di Meglio, and Miroslav Krstic. Boundary exponential stabilization of 1-D inhomogeneous quasilinear hyperbolic systems. *Preprint submitted*, 2018.

[18] Constantinos Kitsos, Gildas Besancon, and Christophe Prieur. High-gain observer design for a class of hyperbolic systems of balance laws. In *Proceedings of the 2018 IEEE Conference on Decision and Control (CDC)*. IEEE, dec 2018.

[19] Wei-Jiu Liu and Miroslav Krstic. Adaptive control of burgers' equation with unknown viscosity. *International Journal of Adaptive Control and Signal Processing*, 15(7):745–766, 2001.

[20] R. Marino and P. Tomei. Global adaptive observers for nonlinear systems via filtered transformations. *IEEE Transactions on Automatic Control*, 37(8):1239–1245, August 1992.

[21] Riccardo Marino and Patrizio Tomei. *Nonlinear control design: geometric, adaptive and robust*, volume 1. Prentice Hall London, 1995.

[22] Ø. N. Stamnes, O. M. Aamo, and G. Kaasa. Adaptive redesign of nonlinear observers. *IEEE Transactions on Automatic Control*, 56(5):1152–1157, May 2011.

[23] Ø. N. Stamnes, J. Zhou, O. M. Aamo, and G. Kaasa. Adaptive observer design for nonlinear systems with parametric uncertainties in unmeasured state dynamics. In *Proceedings of the 48h IEEE Conference on Decision and Control*, pages 4414–4419, December 2009.

[24] Timm Strecker and Ole Morten Aamo. Output feedback boundary control of $2\times2$ semilinear hyperbolic systems. *Automatica*, 83:290–302, 2017.

[25] Timm Strecker, Michael Canton, and Ole Morten Aamo. Exact boundary control of a first-order quasilinear hyperbolic systems by state feedback. In *Submitted*, 2019.

[26] R. Vazquez, J. M. Coron, M. Krstic, and G. Bastin. Local exponential $H^2$ stabilization of a $2\times2$ quasilinear hyperbolic system using backstepping. In *Proceedings of the 50th IEEE Conference on Decision and Control and European Control Conference*, pages 1329–1334, December 2011.

[27] Rafael Vazquez, Miroslav Krstic, and Jean-Michel Coron. Backstepping boundary stabilization and state estimation of a $2\times2$ linear hyperbolic system. In *Proceedings of the 50th IEEE Conference on Decision and Control and European Control Conference*, pages 4937–4942, December 2011.

**Haavard Holta** received his M.Sc. degree from the Department of Engineering Cybernetics at the Norwegian University of Science and Technology in 2017, where he is currently a PhD student.

**Ole Morten Aamo** received the M.Sc. and Ph.D. degrees in engineering cybernetics from the Norwegian University of Science and Technology (NTNU), Trondheim, Norway, in 1992 and 2002, respectively. He is currently a Professor with NTNU. His research interests include control of distributed parameter systems with special emphasis on control of fluid flows. He is a co-author of the books *Flow Control by Feedback* (Springer, 2003) and *Adaptive Control of Hyperbolic PDEs* (Springer, 2019).

## 3.4 Paper [64]: *A heuristic observer design for an uncertain hyperbolic PDE using distributed sensing*

Holta, H. and Aamo, O. M. (2020d). A heuristic observer design for an uncertain hyperbolic PDE using distributed sensing. In *Proceedings of the IFAC world congress 2020*

# A Heuristic Observer Design for an Uncertain Hyperbolic PDE using Distributed Sensing

**Haavard Holta** * **Ole Morten Aamo** **

* *Department of Engineering Cybernetics. Norwegian University of Science and Technology, Trondheim N-7491, Norway (e-mail: haavard.holta@ntnu.no).*
** *Department of Engineering Cybernetics. Norwegian University of Science and Technology, Trondheim N-7491, Norway (e-mail: aamo@ntnu.no).*

**Abstract:** We design an adaptive observer for semi-linear $2 \times 2$ hyperbolic PDEs with parametric uncertainties in both state equations. The proposed method is an extension of a previous result where parametric uncertainties were only allowed in one of the system equation. We utilize partial state measurements of one of the distributed states to estimate the remaining unknown distributed state. The method can be applied to flow rate estimation in fluid flow systems where the pressure is measured.

*Keywords:* Distributed parameter systems, State estimation, Parameter estimation, Adaptive systems, Fluid flow estimation

## 1. INTRODUCTION

### 1.1 Problem formulation

We consider semi-linear $2 \times 2$ hyperbolic systems on the form

$$y_t(x,t) + az_x(x,t) = \phi_1^T(y(x,t),x)\theta_1 \tag{1a}$$

$$z_t(x,t) + by_x(x,t) = \phi_2^T(z(x,t),x)\theta_2. \tag{1b}$$

where $a, b \in \mathbb{R}$ and $\phi_1 : \mathbb{R} \times [0,1] \to \mathbb{R}^p, \phi_2 : \mathbb{R} \times [0,1] \to \mathbb{R}^q$ are known and $\theta_1 \in \mathbb{R}^p, \theta_2 \in \mathbb{R}^q$ are unknown constants with $p, q \in \mathbb{N}$. The distributed state $y : [0,1] \times \mathbb{R}^+ \to \mathbb{R}$ is assumed measured for all $x \in [0,1]$ while $z : [0,1] \times \mathbb{R}^+ \to \mathbb{R}$ is assumed unknown for $x \in (0,1)$, but we assume that both $z(0,t)$ and $z(1,t)$ are measured. In addition, we assume the following.

*Assumption 1.* System (3) with appropriate boundary and initial conditions has a unique bounded solution $(y(\cdot,t), z(\cdot,t)) \in L_2([0,1])$ for all $t \geq 0$.

*Assumption 2.* $||y|| \in \mathcal{L}_\infty \Rightarrow ||\phi_1(y,\cdot)|| \in \mathcal{L}_\infty, ||z|| \in \mathcal{L}_\infty \Rightarrow ||\phi_2(z,\cdot)|| \in \mathcal{L}_\infty$, and $\phi_2$ satisfies the sector condition

$$(\phi_2^T(z_1,x) - \phi_2^T(z_2,x))\theta_2(z_1 - z_2) \leq 0. \tag{2}$$

for any $z_1, z_2 \in L_2([0,1])$

The goal is to estimate the unknown state $z(x)$ as well as the unknown parameters $\theta_1, \theta_2$.

The method presented in this paper can be extended to general hyperbolic systems with $(y(x), z(x)) \in \mathbb{R}^{n+m}$ for $m, n \in \mathbb{N}$ and any coefficient matrix having distinct real eigenvalues. However to simplify the presentation we let $m = n = 1$ and only require $ab > 0$, which implies that (1) is strictly hyperbolic.

### 1.2 Motivation and previous work

The system (1) can be used to model single-phase fluid flow systems (among others, see Bastin and Coron (2016)) and is derived by considering the mass and momentum balances in an open fluid system. In the following we will therefore refer to (1a) as the *mass balance* and (1b) as the *momentum balance*. An example is oil & gas drilling where a drilling fluid called mud is circulated down the hollow drill-string, through the drilling bit down-hole and up in the annulus surrounding the drill-string all the way to the top of the well. The fluid is used to carry cuttings to the top and provide pressure control in the well. Inadequate pressure control might lead to uncontrolled flows of fluid to or from the surrounding oil or gas reservoir. A reservoir pressure exceeding the well pressure leading to a flow of oil or gas into the well, called a *kick*, might have severe consequences if the reservoir fluids reach the surface. The opposite situation where the well pressure exceeds the reservoir pressure by a sufficiently high margin and the drilling fluid flows into the reservoir, which is called a *loss*, is also undesirable as the integrity of the reservoir might weaken, and the pressure drop caused by a loss might lead to a subsequent kick.

Due to the long length of the well which can be up to $10\,\mathrm{km}$, and even though the sound of speed for a typical drilling fluid can be as high as $1000\,\mathrm{m\,s^{-1}}$, the distributed effects caused by the compressibility of the fluid is sometimes significant and should not be neglected (Berg et al., 2019; Landet et al., 2013). In this paper, we utilize the information in the fast traveling pressure waves to estimate unknown states and parameters in a general PDE model. We assume that part of the sate vector is known and design an adaptive observer to estimate the remaining state. The method developed in this paper is an extension of Holta and Aamo (2019) where we only consider uncertainties in the momentum balance of a $2 \times 2$ semi-linear hyperbolic system, and not in the mass balance. The method in Holta and Aamo (2019) is an extension to PDEs of the method developed for non-linear ODEs in Stamnes et al. (2008, 2009) where stability of the observer design is proved by assuming that the non-linearities satisfy a sector condition similar to the condition proposed in Arcak and Kokotovic (1999). Utilizing this special structure avoids the use of canonical transformations (see Marino and Tomei (1992)) which requires that the system is *persistently*

⋆ Economic support from The Research Council of Norway and Equinor ASA through project no. 255348/E30 Sensors and models for improved kick/loss detection in drilling (Semi-kidd) is gratefully acknowledged.

*excited* (PE) (Marino and Tomei, 1995). For non-linearities that satisfy Lipschitz conditions, another approach is to use *high-gain* to dominate the non-linearities. See e.g. Besanon et al. (2004) for ODEs and the recent result in Kitsos et al. (2018) for hyperbolic PDEs.

In the drilling system, a kick or loss is by definition an unexpected event caused by inadequate knowledge about system states and properties. In particular, the reservoir pressure and the flow rate at any single point in the well is often unknown. However, using so-called wired-pipe technology where the pressure inside the well is measured, and under a certain excitation criterion, both flow rate and the properties of the reservoir can be estimated . A local inflow of fluid from the reservoir into the well will likely result in an increase in the local frictional pressure drop, and a local loss of fluids from the well into the reservoir will likely lead to a decrease in friction. So by adapting the observer by estimating local frictional coefficients we can both detect and locate kicks or losses. However, a local increase in frictional momentum loss might also be caused by a pack-off of cuttings, or a wash-out between the drill-string and the annulus. To classify an event as a kick or loss we also need to model in- or out-flow of mass from and to the reservoir and acknowledge that parameters governing the mass balance are dependent on the reservoir properties and therefore uncertain. As the method in Holta and Aamo (2019) assumes that all parameters in the mass balance are perfectly known, the method can not be applied to distinguish between a in- or out-flow and other incidents. However, in this paper we show that if additional flow rate measurements at the top-side boundary are available, a simple parametric model can be used to estimate uncertainties in the mass balance, thus significantly increasing the applicability of the method first proposed in Holta and Aamo (2019).

*Remark 1.* Strictly speaking, the system described above with local inflows might require a model where the uncertain parameters are spatially varying. That is,

$$y_t(x) + az_x(x) = \varphi_1(y(x), x)\vartheta_1(x) \tag{3a}$$
$$z_t(x) + by_x(x) = \varphi_2(z(x), x)\vartheta_2(x) \tag{3b}$$

for some uncertain functions $\vartheta_1, \vartheta_2 : [0, 1] \to \mathbb{R}$. However, in most practical applications $\vartheta_1, \vartheta_2$ will be piece-wise constant (for example due to a geological fault) and we can define

$$\phi_1^i(y(x), x) = \chi_i(x)\varphi(y(x), x) \tag{4}$$

where $\phi_1^i$ is an element in $\phi_1$ and $\chi_i(x) = 1$ in some subset of $[0, 1]$ and zero otherwise,

$$\theta_i = \chi_i\theta(x_i) \tag{5}$$

for any $x_i$ such that $\chi_i(x_i) = 1$, and similarly for $\phi_2$. However, from a mathematical point-of-view the method can straight forwardly be extended to handle spatially varying uncertainties $\theta_2(x)$. That being said, due to implementational concerns regarding robustness and to keep the presentation comparable to Holta and Aamo (2019) we keep the formulation in (1).

### *1.3 Notation*

We avoid arguments in time and write e.g. $y(x)$ for a variable $y : [0, 1] \times \mathbb{R}^+ \to \mathbb{R}$, where $\mathbb{R}^+$ denotes the set of non-negative real numbers. For $f : \mathbb{R}^+ \to \mathbb{R}$, we use the spaces

$$f \in \mathcal{L}_p \leftrightarrow \left( \int_0^\infty |f(t)|^p dt \right)^{\frac{1}{p}} < \infty \tag{6}$$

for $p \geq 1$ with the particular case $f \in \mathcal{L}_\infty \leftrightarrow \sup_{t\geq 0} |f(t)| < \infty$. A function $u : [0, 1] \to \mathbb{R}$ is said to be in $L_2([0, 1])$ if

$$||u|| := \sqrt{\int_0^1 u^2(x)dx} < \infty. \tag{7}$$

The partial derivative of a function is denoted with a subscript, for example $u_t(x, t) = \frac{\partial}{\partial t}u(x, t)$. For a function of one variable, the derivative is denoted using a prime, that is $f'(x) = \frac{d}{dx}f(x)$. The dot notation is reserved for the derivative of functions of time only; $\dot{f}(t) = \frac{d}{dt}f(t)$.

An operator $\Xi : L_2(0, 1) \to \mathbb{R}$ is called *Fréchet differentiable* at $u \in L_2([0, 1])$ if there exists a bounded linear operator $D_u\Xi : L_2([0, 1]) \to \mathbb{R}$ such that

$$\lim_{h\to 0} \frac{|\Xi[u + h] - \Xi[u] - D_u\Xi[h]|}{||h||} = 0 \tag{8}$$

for $h \in L_2([0, 1])$. If such a bounded linear operator exists, it is unique and we call $D_u\Xi$ the *Fréchet derivative* of $\Xi$ at $u$.

## 2. OBSERVER DESIGN

Let $\zeta(x) = ly(x) + z(x)$ for some $l$ such that $\lambda := la > 0$. We have

$$\zeta_t(x) + \lambda\zeta_x(x) = (l^2a - b)y_x(x) + l\phi_1^T(y(x), x)\theta_1 + \phi_2^T(z(x), x)\theta_2 \tag{9}$$
$$\zeta(0) = ly(0) + z(0) \tag{10}$$

To estimate the unknown state $\zeta$, consider the observer

$$\hat{\zeta}_t(x) + \lambda\hat{\zeta}_x(x) = (l^2a - b)y_x(x) + l\phi_1^T(y(x), x)\hat{\theta}_1 + \phi_2^T(\hat{z}(x), x)\hat{\theta}_2 \tag{11a}$$
$$\hat{\zeta}(0) = \zeta(0) \tag{11b}$$

where $\hat{z}(x) = \hat{\zeta}(x) - ly(x)$ and $\hat{\theta}_1, \hat{\theta}_2$ are estimates of $\theta_1, \theta_2$. The error dynamics $\tilde{\zeta}(x) = \zeta(x) - \hat{\zeta}(x)$ then satisfies

$$\tilde{\zeta}_t(x) + \lambda\tilde{\zeta}_x(x) = l\phi_1^T(y(x), x)\tilde{\theta}_1 + \phi_2^T(\hat{z}(x), x)\tilde{\theta}_2 + \tilde{\phi}_2^T(z(x), \hat{z}(x), x)\theta_2 \tag{12a}$$
$$\tilde{\zeta}(0) = 0 \tag{12b}$$

where $\tilde{\phi}_2(z(x), \hat{z}(x), x) := \phi(z(x), x) - \phi(\hat{z}(x), x)$ and $\tilde{\theta}_i = \theta_i - \hat{\theta}_i$, $i = 1, 2$.

The adaptive law generating $\hat{\theta}_1$ is derived in Section 2.1. Stability of the error system (12), which is the main result (Proposition 2), is proved in Section 2.2 under the assumption of an *ideal* adaptive law for $\hat{\theta}_2$ which at first glance can not be implemented. Finally, an implementable adaptive law for $\hat{\theta}_2$ is designed in Section 2.3 and shown to asymptotically converge to the ideal adaptive law.

### *2.1 Estimating the uncertainty in the mass balance*

We utilize both the distributed state measurements $y(x)$, $x \in [0, 1]$ and boundary measurements $z(0), z(1)$ and design a swapping-based parameter estimation scheme.

Let the operators $\Psi, \Omega$ and $\Delta$ be defined as

$$\Psi[y] := \int_0^1 y(x)dx \tag{13a}$$
$$\Omega[y] := \int_0^1 \phi_1(y(x), x)dx \tag{13b}$$
$$\Delta[z] := -a(z(1) - z(0)) \tag{13c}$$

We have

$$\begin{aligned}\dot{\Psi}[y] =&\frac{d}{dt}\int_0^1 y(x)dx = \int_0^1 y_t(x)dx\\ &- a\int_0^1 z_x(x)dx + \int_0^1 \phi_1^T(y(x),x)dx\theta_1\\ =&\Delta[z] + \Omega^T[y]\theta_1. \end{aligned} \tag{14}$$

Consider the filters

$$\dot{\nu} = -\varsigma\nu + \Omega[y] \tag{15a}$$

$$\dot{\rho} = -\varsigma(\rho - \Psi[y]) + \Delta[z] \tag{15b}$$

for some $\varsigma > 0$ and let

$$\bar{\Psi} := \rho + \nu^T\theta_1. \tag{16}$$

Then the error $e := \Psi[y] - \bar{\Psi}$ satisfies

$$\begin{aligned}\dot{e} =&\Delta[z] + \Omega^T[y]\theta_1\\ &- (-\varsigma(\rho - \Psi[y]) + \Delta[z] - \varsigma\nu^T\theta_1 + \Omega^T[y]\theta_1) &(17)\\ =&-\varsigma e &(18)\end{aligned}$$

showing that $e \in \mathcal{L}_2$ and $\bar{\Psi} \to \Psi[y]$ exponentially fast.

*Lemma 1.* For some $\Gamma_1 = \Gamma_1^T \succ 0$, let

$$\dot{\hat{\theta}}_1 = \Gamma_1\epsilon_1\nu \tag{19}$$

where $\epsilon_1 := \Psi[y] - \rho - \nu\hat{\theta}_1$. Then,

(1) $\epsilon_1, \hat{\theta}_1, \dot{\hat{\theta}}_1 \in \mathcal{L}_\infty$.
(2) $\epsilon_1, \dot{\hat{\theta}}_1 \in \mathcal{L}_2$ .
(3) $\Omega^T[y]\tilde{\theta}_1 \in \mathcal{L}_2 \cap \mathcal{L}_\infty$.

If in addition $\Omega[y]$ satisfies the PE condition

$$\alpha_0 I \preceq \frac{1}{T}\int_t^{t+T} \Omega[y]\Omega[y]^T d\tau \preceq \alpha_1 I, \tag{20}$$

for some $\alpha_0, \alpha_1, T > 0$, then $\tilde{\theta}_1 \to 0$ exponentially fast.

**Proof.** Since $\phi_1$ and therefore $\nu$ is bounded by assumption, Property (1) and (2) follow from Ioannou and Sun (2012, Th. 4.3.2). For Property (3), we have $\epsilon_1 = \nu\tilde{\theta}_1 + e$, so that

$$\begin{aligned}\dot{\epsilon}_1 =&\dot{\nu}\tilde{\theta}_1 - \nu\dot{\hat{\theta}}_1 + \dot{e}\\ =&-c\epsilon_1 + \Omega[y]\tilde{\theta}_1 - \epsilon_1\gamma_1\nu\nu^T - \varsigma e\\ =&-\epsilon_1(c + \gamma_1\nu\nu^T) + \Omega[y]\tilde{\theta}_1 - \varsigma e, \end{aligned} \tag{21}$$

so that

$$\begin{aligned}(\Omega[y]\tilde{\theta}_1)^2 \leq& 2\dot{\epsilon}_1^2 + 2\epsilon_1^2(c + \gamma_1\nu\nu^T)^2\\ \leq& 2\frac{d}{dt}(\epsilon_1\dot{\epsilon}_1) - 2\epsilon_1\frac{d^2\epsilon_1}{dt^2} + 4\epsilon_1^2(c + \gamma_1\nu\nu^T)^2\\ &+ 4\varsigma^2 e^2 \end{aligned} \tag{22}$$

Therefore,

$$\begin{aligned}\int_0^t (\Omega[y]\tilde{\theta}_1)^2 d\tau \leq& 2\int_0^t \frac{d}{d\tau}(\epsilon_1\dot{\epsilon}_1)d\tau + 2\bar{\epsilon}_1\int_0^t \frac{d^2\epsilon_1}{d\tau^2}d\tau\\ &+ 2(c + \gamma_1\bar{\nu}^2)^2\int_0^t \epsilon_1^2 d\tau + 4\varsigma^2\int_0^t e^2 d\tau\\ \leq& 4\bar{\epsilon}_1(\dot{\epsilon}_1(t) - \dot{\epsilon}_1(0)) + 2(c + \gamma_1\bar{\nu}^2)^2\int_0^t \epsilon_1^2 d\tau\\ &+ 4\varsigma^2\int_0^t e^2 d\tau \end{aligned} \tag{23}$$

where $\bar{\epsilon}_1 = \sup_{t\geq 0}|\epsilon_1|$ and $\bar{\nu} = \sup_{t\geq 0}||\nu||$ (the latter exists by assumption). Letting $t \to \infty$ on both sides of the above inequality and using the fact that $\epsilon_1, e \in \mathcal{L}_2 \cap \mathcal{L}_\infty$ and $\dot{\epsilon}_1 \in \mathcal{L}_\infty$ shows that the left hand side is bounded which concludes the proof of Property (3). If $\Omega[y]$ is PE, it trivially follows that $\nu$ is PE (Ioannou and Sun, 2012, Lemma 4.8.3 (ii)) and exponential convergence of $\hat{\theta}_1$ to $\theta_1$ follows again from Ioannou and Sun (2012, Th. 4.3.2). □

### 2.2 Main result and stability proof

To study the stability of (12) consider the Lyapunov function candidate

$$V_0 = \frac{1}{2}\int_0^1 W(x)\tilde{\zeta}^2(x)dx \tag{24}$$

for some $W(x) > 0$ satisfying $W'(x) \leq -cW(x)$ for some $c > 0$. Differentiating (24) with respect to time and inserting the dynamics (12a) yield

$$\begin{aligned}\dot{V}_0 =& -\lambda\int_0^1 W(x)\tilde{\zeta}(x)\tilde{\zeta}_x(x)dx\\ &+ \int_0^1 W(x)\tilde{\zeta}(x)l\phi_1^T(y(x),x)\tilde{\theta}_1 dx &(25)\\ &+ \int_0^1 W(x)\tilde{\zeta}(x)\phi_2^T(\hat{z}(x),x)\tilde{\theta}_2 dx\\ &+ \int_0^1 W(x)\tilde{\zeta}(x)\tilde{\phi}_2^T(z(x),\hat{z}(x),x)\theta_2 dx. &(26)\end{aligned}$$

Using integration by parts, splitting the second term using Young's inequality and applying the sector condition in Assumption 2 to the last term, keeping in mind that $\tilde{\zeta}(x) = \tilde{z}(x)$, yield

$$\begin{aligned}\dot{V}_0 \leq& -(c\lambda - 1)V_0 + \frac{1}{2}\int_0^1 W(x)(l\phi_1^T(y(x),x)\tilde{\theta}_1)^2 dx &(27)\\ &+ \int_0^1 W(x)\tilde{\zeta}(x)\phi_2^T(\hat{z}(x),x)\tilde{\theta}_2 dx. &(28)\end{aligned}$$

To deal with the parametric uncertainties we augment the function (24) as follows.

$$V = V_0 + a_1 V_1 + V_2. \tag{29}$$

where

$$V_i = \frac{1}{2}\tilde{\theta}_i^T\Gamma_i^{-1}\tilde{\theta}_i \tag{30}$$

for $i = 1, 2$, $a_1 > 0$ and $\Gamma_2 = \Gamma_2^T \succ 0$. Differentiating with respect to time and inserting (19) and (27) yield

$$\dot{V} \leq -(c\lambda - 1)V_0 + \tilde{\theta}_2^T\Gamma_2^{-1}\left(\dot{\hat{\theta}}_2^* - \dot{\hat{\theta}}_2\right) - \tilde{\theta}_1^T H_1\tilde{\theta}_1 \tag{31}$$

where

$$\begin{aligned}H_1 :=& a_1(\nu\nu^T)\\ &- \frac{l^2}{2}\int_0^1 W(x)\phi_1(y(x),x)\phi_1^T(y(x),x)dx \end{aligned} \tag{32}$$

and

$$\dot{\hat{\theta}}_2^* := \Gamma_2\int_0^1 W(x)\phi_2(\hat{z}(x),x)\tilde{\zeta}(x)dx. \tag{33}$$

We conclude the above discussion by stating the main result.

*Proposition 2.* Consider the state estimation error system (12) with $\hat{\theta}_1$ generated by the adaptive law in Lemma 1 and $\hat{\theta}_2$ satisfying

$$\dot{\hat{\theta}}_2 = \dot{\hat{\theta}}_2^* \tag{34}$$

with any initial estimates

$$\hat{\theta}_2(0) = \hat{\theta}_2^*(0). \tag{35}$$

Then, the state estimation error $||\tilde{\zeta}||$ is bounded. Moreover, if PE condition (20) is satisfied, then

$$||\tilde{\zeta}|| \to 0. \tag{36}$$

**Proof.** Selecting $c$ such that $c_0 := c\lambda - 1 > 0$ and inserting (34) into (31) yield

$$\dot{V} \leq -c_0 V_0 - \tilde{\theta}_1^T H_1 \tilde{\theta}_1. \tag{37}$$

For any $c_2 > 0$ and all

$$V_0 \geq c_0^{-1}(c_2 - \tilde{\theta}_1^T H_1 \tilde{\theta}_1) \tag{38}$$

we have $V \leq -c_2 V_0$. By (Khalil, 1996, Th 4.18), $V$ and consequently $||\tilde{\zeta}||, \hat{\theta}_1, \hat{\theta}_2$ are bounded. Furthermore, if the PE condition (20) holds, then it can be shown that (Ioannou and Sun, 2012, Sec. 4.8.3)

$$\int_t^{t+T} \tilde{\theta}_1^T (\nu\nu^T)\tilde{\theta}_1 d\tau \geq h_1 V_1 \geq 0 \tag{39}$$

for the same $T > 0$ specifying (20) and some $h_1 > 0$. Since $\phi_1$ is bounded by assumption, we can lower bound the second term in (32) which together with (39) for sufficiently large $a_1 > 0$ give the lower bound

$$\int_t^{t+T} \tilde{\theta}_1^T H_1 \tilde{\theta}_1 d\tau \geq \int_t^{t+T} (a_1 h_1 - h_2) V_1 d\tau > 0. \tag{40}$$

for some $h_2 > 0$. Selecting $a_1 > h_2 h_1^{-1}$ in (29) yields

$$\dot{V} \leq -c_0 V_0 \tag{41}$$

so that

$$c_0 \int_0^{\infty} V_0 d\tau \leq V(0) - V(\infty) \tag{42}$$

which since the right hand side is bounded and $V_0 \geq 0$, implies $V_0, ||\tilde{\zeta}||^2 \in \mathcal{L}_1$. By (Liu and Krstic, 2001, Lemma 3.1) it then follows that $V_0 \to 0$ and consequently (36). □

### *2.3 Estimating the uncertainty in the momentum balance*

The *ideal* adaptive law $\hat{\theta}_2^*$ defined by (33) is not implementable as $\tilde{\zeta}$ is a-priori unknown. Instead, we heuristically seek an adaptive law *resembling* the non-implementable law in the sense

$$\dot{\hat{\theta}}_2 \to \dot{\hat{\theta}}_2^* \tag{43}$$

as $t \to \infty$. Simplifying the notation by defining

$$\Phi[\hat{z}](x) := -\int_x^1 W(\xi)\phi_2(\hat{z}(\xi), \xi)d\xi, \tag{44}$$

we have

$$\dot{\hat{\theta}}_2^* = \Gamma_2 \int_0^1 \Phi'[\hat{z}](x)\tilde{\zeta}(x)dx. \tag{45}$$

Utilizing that $\Phi[\hat{z}](1) = \tilde{\zeta}(0) = 0$ and using integration by parts, we equivalently have

$$\dot{\hat{\theta}}_2^* = \Gamma_2 \int_0^1 \Phi[\hat{z}](x)\tilde{\zeta}_x(x)dx. \tag{46}$$

*Proposition 3.* Consider the signal $\hat{\sigma} : \mathbb{R}^{\rightarrow}\mathbb{R}^q$ defined by

$$\dot{\hat{\sigma}} = \int_0^1 \eta[\hat{z}](x)\left(-by_x + \phi_2^T(\hat{z}(x), x)\hat{\theta}_2\right)dx \tag{47a}$$

$$\hat{\sigma}(0) = \hat{\theta}_2^*(0) \tag{47b}$$

where

$$\eta[\hat{z}] = \lambda^{-1}\Gamma_2\Phi[\hat{z}], \tag{48}$$

the operator $\Xi : L_2([0,1]) \to \mathbb{R}^q$ satisfying

$$D_{\hat{z}}\Xi[h] = \int_0^1 \eta[\hat{z}](x)h(x)dx \tag{49a}$$

$$\Xi[\hat{z}(\cdot,0)] = 0, \tag{49b}$$

and let

$$\hat{\theta}_2 = \hat{\sigma} - \Xi[\hat{z}]. \tag{50}$$

If the PE condition (20) in Lemma 1 is satisfied and $||\eta[\hat{z}]|| \in \mathcal{L}_\infty$, then

$$\dot{\hat{\theta}}_2 \to \dot{\hat{\theta}}_2^* \tag{51}$$

exponentially fast.

**Proof.** Consider the auxiliary signal $\sigma : \mathbb{R}^+ \to \mathbb{R}^q$ defined as

$$\sigma := \theta_2 + \Xi[\hat{z}]. \tag{52}$$

It is evident that $\sigma - \hat{\sigma} =: \tilde{\sigma} = \tilde{\theta}_2$ and therefore $\dot{\tilde{\sigma}} = \dot{\tilde{\theta}}_2$. We thus need to show that $\dot{\tilde{\sigma}} \to \dot{\tilde{\theta}}_2^*$. Differentiating (52) with respect to time yields

$$\dot{\sigma} = \frac{d}{dt}\Xi[\hat{z}] = D_{\hat{z}}\Xi[\hat{z}_t]. \tag{53}$$

Inserting (49) gives

$$\begin{aligned}\dot{\sigma} &= \int_0^1 \eta[\hat{z}](x)\hat{z}_t(x)dx \\ &= \int_0^1 \eta[\hat{z}](x)\left(\hat{\zeta}_t(x) + \lambda z_x(x) - l\phi_1^T(y(x),x)\theta_1\right)dx.\end{aligned} \tag{54}$$

Subtracting (47a) from (54) yields

$$\dot{\tilde{\theta}}_2 = \dot{\tilde{\sigma}} = \int_0^1 \eta[\hat{z}](x)\left(\lambda\tilde{z}_x(x) - l\phi_1^T(y(x),x)\tilde{\theta}_1\right)dx \tag{55}$$

which in view of (46) and (48) and the fact that $\tilde{\zeta}(x) = \tilde{z}(x)$, is equivalent to

$$\dot{\tilde{\sigma}} = \dot{\tilde{\theta}}_2^* - \int_0^1 \eta[\hat{z}](x)\left(l\phi_1^T(y(x),x)\tilde{\theta}_1\right)dx. \tag{56}$$

If and $||\eta[\hat{z}]|| \in \mathcal{L}_\infty$ and the PE condition (20) is satisfied, $||\eta[\hat{z}]||||l\phi_1^T(y,\cdot)\tilde{\theta}_1|| \to 0$ and we obtain the desired result (51). From (47b) and (49b) we have that (35) is satisfied. □

To implement the adaptive law (50) at any single time $t_1$, we need to evaluate $\Xi$ at $\hat{z}(\cdot,t_1)$. We proceed by computing the incremental value $\Xi[\hat{z}(\cdot,t_1)] - \Xi[\hat{z}(\cdot,t_0)]$ for any $t_1 > t_0 > 0$. Let $S(\gamma) = \hat{z}(\cdot,t_0) + \gamma[\hat{z}(\cdot,t_1) - \hat{z}(\cdot,t_0)]$. Evaluating $\Xi$ at $S(\gamma)$ and differentiating with respect to $\gamma$ yield

$$\begin{aligned}\frac{d}{d\gamma}\Xi[S(\gamma)] &= D_{S(\gamma)}\Xi[S'(\gamma)] \\ &= D_{S(\gamma)}\Xi[\hat{z}(\cdot,t_1) - \hat{z}(\cdot,t_0)] \\ &= \int_0^1 \eta[S(\gamma)](x)\left(\hat{z}(x,t_1) - \hat{z}(x,t_0)\right)dx\end{aligned} \tag{57}$$

Integrating both sides from $\gamma = 0$ to $\gamma = 1$ and using $S(1) = \hat{z}(\cdot,t_1)$ and $S(0) = \hat{z}(\cdot,t_0)$ yield

$$\begin{aligned}\Xi[\hat{z}(\cdot,t_1)] = &\int_0^1\int_0^1 \eta[S(\gamma)](x)\left(\hat{z}(x,t_1) - \hat{z}(x,t_0)\right)dxd\gamma \\ &+ \Xi[\hat{z}(\cdot,t_0)]\end{aligned} \tag{58}$$

*Remark 2.* Using the adaptive law suggested in Proposition 3, the condition (34) in Proposition 2 is only satisfied asymptotically. Consequently, we have not formally established the boundedness and convergence properties of $||\tilde{\zeta}||$ and $\tilde{\theta}_2$. However,

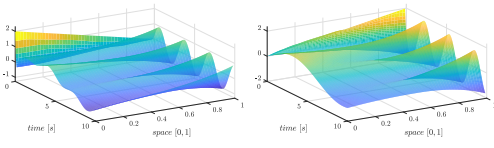


(a) State $y(x,t)$. (b) State $z(x,t)$.

Fig. 1. Case 1. System states.

the two intermediate results in Proposition 2 and 3 suggests an adaptive observer for system (1) that can be tested in simulations or with experimental data. In the next section, the observer is tested in two case simulations.

## 3. SIMULATION

We simulate two cases. Case 1 where the PE condition (20) is satisfied and Case 2 where it is not. The system (1), observer (11), adaptive law (19), filter (47) and operator (58) are simulated in MATLAB for 15 seconds. The PDEs are discretized using 100 spatial discretization points and solved using the *method of lines* by first transforming the hyperbolic system (1) to a Riemann invariant form. In both cases, the system parameters where

$$a = b = 4 \tag{59a}$$

$$\phi_1^T(y(x),x) = \begin{cases} \begin{bmatrix} -5y(x) & 0 \end{bmatrix}, & x < 0 \\ \begin{bmatrix} 0 & -5y(x) \end{bmatrix}, & x \geq 0 \end{cases} \tag{59b}$$

$$\phi_2^T(z(x),x) = \begin{cases} \begin{bmatrix} -z(x) & 0 \end{bmatrix}, & x < 0 \\ \begin{bmatrix} 0 & -z(x) \end{bmatrix}, & x \geq 0 \end{cases} \quad \theta_1 = \begin{bmatrix} 2 & 4 \end{bmatrix} \tag{59c}$$

$$\theta_2 = \begin{bmatrix} 5 & 7 \end{bmatrix}. \tag{59d}$$

Observe that the chosen $\phi_2$ satisfies Assumption 2. For case 1, we used the boundary conditions

$$z(0,t) = \sin(\frac{t}{2}) \tag{60a}$$

$$y(1,t) = \sin(2t) \tag{60b}$$

while for case 2, we used

$$z(0,t) = 0 \tag{61a}$$

$$y(1,t) = \sin(2t). \tag{61b}$$

Compatible initial conditions were selected as

$$y(x,0) = y(1,0) + 2(1-x) \tag{62a}$$

$$z(x,0) = 2x + z(0,0). \tag{62b}$$

Finally, the design parameters are

$$L = 0.8 \tag{63a}$$

$$\hat{\theta}_1(0) = \hat{\theta}_2(0) = 0 \tag{63b}$$

$$\Gamma_1 = \Gamma_2 = \begin{bmatrix} 20 & 0 \\ 0 & 20 \end{bmatrix} \tag{63c}$$

$$W(x) = 2 - x. \tag{63d}$$

For case 1, with states shown in Figure 1, the PE condition (20) is satisfied and $\tilde{\theta}_1 \to 0$ as can be seen in Figure 4. The conditions of Proposition 3 is satisfied and for $\dot{\hat{\theta}}_2 = \dot{\hat{\theta}}_2^*$ it follows from Proposition 2 that $||\tilde{\zeta}|| \to 0$ which can be seen in Figures 2 and 3. The parameter estimates $\hat{\theta}_2$ also converge to their true value as can be seen in Figure 5.

For case 2, with states shown in Figure 6, the PE condition (20) is not satisfied and $\hat{\theta}_1$ converge to a constant $\bar{\theta}_1 \neq \theta_1$ as

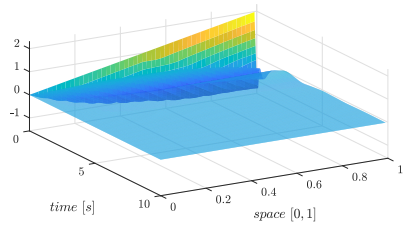


Fig. 2. Case 1. State estimation error $\tilde{z}(x,t)$.

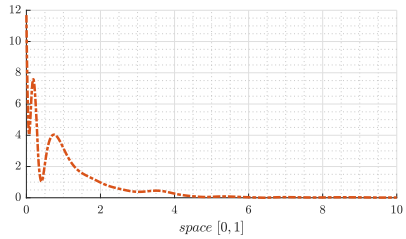


Fig. 3. Case 1. State estimation error $||\tilde{z}||$.

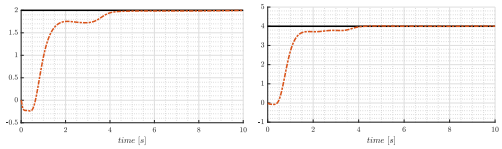


(a) $\hat{\theta}_{1,1}$ vs. $\theta_{1,1}$. (b) $\hat{\theta}_{1,2}$ vs. $\theta_{1,2}$.

Fig. 4. Case 1. Parameter estimates $\hat{\theta}_1$ (red dotted) vs. true parameters $\theta_1$ (solid black).

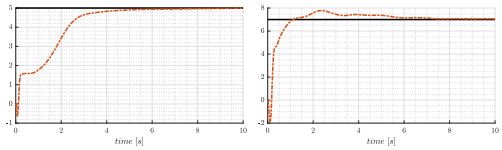


(a) $\hat{\theta}_{2,1}$ vs. $\theta_{2,1}$. (b) $\hat{\theta}_{2,2}$ vs. $\theta_{2,2}$.

Fig. 5. Case 1. Parameter estimates $\hat{\theta}_2$ (red dotted) vs. true parameters $\theta_2$ (solid black).

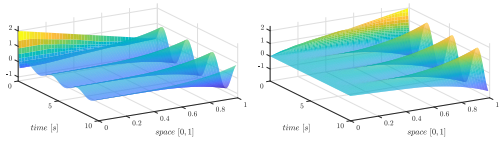


(a) State $y(x,t)$. (b) State $z(x,t)$.

Fig. 6. Case 2. System states.

can be seen in Figure 9. Still, as shown in Figures 7 and 8 the estimation error $||\tilde{\zeta}||$ is bounded and converge to a set close

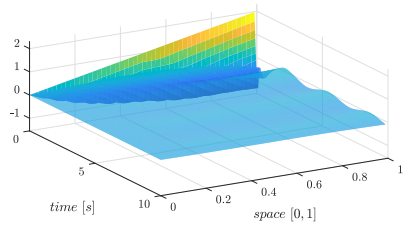


Fig. 7. Case 2. State estimation error $\tilde{z}(x,t)$.

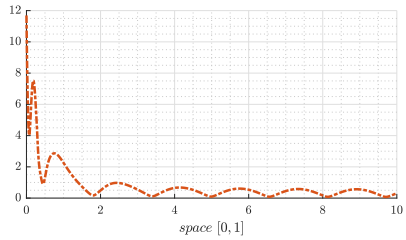


Fig. 8. Case 2. State estimation error $||\tilde{z}||$.

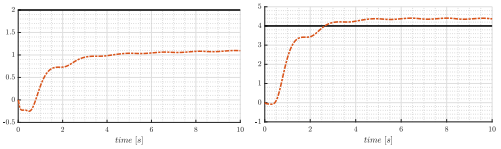

(a) $\hat{\theta}_{1,1}$ vs. $\theta_{1,1}$. (b) $\hat{\theta}_{1,2}$ vs. $\theta_{1,2}$.

Fig. 9. Case 2. Parameter estimates $\hat{\theta}_1$ (red dotted) vs. true parameters $\theta_1$ (solid black).

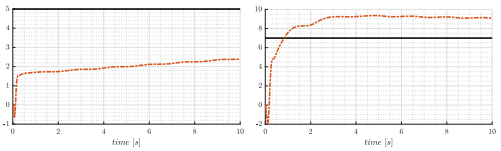

(a) $\hat{\theta}_{2,1}$ vs. $\theta_{2,1}$. (b) $\hat{\theta}_{2,2}$ vs. $\theta_{2,2}$.

Fig. 10. Case 2. Parameter estimates $\hat{\theta}_2$ (red dotted) vs. true parameters $\theta_2$ (solid black).

to zero, as guaranteed by Proposition 2. Figure 10 shows that parameter convergence is not achieved or at least is very slow.

## 4. CONCLUDING REMARKS

We have designed an adaptive observer estimating the distributed state of a semi-linear $2 \times 2$ hyperbolic system and uncertainties appearing in both state equations by relying on partial distributed state measurement and boundary measurements. The scheme can be used to estimate the flow rate in a single-phase fluid flow system where the in-/out-flow of mass and momentum gain/loss are parametrically uncertain by relying on distributed pressure measurements. With no mass in- or out-flux, any uncertain local gain or loss of momentum can be estimated using pressure measurements only. With mass in or out-flux, we use boundary measurements of the flow rate in addition to the pressure measurements to estimate net gain or loss of mass. Remark that for any single point in time, only the aggregate net in-/out-flow can be estimated. Situations with flow-loops, that is inflow in one region and an outflow of equal size in another region, is not detectable using boundary measurements only. However, if the local inflow varies in a certain way and is sufficiently distinct compared to other regions, it is possible to also estimate local in- or out-flow phenomena, and not only the aggregate net flow. These conditions are all covered by the persistence of excitation criterion guaranteeing convergence of the parametric uncertainties in the mass balance.

## REFERENCES

Arcak, M. and Kokotovic, P. (1999). Nonlinear observers: a circle criterion design. In *Proceedings of the 38th IEEE Conference on Decision and Control*, volume 5, 4872–4876. IEEE.

Bastin, G. and Coron, J.M. (2016). *Stability and boundary stabilization of 1-D hyperbolic systems*, volume 88. Springer.

Berg, C., Stakvik, J.Å., Lie, B., Vaagsaether, K., and Kaasa, G.O. (2019). Pressure wave propagation in managed pressure drilling- model comparison with real life data. *Submitted*.

Besanon, G., Zhang, Q., and Hammouri, H. (2004). High-gain observer based state and parameter estimation in nonlinear systems. In *Proceedings of the 6th IFAC Symposium on Nonlinear Control Systems 2004*, volume 37, 327 – 332.

Holta, H. and Aamo, O.M. (2019). An adaptive observer design for $2 \times 2$ semi-linear hyperbolic systems using distributed sensing. In *Proceedings of the 2019 American Control Conference*, 2540–2545.

Ioannou, P.A. and Sun, J. (2012). *Robust Adaptive Control*. Courier Corporation.

Khalil, H.K. (1996). *Nonlinear Systems*. Prentice-Hall, New Jersey.

Kitsos, C., Besancon, G., and Prieur, C. (2018). High-gain observer design for a class of hyperbolic systems of balance laws. In *2018 IEEE Conference on Decision and Control (CDC)*. IEEE.

Landet, I.S., Pavlov, A., and Aamo, O.M. (2013). Modeling and control of heave-induced pressure fluctuations in managed pressure drilling. *IEEE Transactions on Control Systems Technology*, 21(4), 1340–1351.

Liu, W.J. and Krstic, M. (2001). Adaptive control of burgers' equation with unknown viscosity. *International Journal of Adaptive Control and Signal Processing*, 15(7), 745–766.

Marino, R. and Tomei, P. (1992). Global adaptive observers for nonlinear systems via filtered transformations. *IEEE Transactions on Automatic Control*, 37(8), 1239–1245.

Marino, R. and Tomei, P. (1995). *Nonlinear control design: geometric, adaptive and robust*, volume 1. Prentice Hall London.

Stamnes, Ø.N., Zhou, J., Aamo, O.M., and Kaasa, G. (2009). Adaptive observer design for nonlinear systems with parametric uncertainties in unmeasured state dynamics. In *Proceedings of the 48h IEEE Conference on Decision and Control*, 4414–4419.

Stamnes, Ø.N., Zhou, J., Kaasa, G., and Aamo, O.M. (2008). Adaptive observer design for the bottomhole pressure of a managed pressure drilling system. In *Proceedings of the 47th IEEE Conference on Decision and Control*, 2961–2966.

## 3.5 Paper [63]: *Exploiting wired-pipe technology in an adaptive observer for drilling incident detection and estimation*

Holta, H. and Aamo, O. M. (2020c). Exploiting wired-pipe technology in an adaptive observer for drilling incident detection and estimation. *Under review, SPE Journal, submitted January 2020*

This Paper is awaiting publicatin and is not included in NTNU Open

## 3.6 Comments, flaws, limitations and further work

The motivation for extending the observer design from [58] to general heterodirectional systems in [60], was to handle multi-phase systems such as those modeled by the drift-flux model. The same limitation as discussed in Section 2.4 regarding linearization of the flux density matrix applies here. In addition, as discussed in the paper, the adaptive part requires some further assumptions on the type of boundary condition and number of measured states relative to the unmeasured states. In sum, these assumptions are too restrictive to allow applications based on the drift-flux model. Some further work is thus needed for the design to handle faults in multi-phase flow.

It is stressed in [64] that the extension from [58] is justified heuristically. Although we think a formal proof is possible to construct, we did not manage to complete the analysis. Some further work is here needed.

In [63], the fault models are presented without any further justification. Although most of the models are general and/or commonly used, we do make some novel modeling assumptions. The validity of these models should be investigated further and a comment discussing the novelty of these assumptions will be included in the final submitted manuscript.

# CHAPTER 4

# Closed loop kick & loss attenuation

## 4.1 Introduction

The significance of all closed loop kick and loss estimation and attenuation schemes presented in this chapter is that, provided the kick or loss is attenuated, the reservoir pore pressure is simultaneously estimated. That is, using closed loop output regulation, the PE condition is always satisfied and the pore pressure estimates converge to the true value.

In the first paper [57], the state and parameter estimation scheme from [67] is coupled with a closed loop controller for kick & loss estimation. The method is improved in [68] which presents an alternative, simpler solution to the same problem. The first paper is therefore omitted.

In the second paper [68], a closed loop controller is used for loss attenuation in single-phase systems. Down-hole pressure measurements are assumed available using wired drill pipe. The design is compared to a previous result [65] where only top-side flow and pressure measurements are assumed to be available.

In the third paper [62], the state and parameter estimation scheme from [61] is coupled with a closed loop controller for set-point regulation.

## 4.2 Paper [57]: *Boundary set-point regulation of a linear $2 \times 2$ hyperbolic PDE with uncertain bilinear boundary condition (omitted)*

Holta, H. and Aamo, O. M. (2018). Boundary set-point regulation of a linear $2 \times 2$ hyperbolic PDE with uncertain bilinear boundary condition. In *Proceedings of the 2018 IEEE Conference on Decision and Control (CDC)*, pages 2156–2163. IEEE

*This paper is omitted, as the material in this paper is covered by Paper [68].*

## 4.3 Paper [68]: *Adaptive set-point regulation of linear $2 \times 2$ hyperbolic systems with application to the kick problem in MPD*

Holta, H., Anfinsen, H., and Aamo, O. M. (2020a). Adaptive set-point regulation of linear $2 \times 2$ hyperbolic systems with application to the kick and loss problem in drilling. *Automatica*, 119:109078

# Adaptive Set-Point Regulation of Linear $2 \times 2$ Hyperbolic Systems with Application to the Kick and Loss Problem in Drilling ⋆

Haavard Holta [a], Henrik Anfinsen [a], Ole Morten Aamo [a]

[a] *Department of Engineering Cybernetics. Norwegian University of Science and Technology, Trondheim N-7491, Norway*

**Abstract**

We study the kick and loss detection and attenuation problem in managed pressure drilling by modeling the well as a distributed parameter system. Two cases are considered, distinguished by whether down-hole pressure measurements are available or not. The main contribution of the paper is a theoretical result on adaptive stabilization and set-point regulation by boundary control for a general $2 \times 2$ linear hyperbolic system in the case of measurements taken at both boundaries, with stability proven in the $L_2$-sense. The design is applied to the drilling system and shown to solve the kick and loss problem with sensing at both boundaries. An earlier result on adaptive set-point regulation for $2 \times 2$ hyperbolic systems is also applied to the drilling system and shown to solve a kick and loss problem with sensing restricted to the actuated boundary only. The two designs are compared in a simulation of a loss incident, showing a significant reduction in convergence time and total accumulated loss for the design with sensing allowed at both boundaries.

*Key words:* Distributed-parameter systems, adaptive control, parameter estimation, managed pressure drilling, kick and loss detection

## 1 Introduction

### *1.1 Motivation*

A drilling system consists of a drill string with a drill bit at the bottom-hole end and a casing around the drill string called *annulus*. A drilling fluid called *mud* is circulated down the drill string, through the drill-bit and up the annulus to the surface where cuttings are removed and the mud recirculated down the drill string again (see Figure 1). The purpose of the mud is not only to transport the cuttings out of the system, but to provide pressure control throughout the well. If the pressure is too low, the well might collapse, and a too high bottom-hole pressure might lead to fracturing of the formation. Traditionally, pressure is controlled by varying the mud density, viscosity or circulation rate. In *managed pressure drilling* (MPD), with *applied back pressure* (ABP) in particular, the pressure in the annulus is controlled by using a *back pressure valve* top-side to limit the flow and a *back-pressure pump* in the case without circulation. The difficulty in MPD comes from the fact that actuation is located top-side, while the pressure of interest is bottom-hole usually several kilometers away. Sensing is only available at the boundaries and often only top-side.

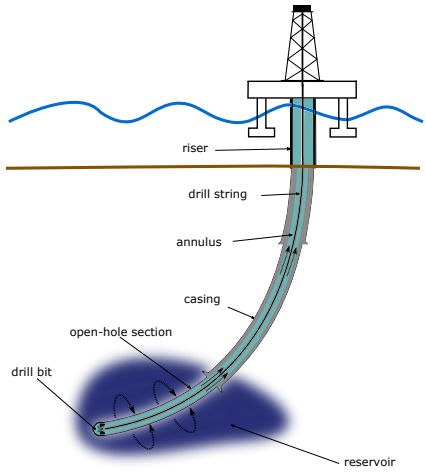


Fig. 1. Schematic of the drilling system.

⋆ Corresponding author: H. Holta. Economic support from The Research Council of Norway and Equinor ASA through project no. 255348/E30 Sensors and models for improved kick/loss detection in drilling (Semi-kidd) is gratefully acknowledged.

*Email addresses:* haavard.holta@ntnu.no (Haavard Holta), henrik.anfinsen@ntnu.no (Henrik Anfinsen), aamo@ntnu.no (Ole Morten Aamo).

Time spent correcting down-hole errors caused by inadequate pressure control accounts for a significant part of the total non-productive time during drilling [24]. To avoid such errors, it is essential to maintain a down-hole pressure within margins dictated by the surrounding reservoir pressure. When the bottom-hole pressure exceeds the formation pressure drilling mud will flow into the formation, called a *loss*, potentially damaging the well-bore (if exceeding the *fracturing* pressure). A higher formation pressure than down-hole pressure will result in formation fluids flowing into the well, called a *gain* or *kick*. If not handled, a kick leads to formation fluids flowing up the annulus, which in severe circumstances, might lead to uncontrolled blowouts on the surface. Often, a kick is preceded by a loss since the loss causes down-hole pressure to drop. Thus, quick handling of the loss is critical for avoiding a kick incident, which is more serious in terms of safety. Since the reservoir pressure is usually unknown, the challenge is now to stabilize the well pressure, estimate the reservoir pressure and at the same time use this estimate together with well pressure and flow estimates to regulate the bottom-hole pressure.

To model the annular pressure and flow in a well using managed pressure drilling, a modification of the model presented in [22] is used. This model is based on a single mass balance law and a momentum balance linearized around a constant mud density. The model is the result of a trade-off between providing the necessary level of simplicity needed for estimation and control design while at the same time capturing the dominating dynamics in a single-phase system with laminar pipe flow. To model the reservoir relation, the bottom-hole boundary condition is replaced by a simple *productivity index inflow* model where the flow between the reservoir and the well-bore is proportional to the bottom-hole and reservoir pressure difference. This gives the following model:

$$p_t(z,t) = -\frac{\beta}{A} q_z(z,t) \tag{1a}$$

$$q_t(z,t) = -\frac{A}{\rho} p_z(z,t) - \frac{F}{\rho} q(z,t) - Ag\cos\psi(z) \tag{1b}$$

$$q(0,t) = J\left(p_r - p(0,t)\right) + q_{bit} \tag{1c}$$

$$p(l,t) = p_l(t) \tag{1d}$$

where $z \in [0,l]$ and $t \geq 0$ are independent variables of space and time respectively, $l$ is the well depth, $p(z,t)$ is pressure, $q(z,t)$ is volumetric flow, $\beta$ is the bulk modulus of the mud, $\rho$ is the density of the mud, $A$ is the cross sectional area of the annulus, $F$ is the friction factor, $g$ is the acceleration of gravity, $\psi(z)$ is the angle between the positive flow direction and gravity at position $z$, $J > 0$ is called the productivity index and is assumed unknown, $p_r$ is the unknown reservoir pressure, and $q_{bit}$ is the known flow through the drill bit. It is assumed that $p_r$ satisfies $0 < p_r \leq \bar{p}_r$ where $\bar{p}_r$ is some known upper bound for the reservoir pressure. Moreover, it is assumed that the choke controller has significantly faster dynamics than the rest of the system so that the actuation dynamics can be ignored and the top-side pressure $p_l$ regarded as a control input. The design goal is to keep the down-hole pressure equal to the unknown reservoir pressure, that is $p(0,t) = p_r$ such that flow between the reservoir and well-bore is zero. This implies that the flow through the annulus is equal to the drill bit flow. Based on the design goal, the control objective

$$\lim_{t\to\infty} \int_t^{t+T} |p_r - p(0,t)|\, d\tau = 0 \tag{2}$$

where $T > 0$ is an arbitrary constant, is selected. To estimate the distributed pressure and flow state and achieve the control objective (2), we assume that the following boundary measurements are available:

- Top-side return flow $q(l,t) =: q_l(t)$ .
- Bottom-hole pressure $p(0,t) =: p_0(t)$.

In particular, recent advances in wired-drillpipe technology now provides down-hole pressure in real time, replacing the older less reliable, low bandwidth *mud-pulse*-based pressure measurements.

### *1.2 Problem statement*

The coefficient matrix of (1a) and (1b) (formed by combining the states into vector form and collecting the coefficients of the spatial derivatives into a single matrix) has two distinct, real eigenvalues ($\pm\sqrt{\beta/\rho}$), which shows that (1) is of type *hyperbolic*. For all linear hyperbolic systems, there exists a coordinate transformation transforming the system to *characteristic* form where the coefficient matrix is diagonalized (see e.g. [9]). To ease the control design process and analysis, but also to make the design slightly more general and thereby possibly applicable to other applications, we will in the following study systems in the form

$$u_t(x,t) + \lambda u_x(x,t) = c_1(x)v(x,t) \tag{3a}$$

$$v_t(x,t) - \mu v_x(x,t) = c_2(x)u(x,t) \tag{3b}$$

$$u(0,t) = rv(0,t) + k(\theta - y_0(t)) \tag{3c}$$

$$v(1,t) = \sigma y_1(t) + U(t) \tag{3d}$$

defined for $x \in [0,1]$, $t \geq 0$, where $u, v$ are the system states, $\lambda, \mu > 0$, $c_1(x), c_2(x) \in C([0,1])$ are the source terms, $r$ is a constant and $y_0$ is a measured signal related to the states by

$$y_0(t) = u(0,t) - b_0 v(0,t) \tag{4}$$

with $b_0 \neq r$. In addition, we have the boundary measurement

$$y_1(t) = u(1,t). \tag{5}$$

The only unknown parameters are $k \in [\underline{k}, \bar{k}] \subset (0,\infty)$ and $\theta \in \mathbb{R}$ where $\underline{k}$ and $\bar{k}$ are known lower and upper bounds on $k$ required for technical reasons in the controller design. In order to select the bounds, we must assume that $r + b_0 k$ is

nonzero with known sign. The control objective (2) can be stated in the new coordinate system as

$$\lim_{t\to\infty} \int_t^{t+T} |\theta - y_0(\tau)|\, d\tau = 0 \tag{6}$$

for some arbitrary $T > 0$.

**Remark 1** *Related to system* (1)*,* $\lambda$ *and* $-\mu$ *represent the eigenvalues of the coefficient matrix which is unchanged by the coordinate transformation, the source terms* $c_1, c_2$ *account for the frictional loss terms, the unknown parameters* $J$ *and* $p_r$ *can be recovered from* $k$ *and* $\theta$*,* $y_0$ *is related to the down-hole pressure measurement while* $y_1$ *is related to the top-side flow measurement, and the parameters* $r$ *and* $b_0$ *are trivially equal to* $-1$ *and* 1*, respectively. The details regarding the diagonalizing change of coordinates from* (1) *to* (3) *can be found in Lemma 5 in Section 3.*

It is assumed that the initial conditions $u(x,0) = u_0(x)$, $v(x,0) = v_0(x)$ satisfy $u_0, v_0 \in \mathscr{B}([0,1])$, where

$$\mathscr{B}([0,1]) = \{f(x) : \sup_{x\in[0,1]} f(x) < \infty\}, \tag{7}$$

in which case it can be shown [30] that (3) has a unique solution that stays in $\mathscr{B}([0,1])$ for all $t \geq 0$ for the form of $U(t)$ used in this paper. The objective is to design a control input $U(t)$ so that system (3) is adaptively stabilized in the $L_2$-sense and such that the objective (6) is achieved. The structure of this problem, with distributed states, and sensing and actuation only at boundaries, fits perfectly into the control framework of infinite-dimensional backstepping for PDEs. In addition, the unknown parameter part of the problem can be handled by combining the backstepping method with an adaptive parameter update law..

### *1.3 Previous work*

The method of infinite-dimensional backstepping for PDEs was first introduced for parabolic PDEs in [23,27,28], where the gain kernel was expressed as a solution to a well-posed PDE. The first result using backstepping applied on hyperbolic PDEs was for first order systems in [19]. The method was later extended to second order hyperbolic systems in [26], and to two coupled first order hyperbolic systems in [32]. The results in the latter were used in [1] for disturbance attenuation in managed pressure drilling which has similarities to the problem considered in this paper. Disturbance attenuation and trajectory tracking problems based on the internal model principle were further studied in [12,20,21]. Adaptive control of parabolic PDEs is extensively studied in [29]. In recent years, results on adaptive state estimation and closed loop stabilization for hyperbolic PDEs have also emerged. Adaptive observers for $n+1$ hyperbolic systems using sensing collocated with the uncertain boundary parameters can be found in [7] using swapping filters, and in [10] using a Lyapunov approach. The extension to stabilization, without additive boundary parameter, and sensing at the non-actuated boundary restricted to the form $y_0(t) = v(0,t)$, is given in [6]. For systems with non-zero additive terms in the un-actuated boundary, the steady-state *profile* is non-zero. For such systems, we study *boundary set-point regulation*, where the goal is to control the un-actuated boundary to a desired set-point, which is unknown a priori. Adaptive set-point regulation for $2 \times 2$ systems with an affine boundary condition is considered in [16] and for a bilinear boundary condition in [15] using a swapping based design. A closed loop controller achieving boundary set-point regulation can be designed by defining a *reference model* and proving stability in terms of a quantity describing the *tracking error*. A model reference adaptive control problem for $2 \times 2$ system with a multiplicative boundary condition is studied in [5].

Previous results on kick attenuation in MPD have mainly focused on using lumped drilling models. A lumped ODE model is applied to a gas kick detection and mitigation problem in [33] by using a method for switched control of the bottom-hole pressure. Another lumped model for estimation and control of in-/outflux is presented in [13]. Kick handling methods for a first-order approximation to the PDE system is presented in [2] using LMI (Linear Matrix Inequality) based controller design. In/out-flux detection using an infinite dimensional observer is presented in [14]. Kick handling using a distributed PDE model incorporating a model of the reservoir inflow relation, has to the best of the authors' knowledge not previously been addressed.

### *1.4 Contributions and paper structure*

The contributions in this paper are twofold. First, a theoretical result on adaptive boundary set-point regulation of system (3) achieving (6) and $L_2$ boundedness of all signals in the closed loop system is derived in Section 2. This is achieved by using some of the ideas on model reference control from [5], but with the additional complexity of having, since the parameter $\theta$ is unknown, an unknown set-point (6). Second, both the design from Section 2 and the theoretical results on set-point regulation using only topside sensing from [16] are applied to the kick & loss problem in managed pressure drilling, solving the non-collocated and collocated sensing and control problem, respectively. Feasibility of applying the designs to the MPD model are stated in Corollaries 1 and 2 in Section 3. Finally, the two designs are compared in a simulation study in Section 4, demonstrating the benefit of having down-hole pressure available. The new design (the theoretical design in Section 2 with non-collocated sensing) is a significant improvement over the design for system (3) offered in [15]. The state- and parameter estimation scheme avoids swapping filters, thereby significantly reducing the dynamic order of the controller, the stability analysis is less involved, and performance when applied to the MPD problem is improved.

### 1.5 Notation

For a signal $z:[0,1]\times[0,\infty)\to\mathbb{R}$, let $||z||=\sqrt{\int_0^1 z^2(x,t)dx}$ denote the $L_2$-norm. For a time-varying, signal $f(t)$, we use the vector spaces

$$f\in\mathscr{L}_p \leftrightarrow \left(\int_0^\infty |f(t)|^p dt\right)^{\frac{1}{p}}<\infty \tag{8}$$

for $p\geq 1$ with the special case $f\in\mathscr{L}_\infty \leftrightarrow \sup_{t\geq 0}|f(t)|<\infty$. The projection operator Proj is defined as

$$\text{Proj}_{a,b}(\tau,\omega)=\begin{cases}0, & \text{if } \omega=a \text{ and } \tau\leq 0\\ 0, & \text{if } \omega=b \text{ and } \tau\geq 0\\ \tau, & \text{otherwise}\end{cases} \tag{9}$$

## 2 Control design with non-collocated sensing

### 2.1 State and parameter estimation

From (4), we see that we can describe the non-actuated boundary in the alternative form

$$u(0,t)=b_0 v(0,t)+y_0(t). \tag{10}$$

Since this form eliminates all unknown parameters from the system, designing an observer estimating the states $(u,v)$ becomes almost trivial. A state observer converging to the true states in finite time is presented in Section 2.1.1. Once the system states are known, we can use boundary condition (3c) to design adaptive laws estimating the unknown parameters. In Section 2.1.2, adaptive laws based on the gradient method for a bilinear parametric model are presented.

#### 2.1.1 Finite-time convergent state observer

Let $\hat{u},\hat{v}$ be the estimates of $u,v$ respectively, and denote the estimation error $\tilde{u}=u-\hat{u}$ and $\tilde{v}=u-\hat{v}$. Choosing the observer

$$\hat{u}_t(x,t)+\lambda\hat{u}_x(x,t)=c_1(x)\hat{v}(x,t)+P_1(x)\tilde{u}(1,t) \tag{11a}$$
$$\hat{v}_t(x,t)-\mu\hat{v}_x(x,t)=c_2(x)\hat{u}(x,t)+P_2(x)\tilde{u}(1,t) \tag{11b}$$
$$\hat{u}(0,t)=b_0\hat{v}(0,t)+y_0(t) \tag{11c}$$
$$\hat{v}(1,t)=\sigma y_1(t)+U(t), \tag{11d}$$

with initial conditions satisfying $\hat{u}(\cdot,0),\hat{v}(\cdot,0)\in\mathscr{B}([0,1])$, gives the error dynamics

$$\tilde{u}_t(x,t)+\lambda\tilde{u}_x(x,t)=c_1(x)\tilde{v}(x,t)-P_1(x)\tilde{u}(1,t) \tag{12a}$$
$$\tilde{v}_t(x,t)-\mu\tilde{v}_x(x,t)=c_2(x)\tilde{u}(x,t)-P_2(x)\tilde{u}(1,t) \tag{12b}$$
$$\tilde{u}(0,t)=b_0\tilde{v}(0,t) \tag{12c}$$
$$\tilde{v}(1,t)=0. \tag{12d}$$

Selecting the injection term $P_1,P_2$ as $P_1(x)=\lambda P^{uu}(x,1)$, $P_2(x)=\lambda P^{vu}(x,1)$, where $(P^{uu},P^{vu})$ is the unique solution to a $2\times 2$ hyperbolic system given in [32, Eq. (67)-(74)], and using the invertible backstepping transformation [32, Eq. (60)-(61)], it is possible to show that (12) is equivalent to a system of cascaded transport equations with a zero boundary condition so that $(\tilde{u},\tilde{v})$ will be identically zero for all

$$t\geq t_F:=\lambda^{-1}+\mu^{-1} \tag{13}$$

since the backstepping transformation is invertible.

#### 2.1.2 Parameter estimation

With $(u,v)$ known for all $t\geq t_F$, we can use boundary condition (3c) to define a known signal $e$ as

$$u(0,t)-rv(0,t)=k(\theta-y_0(t))=:e(t) \tag{14}$$

with the corresponding estimate

$$\hat{e}(t):=\hat{k}(t)(\hat{\theta}(t)-y_0(t)). \tag{15}$$

The *gradient method for bilinear parametric models* in [17, Theorem 4.52] can be used to minimize a cost function based on the square error $\tilde{e}^2(t)=(e(t)-\hat{e}(t))^2$ and thereby forming adaptive laws for the parameter estimates $\hat{\theta},\hat{k}$. Parameter projection is employed to force the estimate of $k$ to satisfy the known conditions on $k$.

**Lemma 1** *Consider the adaptive laws*

$$\dot{\hat{\theta}}(t)=\gamma_1\frac{\tilde{e}(t)}{1+y_0^2(t)} \tag{16a}$$
$$\dot{\hat{k}}(t)=\text{Proj}_{\underline{k},\bar{k}}\left(\gamma_2\left[\hat{\theta}(t)-y_0(t)\right]\frac{\tilde{e}(t)}{1+y_0^2(t)},\hat{k}(t)\right) \tag{16b}$$

*for $t\geq t_F$ and $\dot{\hat{\theta}}=\dot{\hat{k}}=0$ for $t<t_F$, where $\gamma_1,\gamma_2>0$ is the adaptation gain and where we assume $\underline{k}\leq\hat{k}(0)\leq\bar{k}$. The adaptive laws* (16) *have the following properties:*

*(1)* $\hat{\theta},\hat{k},\in\mathscr{L}_\infty$.
*(2)* $\underline{k}\leq\hat{k}(t)\leq\bar{k}$ *for all* $t\geq 0$
*(3)* $\frac{\tilde{e}}{\sqrt{1+y_0^2}}\in\mathscr{L}_2\cap\mathscr{L}_\infty$
*(4)* $\dot{\hat{\theta}},\dot{\hat{k}},\in\mathscr{L}_\infty\cap\mathscr{L}_2$.
*(5) If $y_0$ is bounded for* almost all $t\geq 0$ *and $\hat{\theta}-y_0\in\mathscr{L}_2$, then $\hat{\theta}$ converges to $\theta$ and $\hat{k}$ converges to some constant.*

The proof is given in Appendix A.1.

### 2.2 Closed loop adaptive controller design

In the following stability analysis, it is more convenient to write boundary condition (3c) in linear form

$$\begin{aligned} u(0,t) =& rv(0,t) + \hat{k}(t)(\hat{\theta}(t) - y_0(t)) + \tilde{e}(t) \\ =& \hat{q}(t)v(0,t) + \hat{d}(t) + \hat{\kappa}(t)\tilde{e}(t) \end{aligned} \tag{17}$$

such that

$$\hat{q}(t) := \frac{r + b_0\hat{k}(t)}{1+\hat{k}(t)}, \hat{d}(t) := \frac{\hat{k}(t)\hat{\theta}(t)}{1+\hat{k}(t)}, \hat{\kappa}(t) := \frac{1}{1+\hat{k}(t)}. \tag{18}$$

To derive a closed loop control law, we use the infinite dimensional backstepping method to stabilize the system by decoupling the state dynamics (3). Since the objective is boundary set-point regulation to an unknown set-point, we design a time varying reference signal and a corresponding reference model we would like our system to track, such that the overall control objective is achieved. To give some intuition behind our selection of control law, we apply a certainty equivalence principle in Section 2.2.1 and propose a control law in Theorem 1. To set the stage for the formal stability proof, which is given in Section 2.3, and to give some further intuition, we use the reference model to derive a final target system that describes the *system tracking error*. Instrumental to the design are the backstepping operators $\mathscr{K}_1, \mathscr{K}_2, \mathscr{K}_{10}, \mathscr{K}_{20} : \mathscr{B}([0,1]) \times \mathscr{B}([0,1]) \to \mathscr{B}([0,1])$ given by

$$\begin{aligned} &\mathscr{K}_1[a,b](x,t) = a(x) - \mathscr{K}_{10}[a,b](x,t) \\ &= a(x) - \int_0^x K^{uu}(x,\xi,t)a(\xi) + K^{uv}(x,\xi,t)b(\xi)d\xi \quad (19a) \\ &\mathscr{K}_2[a,b](x,t) = b(x) - \mathscr{K}_{20}[a,b](x,t) \\ &= b(x) - \int_0^x K^{vu}(x,\xi,t)a(\xi) + K^{vv}(x,\xi,t)b(\xi)d\xi \quad (19b) \end{aligned}$$

where $a$, $b \in \mathscr{B}([0,1])$ , $(K^{uu}, K^{uv}, K^{vu}, K^{vv})$ is the solution to the time-varying system of equations

$$\begin{aligned} K^{uu}_x(x,\xi,t)\lambda + K^{uu}_\xi(x,\xi,t)\lambda &= -K^{uv}(x,\xi,t)c_2(x) && (20a) \\ K^{uv}_x(x,\xi,t)\lambda - K^{uv}_\xi(x,\xi,t)\mu &= -K^{uu}(x,\xi,t)c_1(x) && (20b) \\ K^{vu}_x(x,\xi,t)\mu - K^{vu}_\xi(x,\xi,t)\lambda &= K^{vv}(x,\xi,t)c_2(x) && (20c) \\ K^{vv}_x(x,\xi,t)\mu + K^{vv}_\xi(x,\xi,t)\mu &= K^{vu}(x,\xi,t)c_1(x) && (20d) \end{aligned}$$

$$\begin{aligned} K^{uv}(x,x,t)\lambda + K^{uv}(x,x,t)\mu &= c_1(x) && (20e) \\ K^{vu}(x,x,t)\lambda + K^{vu}(x,x,t)\mu &= -c_2(x) && (20f) \\ K^{uu}(x,0,t)\lambda\hat{q}(t) &= K^{uv}(x,0,t)\mu && (20g) \\ K^{vu}(x,0,t)\lambda\hat{q}(t) &= K^{vv}(x,0,t)\mu && (20h) \end{aligned}$$

defined over $\{(x,\xi,t) \,|\, 0 \le \xi \le x \le 1, t \ge t_F\}$. From [11], system (20) has a unique, bounded and continuous solution $(K^{uu}, K^{uv}, K^{vu}, K^{vv})$ for any bounded, nonzero $\hat{q}$. Moreover, the mapping $(a,b) \to (\bar{a},\bar{b})$ given by

$$\begin{aligned} \bar{a}(x) =& \mathscr{K}_1[a,b](x) \\ \bar{b}(x) =& \mathscr{K}_2[a,b](x) \end{aligned} \tag{21}$$

is invertible with unique inverse transformation kernels. In addition, if $\hat{q} \in \mathscr{L}_2 \cap \mathscr{L}_\infty$ then (see [6])

$$||K^{uu}_t||, ||K^{uv}_t||, ||K^{vu}_t||, ||K^{vv}_t|| \in \mathscr{L}_2 \cap \mathscr{L}_\infty. \tag{22}$$

#### 2.2.1 Main result

Let

$$\Psi_1(x,t) := -\lambda K^{uu}(x,0,t) \tag{23a}$$
$$\Psi_2(x,t) := -\lambda K^{uv}(x,0,t). \tag{23b}$$

Furthermore, due to projection of $\hat{k}$ in (16b), $\hat{q}(t)$ given in (18) is bounded. That is

$$|\hat{q}(t)| \le \bar{q} := \max\left|\frac{r+b_0\underline{k}}{1+\underline{k}}, \frac{r+b_0\bar{k}}{1+\bar{k}}\right| \tag{24}$$

for all $t \ge 0$.

**Theorem 1** *Let $\tilde{\sigma}$ be a known constant such that $|\tilde{\sigma}\bar{q}| < 1, \bar{\sigma} =: \sigma - \tilde{\sigma}$. Consider system* (3) *and the adaptive law* (16)*. The control law*

$$\begin{aligned} U(t) =& \mathscr{K}_{20}[\hat{u},\hat{v}](1,t) - \tilde{\sigma}\mathscr{K}_{10}[\hat{u},\hat{v}](1,t) \\ &+ \frac{1-\tilde{\sigma}r}{r-b_0}\hat{\theta}(t) - \bar{\sigma}y_1(t) \\ &- \hat{d}(t)\int_0^1 (\tilde{\sigma}\lambda^{-1}\Psi_1(\xi,t) + \mu^{-1}\Psi_2(\xi,t))d\xi \end{aligned} \tag{25}$$

*guarantees* (6)*. Moreover, all signals in the closed loop system are bounded in the $L_2$-sense, the parameter estimate $\hat{\theta}$ converges to its true value $\theta$ and the parameter estimate $\hat{k}$ converges to some constant.*

A schematic of the design showing how the system plant, observer, control law and adaptive law are interconnected is given in Figure 2. Before proving Theorem 1, some intuition behind the selected control law (25) might be clarifying.

**Remark 2** *If the parameters $(k,\theta)$ are known,we have*

$$q := \frac{r+b_0k}{1+k}, \quad d := \frac{k\theta}{1+k} \tag{26}$$

*known, $\tilde{e} = 0$ from* (18) *and time-invariant kernels* (20) *and* (23) *(since $q = \hat{q}$ is constant). It is possible to show that*

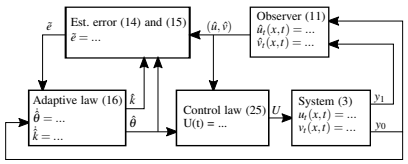


Fig. 2. Structure of the control design.

*system* (3) *is, through the invertible, time-invariant backstepping transformation* $\bar{\omega}(x,t) = \mathscr{K}_1[u,v](x,t)$ *and* $\bar{\zeta}(x,t) = \mathscr{K}_2[u,v](x,t)$ *for* $t \geq t_F$ *and, by selecting*

$$\begin{aligned} U(t) =& \mathscr{K}_{20}[u,v](1,t) - \tilde{\sigma}\mathscr{K}_{10}[u,v](1,t) \\ &+ \zeta^* - \tilde{\sigma} y_1(t), \end{aligned} \tag{27}$$

*equivalent to the system of conservation laws*

$$\bar{\omega}_t + \lambda\bar{\omega}_x = \Psi_1(x)d \tag{28a}$$
$$\bar{\zeta}_t - \mu\bar{\zeta}_x = \Psi_2(x)d \tag{28b}$$
$$\bar{\omega}(0,t) = q\bar{\zeta}(0,t) + d \tag{28c}$$
$$\bar{\zeta}(1,t) = \tilde{\sigma}\bar{\omega}(1,t) + \zeta^*. \tag{28d}$$

*System* (28) *is stable for* $|q\tilde{\sigma}| < 1$ *(see [9, Section 2.1]) and the steady state solution* $\bar{\omega}(0,\cdot) = r\bar{\zeta}(0,\cdot)$ *is obtained if* $\zeta^*$ *solves*

$$\bar{\omega}(0,\cdot) = r\bar{\zeta}(0,\cdot) \tag{29a}$$
$$\bar{\omega}(0,\cdot) = q\bar{\zeta}(0,\cdot) + d \tag{29b}$$
$$\begin{aligned} \bar{\zeta}(0,\cdot) =& d\int_0^1 (\tilde{\sigma}\lambda^{-1}\Psi_1(\xi) + \mu^{-1}\Psi_2(\xi))d\xi \\ &+ \tilde{\sigma}\bar{\omega}(0,\cdot) + \zeta^*. \end{aligned} \tag{29c}$$

*That is, we select*

$$\begin{aligned} \zeta^* =& \frac{d(1-\tilde{\sigma}r)}{r-q} - d\int_0^1 (\tilde{\sigma}\lambda^{-1}\Psi_1(\xi) + \mu^{-1}\Psi_2(\xi))d\xi \\ =& \frac{\theta(1-\tilde{\sigma}r)}{r-b_0} - d\int_0^1 (\tilde{\sigma}\lambda^{-1}\Psi_1(\xi) + \mu^{-1}\Psi_2(\xi))d\xi \end{aligned} \tag{30}$$

*which resembles* (25)*, but with the estimates* $(\hat{u},\hat{v},\hat{\theta})$ *replaced by the true values* $(u,v,\theta)$*. That is, the form of* (25) *is motivated by viewing it as a certainty equivalence design based on* (27) *and* (30)*. If in addition* $\bar{\sigma} = \sigma$*, the system of conservation laws is reduced to a cascaded set of transport equations and we have finite time convergence.*

**Remark 3** *It is shown in [8] that complete cancellation of the top-side reflection* $\sigma$ *by the control law (i.e.* $\bar{\sigma} = \sigma$*) might lead to poor robustness margins in the event of actuator delays. Specifically, it is shown in [8] that systems with* distal reflection $\theta_1$ *(reflection at un-actuated boundary) and* proximal reflection $\sigma$ *(reflection at the actuated boundary) can not be* delay-robustly stabilized *if* $|\sigma\theta_1| > 1$ *and a control law with complete cancellation is unstable if* $|\sigma\theta_1| > \frac{1}{2}$ *for any non-zero delay. Instead, a control law giving up finite time convergence by preserving a small amount of proximal reflection is proposed and shown to delay-robustly stabilize the system for an arbitrary positive delay and any* $|\sigma\theta_1| < 1$*. Here, the parameter* $\bar{\sigma}$*, in the control law, can be viewed as a design parameter enabling a trade-off between performance and robustness with respect to delays.*

### 2.3 Stability analysis

Using the backstepping transformation

$$\omega(x,t) = \mathscr{K}_1[u,v](x,t) \tag{31a}$$
$$\zeta(x,t) = \mathscr{K}_2[u,v](x,t), \tag{31b}$$

we get (see [6] for details) the target system

$$\begin{aligned} \omega_t(x,t) =& -\lambda\omega_x(x,t) + \Psi_1(x,t)(\hat{d}(t) + \hat{\kappa}(t)\tilde{e}(t)) \\ &- \int_0^x K_t^{uu}(x,\xi,t)\mathscr{K}_1^{-1}[\omega,\zeta](\xi,t)d\xi \\ &- \int_0^x K_t^{uv}(x,\xi,t)\mathscr{K}_2^{-1}[\omega,\zeta](\xi,t)d\xi \end{aligned} \tag{32a}$$
$$\begin{aligned} \zeta_t(x,t) =& \mu\zeta_x(x,t) + \Psi_2(x,t)(\hat{d}(t) + \hat{\kappa}(t)\tilde{e}(t)) \\ &- \int_0^x K_t^{vu}(x,\xi,t)\mathscr{K}_1^{-1}[\omega,\zeta](\xi,t)d\xi \\ &- \int_0^x K_t^{vv}(x,\xi,t)\mathscr{K}_2^{-1}[\omega,\zeta](\xi,t)d\xi \end{aligned} \tag{32b}$$
$$\omega(0,t) = \hat{q}(t)\zeta(0,t) + \hat{d}(t) + \hat{\kappa}(t)\tilde{e}(t) \tag{32c}$$
$$\begin{aligned} \zeta(1,t) =& \sigma\omega(1,t) + U(t) \\ &+ \sigma\mathscr{K}_{10}[u,v](1,t) - \mathscr{K}_{20}[u,v](1,t). \end{aligned} \tag{32d}$$

Inspired by [5], we define a reference model the target system should track as

$$\varphi_t(x,t) + \lambda\varphi_x(x,t) = \Psi_1(x,t)\hat{d}(t) \tag{33a}$$
$$\phi_t(x,t) - \mu\phi_x(x,t) = \Psi_2(x,t)\hat{d}(t) \tag{33b}$$
$$\varphi(0,t) = \hat{q}(t)\phi(0,t) + \hat{d}(t) \tag{33c}$$
$$\phi(1,t) = \zeta^*(t) + \sigma\varphi(1,t) \tag{33d}$$

with $\varphi(\cdot,0), \phi(\cdot,0) \in \mathscr{B}([0,1])$.

**Lemma 2** *Consider the reference model* (33) *with parameter estimates* $(\hat{q},\hat{d})$ *provided by the adaptive laws* (16) *and relations* (18)*. If the tracking signal* $\zeta^*$ *is selected as*

$$\begin{aligned} \zeta^*(t) =& \frac{1-\tilde{\sigma}r}{r-\hat{q}(t)}\hat{d}(t) \\ &- \tilde{\sigma}\lambda^{-1}\int_0^1 \Psi_1(\xi,t)\hat{d}(t)d\xi \\ &- \mu^{-1}\int_0^1 \Psi_2(\xi,t)\hat{d}(t)d\xi \end{aligned} \tag{34}$$

*and provided* $|\tilde{\sigma}\tilde{q}|<1$, *then*

$$(\varphi(0,\cdot,)-r\phi(0,\cdot))\in\mathscr{L}_2\cap\mathscr{L}_\infty \tag{35}$$

*and*

$$||\varphi||,||\phi||\in\mathscr{L}_\infty. \tag{36}$$

The proof is given in Appendix A.2.

It now remains to show that the tracking error converges. Defining $\nu=\omega-\varphi$ and $\eta=\zeta-\phi$ and subtracting (33) from (32) and selecting $U(t)$ according to (25) gives the tracking error dynamics

$$\begin{aligned}
\nu_t(x,t)=&-\lambda\nu_x(x,t)+\Psi_1(x,t)\hat{\kappa}(t)\tilde{e}(t)\\
&-\int_0^x K_t^{uu}(x,\xi,t)\mathscr{K}_1^{-1}[\nu+\varphi,\eta+\phi](\xi,t)d\xi\\
&-\int_0^x K_t^{uv}(x,\xi,t)\mathscr{K}_2^{-1}[\nu+\varphi,\eta+\phi](\xi,t)d\xi &\text{(37a)}\\
\eta_t(x,t)=&\mu\eta_x(x,t)+\Psi_2(x,t)\hat{\kappa}(t)\tilde{e}(t)\\
&-\int_0^x K_t^{vu}(x,\xi,t)\mathscr{K}_1^{-1}[\nu+\varphi,\eta+\phi](\xi,t)d\xi\\
&-\int_0^x K_t^{vv}(x,\xi,t)\mathscr{K}_2^{-1}[\nu+\varphi,\eta+\phi](\xi,t)d\xi &\text{(37b)}\\
\nu(0,t)=&\hat{q}(t)\eta(0,t)+\hat{\kappa}(t)\tilde{e} &\text{(37c)}\\
\eta(1,t)=&\tilde{\sigma}\nu(1,t). &\text{(37d)}
\end{aligned}$$

Our strategy is now to prove stability of the tracking error system (37) (in the $L_2$-sense), relate this stability result to our original system (3) and show that the objective (6) is achieved. This relationship is studied in Lemma 3 below. Boundedness and convergence to zero in the $L_2$-sense of the tracking error system (37) is shown in Lemma 4. Finally, these elements are used to prove Theorem 1.

To study the relationship between the tracking error (15) and tracking error dynamics (37), we introduce the auxiliary filter

$$\begin{aligned}
\varpi_t(x,t)-\mu\varpi_x(x,t)=&0 &\text{(38a)}\\
\varpi(1,t)=&\nu(0,t)-r\eta(0,t)=:\varpi_1(t) &\text{(38b)}
\end{aligned}$$

with $\varpi(\cdot,0)\in\mathscr{B}([0,1])$.

**Lemma 3** *Assume the properties of Lemma 2 hold. If in addition* $||\varpi||\in\mathscr{L}_2$, *then*

$$e\in\mathscr{L}_2. \tag{39}$$

*If* $||\varpi||\in\mathscr{L}_\infty$, *then e and* $y_0$ *are bounded a.e.*

The proof is given in Appendix A.3.

**Lemma 4** *Consider the tracking error system* (37) *and the filter* (38). *If*

$$|\tilde{\sigma}\tilde{q}|<1 \tag{40}$$

*then we have*

$$||\nu||,||\eta||,||\varpi||\in\mathscr{L}_2\cap\mathscr{L}_\infty \tag{41}$$

*and*

$$||\nu||,||\eta||,||\varpi||\to 0. \tag{42}$$

The proof is given in Appendix A.4.

We are now ready to prove the main result stated in Theorem 1.

**PROOF.** [Proof of Theorem 1] By Lemma 4, we have $||\varpi||\in\mathscr{L}_2$. It then follows from Lemma 3 that $e\in\mathscr{L}_2$ or equivalently $(\theta-y_0)\in\mathscr{L}_2$ which trivially implies (6). Furthermore, since $||\varpi||\in\mathscr{L}_\infty$ from Lemma 4, we have that $\varpi$ and $y_0$ are bounded for *almost all* $t\geq 0$. We have

$$\begin{aligned}
\hat{e}(t)\leq&|\varphi(0,t)-r\phi(0,t)|+|\nu(0,t)-r\eta(0,t)|\\
&+\frac{\tilde{e}(t)}{1+y_0(t)}(1+y_0(t)),
\end{aligned} \tag{43}$$

which by Property 3 in Lemma 1, Lemma 2 and Lemma 3 implies $\hat{e}\in\mathscr{L}_2$. Property 5 in Lemma 1 then gives $\hat{\theta}\to\theta$ and $\hat{k}\to k_\infty$ for some constant $k_\infty$. Lastly for boundedness, combining the results of Lemma 2 and 4 shows boundedness of $||\omega||\leq||\nu||+||\varphi||$ and $||\zeta||=||\eta||+||\phi||$ and from the invertibility of the transformations $\omega(x,t)=\mathscr{K}_1[\hat{u},\hat{v}](x,t)$ and $\zeta(x,t)=\mathscr{K}_2[\hat{u},\hat{v}](x,t)$, we have $||u||,||v||\in\mathscr{L}_\infty$.

## 3 Application to the kick & loss problem in MPD

As discussed in the introduction, the motivation for studying the control scheme presented in Section 2 and summarized in Theorem 1 is an application to the kick & loss attenuation problem in MPD where the bottom-hole pressure is measured by utilizing wired-drill-pipe technology. In addition to simplifying state estimation, the bottom-hole measurement facilitates using the bilinear form in (3c) and the bilinear adaptive law which results in strong parameter convergence properties. This section and the next will illustrate the advantage in control performance of utilizing bottom-hole pressure measurements for automatic kick & loss handling. So, in addition to an application of the control scheme in Section 2 (Case 1), we present here the alternative control scheme from [16] only utilizing topside measurements (Case 2).

**Case 1** *The* non-collocated *case assumes that both the top-side flow* $q(l,t)=q_l(t)$ *and the down-hole pressure* $p(0,t)$ *are measured. Lemma 5 (see below) ensures that system* (1) *with the specified measurements and control objective* (2) *is equivalent to system* (3) *with measurements* (4) *and* (5) *and control objective* (6), *and provides in explicit form the coordinate transformation.*

**Case 2** *The* collocated *sensing and control case assumes only top side flow $q(l,t)=q_l(t)$ is measured. Since the downhole pressure measurement is unavailable in this case, it is more convenient to write the boundary condition in affine form, giving the system equations*

$$u_t(x,t)+\lambda u_x(x,t)=c_1(x)v(x,t) \tag{44a}$$
$$v_t(x,t)-\mu v_x(x,t)=c_2(x)u(x,t) \tag{44b}$$
$$u(0,t)=\theta_1 v(0,t)+\theta_2 \tag{44c}$$
$$v(1,t)=\sigma y_1(t)+U(t) \tag{44d}$$

*where $u,v,\lambda,\mu,c_1,c_2$ are defined as in the non-collocated case, $\theta_1$ and $\theta_2$ are the unknown boundary parameters and $u(\cdot,0)$, $v(\cdot,0)\in\mathscr{B}([0,1])$. The only measurement is $u(1,t)=y_1(t)$ and the control objective* (2) *can be stated in the new coordinate system as*

$$\lim_{t\to\infty}\int_t^{t+T}|u(0,t)-rv(0,t)|\,d\tau=0 \tag{45}$$

*for some arbitrary $T>0$ where $r\neq\theta_1$. As for Case 1, Lemma 5 provides equivalence between systems* (1) *and* (44) *for Case 2.*

**Lemma 5** *The coordinate transformation*

$$u(x,t)=\frac{1}{2}\left(\frac{A}{\sqrt{\beta\rho}}\left(p(xl,t)+\rho g\int_0^{xl}\cos\psi(s)ds+\frac{F}{A}q_{bit}lx\right)+q(xl,t)-q_{bit}\right)\exp(\frac{lF}{2\sqrt{\beta\rho}}x) \tag{46a}$$
$$v(x,t)=\frac{1}{2}\left(-\frac{A}{\sqrt{\beta\rho}}\left(p(xl,t)+\rho g\int_0^{xl}\cos\psi(s)ds+\frac{F}{A}q_{bit}lx\right)+q(xl,t)-q_{bit}\right)\exp(-\frac{lF}{2\sqrt{\beta\rho}}x) \tag{46b}$$

*where*

$$x=\frac{z}{l} \tag{47}$$

*maps system* (1) *into the forms* (3) *and* (44) *with*

$$\lambda=\mu=\sqrt{\frac{\beta}{\rho}}\frac{1}{l} \tag{48a}$$
$$c_1(x)=c_2(-x)=-\frac{F}{2\rho}\exp(\frac{lF}{\sqrt{\beta\rho}}x) \tag{48b}$$
$$\theta_1=\frac{\left(J\frac{\sqrt{\beta\rho}}{A}-1\right)}{\left(J\frac{\sqrt{\beta\rho}}{A}+1\right)},\quad \theta_2=\frac{J}{\left(J\frac{\sqrt{\beta\rho}}{A}+1\right)}p_r \tag{48c}$$
$$k=J\frac{\sqrt{\beta\rho}}{A},\quad \theta=\frac{A}{\sqrt{\beta\rho}}p_r \tag{48d}$$
$$\sigma=\exp(-\frac{lF}{\sqrt{\beta\rho}}). \tag{48e}$$

*and*

$$U(t)=-\frac{A}{\sqrt{\beta\rho}}\left(p(l,t)+\rho g\int_0^l\cos\psi(s)ds+\frac{F}{A}q_{bit}l\right)\times\exp(-\frac{lF}{2\sqrt{\beta\rho}}) \tag{49a}$$
$$y_1(t)=\frac{1}{2}\left(\frac{A}{\sqrt{\beta\rho}}\left(p(l,t)+\rho g\int_0^l\cos\psi(s)ds+\frac{F}{A}q_{bit}l\right)+q(l,t)-q_{bit}\right)\exp(-\frac{lF}{2\sqrt{\beta\rho}}) \tag{49b}$$
$$y_0(t)=\frac{A}{\sqrt{\beta\rho}}p_0(t). \tag{49c}$$

*The measurement $y_0$ is related to $(u,v)$ by*

$$y_0(t)=u(0,t)-v(0,t) \tag{50}$$

*implying $b_0=1$. Moreover, the control objective* (2) *is transformed to* (6) *or* (45) *with $r=-1$.*

**PROOF.** The constant terms are removed and the origin shifted by defining

$$\bar{p}(z,t)=p(z,t)+\rho g\int_0^z\cos\psi(s)ds+\frac{F}{A}q_{bit}z \tag{51a}$$
$$\bar{q}(z,t)=q(z,t)-q_{bit}. \tag{51b}$$

Next, introducing the diagonalizing change of variables

$$\bar{u}(z,t)=\frac{1}{2}\left(\bar{q}(z,t)+\frac{A}{\sqrt{\beta\rho}}\bar{p}(z,t)\right) \tag{52a}$$
$$\bar{v}(z,t)=\frac{1}{2}\left(\bar{q}(z,t)-\frac{A}{\sqrt{\beta\rho}}\bar{p}(z,t)\right), \tag{52b}$$

the following relations can be found:

$$\bar{u}(z,t)+\bar{v}(z,t)=\frac{1}{2}\left(\bar{q}(z,t)+\frac{A}{\sqrt{\beta\rho}}\bar{p}(z,t)\right)+\frac{1}{2}\left(\bar{q}(z,t)-\frac{A}{\sqrt{\beta\rho}}\bar{p}(z,t)\right)=\bar{q}(z,t) \tag{53}$$

and

$$\frac{\sqrt{\beta\rho}}{A}\left(\bar{u}(z,t)-\bar{v}(z,t)\right)=\frac{\sqrt{\beta\rho}}{2A}\left(\bar{q}(z,t)+\frac{A}{\sqrt{\beta\rho}}\bar{p}(z,t)\right)-\frac{\sqrt{\beta\rho}}{2A}\left(\bar{q}(z,t)-\frac{A}{\sqrt{\beta\rho}}\bar{p}(z,t)\right)=\bar{p}(z,t). \tag{54}$$

Evaluating (51b) at $z = 0$ gives

$$\begin{aligned}\bar{q}(0,t) &= q(0,t) - q_{bit} \\ &= J\left(p_r - p(0,t)\right) + q_{bit} - q_{bit} \\ &= -J\bar{p}(0,t) + Jp_r,\end{aligned} \tag{55}$$

inserting the relations (53) and (54) yield

$$\begin{aligned}\bar{u}(0,t) + \bar{v}(0,t) &= \bar{q}(0,t) \\ &= -J\bar{p}(0,t) + Jp_r \\ &= -J\frac{\sqrt{\beta\rho}}{A}\left(\bar{u}(0,t) - \bar{v}(0,t)\right) + Jp_r\end{aligned} \tag{56}$$

and by reorganizing the terms and using definitions (48c), one obtains (44c). Evaluating (46a) and (46b) at $x = 0$ and adding them together yield

$$\begin{aligned}u(0,t) + v(0,t) =& q(0,t) - q_{bit} = J\left(p_r - p(0,t)\right) \\ =& J\frac{\sqrt{\beta\rho}}{A}\left(\frac{A}{\sqrt{\beta\rho}}p_r - \frac{A}{\sqrt{\beta\rho}}p(0,t)\right)\end{aligned} \tag{57}$$

and the boundary condition (3c) is obtained with $\theta$ and $k$ given in (48d). Subtracting (46a) evaluated at $x = 0$ from (46b) evaluated at $x = 0$ gives

$$u(0,t) - v(0,t) = \frac{A}{\sqrt{\beta\rho}}p(0,t) \tag{58}$$

and the measurement (4) is obtained with $y_0$ given by (49c) and $b_0 = 1$. From (57), it can be seen that $p(0,t) = p_r$ corresponds to $u(0,t) + v(0,t) = 0$ and the objective (2) is transformed to (6) or (45) with $r = -1$. The rest of the proof is similar to the proof of [1, Lemma 10] and therefore omitted.

From (48c) and the fact that $J > 0$, it can be seen that $\theta_1$ satisfies

$$-1 < \theta_1 < 1 \tag{59}$$

which together with $r = -1$ means that the constraint $r \notin [\underline{\theta}_1, \bar{\theta}_1]$ in [16] is satisfied. Inequality (59) can also be used as lower and upper bounds for $\theta_1$. Lower and upper bounds for $\theta_2$ can be found by using that $0 < p_r < \bar{p}_r$ as $\underline{\theta}_2 = 0$ and $\bar{\theta}_2 = \bar{p}_r$ respectively. From (48d) and $J > 0$, we have that $\text{sign}(k)$ is known and positive. The bounds $[\underline{k}, \bar{k}]$ will depend on the specific well considered. Furthermore, it can be seen that the selected $b_0$ and $r$ satisfy the constraint $r \neq b_0$.

**Corollary 1 (Non-collocated sensing and control)** *Consider the system* (1)*. Let $\hat{J}$ and $\hat{p}_r$ be the estimates of the unknown system parameters $J$ and $p_r$ generated using the adaptive law in Lemma 1 and definition* (48d)*. If the system parameters and $r$ are selected according to Lemma 5, the control law*

$$p_l(t) = \frac{\sqrt{\beta\rho}}{A}U(t)\sigma^{-\frac{1}{2}} - \rho g\int_0^l \cos\psi(s)ds - \frac{F}{A}q_{bit}l \tag{60}$$

*with $U(t)$ given by* (25)*, guarantees* (2) *and that all signals in the closed loop system are bounded. Moreover, the estimate $\hat{p}_r$ converges to its true value $p_r$ in the sense*

$$\hat{p}_r(t) \to p_r. \tag{61}$$

**PROOF.** For the first part, it suffices to show that the actuation $p_l(t)$ is related to $U(t)$ through (60), since it is established in Lemma 5 that the system (1) takes the form (3). Solving (49a) for $p(xl,t)$ gives trivially the control law (60). By Theorem 1, the control objective (2) is achieved for some $T > 0$ and all signals in the closed loop are bounded. Convergence in $\hat{p}_r$ follows directly from the definition (48d) and convergence in $\hat{\theta}$ to $\theta$ from Theorem 1.

**Corollary 2 (Collocated sensing and control)** *Consider the system* (1)*. Let $(\hat{p},\hat{q})$ be estimates of the states $(p,q)$ generated from the observer in [16] and transformation* (46)*, and let $\hat{J}$ and $\hat{p}_r$ be estimates of the unknown system parameters $J$ and $p_r$ generated using the adaptive law in [16] and definition* (48c)*. If the system parameters and $r$ are selected according to Lemma 5, the control law*

$$p_l(t) = \frac{\sqrt{\beta\rho}}{A}U(t)\sigma^{-\frac{1}{2}} - \rho g\int_0^l \cos\psi(s)ds - \frac{F}{A}q_{bit}l \tag{62}$$

*with $U(t)$ given by the control law in [16], guarantees* (2) *and all signals in the closed loop system are bounded. Moreover, the estimate $\hat{p}_r$ converges to its true value $p_r$ in the sense*

$$\int_t^{t+T} |\hat{p}_r(\tau) - p_r|\, d\tau \to 0. \tag{63}$$

**PROOF.** For the first part, it suffices to show that the actuation $p_l(t)$ is related to $U(t)$ through (62), since it is established in Lemma 5 that system (1) takes the form (3) with boundary condition (44c). Solving (49a) for $p(xl,t)$ and evaluating the resulting equation at $x = 1$ give trivially the control law (62). By the control law in [16, Theorem 2], the control objective (2) is achieved for some $T > 0$ and all signals in the closed loop are bounded, furthermore it follows that

$$\int_t^{t+T} |\hat{p}(0,\tau) - p(0,\tau)|\, d\tau \to 0 \tag{64}$$

and since the control objective (2) is satisfied, we obtain (63).

**Remark 4** *Comparing the designs presented in Corollaries 1 and 2, we see that when a down-hole pressure measurement is available, it is possible to estimate both the pressure and flow distribution in the well in finite time. The collocated design with only top-side flow measurement on the other hand, achieves only asymptotically converging pressure and flow estimates. Furthermore, with non-collocated control and sensing we are able to prove convergence in the*

*reservoir pressure in the strong sense* (61). *The greatest advantage of using the non-collocated design, however, is the total convergence time of the overall control objective* (2). *This will be apparent in the next section.*

**Remark 5** *In reality, the top-side pressure and flow are related through a choke equation (see eg. [25]). As mentioned in the introduction, we avoid this dynamic by assuming that the top-side pressure is directly controllable. As mentioned in Remark 3, complete cancellation of top-side reflection might lead to instabilities in the event of time delays introduced by the choke actuation system.*

*For a typical set of drilling parameters and productivity indices $J$ in the range $[1,385]$ $bbl/psi/day$, as reported by [4], it can be shown that $|\sigma\theta_1| < \frac{1}{2}$ is usually satisfied. Nonetheless, very large and very small $J$ might fall outside this region. In those cases, using $\bar{\sigma} \neq \sigma$ satisfying $|\sigma - \bar{\sigma}| < 1$ might yield sufficient delay-robustness. A rigorous analysis of the control design in these rare cases is however outside the scope of this paper. In the simulation in the next section, the parameters fall within the region where $|\sigma\theta_1| < \frac{1}{2}$ and we set $\bar{\sigma} = \sigma$.*

## 4 Simulation

Although both methods can be applied to both a kick handling problem and a loss handling handling problem. The original model (1) is based on a single-phase assumption. Even though liquid kicks (oil and water) will introduce new phases of matter into the system in addition to the mud phase (and rock cuttings), the model (1) is still a reasonable approximation as all liquid phases can effectively be lumped into a single liquid phase [3]. Gas kick on the other hand can not accurately be modeled by (1). Of the two, gas kicks is by far the most challenging. For this reason, we will in the following study a loss scenario where the only circulating matter is the drilling mud (in addition to rock cuttings) and the single-phase assumption is satisfied.

Both the control scheme for non-collocated sensing and control (the non-collocated method) developed in this paper and the scheme for collocated sensing and control (the collocated method) presented in [16] are implemented in MATLAB and applied to the loss problem in MPD. For the non-collocated method, the implemented system consists of the adaptive law of Lemma 1, and the control law (25). For the collocated method, the observer, adaptive law and control law from Theorem 1 and 2 in [16] are implemented. The system parameters are chosen as

$$\begin{aligned}
\beta &= 7317 \times 10^5 \,\mathrm{Pa} && (65a)\\
\rho &= 1250 \,\mathrm{kg\,m^{-3}} && (65b)\\
l &= 2500 \,\mathrm{m} && (65c)\\
A &= 0.024 \,\mathrm{m^2} && (65d)\\
F &= 50 \,\mathrm{kg\,m^{-3}} && (65e)\\
g &= 9.81 \,\mathrm{m\,s^{-2}} && (65f)\\
q_{bit} &= 0.1 \,\mathrm{m^3\,s^{-1}} && (65g)\\
J &= 1.068 \times 10^{-8} \,\mathrm{m^3\,s^{-1}\,Pa^{-1}} && (65h)\\
\psi(z) &= 0 \quad \forall z \in [0,l]. && (65i)
\end{aligned}$$

The reservoir pressure is initially set to $p_r(0) = 450\,\mathrm{bar}$ and kept constant until a step to $p_r(t \geq t_0) = 400\,\mathrm{bar}$ occurs at $t_0 = 10\,\mathrm{s}$. The system is at steady state at $t = 0$ with the initial bottom-hole pressure set equal to the reservoir pressure and the bottom-hole flow equal to the drill bit flow. This is the typical scenario of drilling ahead into an unforeseen low-pressure pocket in the reservoir, causing a loss of circulation fluid into the formation. The adaptation gains are selected as $\gamma_1 = \gamma_2 = 5$. From (48d) we find that $k \approx 0.4$ and we use the projection bounds $[\underline{k}, \bar{k}] = [k_0, 1 - k_0]$ with $k_0 = 0.01$.

Figures 3 and 4 compare the bottom-hole pressure and flow when using the two methods. The methods are also compared to a simple control method (the simple method) where the top-side flow is kept equal to the drill bit flow $q(l,t) = q_{bit}$. The figures show that all three methods are able to attenuate the mud loss. The bottom-hole pressure is stabilized at the reservoir pressure and the net loss out of the well converge to zero. It is seen that both the collocated and non-collocated method are significantly faster than the simple method. Figure 10 shows that the collocated method offers a $\sim 40\%$ reduction in accumulated out-flow over the simple method, and the non-collocated an additional $\sim 45\%$ reduction over the collocated method. As can be seen in Figures 5 and 6, this is due to the much faster, finite time convergent observer in the non-collocated design. Figure 9 compares the control input, in terms of controlled top-side pressure. It is clear that the non-collocated controller reacts much quicker than the two other methods. Furthermore, we observe in Figures 7 and 8 that in both designs, the reservoir pressure estimate converges to the true reservoir pressure and the productivity index to some constant.

The non-collocated method also has some implementational advantages over the collocated method: The backstepping kernels used in the collocated observer are time-varying and must therefore be solved on-line. In contrast, the injection terms used in (11) are static and can be solved off-line, yielding a much more computationally efficient observer. Both methods, however, require time-varying controller kernels which must be solved on-line.

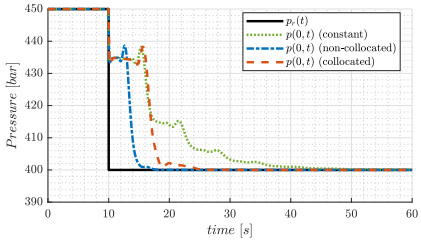


Fig. 3. Bottom-hole pressure.

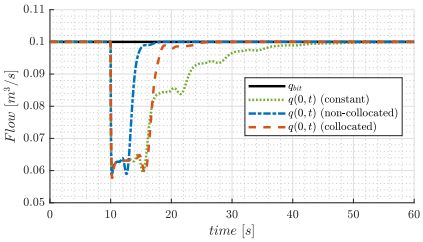


Fig. 4. Bottom-hole flow.

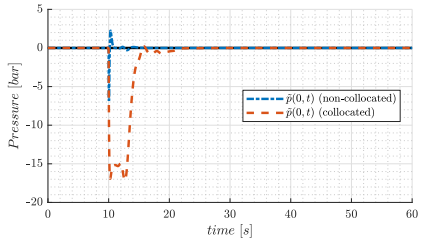


Fig. 5. Bottom-hole pressure estimation error.

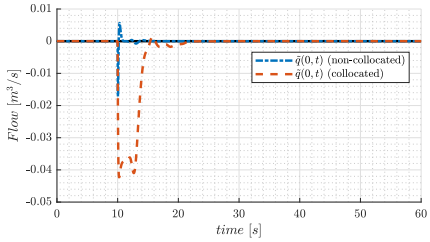


Fig. 6. Bottom-hole flow estimation error.

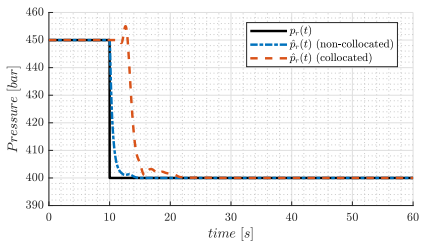


Fig. 7. Reservoir pressure estimate.

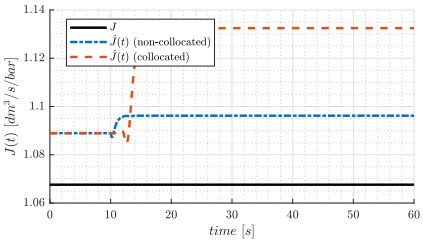


Fig. 8. Productivity index estimate.

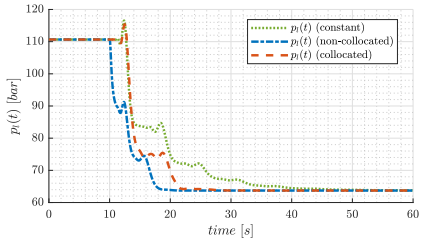


Fig. 9. Control input signal.

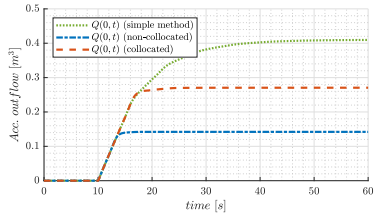


Fig. 10. Accumulated net outflow.

## 5 Concluding Remarks

We have studied set-point regulation of a $2 \times 2$ hyperbolic system with unknown boundary parameters appearing in a special bilinear form. Measurements at both boundaries allowed us to design a finite-time convergent state observer, which in turn was used to design adaptive laws based on a bilinear parametric model. Properties regarding parameter convergence were utilized to design a control law that achieves boundary set-point regulation. The theory was applied to the kick & loss attenuation problem in MPD and compared to an earlier result on stabilization of the same type of system utilizing only top-side sensing. Significant performance improvements was demonstrated for the method utilizing bottom-hole pressure measurements, both in terms of total convergence time and computational complexity, and most importantly in terms of total loss size.

## References


[1] Ole Morten Aamo. Disturbance rejection in $2 \times 2$ linear hyperbolic systems. *IEEE Transactions on Automatic Control*, 58(5):1095–1106, 2013.

[2] Ulf Jakob F Aarsnes, Behçet Açıkmeşe, Adrian Ambrus, and Ole Morten Aamo. Robust controller design for automated kick handling in managed pressure drilling. *Journal of Process Control*, 47:46–57, 2016.

[3] Ulf Jakob F. Aarsnes, Florent Di Meglio, and Steinar Evje. Control-oriented drift-flux modeling of single and two-phase flow for drilling. In *ASME 2014 Dynamic Systems and Control Conference*, October 2014.

[4] Sulaiman Alarifi, Sami AlNuaim, and Abdulazeez Abdulraheem. Productivity index prediction for oil horizontal wells using different artificial intelligence techniques. In *SPE Middle East Oil & Gas Show and Conference*. Society of Petroleum Engineers, 2015.

[5] Henrik Anfinsen and Ole Moren Aamo. Model reference adaptive control of$2 \times 2$coupled linear hyperbolic PDEs. *IEEE Transactions on Automatic Control*, 63(8):2405–2420, Aug 2018.

[6] Henrik Anfinsen and Ole Morten Aamo. Adaptive stabilization of $n+1$ coupled linear hyperbolic systems with uncertain boundary parameters using boundary sensing. *Systems & Control Letters*, 99:72–84, 2017.

[7] Henrik Anfinsen, Mamadou Diagne, Ole Moren Aamo, and Miroslav Krstic. An adaptive observer design for $n+1$ coupled linear hyperbolic PDEs based on swapping. *IEEE Transactions on Automatic Control*, 61(12):3979–3990, December 2016.

[8] Jean Auriol, Ulf Jakob Flo Aarsnes, Philippe Martin, and Florent Di Meglio. Delay-robust control design for two heterodirectional linear coupled hyperbolic PDEs. *IEEE Transactions on Automatic Control*, 63(10):3551–3557, oct 2018.

[9] Georges Bastin and Jean-Michel Coron. *Stability and boundary stabilization of 1-D hyperbolic systems*, volume 88. Springer, 2016.

[10] Michelangelo Bin and Florent Di Meglio. Boundary estimation of parameters for linear hyperbolic PDEs. *IEEE Transactions on Automatic Control*, 62(8):3890–3904, Aug 2017.

[11] Jean-Michel Coron, Rafael Vazquez, Miroslav Krstic, , and Georges Bastin. Local exponential $H^2$ stabilization of a $2 \times 2$ quasilinear hyperbolic system using backstepping. *SIAM Journal on Control and Optimization*, 51(3):2005–2035, 2013.

[12] Joachim Deutscher. Finite-time output regulation for linear $2 \times 2$ hyperbolic systems using backstepping. *Automatica*, 75:54–62, 2017.

[13] Espen Hauge, Ole Morten Aamo, and John-Morten Godhavn. Model-based estimation and control of in/out-flux during drilling. In *Proceeding of the 2012 American Control Conference*, pages 4909–4914. IEEE, 2012.

[14] Espen Hauge, Ole Morten Aamo, and John-Morten Godhavn. Application of an infinite-dimensional observer for drilling systems incorporating kick and loss detection. In *Proceedings of the 12th European Control Conference*, pages 1065–1070. IEEE, 2013.

[15] Haavard Holta and Ole Morten Aamo. Boundary set-point regulation of a linear $2 \times 2$ hyperbolic PDE with uncertain bilinear boundary condition. In *Proceedings of the 2018 IEEE Conference on Decision and Control (CDC)*, pages 2156–2163. IEEE, dec 2018.

[16] Haavard Holta, Henrik Anfinsen, and Ole Morten Aamo. Adaptive set-point regulation of linear $2 \times 2$ hyperbolic systems with uncertain affine boundary condition using collocated sensing and control. In *Proceeding of the 2017 Asian Control Conference*, pages 2766–2771, Dec 2017.

[17] Petros A Ioannou and Jing Sun. *Robust Adaptive Control*. Courier Corporation, 2012.

[18] Miroslav Krstic, Ioannis Kanellakopoulos, and Peter V Kokotovic. *Nonlinear and Adaptive Control Design*. Wiley, 1995.

[19] Miroslav Krstic and Andrey Smyshlyaev. Backstepping boundary control for first-order hyperbolic PDEs and application to systems with actuator and sensor delays. *Systems & Control Letters*, 57(9):750 – 758, 2008.

[20] Pierre-Olivier Lamare and Nikolaos Bekiaris-Liberis. Control of $2 \times 2$ linear hyperbolic systems: Backstepping-based trajectory generation and PI-based tracking. *Systems & Control Letters*, 86:24–33, 2015.

[21] Pierre-Olivier Lamare and Florent Di Meglio. Adding an integrator to backstepping: Output disturbances rejection for linear hyperbolic systems. In *2016 American Control Conference*. IEEE, July 2016.

[22] Ingar Skyberg Landet, Alexey Pavlov, and Ole Morten Aamo. Modeling and control of heave-induced pressure fluctuations in managed pressure drilling. *IEEE Transactions on Control Systems Technology*, 21(4):1340–1351, 2013.

[23] Weijiu Liu. Boundary feedback stabilization of an unstable heat equation. *SIAM Journal on Control and Optimization*, 42(3):1033–1043, 2003.

[24] Rystad Energy. New horizon in the deep watermarket, 2014.

[25] R.B. Schller, T. Solbakken, and S. Selmer-Olsen. Evaluation of multiphase flow rate models for chokes under subcritical oil/gas/water flow conditions. *SPE Production & Facilities*, 18(03):170–181, aug 2003.

[26] Andrey Smyshlyaev, Eduardo Cerpa, and Miroslav Krstic. Boundary stabilization of a 1-D wave equation with in-domain antidamping. *SIAM Journal on Control and Optimization*, 48(6):4014–4031, 2010.

[27] Andrey Smyshlyaev and Miroslav Krstic. Closed-form boundary state feedbacks for a class of 1-D partial integro-differential equations. *IEEE Transactions on Automatic Control*, 49(12):2185–2202, 2004.

[28] Andrey Smyshlyaev and Miroslav Krstic. On control design for PDEs with space-dependent diffusivity or time-dependent reactivity. *Automatica*, 41(9):1601–1608, 2005.

[29] Andrey Smyshlyaev and Miroslav Krstic. *Adaptive Control of Parabolic PDEs*. Princeton University Press, 2010.

[30] Timm Strecker and Ole Morten Aamo. Output feedback boundary control of series interconnections of 2 2 semilinear hyperbolic systems. *IFAC-PapersOnLine*, 50(1):663 – 670, 2017. 20th IFAC World Congress.

[31] Gang Tao. *Adaptive Control Design and Analysis*. John Wiley & Sons, Inc., New York, NY, USA, 2003.

[32] Rafael Vazquez, Miroslav Krstic, and Jean-Michel Coron. Backstepping boundary stabilization and state estimation of a $2 \times 2$

linear hyperbolic system. In *Proceedings of the 50th IEEE Conference on Decision and Control and European Control Conference*, pages 4937–4942, December 2011.

[33] Jing Zhou, Øyvind Nistad Stamnes, Ole Morten Aamo, and Glenn-Ole Kaasa. Switched control for pressure regulation and kick attenuation in a managed pressure drilling system. *IEEE Transactions on Control Systems Technology*, 19(2):337–350, 2011.

## A Proof of Lemma 1 to 4

### *A.1 Proof of Lemma 1*

**PROOF.** Let

$$V_0(t) = k\frac{1}{2\gamma_1}\tilde{\theta}^2(t) + \frac{1}{2\gamma_2}\tilde{k}^2(t) \tag{A.1}$$

for $t \geq t_F$ where $\tilde{\theta} = \theta - \hat{\theta}$ and $\tilde{k} = k - \hat{k}$. Differentiating with respect to time and inserting (16) yield

$$\begin{aligned}
\dot{V}_0(t) &= -k\frac{1}{\gamma_1}\tilde{\theta}(t)\dot{\hat{\theta}}(t) - \frac{1}{\gamma_2}\tilde{k}(t)\dot{\hat{k}}(t) \\
&= -k\tilde{\theta}(t)\frac{\tilde{e}(t)}{1+y_0^2(t)} - \tilde{k}(t)\left[\hat{\theta}(t) - y_0(t)\right]\frac{\tilde{e}(t)}{1+y_0^2(t)} \\
&= -\frac{\tilde{e}(t)}{1+y_0^2(t)}\left(k\tilde{\theta}(t) + \tilde{k}(t)\left[\hat{\theta}(t) - y_0(t)\right]\right) \\
&= -\frac{\tilde{e}(t)}{1+y_0^2(t)}\left(k\left[\theta - y_0(t)\right] - \hat{k}(t)\left[\hat{\theta}(t) - y_0(t)\right]\right) \\
&= -\frac{\tilde{e}^2(t)}{1+y_0^2(t)} \leq 0
\end{aligned} \tag{A.2}$$

implying $V_0 \in \mathscr{L}_\infty$ and Property 1. Property 2 is trivially guaranteed when using projection. Integrating $\dot{V}_0$ from $t = 0$ to $t = \infty$ yields

$$\int_0^\infty \frac{\tilde{e}^2(\tau)}{1+y_0^2(\tau)}d\tau = V_0(0) - V_0(\infty). \tag{A.3}$$

Since $V_0$ is a non-increasing function of time and bounded below, $V_0(\infty)$ is finite, and Property 3 follows. From the adaptive law (16a) we immediately see that $\dot{\hat{\theta}} \in \mathscr{L}_2$. For the $\hat{k}$ update law for $t \geq t_F$, we have

$$\dot{\hat{k}}(t) \leq \gamma_2 \left|\frac{\hat{\theta}(t) + y_0(t)}{\sqrt{1+y_0^2(t)}}\right| \left|\frac{\tilde{e}(t)}{\sqrt{1+y_0^2(t)}}\right| \tag{A.4}$$

which shows that also $\dot{\hat{k}} \in \mathscr{L}_2$. Inserting (15) into the adaptive law (16a) yields

$$\dot{\tilde{\theta}}(t) = -f(t)\left(k\tilde{\theta}(t) + \tilde{k}(t)\left(\hat{\theta}(t) - y_0(t)\right)\right) \tag{A.5}$$

where $f(t) = \gamma_1/(1+y_0^2(t)) > 0$ for all $t > t_F$. Forming $V_0(t) = \frac{1}{2}\tilde{\theta}^2(t)$, time differentiating and applying Young's inequality to the cross term, we get

$$\begin{aligned}
\dot{V}_0(t) &= -f(t)k\tilde{\theta}^2(t) - \tilde{\theta}(t)f(t)\tilde{k}(t)\left(\hat{\theta}(t) - y_0(t)\right) \\
&\leq -\frac{k}{2}f(t)\tilde{\theta}^2(t) + \frac{1}{2k}f(t)\tilde{k}^2(t)\left(\hat{\theta}(t) - y_0(t)\right)^2.
\end{aligned} \tag{A.6}$$

Since by assumption for Property 5, $y_0$ is bounded for almost all $t \geq 0$, it follows that $\operatorname{ess\,inf}_{t\geq 0} f(t) > 0$, which along with Property 1 and boundedness of $f(t)$, provide the existence of constants $b$ and $c > 0$ such that

$$\dot{V}_0(t) \leq -c\tilde{\theta}^2(t) + g(t)\tilde{\theta}^2(t) + b\left(\hat{\theta} - y_0(t)\right)^2, \tag{A.7}$$

where $g(t) = 0$ almost everywhere and therefore $g(t) \in \mathscr{L}_1$. Since $(\hat{\theta} - y_0)^2 \in \mathscr{L}_1$, it follows from [18, Lemma D.6] (Lemma 6 in Appendix B) that $V_0 \in \mathscr{L}_1 \cap \mathscr{L}_\infty$ which together with [31, Lemma 2.7] (Lemma 7 in Appendix B) imply $V_0, \tilde{\theta} \to 0$. Convergence in $\hat{k}$ to some constant can be shown by integrating (16b) from $t = 0$ to $T = \infty$ and applying Cauchy-Schwarz' inequality

$$\begin{aligned}
\int_0^T \left|\dot{\hat{k}}(\tau)\right| d\tau \leq \gamma_2 &\sqrt{\int_0^T \left|\hat{\theta}(\tau) - y_0(\tau)\right|^2 d\tau} \\
&\times \sqrt{\int_0^T \left|\frac{\tilde{e}(\tau)}{1+y_0^2(\tau)}\right|^2 d\tau} < \infty
\end{aligned} \tag{A.8}$$

which, by Property 4 and $(\hat{\theta} - y_0)^2 \in \mathscr{L}_1$, shows that $\dot{\hat{k}} \in \mathscr{L}_1$. Then for any $\varepsilon > 0$ there exists a $T$ such that

$$\int_T^\infty \left|\dot{\hat{k}}(\tau)\right| d\tau < \varepsilon. \tag{A.9}$$

Therefore,

$$\left|\hat{k}(t) - \hat{k}(T)\right| \leq \left|\int_T^t \dot{\hat{k}}(\tau)d\tau\right| \leq \int_T^\infty \left|\dot{\hat{k}}(\tau)\right| d\tau < \varepsilon. \tag{A.10}$$

which shows that $\hat{k}(t)$ has a limit as $t \to \infty$ and the second part of the proof of Property 5 is complete.

### *A.2 Proof of Lemma 2*

**PROOF.** We will in the following use the bounds

$$\sup_{x\in[0,1]} \left|\frac{\partial}{\partial t}\Psi_i(x,t)\right| \leq h_3\mu\left|\dot{\hat{k}}(t)\right|. \tag{A.11}$$

In proving the existence of a solution to the kernel equations (20) in [11], upper bounds on the form $|K^{ij}(x,\xi)| \leq$

$h_1\mu + h_2\mu|\hat{q}(t)|, \{ij\} \in \{uu, uv, vu, vv\}$ are derived. Using the definitions (18) and (23) and differentiating with respect to time yield the upper bound (A.11) for some $h_1, h_2, h_3 > 0$. Solving the reference model (33) along the characteristics for $t \geq t_F$ yields

$$\begin{aligned}\varphi(x,t) =& \lambda^{-1}\int_0^x \Psi_1(\xi, t+\lambda^{-1}(\xi-x))\hat{d}(t+\lambda^{-1}(\xi-x))d\xi \\ &+ \varphi(0, t-\lambda^{-1}x) \qquad \text{(A.12a)}\\ \phi(x,t) =& \mu^{-1}\int_x^1 \Psi_2(\xi, t-\mu^{-1}(\xi-x))\hat{d}(t-\mu^{-1}(\xi-x))d\xi \\ &+ \phi(1, t-\mu^{-1}(1-x)). \qquad \text{(A.12b)}\end{aligned}$$

To simplify the notation let

$$\vartheta(t) = \frac{\hat{d}(t)}{r-\hat{q}(t)}. \qquad \text{(A.13)}$$

Evaluating (A.12) at $x = 0$ and using boundary conditions (33c) and (33d) together with (34) yield

$$\varphi(0,t) = \hat{q}(t)\phi(0,t) + \hat{d}(t) \qquad \text{(A.14)}$$

and

$$\begin{aligned}\phi(0,t) =& \mu^{-1}\int_0^1 \Psi_2(\xi, t-\mu^{-1}\xi)\hat{d}(t-\mu^{-1}\xi)d\xi \\ &+ \tilde{\sigma}\lambda^{-1}\int_0^1 \Psi_1(\xi, t-t_F+\lambda^{-1}\xi)\hat{d}(t-t_F+\lambda^{-1}\xi)d\xi \\ &+ \tilde{\sigma}\varphi(0,t-t_F) + \vartheta(t-\mu^{-1})(1-\tilde{\sigma}r) \\ &- \tilde{\sigma}\lambda^{-1}\int_0^1 \Psi_1(\xi, t-\mu^{-1})\hat{d}(t-\mu^{-1})d\xi \\ &- \mu^{-1}\int_0^1 \Psi_2(\xi, t-\mu^{-1})\hat{d}(t-\mu^{-1})d\xi \\ =& \mu^{-1}\int_0^1\int_{t-\mu^{-1}}^{t-\mu^{-1}\xi} \frac{\partial}{\partial t}\Psi_2(\xi,\tau)\hat{d}(\tau)d\tau d\xi \\ &+ \tilde{\sigma}\lambda^{-1}\int_0^1\int_{t-\mu^{-1}}^{t-t_F+\lambda^{-1}\xi} \frac{\partial}{\partial t}\Psi_1(\xi,\tau)\hat{d}(\tau)d\tau d\xi \\ &+ \tilde{\sigma}\left(\hat{q}(t-t_F)\phi(0,t-t_F) + \hat{d}(t-t_F)\right) \\ &+ \vartheta(t-\mu^{-1})(1-\tilde{\sigma}r). \qquad \text{(A.15)}\end{aligned}$$

Subtracting $\vartheta(t)$ from both sides and grouping similar terms give the following recursion

$$\begin{aligned}&\phi(0,t) - \vartheta(t) \\ &\quad= \mu^{-1}\int_0^1\int_{t-\mu^{-1}}^{t-\mu^{-1}\xi} \frac{d}{d\tau}\Psi_2(\xi,\tau)\hat{d}(\tau)d\tau d\xi \\ &\qquad+ \tilde{\sigma}\lambda^{-1}\int_0^1\int_{t-\mu^{-1}}^{t-t_F+\lambda^{-1}\xi} \frac{d}{d\tau}\Psi_1(\xi,\tau)\hat{d}(\tau)d\tau d\xi \\ &\qquad+ \tilde{\sigma}\left(\hat{q}(t-t_F)\phi(0,t-t_F) + \hat{d}(t-t_F)\right) \\ &\qquad+ \vartheta(t-\mu^{-1}) - \vartheta(t) - \tilde{\sigma}r\vartheta(t-\mu^{-1}) \\ &\quad= \mu^{-1}\int_0^1\int_{t-\mu^{-1}}^{t-\mu^{-1}\xi} \frac{d}{d\tau}\Psi_2(\xi,\tau)\hat{d}(\tau)d\tau d\xi \\ &\qquad+ \tilde{\sigma}\lambda^{-1}\int_0^1\int_{t-\mu^{-1}}^{t-t_F+\lambda^{-1}\xi} \frac{d}{d\tau}\Psi_1(\xi,\tau)\hat{d}(\tau)d\tau d\xi \\ &\qquad+ \tilde{\sigma}\hat{q}(t-t_F)\left(\phi(0,t-t_F) - \vartheta(t-t_F)\right) \\ &\qquad+ \vartheta(t-\mu^{-1}) - \vartheta(t) \\ &\qquad+ \tilde{\sigma}r\vartheta(t-t_F) - \tilde{\sigma}r\vartheta(t-\mu^{-1}) \\ &\quad= \tilde{\sigma}\hat{q}(t-t_F)\left(\phi(0,t-t_F) - \vartheta(t-t_F)\right) \\ &\qquad+ \mu^{-1}\int_0^1\int_{t-\mu^{-1}}^{t-\mu^{-1}\xi} \frac{\partial}{\partial t}\Psi_2(\xi,\tau)\hat{d}(\tau)d\tau d\xi \\ &\qquad+ \tilde{\sigma}\lambda^{-1}\int_0^1\int_{t-\mu^{-1}}^{t-t_F+\lambda^{-1}\xi} \frac{\partial}{\partial t}\Psi_1(\xi,\tau)\hat{d}(\tau)d\tau d\xi \\ &\qquad- \int_{t-\mu^{-1}}^{t} \frac{d\vartheta(\tau)}{d\tau}d\tau - \tilde{\sigma}r\int_{t-t_F}^{t-\mu^{-1}} \frac{d\vartheta(\tau)}{d\tau}d\tau, \qquad \text{(A.16)}\end{aligned}$$

which, since $|\tilde{\sigma}\hat{q}(t)| \leq |\tilde{\sigma}\max_{t\geq t_F}\hat{q}(t)| < 1$, is stable. By Lemma 1, $\frac{d\vartheta(t)}{dt} = \frac{\dot{\hat{\theta}}}{r-b_0}$ and $\dot{\hat{k}}$ are both bounded and square integrable, implying

$$(\phi(0,\cdot) - \vartheta) \in \mathscr{L}_2 \cap \mathscr{L}_\infty \qquad \text{(A.17)}$$

which from (A.14) is seen to be equivalent to

$$(\varphi(0,\cdot) - r\phi(0,\cdot)) \in \mathscr{L}_2 \cap \mathscr{L}_\infty. \qquad \text{(A.18)}$$

Boundedness in the $L_2$-norm can be shown using a similar argument.

### *A.3 Proof of Lemma 3*

**PROOF.**

If $||\varpi|| \in \mathscr{L}_2$ holds, that is

$$\lim_{T\to\infty}\int_0^T\int_0^1 \varpi^2(x,t)dxdt < \infty, \qquad \text{(A.19)}$$

we have after inserting the explicit solution of (38) for $t > \mu^{-1}$

$$\lim_{T\to\infty}\int_{\mu^{-1}}^{T}\int_0^1 \varpi^2(0,t-\mu^{-1}(1-x))dxdt<\infty. \tag{A.20}$$

Substituting $\tau = t-\mu^{-1}(1-x)$ and changing the order of integration yields

$$\lim_{T\to\infty}\left[\int_0^{\mu^{-1}}\int_{\mu^{-1}}^{\tau+\mu^{-1}}+\int_{\mu^{-1}}^{T-\mu^{-1}}\int_{\tau}^{\tau+\mu^{-1}}+\int_{T-\mu^{-1}}^{T}\int_{\tau}^{T}\right] \times\mu\varpi^2(0,\tau)dtd\tau<\infty. \tag{A.21}$$

All the inner integrals evaluate to $\mu^{-1}$ or less, and we have

$$\lim_{T\to\infty}\int_0^T \varpi^2(0,\tau)d\tau<\infty. \tag{A.22}$$

That is, $(\nu(0,\cdot)-r\eta(0,\cdot))\in\mathscr{L}_2$. Since

$$\begin{aligned}|e(t)|=&|u(0,t)-rv(0,t)|=|\omega(0,t)-r\zeta(0,t)|\\ \le&|\varpi_1(t)|+|\varphi(0,t)-r\phi(0,t)|\end{aligned} \tag{A.23}$$

and from Lemma 2 that $\varphi(0,t)-r\phi(0,t)\in\mathscr{L}_2\cap\mathscr{L}_\infty$, $e\in\mathscr{L}_2$ follows. $||\varpi||\in\mathscr{L}_\infty$ implies that $\varpi_1(t)$ is bounded a.e, and in turn that $e$ is bounded a.e, which from the definition (14) also implies boundedness of $y_0$ a.e.

### *A.4 Proof of Lemma 4*

**PROOF.** Let

$$\varepsilon^2(t):=\frac{\tilde e^2(t)}{1+||\varpi||^2}=\frac{\tilde e^2(t)}{1+y_0^2(t)}\frac{1+y_0^2(t)}{1+||\varpi||^2}. \tag{A.24}$$

From the definition (14), upper bound $|e(t)|\le|\varpi_1(t)|+|\varphi(0,t)-r\phi(0,t)|$, and the fact that $|\varphi(0,t)-r\phi(0,t)|$ is bounded from Lemma 2, and that $\varpi_1||\varpi||^{-1}$ is bounded a.e., it follows that the fraction $\frac{1+y_0^2}{1+||\varpi||^2}$ is bounded a.e. and since $\frac{\tilde e^2}{1+y_0^2}\in\mathscr{L}_1$ from Property 3 in Lemma 1, $\varepsilon\in\mathscr{L}_2$ follows. Let

$$V_1(t)=\lambda^{-1}\int_0^1 e^{-\delta\lambda^{-1}x}\nu^2(x,t)dx \tag{A.25a}$$

$$V_2(t)=\mu^{-1}\int_0^1 e^{\delta\mu^{-1}x}\eta^2(x,t)dx \tag{A.25b}$$

$$V_3(t)=\mu^{-1}\int_0^1 e^{\delta\mu^{-1}x}\varpi^2(x,t)dx, \tag{A.25c}$$

where $(\nu,\eta)$ is given by (37) and $\varpi$ by (38). Differentiating (A.25a), inserting the dynamics (37a), integrating by parts, using boundary condition (37) and substituting in (A.24) give

$$\begin{aligned}\dot V_1(t)=&-2\int_0^1 e^{-\delta\lambda^{-1}x}\nu(x,t)\nu_x(x,t)dx,\\ &-2\lambda^{-1}\int_0^1 e^{-\delta\lambda^{-1}x}\nu(x,t)\Psi_1(x,t)\hat\kappa(t)\tilde e(t)dx,\\ &-2\lambda^{-1}\int_0^1 e^{-\delta\lambda^{-1}x}\nu(x,t)\int_0^x K_t^{\mu u}(x,\xi,t)\\ &\qquad\times\mathscr{K}_1^{-1}[\nu+\varphi,\eta+\phi](\xi,t)d\xi dx\\ &-2\lambda^{-1}\int_0^1 e^{-\delta\lambda^{-1}x}\nu(x,t)\int_0^x K_t^{\mu v}(x,\xi,t)\\ &\qquad\times\mathscr{K}_2^{-1}[\nu+\varphi,\eta+\phi](\xi,t)d\xi dx\\ \le&-e^{-\delta\lambda^{-1}}\nu^2(1,t)+(1+\varsigma^{-1})\bar q^2\eta^2(0,t)-\delta V_1(t)\\ &+\lambda^{-1}||\Psi_1||^2\bar\kappa^2\tilde e^2(t)+V_1\\ &+2e^{-\delta\lambda^{-1}}h||K_t^{\mu u}||^2(V_1(t)+V_2(t)+||\varphi||^2+||\phi||^2)\\ &+2e^{-\delta\lambda^{-1}}h||K_t^{\mu v}||^2(V_1(t)+V_2(t)+||\varphi||^2+||\phi||^2)\\ &+(1+\varsigma)\bar\kappa^2\varepsilon^2(t)+(1+\varsigma)\bar\kappa^2\varepsilon^2(t)\mu V_3(t).\end{aligned} \tag{A.26}$$

for some $\varsigma>0$ and where we have defined $\bar\kappa:=\sup_{t\ge0}\hat\kappa(t)=(1+\underline{k})^{-1}$ and used $\sup_{t\ge t_F}\hat q^2(t)\le\bar q^2$, $\varsigma>0$ and $||\mathscr{K}_i^{-1}[\nu+\varphi,\eta+\phi]||\le h(||\omega||+||\eta||+||\varphi||^2+||\phi||^2)$ for some $h>0$. Differentiating (A.25b) and inserting the dynamics (37b), we get similarly

$$\begin{aligned}\dot V_2(t)=&2\int_0^1 e^{\delta\mu^{-1}x}\eta(x,t)\eta_x(x,t)dx,\\ &-2\mu^{-1}\int_0^1 e^{\delta\mu^{-1}x}\eta(x,t)\Psi_2(x,t)\hat\kappa(t)\tilde e(t)dx,\\ &-2\int_0^1 e^{\delta\mu^{-1}x}\eta(x,t)\int_0^x K_t^{\nu u}(x,\xi,t)\\ &\qquad\times\mathscr{K}_1^{-1}[\nu+\varphi,\eta+\phi](\xi,t)d\xi dx\\ &-2\int_0^1 e^{\delta\mu^{-1}x}\eta(x,t)\int_0^x K_t^{\nu v}(x,\xi,t)\\ &\qquad\times\mathscr{K}_2^{-1}[\nu+\varphi,\eta+\phi](\xi,t)d\xi dx\\ \le&e^{\delta\mu^{-1}}\bar\sigma^2\nu^2(1,t)-\eta^2(0)-\delta V_2(t)\\ &+2e^{\delta\mu^{-1}}h||K_t^{\nu u}||^2(V_1(t)+V_2(t)+||\varphi||^2+||\phi||^2)\\ &+2e^{\delta\mu^{-1}}h||K_t^{\nu v}||^2(V_1(t)+V_2(t)+||\varphi||^2+||\phi||^2)\\ &+\mu^{-1}e^{\delta\mu^{-1}}||\Psi_2||^2\bar\kappa^2\tilde e^2(t)+V_2(t).\end{aligned} \tag{A.27}$$

Lastly, differentiating (A.25c), inserting the dynamics (38), and upper bounding $\varpi(0,t)$ by defining $\bar q_r:=\sup_{t\ge0}2(\hat q(t)-r)^2=2(r-b_0)^2\bar\kappa$, we get

$$\begin{aligned}\dot V_3(t)=&2\int_0^1 e^{\delta\mu^{-1}x}\varpi(x,t)\varpi_x(x,t)dx\\ =&e^{\delta\mu^{-1}}\varpi_1^2(t)-\varpi^2(0,t)-\delta V_3(t)\\ \le&e^{\delta\mu^{-1}}(\bar q_r\eta^2(0,t)+2\bar\kappa^2\varepsilon^2(t)+2\bar\kappa^2\varepsilon^2(t)\mu V_3(t))\\ &-\delta V_3(t).\end{aligned} \tag{A.28}$$

Now forming the Lyapunov function candidate

$$V_4(t) = a_1 V_1(t) + a_2 V_2(t) + a_3 V_3(t), \tag{A.29}$$

and defining the integrable functions

$$\begin{aligned} l_1(t) :=& (2+\varsigma+\lambda^{-1}||\Psi_1||^2+\mu^{-1}e^{\delta\mu^{-1}}||\Psi_2||^2)\bar{\kappa}^2\varepsilon^2(t) \\ &+2e^{-\delta\lambda^{-1}}h(||\varphi||^2+||\phi||^2) \\ &\times(||K_t^{uu}||^2+||K_t^{uv}||^2+||K_t^{vu}||^2+||K_t^{vv}||^2) \end{aligned} \tag{A.30a}$$

$$\begin{aligned} l_2(t) :=& (\mu(2+\varsigma)+||\Psi_1||^2+e^{\delta\mu^{-1}}||\Psi_2||^2)\bar{\kappa}^2\varepsilon^2(t) \\ &2e^{-\delta\lambda^{-1}}h \\ &\times(||K_t^{uu}||^2+||K_t^{uv}||^2+||K_t^{vu}||^2+||K_t^{vv}||^2) \end{aligned} \tag{A.30b}$$

and using $a_3 = a_1\bar{q}_r^{-1}e^{-\delta\mu^{-1}}\varsigma^{-1}$ gives the upper bound

$$\begin{aligned} V_4(t) \leq& -(\delta-1)V_4 + l_1(t) + l_2(t)V_4(t) \\ &-(a_1e^{-\delta\lambda^{-1}} - a_2e^{\delta\mu^{-1}}\tilde{\sigma}^2)v^2(1,t) \\ &-(a_2 - a_1(1+2\varsigma^{-1})\bar{q}^2)\eta^2(0,t). \end{aligned} \tag{A.31}$$

Following [9, Theorem 2.4], if $|\bar{\sigma}\bar{q}|<1$, we can select $\delta>1$ and $\varsigma>0$ such that

$$(e^{\delta(\mu^{-1}+\lambda^{-1})})\tilde{\sigma}^2(1+2\varsigma^{-1})\bar{q}^2 < 1 \tag{A.32}$$

and $a_1, a_2$ such that

$$e^{\delta(\mu^{-1}+\lambda^{-1})}\tilde{\sigma}^2 < \frac{a_1}{a_2} < \frac{1}{(1+2\varsigma^{-1})\bar{q}^2} \tag{A.33}$$

obtaining $\dot{V}_4(t) \leq -V_4(t) + l_1(t) + l_2(t)V_4(t)$. It follows from [18, Lemma B.6] that $V_4 \in \mathscr{L}_1 \cap \mathscr{L}_\infty$, and hence (41). Furthermore, from [31, Lemma 2.17] we have that $V_8 \to 0$, which implies (42).

## B Additional stability and convergence lemmas

**Lemma 6 (Lemma B.6 from [18])** *Let $v(t)$, $l_1(t)$, $l_2(t)$ be real-valued functions defined for $t \geq 0$. Suppose*

$$0 \leq v(t), l_1(t), l_2(t), \ \forall t \geq 0 \tag{B.1a}$$

$$l_1, l_2 \in \mathscr{L}_1 \tag{B.1b}$$

$$\dot{v}(t) \leq -cv(t) + l_1(t)v(t) + l_2(t) \tag{B.1c}$$

*for some positive constant $c$. Then $v \in \mathscr{L}_1 \cap \mathscr{L}_\infty$.*

**Lemma 7 (Lemma 2.17 from [31])** *Consider a signal $g$ satisfying*

$$\dot{g}(t) = -ag(t) + bh(t) \tag{B.2}$$

*for a signal $h \in \mathscr{L}_1$ and some constants $a, b > 0$. Then*

$$g \in \mathscr{L}_\infty \tag{B.3}$$

*and*

$$\lim_{t\to\infty} g(t) = 0. \tag{B.4}$$

## 4.4 Paper [62]: *Adaptive set-point regulation of linear $n+1$ hyperbolic systems with uncertain affine boundary condition using collocated sensing and control*

Holta, H. and Aamo, O. M. (2020b). Adaptive set-point regulation of linear n+1 hyperbolic systems with uncertain affine boundary condition using collocated sensing and control. *Under review, Systems & Control Letters, submitted January 2020*

## 4.5 Comments, flaws, limitations and further work

All boundary control schemes seeking finite time convergence in systems with natural boundary reflections, involve counteracting the unwanted boundary reflection. This counteracting or cancellation of boundary terms has some robustness issues related to actuator and sensor delay. This problem was first studied in [13]. The reviewers of paper [68] (Section 4.3) made us aware of this potential problem and we modified the paper accordingly. This potential problem is however common to all boundary feedback control systems seeking attenuation in finite time and is an important topic for further research.

The same limitation as discussed in Section 2.4 regarding linearization of the flux density matrix applies to [62].

# CHAPTER 5

# Gas kick detection & estimation

## 5.1 Introduction

The first paper [59] presents an early-lumping design for gas detection and estimation. This is the only early-lumping design in this thesis. An important model-reduction assumption is made, namely the approximation of the $3 \times 3$ quasi-linear drift-flux model by a simple transport equation plus a coupled $2 \times 2$ quasi-linear system. The validity of this model reduction is investigated further in [69].

## 5.2 Paper [59]: *A least squares scheme utilizing fast propagating shock waves for early kick estimation in drilling*

Holta, H. and Aamo, O. M. (2019b). A least-squares scheme utilizing fast propagating shock waves for early kick estimation in drilling. In *Proceedings of the 2019 IEEE Conference on Control Technology and Applications (CCTA)*, pages 1081–1086

## 5.3 Paper [69]: *Observer design for a two-time-scale quasi-linear system*

Holta, H., Anfinsen, H., and Aamo, O. M. (2020b). Observer design for a two-time-scale quasi-linear system. *Unpublished*

This Paper is awaiting publication and is not included in NTNU Open

## 5.4 Comments, flaws, limitations and further work

In the first paper [59], the initial state value is assumed known, and only the unknown boundary parameters $J_G$, $J_L$ and $p_r$ are estimated. In the second paper [69], the boundary parameters are assumed known, and only the unknown states $u$ and $v$ are estimated. While the assumptions in [59] might be justified in a kick scenario where the pre-kick drilling conditions can be estimated trivially off-line, the known-parameter-assumption in [69] is untenable. A kick, by definition, is an unexpected event caused by insufficient information about the reservoir – well-bore interface. An important area for further work is therefore to extend the method in [69] to include parameter adaptation. Moreover, in [69], the slowly propagating state $\chi$ is assumed known. In a drilling application with limited down-hole measurements, an observer estimating the state $\chi$ must be included. This inclusion, however, introduces some problems related to observability which seems to be a fundamental problem in all kick estimation scenarios with similar limited measurements. Lastly, the recently published backstepping controller for non-autonomous systems presented in [34] might be extended to observer design and thus present a better, more robust solution, to the same problem. The method presented in [106] might also be promising in that regard. Due to all these circumstances, the authors have decided not to publish the second paper [69]. Nonetheless, the paper substantiates the utility of the methods presented in Chapter 3 and it is therefore included in this thesis as an unpublished paper.

# CHAPTER 6

## Concluding remarks

Estimating the states and parameters in a drilling system is associated with the kick & loss *estimation* problem. The kick & loss *detection* problem is a statistical problem which involves the identification of a single explanatory model from a large set of possible models (one for every conceivable drilling incident). No detection scheme should be deployed on a stand-alone basis and caution must be taken when assessing the reliability of the estimates.

There is a reason distributed models, so far, has not been used for real-time kick and loss estimation. Firstly, the estimation schemes all depend on accurate top-side flow and pressure measurements. Especially the return flow measurements are troubled by high levels of noise, significant bias, drifting, and low sampling rate. Secondly, few theoretical observer and control results have been available for hyperbolic PDE systems. The control toolbox for ODEs, on the other hand, is rich. Of course, early lumping is always an alternative, but the loss of fundamental properties and increased dimensionality makes early lumping designs ill-suited for on-line implementation. My work has focused on overcoming the second limitation. Still, much work and investments in measurement technology is needed to overcome the first limitations. So, at the moment I doubt the designs presented in this thesis will work using todays measurement equipment. In addition, other important qualities such as robustness to modeling errors, delays and measurement noise have only been studied to a limited degree. Nevertheless, some of the results presented in this thesis might serve as building blocks to yet better estimation and control schemes that can be used in the future if sufficiently accurate measurement technologies are implemented in the drilling industry.

# References


[1] Aamo, O. M. (2013). Disturbance rejection in $2 \times 2$ linear hyperbolic systems. *IEEE Transactions on Automatic Control*, 58(5):1095–1106.

[2] Aamo, O. M., Salvesen, J., and Foss, B. A. (2006). Observer design using boundary injections for pipeline monitoring and leak detection. *IFAC Proceedings Volumes*, 39(2):53–58.

[3] Aarsnes, U. J. F., Ambrus, A., Meglio, F. D., Vajargah, A. K., Aamo, O. M., and van Oort, E. (2016a). A simplified two-phase flow model using a quasi-equilibrium momentum balance. *International Journal of Multiphase Flow*, 83:77–85.

[4] Aarsnes, U. J. F., Flåtten, T., and Aamo, O. M. (2016b). Review of two-phase flow models for control and estimation. *Annual Reviews in Control*, 42:50 – 62.

[5] Aarsnes, U. J. F., Gleditsch, M. S., Aamo, O. M., and Pavlov, A. (2014a). Modeling and avoidance of heave-induced resonances in offshore drilling. *SPE Drilling & Completion*, 29(04):454–464.

[6] Aarsnes, U. J. F., Meglio, F. D., Aamo, O. M., and Kaasa, G.-O. (2014b). Fit-for-purpose modeling for automation of underbalanced drilling operations. In *SPE/IADC Managed Pressure Drilling & Underbalanced Operations Conference & Exhibition*. Society of Petroleum Engineers.

[7] Ali, T. H., Sas, M., Hood, J. A., Lemke, S. R., Srinivasan, A., McKay, J., Mondragon, C., Townsend, S. C., Edwards, S., Fereday, K. S., Hernandez, M., and Reeves, M. (2008). High speed telemetry drill pipe network optimizes drilling dynamics and wellbore placement. In *IADC/SPE Drilling Conference*. Society of Petroleum Engineers.

[8] Ambrus, A., Aarsnes, U. J. F., Vajargah, A. K., Akbari, B., van Oort, E., and Aamo, O. M. (2016). Real-time estimation of reservoir influx rate and pore pressure using a simplified transient two-phase flow model. *Journal of Natural Gas Science and Engineering*, 32:439–452.

[9] Anfinsen, B. and Rommetveit, R. (1992). Sensitivity of early kick detection parameters in full-scale gas kick experiments with oil- and water-based drilling muds. In *IADC/SPE Drilling Conference*. Society of Petroleum Engineers.

[10] Anfinsen, H. and Aamo, O. M. (2019). *Adaptive Control of Hyperbolic PDEs (Communications and Control Engineering)*. Springer.

[11] Anfinsen, H., Holta, H., and Aamo, O. M. (2020a). Adaptive control of a linear hyperbolic PDE with an uncertain transport speed and a spatially varying coefficient. In *Proceedings of the 28th Mediterranean Conference on Control and Automation (MED)*.

[12] Anfinsen, H., Holta, H., and Aamo, O. M. (2020b). Adaptive control of a scalar 1-D linear hyperbolic PDE with an uncertain transport speed using boundary sensing. In *Proceedings of the 2020 American Control Conference (ACC)*.

[13] Auriol, J., Aarsnes, U. J. F., Martin, P., and Meglio, F. D. (2018). Delay-robust control design for two heterodirectional linear coupled hyperbolic PDEs. *IEEE Transactions on Automatic Control*, 63(10):3551–3557.

[14] Auriol, J. and Meglio, F. D. (2016). Minimum time control of heterodirectional linear coupled hyperbolic PDEs. *Automatica*, 71:300 – 307.

[15] Babu, D. R. (1998). Effect of $p$-$\rho$-$t$ behavior of muds on loss/gain during high-temperature deep-well drilling. *Journal of Petroleum Science and Engineering*, 20(1-2):49–62.

[16] Balogh, A. and Krstic, M. (2002). Infinite dimensional backstepping-style feedback transformations for a heat equation with an arbitrary level of instability. *European journal of control*, 8(2):165–175.

[17] Bastin, G. and Coron, J.-M. (2010). Further results on boundary feedback stabilisation of $2 \times 2$ hyperbolic systems over a bounded interval. *IFAC Proceedings Volumes*, 43(14):1081–1085.

[18] Bastin, G. and Coron, J.-M. (2016). *Stability and boundary stabilization of 1-D hyperbolic systems*, volume 88. Springer.

[19] Bellman, R. (1957). *Dynamic Programming*. Rand Corporation research study. Princeton University Press.

[20] Benzoni-Gavage, S. (1991). *Analyse numérique des modèles hydrodynamiques d'écoulements diphasiques instationnaires dans les réseaux de production pétrolière*. PhD thesis, Lyon 1.

[21] Berg, C., Malagalage, A., Agu, C., Kaasa, G.-O., Vaagsaether, K., and Lie, B. (2015). Model-based drilling fluid flow rate estimation using Venturi flume. *IFAC-PapersOnLine*, 48(6):171–176.

[22] Besançon, G., Georges, D., Begovich, O., Verde, C., and Aldana, C. (2007). Direct observer design for leak detection and estimation in pipelines. In *Proceedings of the 2007 European Control Conference*, pages 5666–5670. IEEE.

[23] Billmann, L. and Isermann, R. (1987). Leak detection methods for pipelines. *Automatica*, 23(3):381–385.

[24] Bisgaard, C., Sørensen, H. H., and Spangenberg, S. (1987). A finite element method for transient compressible flow in pipelines. *International Journal for Numerical Methods in Fluids*, 7(3):291–303.

[25] Boskovic, D. M., Krstic, M., and Liu, W. (2001). Boundary control of an unstable heat equation via measurement of domain-averaged temperature. *IEEE Transactions on Automatic Control*, 46(12):2022–2028.

[26] Caenn, R., Darley, H. C., and Gray, G. R. (2011). *Composition and properties of drilling and completion fluids*. Gulf professional publishing.

[27] Carlsen, L. A., Nygaard, G., Gravdal, J. E., Nikolaou, M., and Schubert, J. (2008). Performing the dynamic shut-in procedure because of a kick incident when using automatic coordinated control of pump rates and choke-valve opening. In *SPE/IADC Managed Pressure Drilling and Underbalanced Operations Conference and Exhibition*. Society of Petroleum Engineers.

[28] Cayeux, E. and Daireaux, B. (2013). Precise gain and loss detection using a transient hydraulic model of the return flow to the pit. In *SPE/IADC Middle East Drilling Technology Conference & Exhibition*. Society of Petroleum Engineers.

[29] Cayeux, E. and Daireaux, B. (2016). Insights into the physical phenomena that influence automatic gain/loss detection during drilling operations. *SPE Drilling & Completion*, 32(01):13–24.

[30] Chhantyal, K. (2018). *Sensor Data Fusion based Modelling of Drilling Fluid Return Flow through Open Channels*. PhD thesis, University of South-Eastern Norway.

[31] Colton, D. (1977). The solution of initial-boundary value problems for parabolic equations by the method of integral operators. *Journal of Differential Equations*, 26(2):181–190.

[32] Coron, J., D'Andrea-Novel, B., and Bastin, G. (1999). A Lyapunovapproach to control irrigation canals modeled by Saint-Venant equations. *Proc. Eur. Control Conf.* cited By 36.

[33] Coron, J.-M., Bastin, G., and d'Andréa Novel, B. (2008). Dissipative boundary conditions for one-dimensional nonlinear hyperbolic systems. *SIAM Journal on Control and Optimization*, 47(3):1460–1498.

[34] Coron, J.-M., Hu, L., Olive, G., and Shang, P. (2020). Boundary stabilization in finite time of one-dimensional linear hyperbolic balance laws with coefficients depending on time and space. *Preprint available at* http://arxiv.org/abs/2004.12594v1.

[35] Coron, J.-M., Vazquez, R., Krstic, M., , and Bastin, G. (2013). Local exponential $H^2$ stabilization of a $2 \times 2$ quasilinear hyperbolic system using backstepping. *SIAM Journal on Control and Optimization*, 51(3):2005–2035.

[36] Dake, L. P. (1978). *Fundamentals of reservoir engineering*, volume 8 of *Developments in petroleum science*. Elsevier, Amsterdam.

[37] Di Meglio, F. (2011). *Dynamics and control of slugging in oil production*. PhD thesis, École Nationale Supérieure des Mines de Paris.

[38] Di Meglio, F. and Aarsnes, U. (2015). A distributed parameter systems view of control problems in drilling. *IFAC-PapersOnLine*, 48(6):272 – 278. 2nd IFAC Workshop on Automatic Control in Offshore Oil and Gas Production OOGP 2015.

[39] Di Meglio, F., Bresch-Pietri, D., and Aarsnes, U. J. F. (2014). An adaptive observer for hyperbolic systems with application to underbalanced drilling. *IFAC Proceedings Volumes*, 47(3):11391 – 11397. 19th IFAC World Congress.

[40] Di Meglio, F., Vazquez, R., and Krstic, M. (2013). Stabilization of a system of $n + 1$ coupled first-order hyperbolic linear PDEs with a single boundary input. *IEEE Transactions on Automatic Control*, 58(12):3097–3111.

[41] Dowell, I., Mills, A., and Lora, M. (2006). Chapter 15: Drilling-data acquisition. *RF Mitchell. Petroleum Engineering Handbook. II-Drilling Engineering. Society of Petroleum Engineers*, na:647–685.

[42] Dulhoste, J.-F., Georges, D., and Besançon, G. (2004). Nonlinear control of open-channel water flow based on collocation control model. *Journal of Hydraulic Engineering*, 130(3):254–266.

[43] Evje, S. (2013). A compressible two-phase model with pressure-dependent well-reservoir interaction. *SIAM Journal on Mathematical Analysis*, 45(2):518–546. Incompressible liquid, no source terms, pressure-inflow relationship.

[44] Fjelde, K. K., Rommetveit, R., Merlo, A., and Lage, A. C. V. M. (2003). Improvements in dynamic modeling of underbalanced drilling. In *Proceedings of the IADC/SPE Underbalanced Technology Conference and Exhibition*, page 8, Houston, Texas. Society of Petroleum Engineers.

[45] Florence, F. R. and Burks, J. (2012). New surface and down-hole sensors needed for oil and gas drilling. In *2012 IEEE International Instrumentation and Measurement Technology Conference Proceedings*. IEEE.

[46] Fraser, D., Lindley, R., Moore, D. D., and Staak, M. V. (2014). Early kick detection methods and technologies. In *SPE Annual Technical Conference and Exhibition*. Society of Petroleum Engineers.

[47] Gabaldon, O., Culen, M., and Brand, P. (2014). Enhancing well control through managed pressure drilling. In *Offshore Technology Conference*. Offshore Technology Conference.

[48] Gavrilyuk, S. and Fabre, J. (1996). Lagrangian coordinates for a drift-flux model of a gas-liquid mixture. *International Journal of Multiphase Flow*, 22(3):453–460.

[49] Ghidaoui, M. S., Zhao, M., McInnis, D. A., and Axworthy, D. H. (2005). A review of water hammer theory and practice. *Applied Mechanics Reviews*, 58(1):49–76.

[50] Godhavn, J.-M., Pavlov, A., Kaasa, G.-O., and Rolland, N. L. (2011). Drilling seeking automatic control solutions. *IFAC Proceedings Volumes*, 44(1):10842–10850.

[51] Grace, R. D. (2017). *Blowout and well control handbook*. Gulf Professional Publishing.

[52] Gravdal, A. E., Lorentzen, R. J., and Time, R. W. (2010). Wired drill pipe telemetry enables real-time evaluation of kick during managed pressure drilling. In *SPE Asia Pacific Oil and Gas Conference and Exhibition*. Society of Petroleum Engineers.

[53] Hauge, E., Aamo, O., Godhavn, J.-M., and Nygaard, G. (2013a). A novel model-based scheme for kick and loss mitigation during drilling. *Journal of Process Control*, 23(4):463–472.

[54] Hauge, E., Aamo, O. M., and Godhavn, J.-M. (2013b). Application of an infinite-dimensional observer for drilling systems incorporating kick and loss detection. In *Proceedings of the 12th European Control Conference*, pages 1065–1070. IEEE.

[55] Hauge, E., Stamnes, Ø. N., Aamo, O. M., and Godhavn, J.-M. (2012). A dynamic model of percolating gas in a wellbore. *SPE Drilling & Completion*, 27(02):204–215.

[56] Helstrup, O. A., Chen, Z., and Rahman, S. S. (2004). Time-dependent wellbore instability and ballooning in naturally fractured formations. *Journal of Petroleum Science and Engineering*, 43(1-2):113–128.

[57] Holta, H. and Aamo, O. M. (2018). Boundary set-point regulation of a linear $2\times2$ hyperbolic PDE with uncertain bilinear boundary condition. In *Proceedings of the 2018 IEEE Conference on Decision and Control (CDC)*, pages 2156–2163. IEEE.

[58] Holta, H. and Aamo, O. M. (2019a). An adaptive observer design for $2 \times 2$ semi-linear hyberbolic systems using distributed sensing. In *Proceedings of the 2019 American Control Conference (ACC)*, pages 2540–2545.

[59] Holta, H. and Aamo, O. M. (2019b). A least-squares scheme utilizing fast propagating shock waves for early kick estimation in drilling. In *Proceedings of the 2019 IEEE Conference on Control Technology and Applications (CCTA)*, pages 1081–1086.

[60] Holta, H. and Aamo, O. M. (2019c). Observer design for a class of semi-linear hyperbolic PDEs with distributed sensing and parametric uncertainties. *Under review, IEEE Transactions on Automatic Control, submitted September 2019.*

[61] Holta, H. and Aamo, O. M. (2020a). Adaptive observer design for an n+1 hyperbolic PDE with uncertainty and sensing on opposite ends. In *Proceedings of the 2020 European Control Conference (ECC)*, pages 1159–1164.

[62] Holta, H. and Aamo, O. M. (2020b). Adaptive set-point regulation of linear n+1 hyperbolic systems with uncertain affine boundary condition using collocated sensing and control. *Under review, Systems & Control Letters, submitted January 2020.*

[63] Holta, H. and Aamo, O. M. (2020c). Exploiting wired-pipe technology in an adaptive observer for drilling incident detection and estimation. *Under review, SPE Journal, submitted January 2020.*

[64] Holta, H. and Aamo, O. M. (2020d). A heuristic observer design for an uncertain hyperbolic PDE using distributed sensing. In *Proceedings of the IFAC world congress 2020.*

[65] Holta, H., Anfinsen, H., and Aamo, O. M. (2017a). Adaptive set-point regulation of linear $2 \times 2$ hyperbolic systems with uncertain affine boundary condition using collocated sensing and control. In *Proceedings of the 2017 Asian Control Conference (ASCC)*, pages 2766–2771.

[66] Holta, H., Anfinsen, H., and Aamo, O. M. (2017b). Estimation of an uncertain bilinear boundary condition in linear $2 \times 2$ hyperbolic systems with application to drilling. In *Proceedings of the 17th International Conference on Control, Automation, and Systems (ICCAS)*, pages 188–193.

[67] Holta, H., Anfinsen, H., and Aamo, O. M. (2018). Improved kick and loss detection and attenuation in managed pressure drilling by utilizing wired drill pipe. *In Proceedings of the 3rd IFAC Workshop on Automatic Control in Offshore Oil and Gas Production (OOGP)*, 51(8):44–49.

[68] Holta, H., Anfinsen, H., and Aamo, O. M. (2020a). Adaptive set-point regulation of linear $2 \times 2$ hyperbolic systems with application to the kick and loss problem in drilling. *Automatica*, 119:109078.

[69] Holta, H., Anfinsen, H., and Aamo, O. M. (2020b). Observer design for a two-time-scale quasi-linear system. *Unpublished*.

[70] Hu, L., Di Meglio, F., Vazquez, R., and Krstic, M. (2016). Control of homodirectional and general heterodirectional linear coupled hyperbolic PDEs. *IEEE Transactions on Automatic Control*, 61(11):3301–3314.

[71] Hu, L., Vazquez, R., Meglio, F. D., and Krstic, M. (2018). Boundary exponential stabilization of 1-D inhomogeneous quasilinear hyperbolic systems. *Preprint submitted*.

[72] Jinasena, A. (2019). *Models and Estimators for Flow of Topside Drilling Fluid*. PhD thesis, University of South-Eastern Norway.

[73] Jinasena, A., Holta, H., Jondahl, M. H., Welahettige, P., Sharma, R., Aamo, O. M., and Lie, B. (2020). Model based early kick/loss detection and attenuation in managed pressure drilling with topside sensing using a Venturi flowmeter. *Submitted to the 61st International Conference of Scandinavian Simulation Society, SIMS*.

[74] Jondahl, M. H. (2020). *Data Driven Models for Estimation of Drilling Fluid Rheological Properties and Flow Rate*. PhD thesis, University of South-Eastern Norway.

[75] Kaasa, G.-O., Stamnes, Ø. N., Aamo, O. M., and Imsland, L. S. (2012). Simplified hydraulics model used for intelligent estimation of downhole pressure for a managed-pressure-drilling control system. *SPE Drilling & Completion*, 27(01):127–138.

[76] Kowalczuk, Z. and Gunawickrama, K. (2000). Leak detection and isolation for transmission pipelines via nonlinear state estimation. *IFAC Proceedings Volumes*, 33(11):921–926.

[77] Krstic, M. and Smyshlyaev, A. (2008a). Backstepping boundary control for first-order hyperbolic PDEs and application to systems with actuator and sensor delays. *Systems & Control Letters*, 57(9):750 – 758.

[78] Krstic, M. and Smyshlyaev, A. (2008b). *Boundary Control of PDEs: A Course on Backstepping Designs*, volume 16. Siam.

[79] Landet, I. S., Pavlov, A., and Aamo, O. M. (2013). Modeling and control of heave-induced pressure fluctuations in managed pressure drilling. *IEEE Transactions on Control Systems Technology*, 21(4):1340–1351.

[80] Le Blay, F., Villard, E., Hilliard, S. C., and Gronas, T. (2012). A new generation of well surveillance for early detection of gains and losses when drilling very high profile ultradeepwater wells, improving safety, and optimizing operating procedures. In *SPETT 2012 Energy Conference and Exhibition*. Society of Petroleum Engineers.

[81] Liu, W. (2003). Boundary feedback stabilization of an unstable heat equation. *SIAM Journal on Control and Optimization*, 42(3):1033–1043.

[82] Malloy, K. P., Stone, R., Medley, G. H., Hannegan, D. M., Coker, O. D., Reitsma, D., Santos, H. M., Kinder, J. I., Eck-Olsen, J., McCaskill, J. W., May, J. R., Smith, K. L., and Sonnemann, P. (2009). Managed-pressure drilling: What it is and what it is not. In *IADC/SPE Managed Pressure Drilling and Underbalanced Operations Conference & Exhibition*. Society of Petroleum Engineers.

[83] Mehrabi, M., Zeyghami, M., and Shahri, M. P. (2012). Modeling of fracture ballooning in naturally fractured reservoirs: A sensitivity analysis. In *Nigeria Annual International Conference and Exhibition*. Society of Petroleum Engineers.

[84] Miller, J. and Young, R. (1985). Influence of mud column dynamics on top tension of suspended deepwater drilling risers. In *Offshore Technology Conference*. Offshore Technology Conference.

[85] Nikolaou, M. (2013). Computer-aided process engineering in oil and gas production. *Computers & Chemical Engineering*, 51:96–101.

[86] Nikoofard, A., Aarsnes, U. J. F., Johansen, T. A., and Kaasa, G.-O. (2017). State and parameter estimation of a drift-flux model for underbalanced drilling operations. *IEEE Transactions on Control Systems Technology*, 25(6):2000–2009.

[87] Nikoofard, A., Johansen, T. A., and Kaasa, G.-O. (2014). Nonlinear moving horizon observer for estimation of states and parameters in under-balanced drilling operations. In *ASME 2014 Dynamic Systems and Control Conference*. ASME.

[88] Nikoofard, A., Johansen, T. A., and Kaasa, G.-O. (2018). Reservoir characterization in under-balanced drilling using low-order lumped model. *Journal of Process Control*, 62:24–36.

[89] Nygaard, G., Naedal, G., and Mylvaganam, S. (2006). Evaluating nonlinear Kalman filters for parameter estimation in reservoirs during petroleum well drilling. In *2006 IEEE Conference on Computer Aided Control System Design*. IEEE.

[90] Nygaard, G. H., Vefring, E. H., Fjelde, K. K., Naevdal, G., Lorentzen, R. J., and Mylvaganam, S. (2007). Bottomhole pressure control during drilling operations in gas-dominant wells. *SPE Journal*, 12(01):49–61.

[91] Orban, J., Zanner, K., and Orban, A. (1987). New flowmeters for kick and loss detection during drilling. In *SPE Annual Technical Conference and Exhibition*. Society of Petroleum Engineers.

[92] Pink, A. P., Kverneland, H., Bruce, A., and Applewhite, J. B. (2012). Building an automated drilling system where the surface machines are controlled by downhole and surface data to optimize the well construction process. In *IADC/SPE Drilling Conference and Exhibition*. Society of Petroleum Engineers.

[93] Rayleigh, John William Strutt, r. B. (1896). *Theory of sound*. Macmillan.

[94] Reitsma, D. (2010). A simplified and highly effective method to identify influx and losses during managed pressure drilling without the use of a Coriolis flow

meter. In *SPE/IADC Managed Pressure Drilling and Underbalanced Operations Conference and Exhibition*. Society of Petroleum Engineers.

[95] Russell, D. L. (1978a). Canonical forms and spectral determination for a class of hyperbolic distributed parameter control systems. *Journal of Mathematical Analysis and Applications*, 62(1):186–225.

[96] Russell, D. L. (1978b). Controllability and stabilizability theory for linear partial differential equations: Recent progress and open questions. *SIAM Review*, 20(4):639–739.

[97] Saba, D. B., Argomedo, F. B., Auriol, J., Loreto, M. D., and Meglio, F. D. (2019). Stability analysis for a class of linear $2 \times 2$ hyperbolic PDEs using a backstepping transform. *IEEE Transactions on Automatic Control*, pages 1–1.

[98] Schafer, D., Loeppke, G., Glowka, D., Scott, D., and Wright, E. (1992). An evaluation of flowmeters for the detection of kicks and lost circulation during drilling. In *IADC/SPE Drilling Conference*. Society of Petroleum Engineers.

[99] Shayegi, S., Kabir, C. S., If, F., Christensen, S., Ken, K., Casasus-Bribian, J., Hasan, A. K., and Moos, D. (2012). Reservoir characterization begins at first contact with the drill bit. *SPE Drilling & Completion*, 27(01):11–21.

[100] Shields, D., Ashton, S., and Daley, S. (2001). Design of nonlinear observers for detecting faults in hydraulic sub-sea pipelines. *Control Engineering Practice*, 9(3):297–311.

[101] Shu, J.-J. (2003). A finite element model and electronic analogue of pipeline pressure transients with frequency-dependent friction. *Journal of Fluids Engineering*, 125(1):194–198.

[102] Smith, J. R. and Patel, B. M. (2012). A proposed method for planning the best initial response to kicks taken during managed-pressure-drilling operations. *SPE Drilling & Completion*, 27(02):194–203.

[103] Smyshlyaev, A. and Krstic, M. (2004). Closed-form boundary state feedbacks for a class of 1-D partial integro-differential equations. *IEEE Transactions on Automatic Control*, 49(12):2185–2202.

[104] Smyshlyaev, A. and Krstic, M. (2005). On control design for PDEs with space-dependent diffusivity or time-dependent reactivity. *Automatica*, 41(9):1601–1608.

[105] Stecki, J. S. and Davis, D. C. (1986). Fluid transmission lines—distributed parameter models part 1: A review of the state of the art. *Proceedings of the Institution of Mechanical Engineers, Part A: Power and Process Engineering*, 200(4):215–228.

[106] Strecker, T., Aamo, O. M., and Cantoni, M. (2019). Direct predictive boundary control of a first-order quasilinear hyperbolic PDE. In *2019 IEEE 58th Conference on Decision and Control (CDC)*. IEEE.

[107] Szymkiewicz, R. and Mitosek, M. (2004). Analysis of unsteady pipe flow using the modified finite element method. *Communications in Numerical Methods in Engineering*, 21(4):183–199.

[108] Tijsseling, A. and Anderson, A. (2008). Thomas Young's research on fluid transients: 200 years on. In Hunt, S., editor, *Proceedings 10th International Conference on Pressure Surges (Edinburgh, UK, May 14-16, 2008)*, pages 21–33. BHR Group Limited.

[109] Torres, L., Besancon, G., and Georges, D. (2008). A collocation model for water-hammer dynamics with application to leak detection. In *Proceedings of the 2008 47th IEEE Conference on Decision and Control*. IEEE.

[110] Torres, L., Besanon, G., and Georges, D. (2009). Multi-leak estimator for pipelines based on an orthogonal collocation model. In *Proceedings of the 48h IEEE Conference on Decision and Control (CDC) held jointly with 2009 28th Chinese Control Conference*. IEEE.

[111] Vazquez, R., Krstic, M., and Coron, J.-M. (2011). Backstepping boundary stabilization and state estimation of a $2 \times 2$ linear hyperbolic system. In *Proceedings of the 50th IEEE Conference on Decision and Control and European Control Conference*, pages 4937–4942.

[112] Vefring, E. H., Nygaard, G., Fjelde, K. K., Lorentzen, R. J., Nævdal, G., and Merlo, A. (2002). Reservoir characterization during underbalanced drilling: Methodology, accuracy, and necessary data. In *SPE Annual Technical Conference and Exhibition*. Society of Petroleum Engineers.

[113] Vefring, E. H., Nygaard, G., Lorentzen, R. J., Nævdal, G., and Fjelde, K. K. (2003). Reservoir characterization during UBD: Methodology and active tests. In *IADC/SPE Underbalanced Technology Conference and Exhibition*. Society of Petroleum Engineers.

[114] Vefring, E. H., Nygaard, G. H., Lorentzen, R. J., Naevdal, G., and Fjelde, K. K. (2006). Reservoir characterization during underbalanced drilling (UBD): Methodology and active tests. *SPE Journal*, 11(02):181–192.

[115] Velmurugan, N. and Meglio, F. D. (2018). Transient modelling of influx and observer implementation for estimation while drilling. In *2018 IEEE Conference on Decision and Control (CDC)*. IEEE.

[116] Wasserman, I., Hahn, D., Nguyen, D. H., Reckmann, H., and Macpherson, J. (2008). Mud-pulse telemetry sees step-change improvement with oscillating shear valves. *Oil & gas journal*, 106(24):39–40.

[117] Welahettige, P. K. W. (2019). *Transient drilling fluid flow in Venturi channels: comparing 3D and 1D models to experimental data*. PhD thesis, University of South-Eastern Norway.

[118] Willersrud, A., Blanke, M., and Imsland, L. (2015a). Incident detection and isolation in drilling using analytical redundancy relations. *Control Engineering Practice*, 41:1–12.

[119] Willersrud, A., Blanke, M., Imsland, L., and Pavlov, A. (2015b). Fault diagnosis of downhole drilling incidents using adaptive observers and statistical change detection. *Journal of Process Control*, 30:90–103.

[120] Zhou, J., Stamnes, Ø. N., Aamo, O. M., and Kaasa, G.-O. (2009). Pressure regulation with kick attenuation in a managed pressure drilling system. In *Proceedings of the 48th IEEE Conference on Decision and Control and 28th Chinese Control Conference*, pages 5586–5591. IEEE.

[121] Zhou, J., Stamnes, Ø. N., Aamo, O. M., and Kaasa, G.-O. (2011). Switched control for pressure regulation and kick attenuation in a managed pressure drilling system. *IEEE Transactions on Control Systems Technology*, 19(2):337–350.

# APPENDIX A

## Drilling coordinate transformations

The following result is shown for the annulus system $i = a$. A similar result holds for the drill-pipe system $i = d$. For simplicity the subscript $i$ is omitted.

**Lemma A.1.** *For the annulus system $i = a$, the coordinate transformation*

$$u(x,t) = \frac{1}{2}\left(\frac{A(x)}{\sqrt{\beta\rho}}\left(p(xl,t) + \rho g\int_0^x (\cos\psi(s) + \frac{f(x)}{A(x)}q_{bit})ds\right) + q(xl,t) - q_{bit}\right)$$
$$\times \exp\left(-\frac{1}{2}\int_0^x l\sqrt{\frac{\rho}{\beta}}(-f(sl) + \frac{A'(sl)}{A(sl)}\sqrt{\frac{\beta}{\rho}})ds\right) \tag{A.1a}$$

$$v(x,t) = \frac{1}{2}\left(-\frac{A(x)}{\sqrt{\beta\rho}}\left(p(xl,t) + \rho g\int_0^x (\cos\psi(s) + \frac{f(x)}{A(x)}q_{bit})ds\right) + q(xl,t) - q_{bit}\right)$$
$$\times \exp\left(-\frac{1}{2}\int_0^x l\sqrt{\frac{\rho}{\beta}}(-f(sl) - \frac{A'(sl)}{A(sl)}\sqrt{\frac{\beta}{\rho}})ds\right) \tag{A.1b}$$

*maps system (1.16) with source terms (1.19) into the form (1.10) with*

$$\lambda = \mu := \sqrt{\frac{\beta}{\rho}}\frac{1}{l} \tag{A.2a}$$

$$c_1(x) := \frac{1}{2}(-f(xl) - \frac{A'(xl)}{A(xl)}\sqrt{\frac{\beta}{\rho}})$$
$$\times \exp\left(-\int_0^x l\sqrt{\frac{\rho}{\beta}}(-f(sl) + \frac{A'(sl)}{A(sl)}\sqrt{\frac{\beta}{\rho}})ds\right) \tag{A.2b}$$

$$c_2(x) = \frac{1}{2}(-f(xl) + \frac{A'(xl)}{A(xl)}\sqrt{\frac{\beta}{\rho}})$$
$$\times \exp\left(-\int_0^x l\sqrt{\frac{\rho}{\beta}}(-f(sl) - \frac{A'(sl)}{A(sl)}\sqrt{\frac{\beta}{\rho}})ds\right). \tag{A.2c}$$

*The boundary condition* (1.50) *is mapped into the form* (1.55) *with*

$$Q_0 = -(1+k) := \frac{\left(J\frac{\sqrt{\beta\rho}}{A(0)} - 1\right)}{\left(J\frac{\sqrt{\beta\rho}}{A(0)} + 1\right)}, \quad d = k\theta := \frac{J}{\left(J\frac{\sqrt{\beta\rho}}{A(0)} + 1\right)}p_r. \tag{A.3}$$

*Or, if* $p(0,t)$ *is measured, into the form* (1.56) *with*

$$k_0 := J\frac{\sqrt{\beta\rho}}{A(0)}, \quad \theta_0 := \frac{A(0)}{\sqrt{\beta\rho}}p_r \tag{A.4}$$

*and*

$$y_0(t) := \frac{A(0)}{\sqrt{\beta\rho}}p_0(t) = u(0,t) - v(0,t). \tag{A.5}$$

*The top-side boundary condition* (1.20c)*, is mapped into the form* (1.14b)*,*

$$v(1,t) = R_1 y_1(t) + U(t), \tag{A.6}$$

*where the boundary control law* $U(t)$ *and measurement* $y_1(t)$ *are defined as*

$$\begin{aligned} U(t) := &\left(-\frac{A(l)}{\sqrt{\beta\rho}}\left(p(l,t) + \rho g\int_0^l (\cos\psi(s) + \frac{f(x)}{A(x)}q_{bit})ds\right)\right) \\ &\times \exp\left(-\frac{1}{2}\int_0^l l\sqrt{\frac{\rho}{\beta}}(-f(sl) + \frac{A'(sl)}{A(sl)}\sqrt{\frac{\beta}{\rho}})ds\right) \end{aligned} \tag{A.7a}$$

$$y_1(t) := u(1,t) \tag{A.7b}$$

*and*

$$R_1 := \exp\left(-\int_0^l l\sqrt{\frac{\rho}{\beta}}(-f(sl) + \frac{A'(sl)}{A(sl)}\sqrt{\frac{\beta}{\rho}})ds\right). \tag{A.8}$$

*Moreover, the control objective* (1.57) *is equivalent to* (1.58) *and* (1.59)*.*

*Proof.* To improve the condition number of the solution, constant terms are removed and the origin shifted by defining

$$\bar{p}(x,t) = p(x,t) + \rho g\int_0^x (\cos\psi(s) + \frac{f(x)}{A(x)}q_{bit})ds \tag{A.9a}$$

$$\bar{q}(x,t) = q(x,t) - q_{bit}. \tag{A.9b}$$

The solution in terms of the new coordinates $(\bar{p}(x,t), \bar{q}(x,t))$ satisfy

$$\bar{p}_t = -\frac{\beta}{A(x)}\bar{q}_x \tag{A.10a}$$

$$\bar{q}_t = -\frac{A(x)}{\rho}\bar{p}_x - f(x)\bar{q}. \tag{A.10b}$$

The similarity transformation

$$\begin{bmatrix}\bar{u}\\ \bar{v}\end{bmatrix} := \frac{1}{2}\begin{bmatrix}\frac{A(x)}{\sqrt{\beta\rho}} & 1\\ -\frac{A(x)}{\sqrt{\beta\rho}} & 1\end{bmatrix}\begin{bmatrix}\bar{p}\\ \bar{q}\end{bmatrix} \tag{A.11}$$

maps (A.10) into the characteristic form

$$\bar{u}_t + \sqrt{\frac{\beta}{\rho}}\bar{u}_x = \frac{1}{2}(S_1(xl) + S_2(xl))\bar{u} + \frac{1}{2}(S_1(xl) - S_2(xl))\bar{v} \tag{A.12a}$$

$$\bar{v}_t + \sqrt{\frac{\beta}{\rho}}\bar{v}_x = \frac{1}{2}(S_1(xl) + S_2(xl))\bar{u} + \frac{1}{2}(S_1(xl) - S_2(xl))\bar{v}. \tag{A.12b}$$

where

$$S_1(x) = -f(x), \quad S_2(x) = \frac{A'(x)}{A(x)}\sqrt{\frac{\beta}{\rho}}. \tag{A.13}$$

Finally, the diagonal elements can be removed and the domain scaled by applying the transformation

$$u(x,t) = \bar{u}(xl,t)\exp\left(-\frac{1}{2}\int_0^x l\sqrt{\frac{\rho}{\beta}}(S_1(sl) + S_2(sl))ds\right) \tag{A.14a}$$

$$v(x,t) = \bar{v}(xl,t)\exp\left(\frac{1}{2}\int_0^x l\sqrt{\frac{\rho}{\beta}}(S_1(sl) - S_2(sl))ds\right), \tag{A.14b}$$

mapping (A.12) into

$$u_t + \frac{1}{l}\sqrt{\frac{\beta}{\rho}}u_x = \frac{1}{2}(S_1(xl) - S_2(xl))\left(-\frac{1}{2}\int_0^x l\sqrt{\frac{\rho}{\beta}}(S_1(sl) + S_2(sl))ds\right)v \tag{A.15a}$$

$$v_t + \frac{1}{l}\sqrt{\frac{\beta}{\rho}}v_x = \frac{1}{2}(S_1(xl) + S_2(xl))\left(-\frac{1}{2}\int_0^x l\sqrt{\frac{\rho}{\beta}}(S_1(sl) - S_2(sl))ds\right)u \tag{A.15b}$$

which is in the form (1.10) with transport velocities and source terms (A.2).

For the bottom-hole boundary condition, evaluating (A.9) and (A.11) at $x = 0$ and inserting (1.50) gives

$$\begin{aligned} u(0,t) + v(0,t) =& q(0,t) - q_{bit} = J\left(p_{res} - p(0,t)\right)\\ =& J\frac{\sqrt{\beta\rho}}{A(0)}\left(\frac{A(0)}{\sqrt{\beta\rho}}p_{res} - \frac{A(0)}{\sqrt{\beta\rho}}p(0,t)\right)\end{aligned} \tag{A.16}$$

and the boundary condition (1.56) is obtained with $\theta_0$ and $k_0$ given in (A.4). Now if, $y_0(t) = u(0,t) - v(0,t)$ is not measured, starting from (1.56), the boundary condition

$$u(0,t) + v(0,t) = k_0(\theta_0 - (u(0,t) - v(0,t))) \tag{A.17}$$

can be solved for $u(0,t)$ as

$$u(0,t) = -2\frac{k_0}{1+k_0}(-\frac{1}{2}\theta_0 - v(0,t)). \tag{A.18}$$

Let

$$k = -2\frac{k_0}{1+k_0}, \quad \theta = -\frac{1}{2}\theta_0 \tag{A.19}$$

which by inserting (A.4) into (A.19) is equal to (A.3).

For the top-side boundary condition, inserting (A.7) into (A.1) with $x = 1$ gives

$$\begin{aligned} v(1,t) =& \frac{1}{2}(U(t) + (q(xl) - q_{bit})R_1^{\frac{1}{2}}) && \text{(A.20)} \\ =& \frac{1}{2}(U(t) + (u(1,t)R_1^{\frac{1}{2}} + v(1,t)R_1^{-\frac{1}{2}})R_1^{\frac{1}{2}}) && \text{(A.21)} \\ =& \frac{1}{2}(U(t) + u(1,t)R_1 + v(1,t)) && \text{(A.22)} \end{aligned}$$

and (A.6) follows.

The equivalence between the control objectives (1.57), (1.58) and (1.59) can be seen from (A.16) and (1.55). □

ISBN 978-82-326-4814-6 (printed version)
ISBN 978-82-326-4815-3 (electronic version)
ISSN 1503-8181

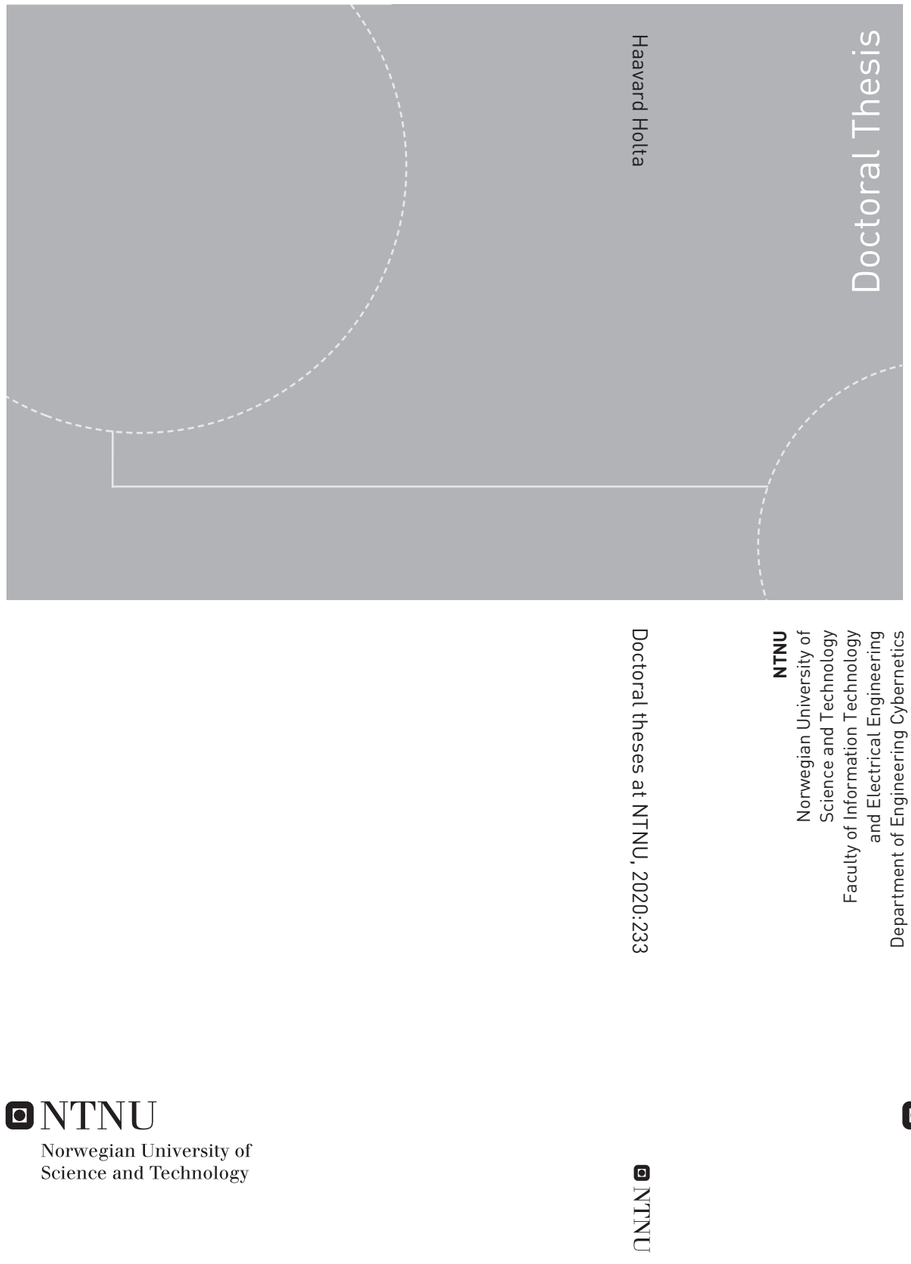


Doctoral theses at NTNU, 2020:233

Haavard Holta

# Kick & Loss Detection and Estimation using Distributed Models

**NTNU**
Norwegian University of
Science and Technology
Faculty of Information Technology
and Electrical Engineering
Department of Engineering Cybernetics

NTNU
Norwegian University of
Science and Technology

Doctoral theses at NTNU, 2020:233

NTNU

NTNU
Norwegian University of
Science and Technology